Nanoscale Molecular Systems: Designed Phenyl-Acetylene Architectures

Inauguraldissertation

zur

Erlangung der Würde eines Doktors der Philosophie

vorgelegt der

Philosophisch-Naturwissenschaftlichen Fakultät

der Universität Basel

von

Thomas R. Eaton

von Grossbritannien

Basel 2015

Genehmigt von der Philosophisch-Naturwissenschaftlichen Fakultät
auf Antrag von;

Prof. Dr. Marcel Mayor

Prof. Dr. Edwin Constable

Basel, 18 June 2013

Prof. Dr. Jörg Schibler
- Dekan -

To my parents,

Mark and Diana Eaton

for aligning all the building blocks

Le savant n'étudie pas la nature parce que cela est utile; il l'étudie parce qu'il y prend plaisir et il y prend plaisir parce qu'elle est belle. Si la nature n'était pas belle, elle ne vaudrait pas la peine d'être connue, la vie ne vaudrait pas la peine d'être vécue.

– Henri Poincaré,

Science et méthode (1908)

The scientist does not study nature because it is useful to do so. He studies it because he takes pleasure in it, and he takes pleasure in it because it is beautiful. If nature were not beautiful it would not be worth knowing, and life would not be worth living. – Henri Poincaré

(Translation by Francis Maitland, 1914)

Summary:

Molecular design should be about fulfilling function. However designing molecular structures that will fulfill a particular function is incredibly difficult. The delicate interplay of structure-property relationships and further emergent phenomena that arise when molecules come together are very unpredictable. This thesis sets out tools to guide the budding molecular architect in successfully making the transition in mindset from structure-property relationships to structure-function relationships.

In chapter 1, after covering briefly the tools currently used to investigate the nano world, we explore the chemistry of acetylenes applied in coupling reactions to form phenyl-acetylene bonds. We then turn our attention to supramolecular chemistry as a driver for the formation of self-assembled networks, allowing for a bottom-up approach to achieve nanopatterned, functional surfaces.

In chapter 2, the concept of phenyl-acetylene building blocks is presented. This modular approach to the assembly nano scale architectures makes the 'mass production' of a library of interesting building materials viable through organic synthesis. Both aryl and carbazole building blocks are explored, with a focus on their scope for further assembly to larger architectures.

Chapter 3 discusses applications of the building block approach to molecular electronics. Computing devices could become much faster, smaller, and cheaper to run if we move away from the silicon-based transistor towards functional single molecules. We have synthesised a series of linear, fully conjugated nano-rods and stars to act as molecular wires in an attempt to fabricate the first functional three-terminal device.

In chapter 4 we investigate the synthetic route towards an organic metamaterial. The building block methodology is applied an refined in the 26 step synthesis of a giant, fully conjugated carbazole based macrocyle

Finally, in Chapter 5 we look to the synthesis and STM investigations of a family of star-shaped molecular rods demonstrating an unprecedented level of control of single molecular organisation in an extended array.

Table of Contents

Summary: i
Table of Contents iii
Abbreviations vii
Carbazole Nomenclature xi

1 Introduction 1

1.1 Room at the bottom 2

1.2 Phenyl-Acetylene bond assembly 3

1.2.1 Introduction to phenyl-acetylenes 3
1.2.2 Synthetic strategy: where to make the disconnection 6
1.2.3 Mechanism of the Sonogashira reaction 9
1.2.4 Reactivity and chemoselectivity of phenyls 12
1.2.5 Masking: using FG interconversions to control reactivity 16
1.2.6 Acetylene protecting groups (PGs) 19
1.2.7 Breaking the symmetry – I: statistical coupling 23
1.2.8 Breaking the Symmetry – II: statistical deprotection 24
1.2.9 In Situ generation of free acetylene 26
1.2.10 Concepts applied to representative syntheses 27
1.2.11 Summary and outlook 32

1.3 Nanopatterning by molecular self-assembly on surfaces 33

1.3.1 Supramolecular chemistry in solution 34
1.3.2 Supramolecular chemistry on surfaces 35
1.3.3 Templation and molecular dynamics on surfaces 36
1.3.4 Porous honeycomb networks 37
1.3.5 Melamine-PTCDI honeycomb networks 40
1.3.6 Outlook for molecules on surfaces 42

2 Building Blocks for Synthesis 45

2.1 Building Block Design 46

2.1.1 Acetylene as a glue 47
2.1.2 Phenyl-acetylenes: the modular approach 48
2.1.3 Statistical coupling of acetylenes 49
2.1.4 Generating a library of aromatic building blocks 51

2.2 Carbazole as a building block 53

2.2.1 Carbazole functionalization 53

2.2.2 Synthesis of 2,7-substituted carbazoles 55
2.2.3 Sonogashira coupling to carbazole 58
2.2.4 Halogen exchange on carbazole building blocks 60
2.3 Applying Building Blocks in Synthesis 61
2.3.1 Monomers for Polymer dispersion of SWCNT 61
2.3.2 Push-pull carbazoles in D–π–A systems 63
2.4 Conclusion and outlook: 65

3 Molecular Wires: OPE Rods & Stars 67
3.1 Single molecule wires 68
3.2 Synthetic approaches to an organic single-molecular wire 68
3.2.1 OPE and OPV rods 69
3.2.2 Bridging larger gaps 70
3.3 A single-molecule three-terminal device 73
3.3.1 Synthetic target of a three arm star 74
3.3.2 Divergent approach to synthesize the star 75
3.3.3 Convergent approach to synthesize the star 77
3.3.4 Three-arm star characterisation 78
3.3.5 Removal of thiol protecting groups 81
3.4 Conclusion and Outlook: 83

4 Nano-Scale Carbazole Architectures 85
4.1 Investigations of a nanoscale carbazole based architecture 86
4.1.1 Design of an organic metamaterial 86
4.1.2 Molecular Requirements 87
4.1.3 Target Structure: a novel carbazole macrocycle 88
4.1.4 Retrosynthesis of a symmetric carbazole ring 90
4.2 Synthetic approaches to assemble the macrocycle 92
4.2.1 Synthesis of the 1/8th cycle rim from bromo-carbazoles 92
4.2.2 Synthesis of the linker to make quarter cycle rim 95
4.2.3 Synthesis of the 1/8th cycle rim accelerated with iodo-carbazoles 97
4.2.4 Assembly of the quarter cycle and characterisation 98
4.2.5 Synthetic approaches to suitable template scaffolds 102
4.2.6 Connecting the template to the quarter cycle rim 106
4.2.7 Attempts at cyclisation 109
4.3 Conclusions and outlook 111

5 Supramolecular Architectures....113
5.1 Initial studies – probing the size of the pore....115
5.1.1 Phenyl-acetylene star synthesis....115
5.1.2 Phenyl-acetylene star characterisation....116
5.1.3 Biphenyl and a stilbene star synthesis....118
5.1.4 Biphenyl and stilbene star characterisation....119
5.2 Molecular dynamics in the pore....121
5.2.1 Tri-hydroxy biphenyl star synthesis....121
5.2.2 Surface investigations on the tri-hydroxy biphenyl star....122
5.3 Controlled motion of stars inside the pore....123
5.3.1 Templating of the network using C_{60}....123
5.3.2 Hexa- and octa- hydroxy star synthesis....124
5.3.3 Surface investigations of the three and four arm biphenyl stars....127
5.4 Conclusion and Outlook....130
6 Conclusion....133
7 Experimental Section....135
7.1 Compounds from Chapter 2....136
7.2 Compounds from Chapter 3....157
7.3 Compounds from Chapter 4....166
7.4 Compounds from Chapter 5....186
7.5 X-ray Crystal Structures....193
8 References:....197
9 Appendices:....207
9.1 Acknowledgements
9.2 Carbazole poster
9.3 Stars poster
9.4 Curriculum vitae

Abbreviations

A	acceptor
Å	angstrom
Ac	acetate group (–CO2Me)
aq	aqueous
Ar	aryl
Boc	*tert*-butyloxycarbonyl
br.s	broad singlet
brine	saturated aqueous NaCl solution
CNT	carbon nano tube
COSY	correlation spectroscopy
Cp	primary carbon
CPDIPS-A	[(3-cyanopropyl)diisopropylsilyl]-acetylene
CPDMS-A	[(3-cyanopropyl)dimethylsilyl]-acetylene
Cq	quartenery carbon
Cs	secondary carbon
Ct	tertiary carbon
d	doublet
D	donor
dba	dibenzyldenacetone
DCB	dichlorobenzene
DCM	dichloromethane
δH	proton chemical shift
δC	carbon chemical shift
DIPA	diisopropylamine
DMAP	4-dimethylaminopyridine
DMF	*N,N*-dimethylformaide
DMSO	dimethylsulfoxide
dppf	1,1'-bis(diphenylphosphino)ferrocene
ε	extinction coefficient
EA	elemental analysis
EDG	electron donating group

EI	electron impact
eq.	equivalent
ESI	electrospray ionisation
Et	ethyl group (–CH2Me)
Et_2O	diethyl ether
EtOAc	ethyl acetate
EtOH	ethanol
EWG	electron withdrawing group
GPC	gel permeation chromatography
HMBC	heteronuclear multiple bond coherence
HMQC	heteronuclear multiple quantum choherence
HOMO	highest occupied molecular orbital
HPLC	high performance liquid chromatography
hr	hours
hv	light
^{i}Pr	*iso*-propyl group (–CHMe)
J	coupling constant
λ	wavelength
LUMO	lowest unoccupied molecular orbital
m	meta
m	multiplet
M	molar
m/z	mass per charge
MALDI-TOF	matrix-assisted laser desorption ionisation
MCBJ	mechanically controled break junction
Me	methyl group (–CH3)
MeCN	aetonitrile
MeOH	methanol
min	minutes
mp	melting point
MS	mass spectrometry
MW	microwave
n-BuLi	*n*-butyl lithium
NBS	*N*-bromosuccinimide

NMR	nuclear magnetic resonance
NOESY	nuclear Overhauser effect spectroscopy
o-	ortho
OPE	oligo(phenylene ethynylene)
OPV	oligo(phenylene vinylene)
OTf	triflate
p-	para
PG	protecting group
Ph-	phenyl group (–C6H5)
PPh_3	triphenylphosphine
PTCDI	perylene tetracarboxylic diimide
q	quartet
qnt.	quantitative yield
R	alkyl or organic group
R_f	retention factor
RT	room temperature
s	singlet
SAM	self assembled monolayer
STM	scanning tunneling microscopy
SWCNT	single walled carbon nanotube
t	triplet
TBAF	tetra-N-butylammonium fluoride
TBME	*tert*-butyl methyl ether
^{t}Bu	*tert*-butyl group (–CMe3)
TFA	trifluoroacetic acid
THF	tetrahydrofuran
THS-A	trihexylsilyl-acetylene
TIPS-A	triisopropylsilyl-acetylene
TLC	thin layer chromatography
TMS-A	trimethylsilyl-acetylene
TOCSY	totally correlated spectroscopy
UV-vis	ultraviolet- visible
w/w	weight for weight

Carbazole Nomenclature

Carbazole is a naturally occurring, organic aromatic compound belonging to the indole family of heterocyclic compounds, and was first isolated from coal tar by C. Graebe and C. Glaser in 1872. It is still obtained industrially from coal tar in the thousands of tons per annum, or recovered as a side product from the industrial formation of anthracene, for use in the synthesis of dyes. The IUPAC naming of substituted carbazoles follows a strict numbering, in this thesis we focus on substitution in either the 2,7- positions or the 3,6- positions as depicted below:

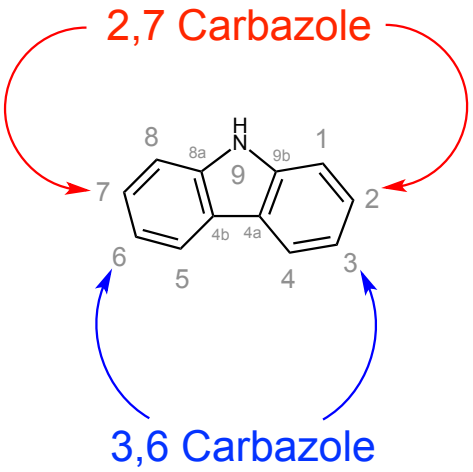

9*H*-Carbazole

In the following, carbazoles are systematically named using an abbreviated form for the sake of clarity. Where the full name is given, the substituents attached to the ring are named first, followed by the -9*H*- position.

All compounds are numbered sequentially by chapter in order of appearance, in the form 1.23 which is the 23rd compound introduced in chapter 1. All reaction arrows were carried out at room temperature unless stated otherwise.

1 Introduction

Chapter 1 presents the synthetic strategies for the formation of phenyl-acetylene bonds by Sonogashira cross- couplings. Chemoselectivity, masking, protecting group strategies and statistical reactions are presented as synthetic techniques for the formation of building blocks, geared towards the design and assembly of larger molecular architectures. We then turn to the use of supramolecular chemistry to drive the formation of self-assembled networks allowing for a bottom-up approach to achieve nanopatterned surfaces, and area where phenyl-acetylene based structures afford a high degree of surface control.

Sections of this chapter are adapted from two published review articles, which appeared in The European Journal of Organic Chemistry, and Chimia respectively. I would like to highlight the important contribution of my co-authors; Nicolas Jenny, David Muñoz, Manfred Buck and Marcel Mayor whose voice you may hear and see in portions of the text.

1.1 Room at the bottom

"There's plenty of room at the bottom" – Richard Feynman's famous lecture delivered on the 29th December, 1959 challenged the worlds scientists to push nature to its limits.[1] This challenge spawned a new paradigm in the physical sciences – one of nano proportions but boundless scale and scope. Nanotechnology now pervades the physical sciences both as a field of study, but also increasingly in its application, under a new paradigm. Using a reductionist approach it's incredibly tempting to assume that we could take a function and stripping it down to its core components in order to understand how it works, by characterising its constituent parts, however this assumption while logical in its deduction – misses the reality of nature. An inductive, emergent approach is required.

This thesis is built on the premise that if we can induce structure-property relationships from the bottom-up, we can also extend the idea to structure-function relationships. The utility of chemistry comes from its application, not just from understanding and characterising a system. This ideology requires new approaches to synthesis target molecular architectures of interest.

When looking to the function of a system and not just its structure, the interaction of the individual components when they come together is incredibly important as the whole quickly becomes more than some of its parts. This is more true than ever down at the molecular length scale. We therefore cannot be successful looking from the top-down, rather we must approach from the bottom-up, adding different combinations of structures that can give rise to emergent properties. In this way we aim to define structure-to-function relationships. It is in understanding this emergence where reductionism fail us, and why a bottom-up approach, as outlined in this treatise, is required.

At the outset, it is assumed that the reader is familiar with the normal analytical tools of molecular analysis, in particular the scanning tunnelling microscope (STM), first presented by Gerd Binnig and Heinrich Rohrer in 1982,[2] for which they received the 1986 Nobel Prize in physics has become a main stay in the analysis at the molecular length scale. We will here more about STM measurements and the exciting insight it provides in chapter 5.

The aim of this thesis is to present synthetic methodologies that allow for defining of structure-to-property and structure-to-function relationships, using phenyl-acetylene building blocks as the primary tool to drive this emergent behaviour.

1.2 Phenyl-Acetylene bond assembly

As A Powerful Tool for the Construction of Nanoscale Architectures

This introductory section summarises fundamental strategies and basic considerations for the design and synthesis of nanoscale architectures assembled by the formation of acetylene-phenyl bonds. Since its first appearance in 1975 the *Sonogashira-Hagihara* reaction has allowed the formation of bonds between sp1 and sp2 carbon centres under mild conditions. This palladium catalysed cross-coupling quickly found application in almost every area of synthetic organic chemistry. The biggest impact of this new method was probably observed in nanoscale architectures giving rise to a new field of "Acetylene Scaffolding". Here we present a summary of the underlying concepts and important strategies for the formation of acetylene-phenyl bonds geared towards the assembly of nanoscale architectures illustrated with a few beautiful examples from the literature. It is not meant to be a comprehensive overview of the Sonogashira cross-coupling reaction nor of the area of acetylene scaffolding but should serve as guide to those new to the field.

Starting with a short discussion of the reaction mechanism, the proper choice of precursors is discussed. Chemoselectivity introduced by various leaving groups or by masking their reactivity follows. The most common acetylene protection groups are summarized, compared with respect to their functional group tolerances and strategic concepts including orthogonality, sequential deprotection and in situ deprotection. Strategies for quick access to highly functionalised building blocks such as chemo selective halogenations and symmetry breaking are considered. Finally, the potential of the strategies discussed are documented with a few examples from the current literature.

1.2.1 Introduction to phenyl-acetylenes

Structure-property relationships are at the heart of a scientists' interaction with nature. From peptides to molecules, the spatial arrangement of functional groups in a substance plays a dominant role on its properties and function.[3] Defining the structural architecture of a molecule in order to systematically investigate the effect this has on its physical properties requires the synthesis of complex organic molecules from much smaller, simpler building blocks. Palladium catalysed coupling chemistry has provided a fast and efficient method for the formation of new C–C bonds[4][5] and has revolutionized the synthesis of macromolecular

structures. The importance of cross-couplings to synthetic organic chemistry has finally been recognised at the highest levels, the topic being awarded the 2010 Nobel Prize in Chemistry.[5][6] To our surprise, sp^1–sp^2 cross-couplings were not mentioned by the Committee in their announcement, despite the importance of this coupling reaction.

The acetylene functional group in particular provides its own advantages over other C–C bonds providing both enhanced rigidity and conjugation.[7] *Sonogashira* couplings are a facile way to introduce acetylenes,[8][9] classically involving the coupling of an acetylene to an aryl halogen centre[10] allowing for conjugated π-systems to be formed from suitable building blocks. This micro-review describes synthetic strategies for the formation of suitable building blocks geared towards the assembly of larger molecular architectures. The structural motif of phenyl-acetylene bonds finds use in applications as diverse as; molecular electronics,[11] nano-sensors,[12] liquid crystals,[13] natural products,[14][15] optoelectronics,[16] organic-inorganic hybrid structures[17][18], surface functionalisation[19] and cell imaging[20] amongst many others. In many instances acetylene couplings are preferential to *Suzuki*[21] or *Stille*[22] direct sp^2–sp^2 couplings as they can be essential to achieve coplanarity, increasing the π-conjugation length and decreasing the HOMO–LUMO gap. This has been shown for various chromophores including NDIs,[23] oligophenylethynylenes (OPEs),[24][25] BODIPYs[26] and substituted porphyrins[27] which show a marked bathochromic shift in absorption.

Phenyl-acetylene scaffolds became very popular through the 90's as a facile method to assemble large organic molecular architectures focusing on the synthetic challenge, function being a secondary consideration. [7][28] Since then the function of molecules has displaced structure as an objective, as has been demonstrated with bottom-up approaches towards functional graphene sheets.[29] Acetylenes in shape-persistent macrocycles[30] have been shown to display liquid crystalline behaviour[13] and self organisation on a surface.[31] These properties require precise control over functional group orientation within the building blocks prior to macrocyclisation. With the correct spatial orientation π-π aggregation can also be induced.[32][33]

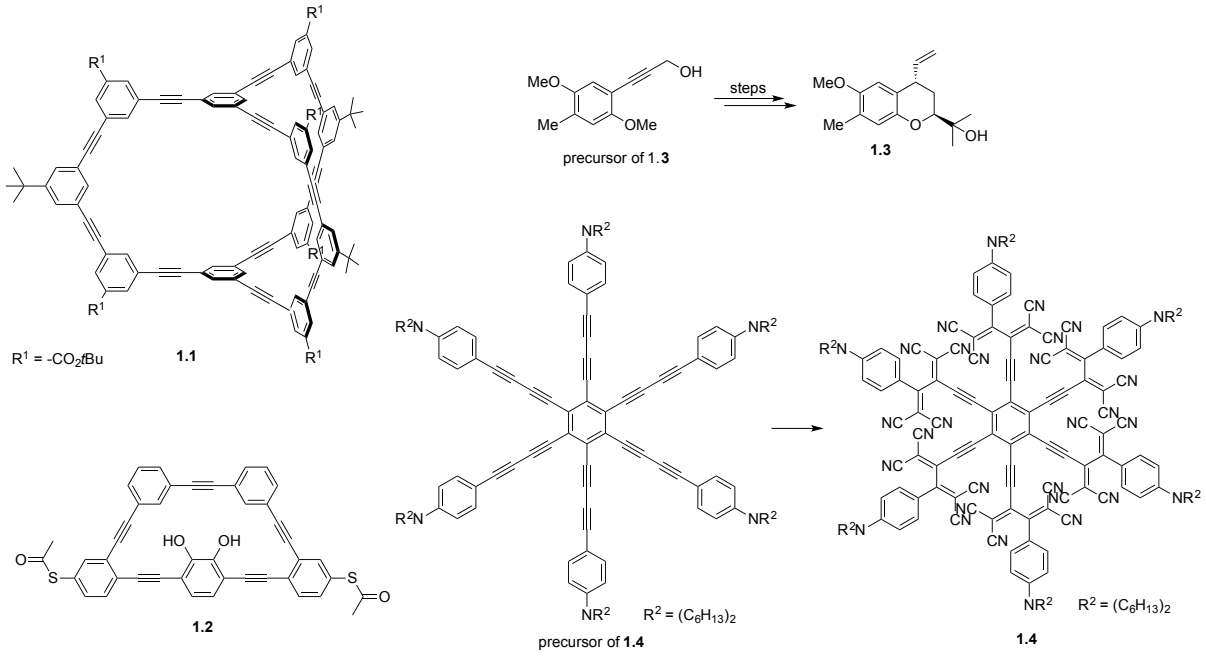

Figure 1.1: Examples of phenyl-acetylene structures.

In Figure 1.1 four typical examples from different areas of synthetic chemistry illustrate the breadth of systems in which phenyl-acetylene bonds are found. Three dimensional (3D) structures in particular represent another level of complexity in structure-property relationships. Protein folding and DNA helices are naturally occurring examples of the bearing structure can have on function at the molecular level. Chemical approaches to mimic the controlled assembly of such massive biological systems are very difficult to replicate. As synthetic organic chemists we can try to imitate this complexity, using a bottom up approach by combining suitable building blocks. Pioneering work by Jeffery Moore and co-workers[34] on 3D cages required precise control over the substitution patterns of their building blocks in order to achieve 3D architectures such as compound **1.1**. The context of this micro-review is to cover the relevant synthetic tool kit required to imitate such syntheses.

In the field of molecular electronics structure-property relationships of single molecules can be investigated using phenyl-acetylenes. Structure **1.2** was designed around the macrocyclic turnstile from Jeffery Moore[35] in order to study switching behaviour by molecular rotation.[36] The synthesis of such a complex structure with the substitution pattern found in **1.2** is a challenge, requiring a well planned strategy involving the correct choice of disconnections and suitable protecting groups in order to overcome issues of reactivity and stability.[37] The successful synthesis of **1.2** made extensive use of the strategies discussed in this micro-review.

In natural product synthesis phenyl-acetylenes are found both in synthetic intermediates and in target compounds, often introduced by *Sonogashira* reactions.[14] A phenyl-acetylene bond was introduced to a precursor en route to (–)-Heliannuol E (**1.3**)[38] a natural product found in sunflowers.

In materials chemistry dendrimer-like structures such as **1.4** have shown very large intramolecular charge transfer interactions, and therefore a very high uptake of electrons. This allows for the possibility of making a molecular battery. François Diederich and co-workers[39] required the formation of an electron rich acetylene moiety in order to facilitate a [2+2] cycloaddition reaction to form molecule **1.4**. This demonstrates the tunability of acetylene reactivity possible by changing the local electronic environment. The enhanced reactivity of acetylenes has recently been popularised with the advent of "click'' chemistry.[40] The scope of this micro-review is limited to the most important tools and strategies required for the assembly of acetylene-phenyl building blocks, with a view towards the formation of larger nanoscale architectures, as acetylene scaffolds and the formation of substituted 1,4-butadienes is well reviewed elsewhere.[7][41]

1.2.2 Synthetic strategy: where to make the disconnection

The first step in any synthesis is to settle upon a target structure, this will depend upon the required mechanical, optical, or binding properties of the compound in question. Once a target has been decided upon, retrosynthetic analysis, as reviewed by Elias Corey[42] represents a powerful tool in the design of a successful synthesis. When making a retrosynthetic analysis of sp^1 and sp^2 hybridised carbon systems, with the intention of performing palladium catalysed cross-coupling reactions, there are a few important generalisations to bear in mind (Figure 1.2). The principle consideration is which phenyl group contains the halogen (acceptor) component and which contains the acetylene (donor) component.

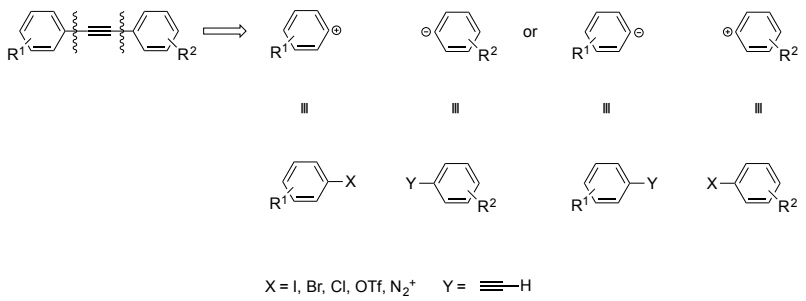

Figure 1.2: Retrosynthesis of the phenyl-acetylene bond.

This seemingly arbitrary decision about where to place a disconnection and which side should be a1 (acceptor) and which d1 (donor), can make the difference between success and failure in the elucidation of the target compound. Most syntheses can be classified as either following the principles of convergence or divergence,[43] where the building blocks are assembled together before attachment to a central unit (convergent) or building blocks are assembled directly onto a core substituent (divergent). Narita et al.[44] have employed the use of just such a change in disconnection in their convergent synthesis of star-shaped oligothiophenes (Scheme 1.1). Under the same coupling conditions of $Pd(PPh_3)_4$, CuI and NEt_3 but by changing which building block was the acceptor and which was the donor, they were able to obtain their target stars. Method A involves the coupling of iodo-polythiophene **1.5** (acting as a1) to acetylene functionalised benzene rings **1.7, 1.10** and **1.13** (acting as d1). Method B exchanges the position of the acetylene onto the acetylene-functionalised polythiophene **1.6** (acting as d1) and the halogen benzenes **1.8**, **1.11** and **1.14** (acting as a1). For the tri-functionalised star **1.9** method B afforded a higher yield. For **1.12** both approaches are comparable and for **1.15** only method A formed the product. This could be due to the switch to hexabromobenzene (**1.14**) in place of hexaiodobenzene for method B, possibly required due to the very low solubility of hexaiodobenzene. This example illustrates the bearing which the choice of disconnection can have on the outcome of a synthetic strategy.

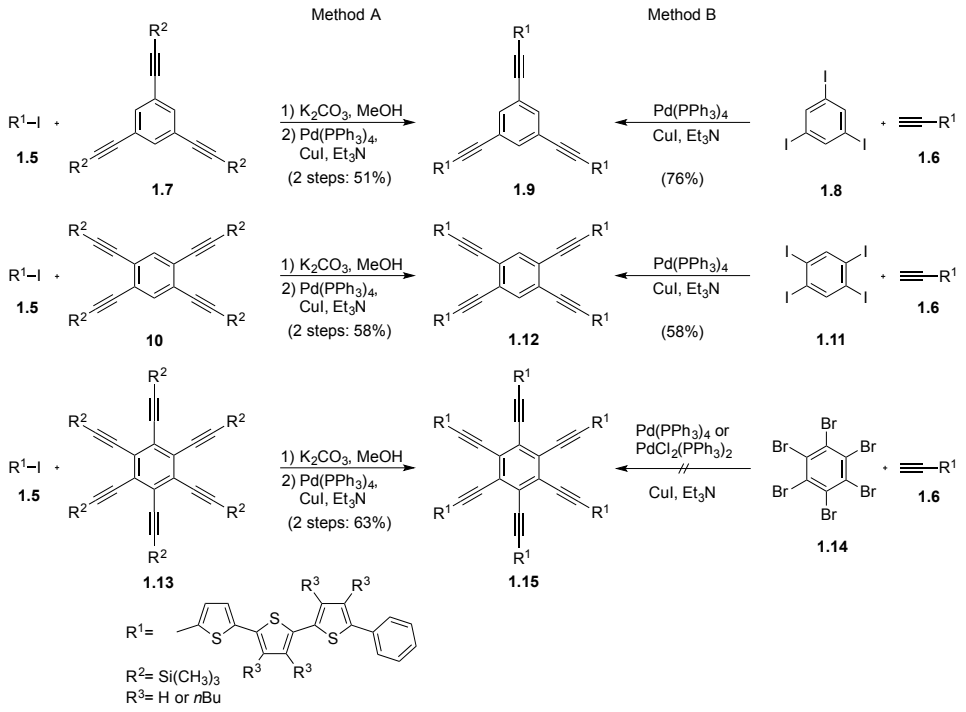

Scheme 1.1: The effect of changing the acetylene disconnection.

After proposing which disconnections should be made, and which mode of assembly, either convergent or divergent, shall be employed one can then turn to the formation of these proposed building blocks. In section 1.2.4 on chemoselectivity we will discuss the tuning of the acceptor (halogen, triflate, N_2^+) and how the insertion of more than one of these components allows for selective couplings providing a great deal of control over building block assembly. When it becomes difficult to obtain this precise control one can employ the technique of masking which we discuss in section 1.2.5. Masking deals with the transformation of one functional group into another, presenting the best in reaction control. It differs from a protecting group (PG) in that direct cleavage of the masking group is not possible. A functional group interconversion (FGI) is first required before the site would become active to the reaction conditions. This allows for greater functional group tolerances to be achieved with the same building block. Differing electronic properties and subsequent reactivity can also be achieved through masking, for example in the conversion from a nitro to an amine and finally into an iodine.

Addition of an acetylene moiety to any building block usually requires a PG unless one uses molecular acetylene. The range of available PGs is discussed in section 1.2.6 where the relative advantages of processability, solubility, ease of deprotection and the matching of different PGs to achieve orthogonality are explained. Then we turn to the special case of statistical coupling and deprotection reactions which allow for the introduction of asymmetry

to an otherwise symmetric (for example containing the ideal symmetry elements C_2 or σ_v) building block. By this, we mean performing a 'statistical reaction' on only one reactive site where two identical ones are present, thereby introducing 'asymmetry' to the molecule. This asymmetry can be introduced either by manipulation of functional groups prior to application of cross-coupling reactions, an idea expanded upon in section 1.2.2, or by performing a statistical cross-coupling as discussed in section 1.2.7 below. A third option is to perform a statistical deprotection of protected acetylenes bearing the same protecting groups. Oligomer and macrocyclic syntheses often contain examples of these strategies[45][46] as a library of functionalized compounds are desired and it can be easier to use the same building blocks which can be statistically functionalised to introduce diversification in the number of target structures.

When side-products, including diacetylenes or polymerisations in a macrocycle forming reaction are an issue, in situ deprotection of the acetylene moiety in the presence of the *Sonogashira* coupling agents can lead to improved yields or even elicit an otherwise unattainable compound. These in situ reaction strategies are discussed in section 1.2.9 followed by examples in section 1.2.10 bringing all the concepts we have mentioned together, but first we turn to the role of palladium and copper in *Sonogashira* cross-couplings.

1.2.3 Mechanism of the Sonogashira reaction

Below we briefly summarise the currently accepted mechanism of the *Sonogashira* reaction, with a focus on gaining a better understanding of the problems which can occur and how to avoid the formation of side-products, such as di-acetylene homocoupled product or conjugated enynes.[47] The generally accepted catalytic cycle[8][10] for the copper co-catalyzed cross-coupling reaction is believed to take place through two independent catalytic cycles (Scheme 1.2). The palladium catalysed reaction (cycle A) starts with a fast oxidative addition of the a1 acceptor (Ar-X; where X = I, Br, Cl, OTf, N_2^+) to the active catalyst generated from the initial palladium complex.

It is known that electron donors such as phosphanes, amines and ethers, used as ligands and solvents can reduce palladium(II) species, to the palladium(0) complex.[48] The electronic nature of the substrate which adds to the palladium(0) is very important. Electron withdrawing groups on the substrate reduce the electronic density of the Ar-X bond and therefore facilitate the oxidative addition.[49][50]

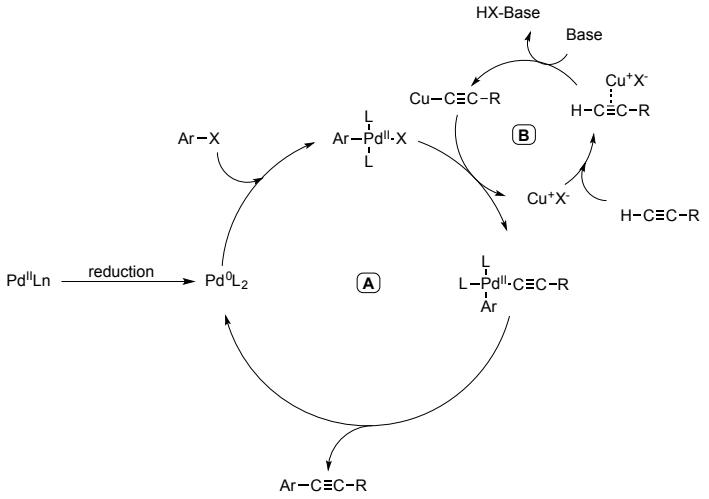

Scheme 1.2: Catalytic cycle of the palladium/copper co-catalysed *Sonogashira* cross-coupling reaction.

The second step is a transmetallation with a copper acetylide generated in cycle B (Scheme 1.2). This is usually the rate determining step. After a *cis/trans* isomerization and a reductive elimination the cross-coupled product is formed and the catalyst is regenerated. The copper cycle (cycle B) is still poorly understood. It is believed that the base abstracts the acetylenic proton of the terminal alkyne, thus forming a copper acetylide in the presence of the copper(I) salt, but the amines used are usually not basic enough to deprotonate the alkyne to make the anionic nucleophile that should form the copper acetylide. Therefore, a π-alkyne-Cu complex could be formed. The coordination of the copper would make the proton much more acidic and therefore easier to abstract by a weaker base. These copper acetylides could also be involved in the formation of the active Pd^0L_2 complex (Scheme 1.3).[8]

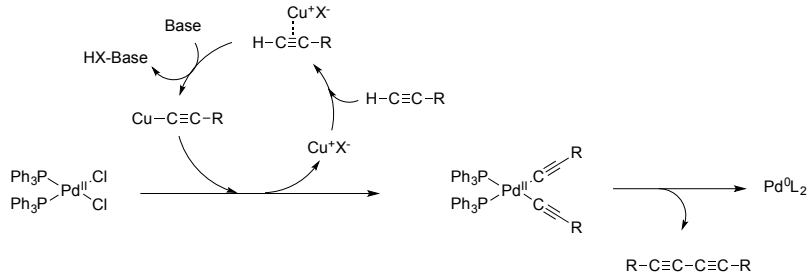

Scheme 1.3: Possible formation step of the active catalytic species.

Some questions still arise about the nature of the real active catalyst. Some results indicate that an anionic palladium complex would be the active species if anions or halides are present.[51] The mechanism of the copper free *Sonogashira* cross-coupling reaction is also not very well understood (Scheme 1.4). It should be noted that the absence of trace copper in

otherwise ‘pure’ metals such as palladium is an area of contention. Traces of copper below current detection limits may still be present which could influence the reaction mechanism. In any case the first step must be the same oxidative addition of an Ar-X to a Pd^0L_2 complex as in the copper co-catalyzed cycle discussed previously (Scheme 1.3). It is commonly accepted that the alkyne coordinates via a ligand exchange process to the palladium(II) complex. This complexation increases the acidic nature of the proton which is then abstracted from the base to form the new complex $ArPd(C{\equiv}CR)L_2$, which affords the coupling product by reductive elimination.

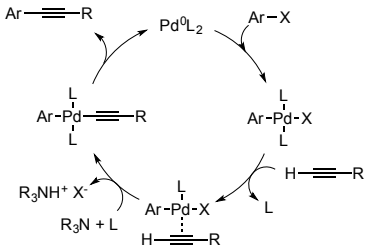

Scheme 1.4: Proposed mechanism of a copper-free *Sonogashira* cross-coupling reaction.

Terminal acetylenes can also play an important role in the palladium cycle. It is possible that the terminal alkynes coordinate the palladium(0) complex prior to the oxidative addition step, thereby producing a decelerating effect by formation of unreactive or slow-reacting (η^2-$RC{\equiv}CH)Pd^0L_2$ complexes.[52] The stationary regime of a catalytic cycle is more easily reached if the reaction rates of all the elemental steps are as close as possible to each other. This can be achieved by accelerating the rate-determining step or decelerating the fast reactions by stabilizing high-energy species.[53] If the oxidative addition step is faster than the transmetallation step, the decelerating effect of the alkynes provides a better efficiency for the catalytic cycle, bringing the rates of the two steps closer together. This can be enhanced by increasing the reaction temperature. However, if the oxidative addition step is slower than the transmetallation step, as is the case for arylbromides or arylchlorides, it becomes even slower in the presence of the nucleophilic alkynes and the catalytic reaction would become less efficient.

To improve the yield of a *Sonogashira* cross-coupling reaction one should screen a few standard palladium catalysts such as; $Pd(PPh_3)_4$, $PdCl_2(PPh_3)_2$, $Pd(OAc)_2$ and $Pd(dba)_2$ combined with different bases at different temperatures. If the yields are still not satisfactory the design of new ligands for the palladium complex should be considered or a change in the retro synthetic strategy is required. In this review we want to focus on the strategic approach

and not on the optimization of the palladium catalyst as this has already been extensively covered in other reviews.[48][54][55]

1.2.4 Reactivity and chemoselectivity of phenyls

While symmetric systems are more easily assembled than asymmetric ones there are many applications where an inherent asymmetry is required, such as push-pull systems and molecules for use in the field of molecular electronics.[56][11][57] Building blocks for *Sonogashira* cross-coupling reactions require the presence of acceptor groups to undergo oxidative addition. The order of reactivity of halobenzenes towards oxidative addition to $Pd(PPh_3)_4$ was found by Fitton et al. [49][50] to be Ar-I > Ar-Br > Ar-Cl with large enough a difference in reaction rates to allow for high chemoselectivity. Over the past decades, many research groups have developed catalytic systems which promote the oxidative addition of arylbromides[58][59] and arylchlorides.[60][61] Besides arylhalides, aryltriflates[62] and aryldiazo-compounds[63][64] have drawn a lot of attention over the past few years. The use of these functional groups as acceptors will be discussed later.

The order of reactivity of the arylhalides can be used to sequentially introduce acetylenes bearing orthogonal protecting groups onto a multi-functionalized building block. This method stands in contrast to a statistical approach, which works well as long as the central parts of the desired building blocks are symmetric[65][66] and as long as chemical waste is not an issue. However, if the building block is asymmetric a statistical approach leads to more side products and the purification can become difficult and time consuming. On the other hand, designing an asymmetric iodo-bromo-benzene compound which has an extra functionality in a preferred position can also be difficult. Sigurd Höger[67] demonstrated a nice approach to control the chemoselectivity to form such an asymmetric iodo-bromo-benzene building block (Scheme 1.5).

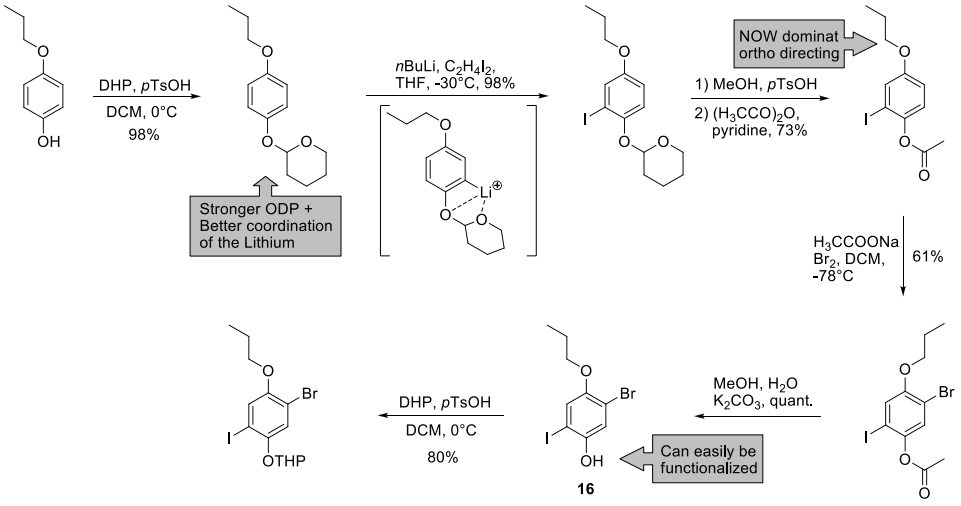

Scheme 1.5: Chemoselective introduction of halides using substituent control.

He reported two strategies for the synthesis of monoalkylated hydroquinones **1.16** and **1.17** containing a bromine and an iodine in the 2- and 5-positions (Scheme 1.5 and Scheme 1.6). The difference in reactivity of the halogens in **1.16** and **1.17** towards palladium(0) species allows for selective transformations to orthogonally protected acetylenes. This allows these positions, as well as the phenolic groups present, to be further functionalized.[68] The different *ortho*-directing-powers[69] (ODP) of the substituents on the benzene ring were used to selectively introduce an electrophile such as iodine or bromine.

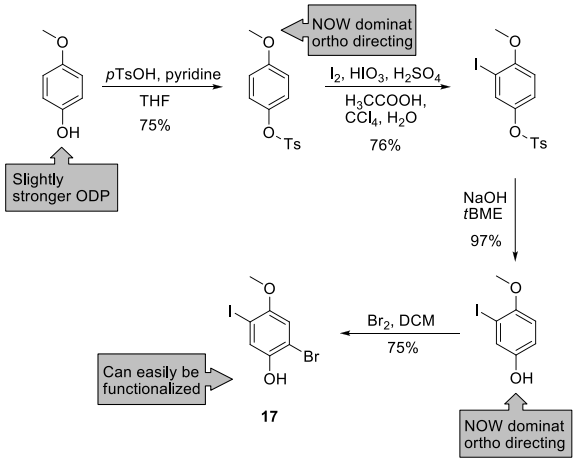

Scheme 1.6: Chemoselective introduction of halides using substituent control.

The fastest route to an asymmetric molecule can often be to start with a symmetric compound, and introduce the asymmetry by controlling the equivalents of reagent added. Manipulation of functional groups, such as halogen exchange or –OH protection[70] are good

examples. Statistical couplings and deprotections are further expanded upon in sections 1.2.7 and 1.2.8.

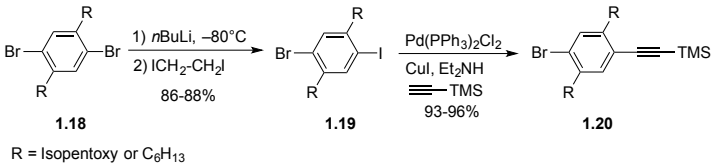

Scheme 1.7: Halide exchange to allow selective introduction of TMS-acetylene.

In order to avoid a statistical coupling to make **1.20**, Adelheid Godt and co-workers[71] found conditions for a selective halogen exchange in their synthesis of monodispersed OPEs (scheme 7). Using *n*BuLi at –80°C was necessary in order for a clean transformation from **1.18** to **1.19** after quenching the lithium salt with I-CH_2-CH_2-I. Chemoselective palladium catalysed coupling of TMS-acetylene with the iodine of **1.19** afforded the asymmetric building block **1.20**. This was then used in a successful coupling sequence, eventually forming an octomeric OPE.

The use of alternative acceptor groups for performing the oxidative addition in palladium catalysed reactions are becoming more prevalent. A triflate (–OTf) leaving group is not as reactive as iodine but has a similar reactivity to that of bromine. The biggest advantage of a triflate-strategy is the possibility to have a hydroxy group present on a building block which can be transformed into a triflate at any time. The hydroxy group can be protected if other reaction sequences do not tolerate the presence of a free alcohol. Many protection/deprotection protocols for hydroxy groups are known[72] and a suitable strategy can be chosen for a longer reaction sequence. A selective alkynylation of bromo-aryl-triflate **1.21** (Scheme 1.8) was reported by Tamio Hayashi and co-workers[73] They showed that aromatic compounds bearing both bromine and triflate can undergo a selective replacement of either bromine or triflate by an acetylene group. It was found that the triflate group was selectively replaced by the acetylene group to give **1.24** in 96% yield when $PdCl_2$(alaphos) and phenylethynylmagnesium bromide (**1.22**) were used. On the other hand, under standard *Sonogashira* conditions, preferential substitution of bromine to give **1.25** was observed, although the selectivity was lower, with a purified yield of 73%.

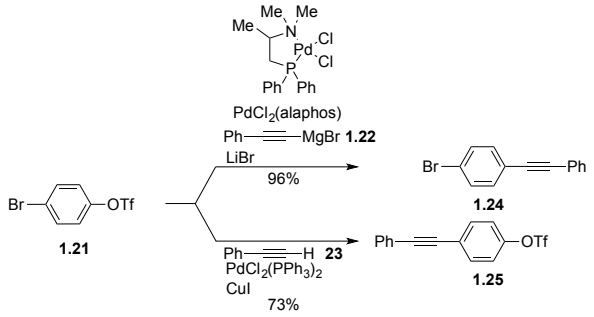

Scheme 1.8: Control of acceptor group substitution by changing the donor and active catalyst species.

To compare the order of reactivity towards the $PdCl_2$(alaphos) catalyst an iodoaryl triflate derivative **1.26** was used instead of the bromoaryl triflate **1.21** to make **1.27** (Scheme 1.9). It was shown that the order of reactivity of the leaving groups on an aromatic ring is iodine > triflate > bromine in the *Grignard* cross-coupling reaction catalyzed by $PdCl_2$(alaphos).

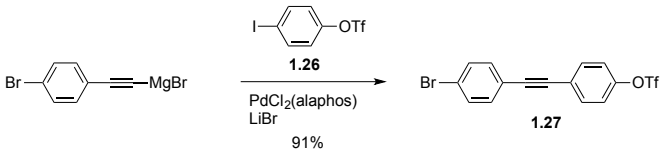

Scheme 1.9: *Grignard* cross-coupling reaction.

Aryldiazonium salts, such as **1.28,** represent an attractive alternative to aryl-halides or triflates because of their higher reactivity,[64] their formation under milder conditions, their availability from inexpensive anilines, and because additional base is not required in several applications (Scheme 1.10). The reaction of **1.23** and **1.28** occurs under mild conditions in the presence of nBu$_4$NI and proceeds through a domino iododediazoniation/*Sonogashira* cross-coupling sequence to give **1.29**. Good to excellent yields are usually obtained. A variety of alkyl, aryl, and heteroaryl substituents on the alkyne substrate can be used and many useful functionalities including bromo-, chloro-, keto-, ester-, ether-, cyano-, and nitro-substituents on the aryldiazonium salt are tolerated. The entire aryldiazonium salt synthesis/iododediazoniation/cross-coupling sequence can also be performed as a one-pot domino process, omitting the isolation of the arenediazonium salt.[64]

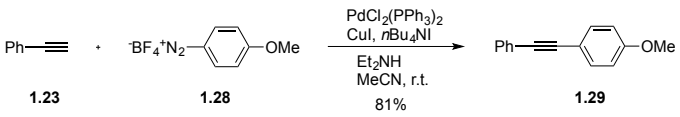

Scheme 1.10: Diazonium salt as acceptor in a Sonogashira cross-coupling reaction.

While the use of different acceptor groups to enable selective couplings to a building block may be more aesthetically pleasing, in some instances a statistical approach incorporating orthogonal protecting groups can afford target structures in fewer transformations. It is often possible to obtain a higher yield of product from a single step statistical reaction than the overall yield from a series of non-statistical reactions. These possibilities of breaking the symmetry of a building block are discussed in section 1.2.7 and we hope that by using a combination of these approaches a best fit to any synthetic route can be made.

1.2.5 Masking: using FG interconversions to control reactivity

With increasing demand for enhanced functionalities of macromolecules, the design and the retrosynthetic strategies have become more and more challenging. Multiple aromatic substitutions of arylhalides do not always work with a statistical approach. Reasons for this can be ecological (additional waste), economical (increased costs) or simply isolation problems in the lab. Therefore a more selective and efficient strategy must be chosen. As described above, the different reactivity of aryl halides towards oxidative addition to the palladium(0) species could be a useful tool. This strategy is limited to building blocks, which can survive harsher coupling conditions such as high temperatures or long reaction times owing to the reduced reactivity of arylbromides and arylchlorides.[49][50] If the nature of the building block does not allow for these harsher conditions, one is limited to the more reactive aryliodides. This again raises the issue of the selectivity when more than one iodine coupling site is required.

To avoid a statistical coupling approach, masking of the halide should be considered. The ideal masking group should be readily available, stable to a variety of chemical conversions and conveniently transformed under mild conditions in a high yield to the desired aryl halide. A useful masking group for an iodine is an amine, which has additional advantages and disadvantages for further functionalization on the benzene core by means of activation or deactivation[37]. The reactivity of the aromatic system can be tuned by the introduction of a nitro group as a precursor to the amine, switching from an electron rich to an electron poor system. The transformation from an amine to an iodine is well known and was first reported by *Traugott Sandmeyer* in 1884.[74] However a free amine can also act as a d1 coupling partner, known as a *Hartwig-Buchwald* reaction,[75][76] leading to side products. As a consequence the amine may need to be protected in order to increase its stability towards the reaction conditions and yet it should still be labile enough to be deprotected and subsequently

transformed into an iodine. Jorge Barrio has reported on the conversion of 1-aryl-3,3-dialkyltriazene **1.31** to aryl iodides using either trimethylsilyl iodide[77] or sodium iodate.[78] This protocol was later improved by Moore et al.[79] using methyl iodide as the iodine source to make **1.31** (Scheme 1.11).

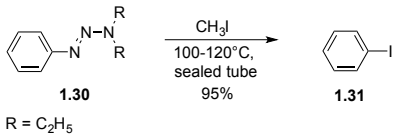

Scheme 1.11: Functional group interconversion of triazine into iodine.

The triazene **1.30** can easily be made from the amine derivative[77] (see Scheme 1.13) and the reaction can be performed with equal success using various N,N-dialkyl substituents. In fact, it was found that pyrrolidine triazenes have a greater tendency to form crystalline solids than the corresponding N,N-dialkyl derivatives. Thus, the pyrrolidine triazenes can easily be purified by recrystallization.

A very nice example was shown by Jeffrey Moore and co workers.[80] They used a divergent-convergent approach to synthesize an oligo-phenylene-ethynyne (OPE) structure **1.34** (Scheme 1.12).

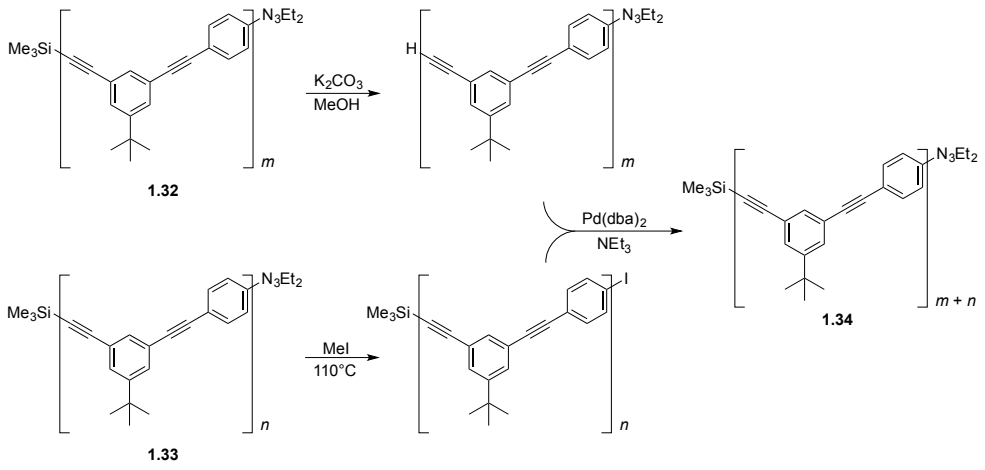

Scheme 1.12: The final convergent step in the divergent-convergent OPE synthesis.

The diethyltriazenyl/trimethylsilyl functionalised structures **1.32** and **1.33** are the parent compounds. Desilylation and exchange of the triazenyl substituent for an iodo substituent are the two divergent steps, followed by the alkynyl–aryl coupling, the convergent step.

Another interesting strategy is masking the acetylene itself. This requires having a functional group in place which can later be transformed into an acetylene. There are several methods described in the literature of how to convert a carbonyl into an acetylene (*Corey-Fuchs*[81], *Seyferth-Gilbert*[82]). The problem with such an approach is the reactivity of the carbonyl

towards a nucleophile. An extra protection/deprotection step would be necessary. A very nice alternative was reported from Ei-ichi Negishi and James Tour.[83] They used an acetyl group to mask the acetylene (Scheme 1.13). First an enolate was formed using LDA, which was then trapped with diethyl chlorophosphate to afford an enol intermediate. After elimination to form an acetylene, a further equivalent of LDA formed an acetylide anion. This was then quenched with trimethylsilyl chloride to afford the TMS-protected acetylene **1.35**. Tour et al.[84] (Scheme 1.13) nicely showed the synthetic power of these two masking strategies to synthesize **1.36** using an iterative approach.

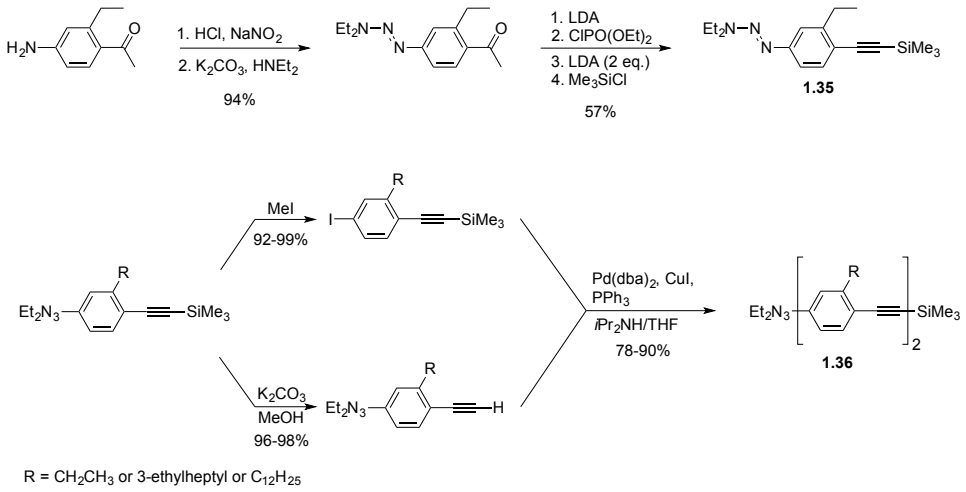

Scheme 1.13: Masking of both the donor and acceptor.

Another Masking group was used by Arne Lützen and co-workers.[85][86] They introduced a dimethylpyrrole moiety to protect the amine in **1.37**. This masking group is suitable for cross-coupling reactions followed by a diazo formation and iodine substitution to form **1.38** (Scheme 1.14).

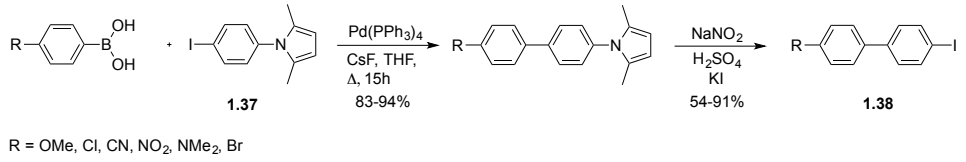

Scheme 1.14: Functional group interconversion of dimethylpyrrole into an iodine.

This method is an alternative to the triazene strategy introduced above. The advantage of the pyrrole masking group is its fast transformation into an iodine at room temperature. It typically leads to fewer side products during a coupling reaction compared to a free amine.

1.2.6 Acetylene protecting groups (PGs)

During the design of a successful synthetic route disconnections must be made which correspond to viable building blocks. Consideration should be given to which moiety should act as the acceptor and which as the donor, as was discussed in section 1.2.2. At the same time suitable PGs should also be considered. In order to aid this process below is a selection of known acetylene PGs. Each is discussed in turn, listing the relative advantages, disadvantages and the conditions under which the acetylene-H will be revealed and therefore made active to coupling conditions.

Protecting groups currently play a vital role in organic synthesis allowing very complex structures to be assembled by careful choice of the PG and the order of assembly.[70] In most syntheses PGs are required due to a lack of reaction selectivity. In acetylene based molecular structures PGs are used to enable the introduction of acetylene units. The use of acetylene gas would simply give rise to the di-coupled product,[87] leaving aside the obvious difficulty of using such a reagent. In this section we will focus on the most common acetylene protecting groups representing the donor moiety of the cross-coupling cycle. See section 1.2.4 for a discussion of the acceptor moiety.

The choice of acetylene PG should consider its functional group tolerance and ease of removal, however these are not the only considerations. The PG may also engender other favourable properties to a synthesis including, orthogonality (expanded upon below), increased polarity to aid in purification on silica gel, increased solubility, stability, and the possibility of statistical or in situ deprotection.

Acetylene Protecting Groups

Silyl based protecting groups have been particularly popular due to their early adoption and ease of removal, either under mild basic conditions or using fluoride ions (F^-) in protic solvents. Increasing bulk around the silicon centre engenders increased stability which can be used for selective removal of less bulky silyls faster than bulkier ones.[88] This range of stabilities to basic conditions can be employed, culminating in the use of an F^- source, which will cleave all silyl PGs. Thus when multiple silyl protecting groups are present, sequential lability can be employed to deprotect specific acetylenes and after further coupling build up larger structures with a specified substitution pattern. They are most often formed by the reaction of a chlorine substituted silicon centre with ethynlmagnesiumbromide. There are many possible acetylene PGs[72] however we shall only summarise the most popular ones

here as, in practise, most researches stick to the following easily accessible acetylenes (Figure 1.3).

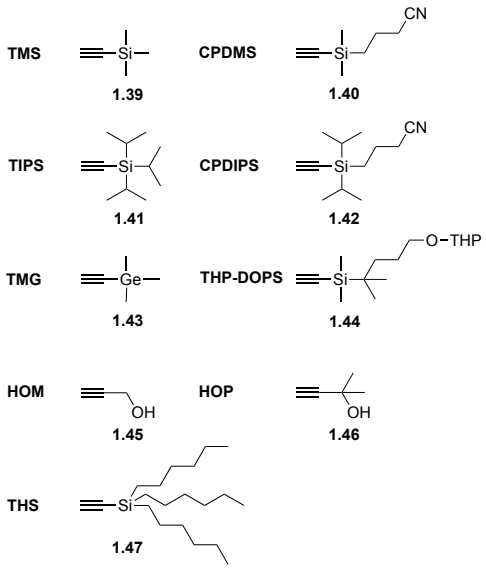

Figure 1.3: Commonly used acetylene protecting groups.

Trimethylsilyl acetylene 1.39 (TMS) is one of the most common acetylene protecting groups. It was employed by *Kenkichi Sonogashira* in the early days of cross-coupling synthesis,[87] and was also used as a PG in *Cadiot-Chodkiewicz* cross-coupling reactions.[88] The TMS PG is best used when all that is required is insertion of an acetylene, and where no other properties are sought from the PG itself. Easy removal of TMS is made by application of mild basic conditions; usually K_2CO_3 in the presence of a protic solvent. TMS will also be cleaved readily in the presence of an F^- source such as KF with 18-crown-6 as a chelator or TBAF (see TIPS for details). The addition of silver salts (Ag^+) can also be used to deprotect TMS,[89] and is usually preferable to the in situ use of alkali metal hydroxides,[90] owing to its greater functional group tolerance.

(3-Cyanopropyl)dimethylsilyl acetylene 1.40 (CPDMS) was introduced by Sigurd Höger to develop a polar analogue of the popular TMS PG using a CN alkyl chain bonded to the silicon centre.[91] The CPDMS adds polarity to the acetylene moiety making purification on silica gel much easier, but is still as easily removed as TMS under the same mild alkali conditions in the presence of a protic solvent. It will also be removed by an F^- source.

Triisopropylsilyl acetylene 1.41 (TIPS) is another very popular PG used for its increased stability to acidic and basic conditions owing to the steric bulk of the three isopropyl groups around the silyl centre. It is easily removed in the presence of an F^- source making it a very tolerant PG to most other functional groups, while still maintaining a facile

deprotection.[92][93] It has been reported that the yield of the deprotection can be increased in the presence of small quantities of water, moderating the reactivity of the fluoride anion.[94] Commercial TBAF is sold as a 1M solution in THF containing wt.-5% water, which is usually sufficient. Deprotection using AgF offers an alternative to TBAF, and in the presence of a bromine source it can be used to insert a halogen en route towards the formation of 1,4-butadyenes.[95]

(3-Cyanopropyl)diisopropylsilyl acetylene 1.42 (CPDIPS) was also introduced by the group of Sigurd Höger[96] as a more stable version of the CPDMS PG which behaves as a polar analogue of the popular TIPS PG requiring an F^- source for deprotection but still engendering the increased polarity of the CPDMS, but also added stability to temperature, acidic and basic conditions.

Trimethylgermanium 1.43 (TMG) is a relatively old PG[88][92] which has not seen wide adoption. It can be cleaved with catalytic CuBr in MeOH and has been used as an orthogonal protecting group to TMS in the synthesis of acetylene interlinked oligosaccharides (Scheme 1.15).[97]

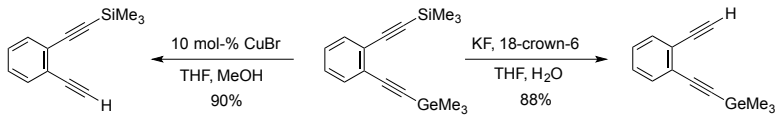

Scheme 1.15: Orthogonal deprotection of TMS and TMG groups.

The acetylene-$GeMe_3$ is made by reacting $ClGeMe_3$ with ethynlmagnesiumbromide. Recently TMG has been employed in an in situ deprotection and subsequent azide click reaction by washing a functionalised surface with Cu(I) to act as both the deprotecting agent and as catalyst of the click reaction.[98]

Dimethyl[1,1-dimethyl-3-(tetrahydro-2*H*-pyran-2-yloxy)propylsilylalkyne)] 1.44(DOPS). Chengzhi Cai and Andrea Vasella[99] introduced a new application of silyl protecting groups to acetylene chemistry with their use of DOPS.. This group is orthogonal to TMS and sequentially labile to other silyl PGs. The deprotection of the THP PG under acidic conditions reveals a free alcohol. Then treatment of the compound with a suitable base (eg LiDBB lithium 4',4'-ditert-butylbiphenylide) in a dry aprotic solvent deprotonates this alcohol and leads to intramolecular attack of the silicon centre, thereby revealing the free acetylide. These conditions would leave a TMS protected acetylene intact.

Hydroxymethyl acetylene 1.45 (HOM) as a PG was introduced by Bumagin et al.[100] and has the advantage of affording polarity and orthogonality to the silyl PGs. It is cleaved within 20 minutes after treatment with MnO_2 and KOH to afford the free acetylene upon workup and

has been used in the successful synthesis of long-chain oligomers, where the effectiveness of the HOM as a polar tag steadily decreased with increasing chain length.[66]

2-Hydroxypropyl acetylene 1.46 (HOP) This polar PG is most useful when the purification of reaction products will be a problem. This can be especially useful when more than one HOP group is statistically added or removed on a building block and requires isolation. It can be removed by heating with alkali metal hydroxides or hydrides, usually in refluxing toluene[101] via a retro-*Favorskii* reaction.[102] This treatment does mean that this PG may be incompatible with base sensitive functional groups, but as long as dry toluene is used it can be removed selectively in the presence of silyl PGs including TMS.[103]

Trihexylsilyl acetylene 1.47 (THS) adds long alkyl chains allowing for increased solubility of the unit to which it is attached. This can allow for easier processability of a building block prior to its removal and subsequent coupling to another, hopefully soluble, partner. It was successfully used by Reeve et al.[20] in the synthesis of a series of push-pull porphyrin molecules, which without the increased solubility of the alkyl chains, would be too difficult to purify. Using a statistical deprotection of the THS with TBAF they were able to introduce the push-pull units after *Sonogashira* coupling from their initial symmetric diprotected prophyrin.

Orthogonality of PGs

Orthogonality is a desirable trait in PG strategies where one PG can be selectively removed in the presence of another PG in any order (Figure 1.4). The conditions for cleaving one PG must be tolerated by the other, and vice versa. (X off, Y stays, or Y off and X stays).

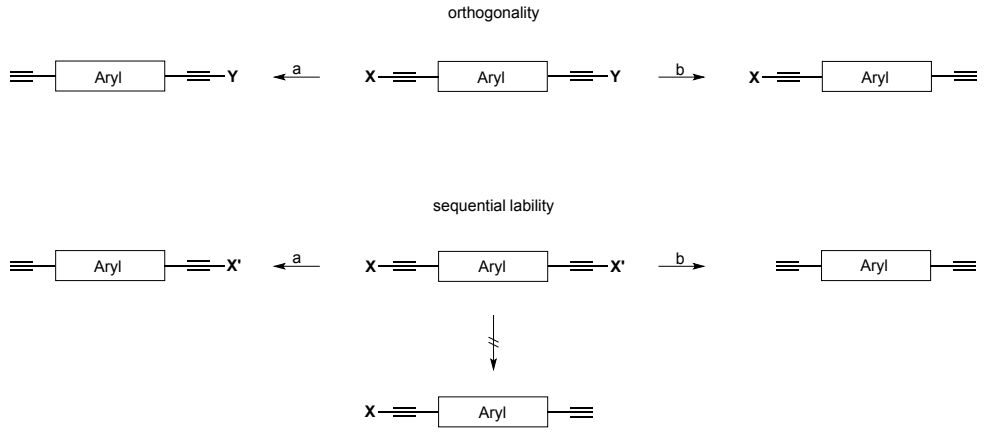

Figure 1.4: Concept of orthogonal and sequentially labile acetylene protecting groups.

True orthogonality is very difficult to achieve using a combination of silyl PGs as addition of an F^- source will cleave all, with the rate determined by the degree of steric bulk around the silyl centre. This can be seen in the case of the DOPS PG. So only sequential removal is

practical (X off, then X'), but the order of deprotection is limited as the 'least stable' group must be removed first. (e.g. the TMS in a TIPS/TMS combination). Sequential removal of silyl groups is therefore possible, but this places severe limitations on the sequence in which reactions can be performed.

Adelheid Godt and co-workers[66] were able to use a combination of the HOM and TIPS PGs in their synthesis of OPE rods (see Scheme 1.16) where removal of TIPS from **1.48** using TBAF gave **1.49** in 96% yield without affecting the HOM group and removal of HOM from **1.48** to afford **1.50** was possible in 89% yield.

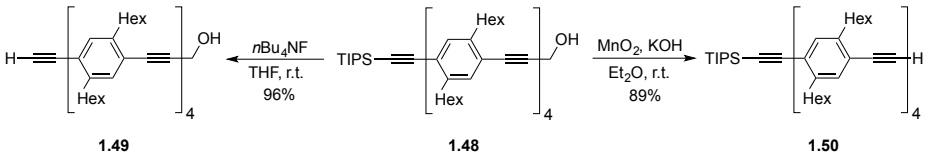

Scheme 1.16: Orthogonal deprotection of HOM and TIPS groups.

This work has recently been expanded upon by Sahoo et al.[65] using the same orthogonal PGs and also incorporating ether linkers as polar tags on their OPE rods.

1.2.7 Breaking the symmetry – I: statistical coupling

So far we have discussed how to use the selectivity of different Ar-X to introduce acetylenes bearing different protecting groups. This approach is especially helpful if an asymmetric building block is required. Whenever the a1 coupling component is symmetrically arranged with respect to any other R-groups (usually containing a C_2 or σ_v ideal symmetry element) in a building block, statistical reactions can be employed. A statistical reaction usually leads to a mixture of starting material, mono-substituted product and di-substituted product. These mixtures are not always easy to separate, especially when apolar protecting groups such as TIPS or TMS are used, or if the molecules are already very large. To overcome this problem one should introduce more polar protecting groups such as the HOM/HOP[65] or the CPDMS[91] and CPDIPS,[96] developed by Sigurd Höger for this purpose. These building blocks can now be used to build up larger asymmetric molecules or can be used in a divergent synthesis towards a macro molecular structure.[66] Yields of the mono-functionalized species can be increased by using an excess of the acceptor component **1.51** relative to the equivalents of acetylene used. Yields as high as 80% have been achieved this way.[104] It is possible to introduce orthogonal protecting groups in a one-pot reaction[105] or

stepwise[106] (Scheme 1.17). Even though the stepwise approach includes an extra purification step, it usually provides higher overall yields.

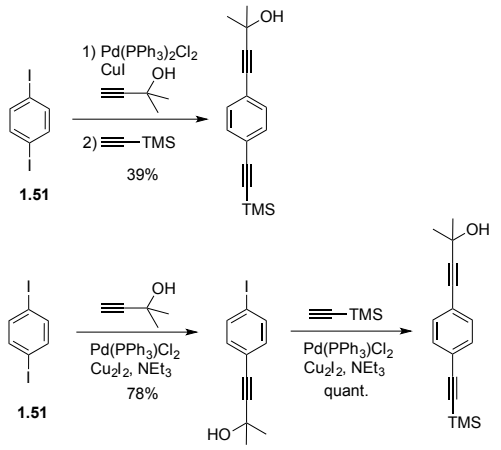

Scheme 1.17: Statistical coupling: one-pot versus a step-wise introduction of acetylene.

1.2.8 Breaking the Symmetry – II: statistical deprotection

When two or more identically protected acetylenes are present in a molecule then a statistical deprotection procedure may be employed (Scheme 1.18). The HOP PG is particularly well suited to this approach as the polarity it engenders to a compound allows for easy purification on silica gel of the fully-protected, mono-deprotected and fully-deprotected derivatives. By varying the strength of the base, temperature and reaction time used for the deprotection one can reliably optimize the formation of the required component. However it is often difficult to determine which of these variables is predominant for each particular deprotection.

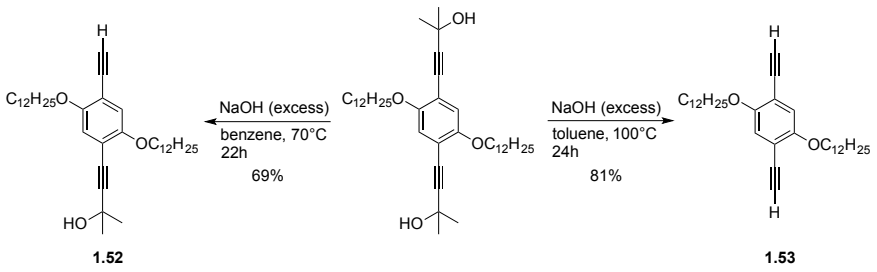

Scheme 1.18: Statistical and complete deprotection depending upon the conditions applied.

Abderrahim Khatyr and Raymond Ziessel[107] showed that an excess of NaOH in benzene at 70°C for 22 h gave **1.52** in 69% yield. However at 100°C in toluene for the same time **1.53** was obtained in 81% yield. The Raymond Ziessel group performed the same transformation under similar conditions (NaOH in benzene at 70°C) for 14 h. They only obtained a 45% yield with the majority of starting material re-isolated[108] indicating the relative difficulty in

reproducing this statistical deprotection. Luo et al.[109][110] have recently shown that by monitoring the deprotection more closely by TLC the monodeprotected product can be obtained within 20 min. By dissolving **1.54** in toluene in the presence of 4.4 equiv. of K_2CO_3 and then adding 0.9 equiv. of KOH at 70°C and monitoring the reaction by TLC every 5 min for the observation of fully deprotected **1.56**, and after about 20 min, on the first appearance of **1.56** the reaction was worked up yielding **1.55** in 66-69% yield after column chromatography on silica gel.

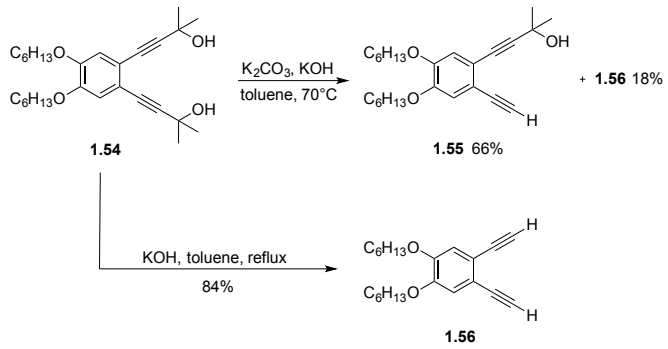

Scheme 1.19: Statistical and complete deprotection depending upon the conditions applied.

Using only KOH **1.56** was obtained in 84% yield after 2 h (Scheme 1.19).[109]

Statistical deprotection of the TIPS PG can be achieved in a similar manner. Slow addition of TBAF as an F^- source followed by close monitoring by TLC can afford the mono-deprotected product in good yield. This method is exemplified by Sigurd Höger and co-workers[96] in their seminal work on CPDIPS where the polar TIPS analogue is proven to be efficiently deprotected with TBAF in the presence of 5 vol.-% water as shown in the reaction of **1.57** to **1.58** in a yield of 55% after stirring for six hours (Scheme 1.20). Owing to the polarity endowed by the CN group a large difference in R_f allows facile separation on silica.

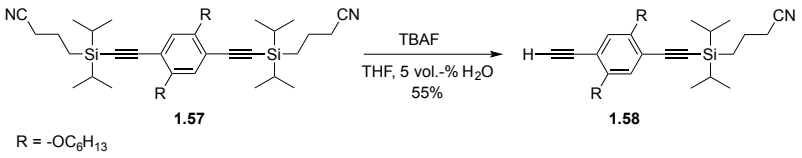

Scheme 1.20: Statistical deprotection of CPDIPS-acetylene.

This approach is not limited to the TIPS or CPDIPS group. Under acidic conditions of 1.5 equiv. acetic acid in wet THF, a thiophenyl substituted benzene with two TBDMS protected acetylenes was mono-deprotected using TBAF to afford the monosilytaed product in a yield of 48%.[45]

1.2.9 In Situ generation of free acetylene

After talking about the order of reactivity of arylhalides towards oxidative addition to palladium(0) complexes we should also mention the oxidative addition of acetylenes to palladium(0) complexes. If the oxidative addition of the acetylene is much faster than the oxidative addition of the arylhalide then formation of the homo-coupled product can be favoured. This process can also be promoted in the presence of trace quantities of oxygen, facilitating a *Hay*-type coupling. The exact origin of 1,4-butadiyene side-products is often ambiguous, as the precise oxygen content is usually not investigated. To prevent the formation of the homo-coupled product one could accelerate the oxidative addition step of the arylhalide. It often helps to change the ligands of the palladium(0) complex.[54] Bulkier and more electron-donating ligands usually accelerate the oxidative addition of the arylhalide which leads to the intended cross-coupled product. An alternative would be to slow down the oxidative addition of the acetylene by reducing the amount of free acetylene in the reaction. To do so, one could slowly add the free acetylene to the reaction mixture or one could slowly generate the free acetylene in the reaction. The second approach is called in situ generation or in situ deprotection.

A useful method is the deprotection of TMS-acetylene with small amounts of hydroxide ions. Haley et al.[111] used this method for the synthesis of benzannelated dehydroannulene **1.61** (Scheme 1.21). By reducing the amount of free acetylene coming from **1.59** in the first step they favoured the cross-coupled product over the homo-coupled product. The small amount of hydroxide ions slowly deprotected the TMS-acetylene but not the TIPS-acetylene. Once the TMS acetylene was deprotected it reacted with the excess aryliodide.

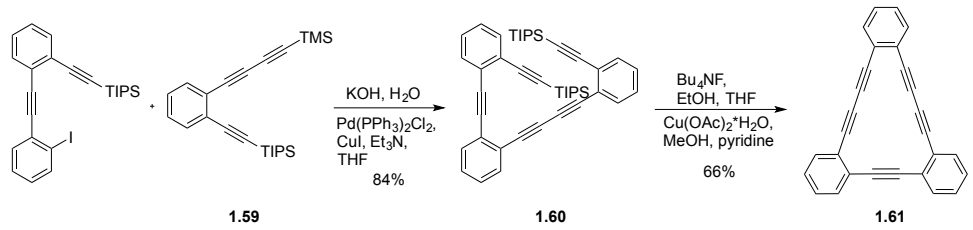

Scheme 1.21: Demonstration of in situ deprotection coupling reactions.

Applying the same strategy for the second step an intramolecular ring closing reaction was favoured over the intermolecular polymerization reaction. In this case, a large excess of TBAF was used to deprotect the TIPS-acetylene **1.60** and a highly diluted reaction mixture helped to favour the intramolecular homo-coupling reaction to form **1.61**.

Another example using in situ deprotection was reported by Mio et al.[112] They demonstrated a divergent approach to generate symmetric and asymmetric tolanes **1.62** in a one-pot reaction (Scheme 1.22). In addition, a convergent strategy was applied to synthesize triarylethynylene and tetraarylethynylene **1.64** from **1.63** (Scheme 1.23).

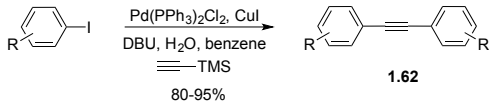

Scheme 1.22: Formation of symmetric tolanes using an in situ deprotection.

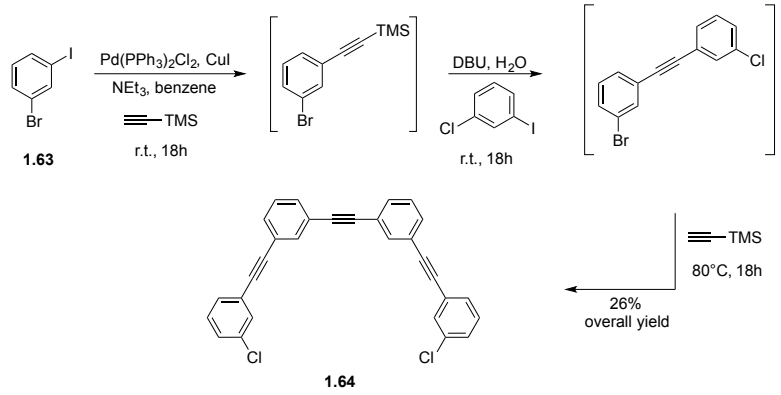

Scheme 1.23: Four sequential *Sonogashira* reactions in one pot controlled by in situ deprotection.

These examples show nice methodologies for in situ deprotection of TMS acetylenes and TIPS acetylenes. If very high reaction temperatures and reaction times are necessary, control over the in situ removal of TMS is not very effective. Chow et al.[113] reported in 2001 on another modified *Sonogashira* cross-coupling reaction. HOP was used as the protection group and it was in situ deprotected using sodium hydroxide in a water/toluene mixture.

1.2.10 Concepts applied to representative syntheses

Below is a collection of examples which brings together all of the strategic tools we have described in this review. By using the right combination of retrosynthesis, catalyst, masking and protecting groups it should be possible to elicit any plausible phenyl-acetylene structure.
Paul Baxter[114] in his synthesis of a hexagonal macrocycle used a selective halogen exchange followed by a chemoselective cross-coupling of an acetylene (see section 1.2.4). Initially statistical introduction of TMS-acetylene from **1.65** to **1.66** yielded a mixture of mono, di and tri substituted aryls which could not be easily separated. But the stepwise introduction of an iodine gave control over assembly of the asymmetric building block **1.67** in high yields (Scheme 1.24).

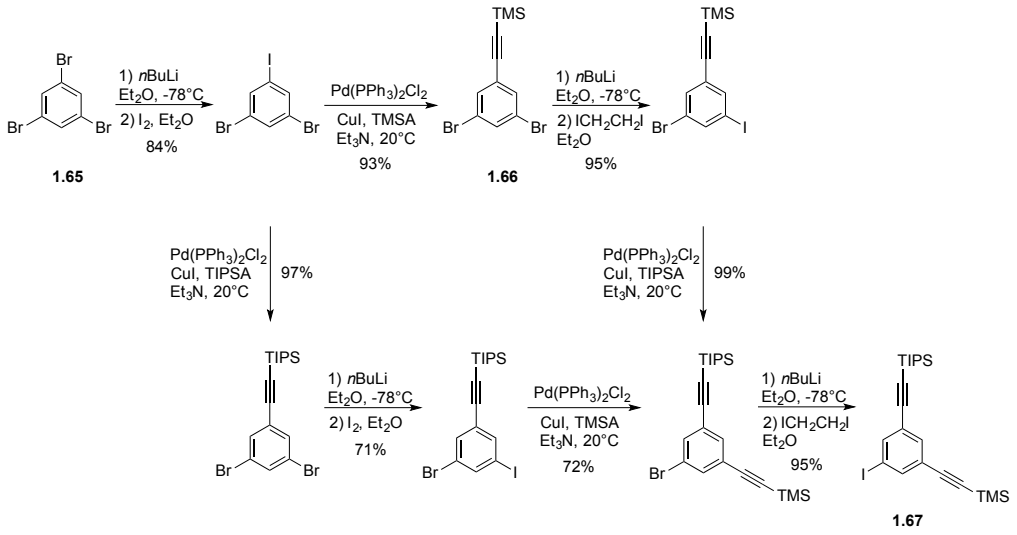

Scheme 1.24: Use of chemoselective control in the formation of phenyl-acetylene building blocks.

Paul Baxter[114] also illustrates an example of a selective assembly using the tools of chemoselectivity (see section 1.2.4) and masking (see section 1.2.5) (Scheme 1.25). Initially a bromine in **1.68** was replaced with an aldehyde using *n*butyl-lithium and DMF to form **1.69**. Aldehyde **1.69** was transformed into acetylene derivative **1.70** via a *Croey-Fuchs* reaction[81] and then protected with TMS to afford **1.71**. Using this strategic approach they could selectively introduce the acetylene and the tin functional group in **1.72**. The yields of the *Stille* coupling to form **1.73** were further improved by changing the disconnection for the last cross-coupling reaction by exchanging the acceptor and donor moieties (see section 1.2.2) This reaction sequence demonstrates that the tools discussed in this review are not restricted to *Sonogashira* couplings, but can be applied more generally to other reaction types in the assembly of larger structures from their constituent parts.

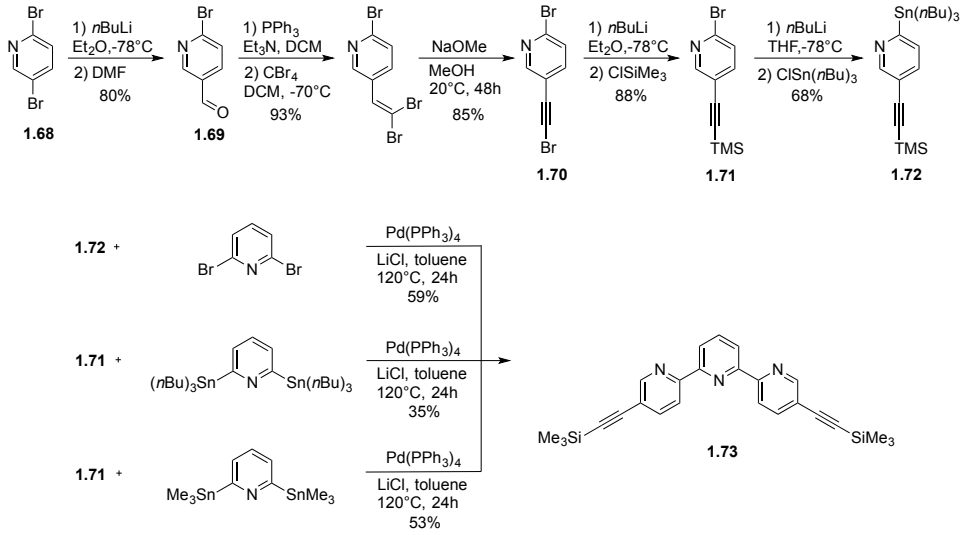

Scheme 1.25: Functional group interconversions and change of disconnection to form a terpyridine.

The synthesis of star shaped or branched molecules present their own particular challenge. It is usually possible to form the desired product as part of a reaction mixture but purification of the target can be very troublesome. As a consequence this can mean that a synthetic route becomes unviable. The synthesis of such compounds are usually described as following the principles of convergence, where an OPE is coupled to the central motif forming the star in the final step, or divergence, where the star is built up by iterative couplings using protection/deprotection procedures (see section 1.2.2).

McDonagh et al.[115] attempted a convergent route towards organic/inorganic hybrid star **1.76** (Scheme 1.26) starting from OPE **1.74** coupling with triiodobenzene (**1.75**) but were unable to separate it from the diacetylene linear rod **1.77**, even after rigorous de-oxygenation of the reaction mixture in an attempt to hinder its formation.

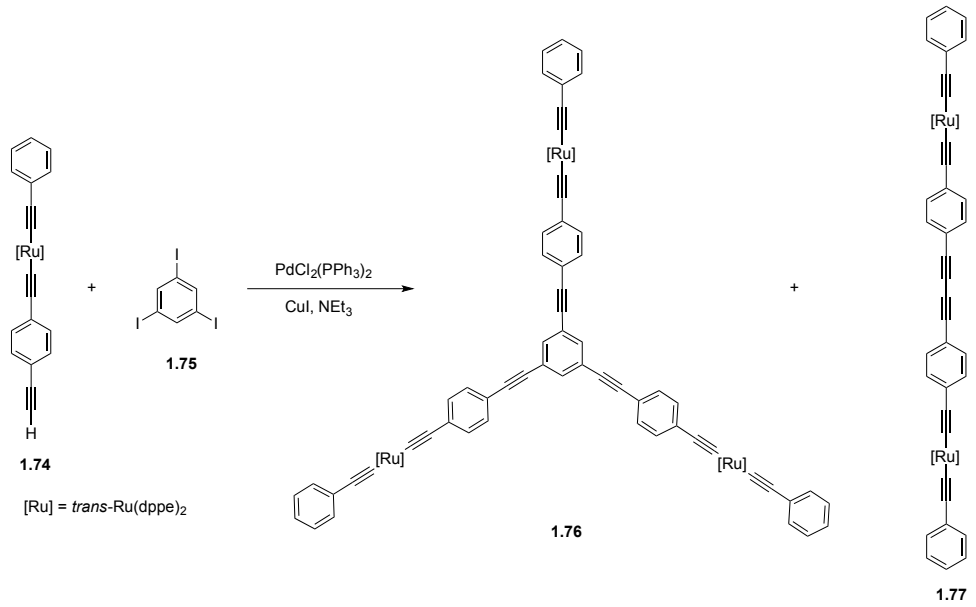

Scheme 1.26: Difficulty of a convergent approach to star synthesis due to the formation of 1,4-butadiynes.

Instead they decided to use a divergent synthetic route building up the star from triethynylbenzene (**1.78**) and sequential coupling of **1.79** (Scheme 1.27). After insertion of Ruthenium and a final divergent coupling they were able to obtain **1.76** avoiding any inseparable reaction mixtures.

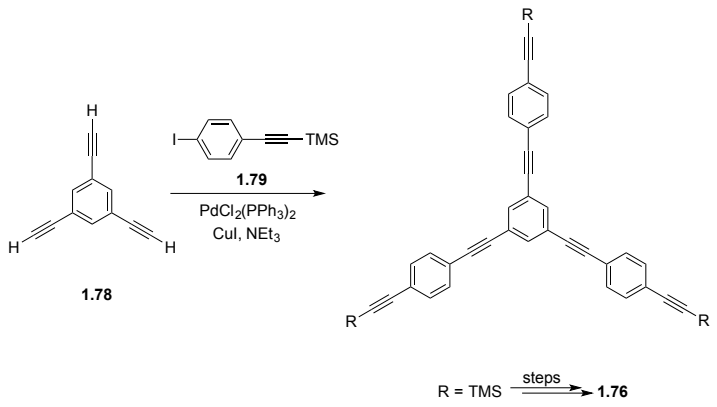

Scheme 1.27: Divergent approach to star synthesis.

However the presence of substituents at the 2- and 5-positions appears to allow for a successful convergent approach as shown in the coupling of **1.85** to **1.75** as the side chains appear to shift the balance in the formation of diacetylene side products. James Tour and co-workers[116] comment specifically on this effect, further expanded upon in their work towards the synthesis of C_{60} terminated star OPEs[117] (Scheme 1.28).

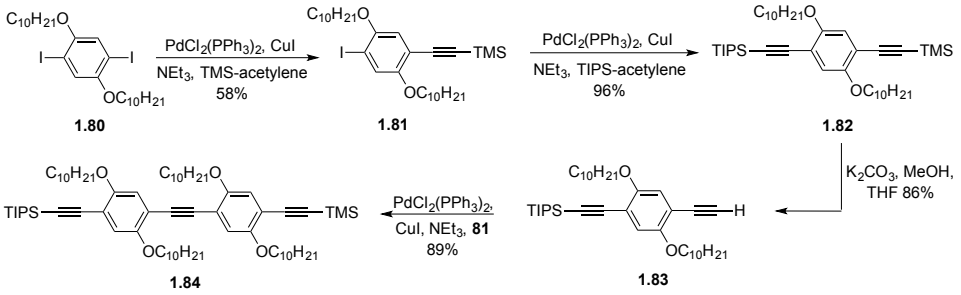

Scheme 1.28: Asymmetric OPE synthesis using orthogonal protecting groups.

They formed the asymmetric OPE **1.84** via a statistical coupling procedure (see section 1.2.7) in order to introduce two sequentially labile PGs (see section 1.2.6). Statistical coupling of TMS acetylene to **1.80** broke the inversion centre present in this molecule. This was followed by subsequent coupling with TIPS-acetylene, to afford the asymmetric building block **1.82** containing the sequentially labile PGs TMS and TIPS. Selective removal of TMS using standard conditions afforded **1.83** which could be extended with a further cross-coupling with **1.81**. After removal of TMS they were able to couple OPE **1.85** to tri-iodobenzene **1.75** constituting a successful convergent synthesis of star **1.86** (Scheme 1.29). The authors describe an easier purification of this product from its reaction mixture than expected as there was less diacetylene homocoupled product than they had observed in other OPE syntheses. They attribute this to the steric hinderance of the $-OC_{10}H_{21}$ chains on the aryl monomers.[117]

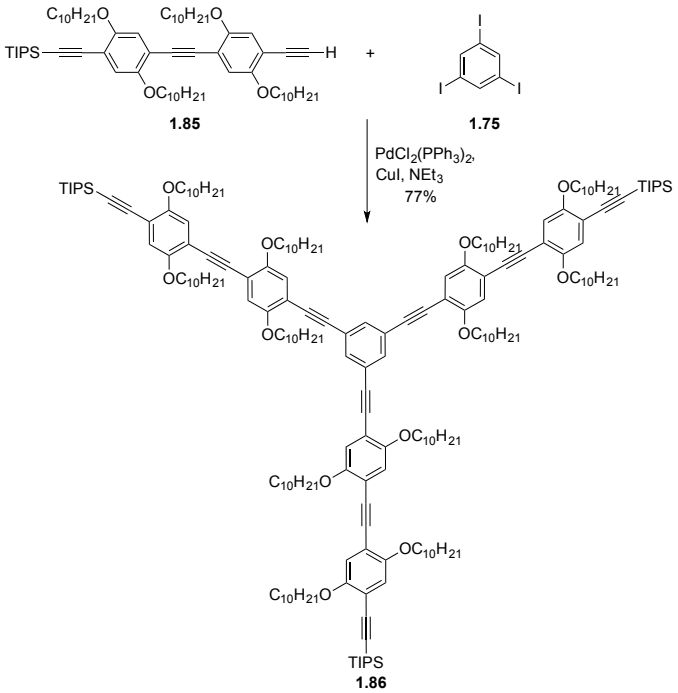

Scheme 1.29: Convergent approach to the synthesis of a branched OPE.

The strategies described in this micro-review are also applicable to natural product synthesis.[14] (5*S*,15*S*)-dihydroxy-6,13-trans-8,11-cis-eicosatetraenoic acid (**1.92**) was synthesized starting from a *Sonogashira* coupling of **1.87** with mono-protected bis-acetylene **1.88** as a masked *Z*-alkene (see section 3).[118] This structural geometry would be very difficult to form via other methods. Deprotection of the TMS protecting group on **1.89** followed by a second *Sonogashira* coupling with **1.90** allows for the formation of the asymmetric compound **1.91**. After further functional group interconvertions the final target **1.92** was obtained (Scheme 1.30).

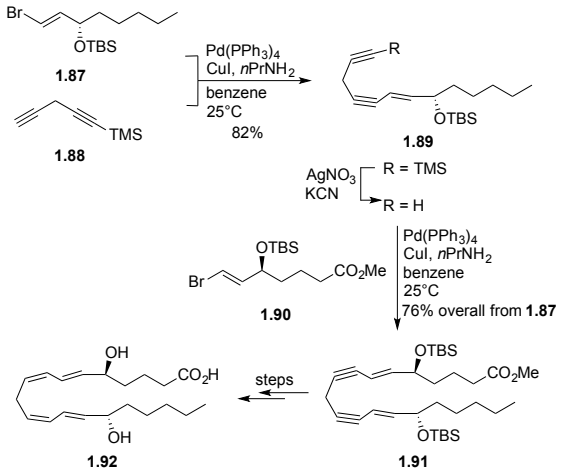

Scheme 1.30: Part of a natural product synthesis where *Sonogashira* cross-coupling reactions were applied.

We have chosen this particular example to show that the *Sonogashira* reactions are not limited to arylhalides as the a1 moiety. Vinylhalides such as **1.87** or heteroaromatic halides can also be successfully coupled with acetylenes.[10]

1.2.11 Summary and outlook

In this section synthetic tools including retrosynthetic analysis, chemoselectivity, masking, choice of protecting group and statistical approaches towards the formation of phenyl-acetylene building blocks were discussed. Gaining control of the substitution pattern of smaller building blocks was shown to be a method for guiding the interlinking of phenyl-acetylenes to build larger architectures. Taking into account the relative advantages and disadvantages of each synthetic technique may reduce the time spent synthesizing molecules so that one may focus on applications, discovering what role structure plays in function. The emerging inter-disciplinary fields including; molecular electronics, photovoltaics, energy

storage, and medicinal chemistry among many others strongly depend on the bottom-up assembly of molecular building blocks and therefore on classical organic chemistry.
We hope that using this collection of synthetic tools young researches will find it easier to synthesize even larger macromolecular structures expanding the art of synthesis by design. It is hard to predict what new application may be found for molecular systems, but what is certain is that being able to control the spatial arrangement of functional groups will always be important.

We now turn our attention to supramolecular methods to exert control on the assembly of molecules on surfaces.

1.3 Nanopatterning by molecular self-assembly on surfaces

The ability to pattern surfaces down to the nanoscale is of increasing importance in nanoscience research. The use of supramolecular chemistry to drive the formation of self-assembled networks allows for a bottom-up approach to achieve nanopatterned surfaces. This short review highlights some of the recent breakthroughs in achieving long-range order in such molecular based systems, complemented with examples from our own work. The tuning of molecular architectures can exert control on the emergent properties and function of molecules at interfaces. In particular the formation of porous honeycomb networks allows for the rational design of highly ordered patterned surface domains and the investigation of molecular dynamics, chirality and templation effects on surfaces.

Synthetic organic chemistry is most commonly conducted in solution for ease of processability, however natural living systems perform much of their magic at interfaces through the exclusion of solvent. In cells proteins create folded surfaces to obtain regio- and stero-selective reaction control.[119] Physical processes involving electron transfer such as photosynthesis[120] or the transport of charges across membranes to generate local electric fields and propagate neural signals[121] all occur at well-defined interfaces.
For many promising developments in nanoscience and technology in the areas of; molecular electronics,[122] optoelectronic metamaterials,[123] photonic crystals,[124] DNA sequencing[125] and organic photovoltaics[126] the precise design of interfaces is essential, however we are

currently limited by our ability to control interfacial structures both on an extended length scale and down to the bottom of the nanoscale.

Using nature as our guide, crystal growth is a nice example of how this control can be achieved. The process of crystallization can be characterized by two primary factors, symmetry and branching.[127] The intrinsic property of molecular structure controls the symmetry of the system under thermodynamic control. The extrinsic environment including temperature, pressure and concentration affects the branching under entropic control.

The simple molecule H_2O crystalizes into a hexagonal lattice whose symmetry is determined by its three coordination sites available to form four H-bonds. But the localized crystalline domains quickly diverge in a random fashion in the formation of a snow flake.[128] This branching effect is due to the external conditions at the site of crystal growth. It is commonly said that 'no two snow flakes are the same', however they all have hexagonal symmetry. These emergent properties arise from the interplay of the intrinsic molecular structure with the localized external environment, so that even starting from the same initial conditions highly divergent outcomes are achieved.

Intermolecular, non-covalent interactions can increase the enthalpy term for the same free energy, thereby reducing the effect of the entropy term on the system.[129] By tuning the molecular structure we can exert control on the emergent properties and function of molecules, allowing for the rational design of highly ordered, patterned surfaces.[130]

1.3.1 Supramolecular chemistry in solution

Supramolecular chemistry is a maturing field in the synthesis of organic molecules and offers a way to overcome the entropic barriers of the free energy of association to achieve self-ordered systems.[131] There are many possible non-covalent intermolecular interactions that can be used to drive self-assembly. Most well known is H-bonding,[132] and its related halogen bonding,[133] not forgetting van der Waals interactions,[134] metal coordination,[135] π–π,[136] cation-π[137] and even anion-π interactions.[138] Supramolecular approaches have recently resulted in the first functional artificial synthetic machine, mimicking the function of a ribosome.[139] Dynamic covalent chemistry has greatly increased our understanding of biological and chemical systems.[140] The group of Samuel Stupp have pioneered the application of supramolecular interactions in polymeric systems which mimic analogues of human tissues.[141] The Mayor group recently reported the synthesis and self-aggregation of molecular daisy chains in solution.[142] These solution based, non-covalent aggregates are

held together by mechanically interlocked supramolecular binding concepts.[143] The focus of this work is to illustrate approaches and advantages of applying these solution based concepts onto surfaces.

1.3.2 Supramolecular chemistry on surfaces

Currently, patterned surfaces are usually formed by the top-down approach using lithographic techniques, however in order to enter the sub-5 nm regime and achieve single-molecule resolution bottom-up approaches based on self-organised molecular scale architectures are required.[144] This length scale also defines the requirements for imaging techniques, of which scanning tunneling microscopy (STM), among others,[145] is a very powerful method to investigate molecules at surfaces. Typically higher-resolution STM images are obtained at reduced temperatures under ultra high vacuum (UHV) conditions.[146] The compound of interest is either sublimed or sputtered onto a substrate, and consequently the molecules used must also be well matched to these harsh deposition conditions.[147] The alternative of measurements at the solid-liquid interface typically implies a limited temperature range and lower resolution, as thermally induced motion and migration of the adsorbate often occurs, giving rise to different structural phases.[148] These limitations can be somewhat overcome by first preparing the sample at the liquid-solid interface and then measuring ex situ under ambient conditions.[149]

Patterns of molecules can be achieved with control dictated by either the substrate or by the molecular structure, often adapting ideas borrowed from crystal engineering applied to 2-D networks.[150–152] When porous networks are formed, further functionalization of the surface becomes possible.[153] Chemical reactions can be induced by manipulation from the STM tip[154] leading to the exciting prospect of growing 2-D covalent sheets that form graphene nanoribbons.[155] Light activated functional surfaces can even release drug targets on demand.[156]

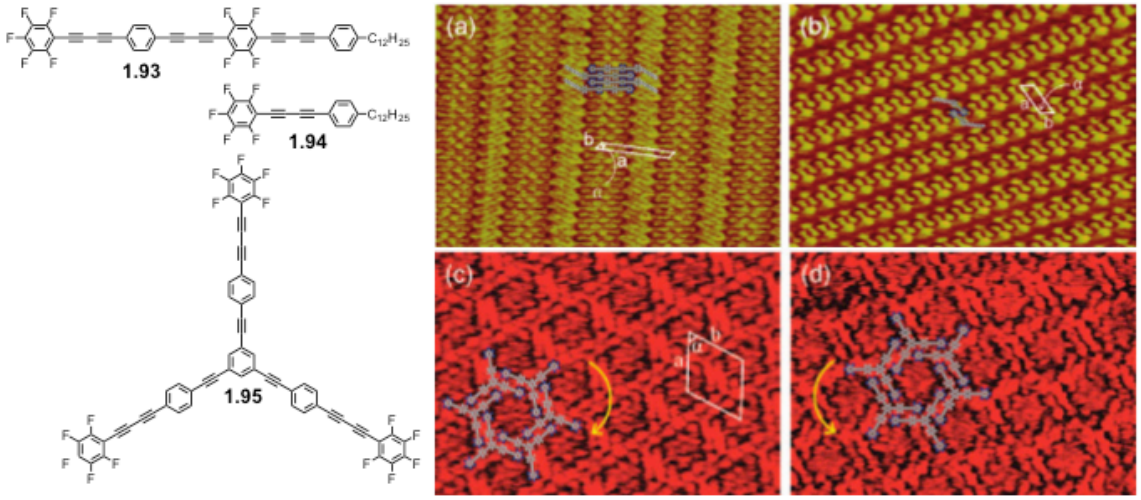

Figure 1.5: Pentafluorophenyl OPE rods 1.93, 1.94 and star 1.95 were deposited on HOPG surfaces and imaged by STM in constant current mode. a) Overlaid modeling of OPE 1.93 on STM, V_{bias} = –0.95V, I_{set} = 0.6nA. b) Overlaid modeling of OPE 1.94 on STM, V_{bias} = –0.90 V, I_{set} = 0.6 nA. c and d) High resolution STM images V_{bias} = –0.5 V, I_{set} = 1.43 nA. d) a mirrored arrangement of the domain in c) demonstrating change in chiral domain. Both are overlaid with modeling of OPE star 1.95. (Images a and b reprinted with permission from ref. [157]. Copyright 2011, Langmuir. Images c and d reprinted with permission from ref. [158]. Copyright 2008, American Chemical Society.)

The Mayor group have investigated acetylene based π-oligomers on surfaces,[159] however the most ordered pattern domains were obtained from a series of investigations applying halogen-π interactions. Electron rich acetylenes are a unique moiety for H-bonding motifs on surfaces because the terminal acetylene can act as an H-donor and their high π-density can act as a proton acceptor.[160] In our case molecular rods of pentafluorophenyl subunits **1.93** and **1.94** linked by a diacetylene, self-assembled into ordered domains of interlocked parallel lines[157,161] (see Figure 1.5a,b). A bent rod and star structure **1.95** with acetylene linkers assembled into interdigitated 2-D chiral porous networks driven by Aryl–H···F bonding[158] (Figure 1.5c,d). It was also possible to design and synthesize halide-end capped oligo-phenyl-ethynylene (OPE) rods and compare their 3-D crystal structure to their 2-D arrangement on surfaces.[162] Currently we are working to combine such phenyl-acetylene architectures with a porous network to investigate template effects and even the dynamics of molecular motion at the interface.

1.3.3 Templation and molecular dynamics on surfaces

The use of templating and host-guest interactions allows organization of molecules on a surface that would not otherwise self assemble in a given pattern. The group of Dieter Schlüter have been able to form 2-D polymer sheets at the water/air interface, which can

coordinate Fe^{2+} metal centers.[163] Jay Siegel and coworkers[164] used corannulene buckybowls as hosts for C_{60}. These templating concepts are analogous to those seen in solution, however an interface is also a pro-chiral environment dictated by the facial selectivity of an adsorbed molecule and the generation of surface confined networks, which can both lead to chiral recognition.[165]

Identification of different conformational geometries of a molecule on a surface was first reported by Jung et al.[166] for a tetra-substituted porphyrin determined by STM. They were able to assign the different 'landing geometries' of the porphyrin and investigate conformational changes governed by the interaction of the molecule with the surface. Schramm et al.[167] experienced first hand the difficulties that arise when a desired 'landing geometry' is disfavored.

Thermally induced motion was used by Gimzewski et al.[168] to investigate the mechanics of a single molecule, supramolecular bearing. Directionally controlled, concerted molecular motion was recently achieved by Ben Feringa and co-workers[169] by manipulation of an STM tip on a nanocar. Careful design and synthesis of the 'wheels' of the car was required to ensure that the axels were of opposite handed-ness, however they too had to first search for molecules that had the correct 'landing geometry'. It may be possible to obtain directional motion of single molecules by confinement within a cavity to overcome this limitation, so long as there is still sufficient space to allow for molecular rotations. Below we discuss the approaches towards such surfaced confined rotors.

1.3.4 Porous honeycomb networks

Ludwig Bartels and co-workers found an anthraquinone based H-bonded network on a Cu(111) surface that arranged spontaneously at low surface coverage and low temperatures (between 10–200 K) into a honeycomb network with long range ordering[170] (see Figure 1.6a). This network formation was notable for two key features. The H-bonding that drove the self-assembly was mediated between a carbonyl group and an aromatic proton (see Figure 1.6b). Secondly, the cavity that was formed was roughly 50Å, more than five times the space filling of the individual anthraquinone units, seemingly driven by the delicate interplay of weakly attractive H-bonding and substrate mediated adsorbate–adsorbate repulsion. At higher anthraquinone densities islands of closed packed molecules were preferred, indicative of a shift to another polymorphic state.

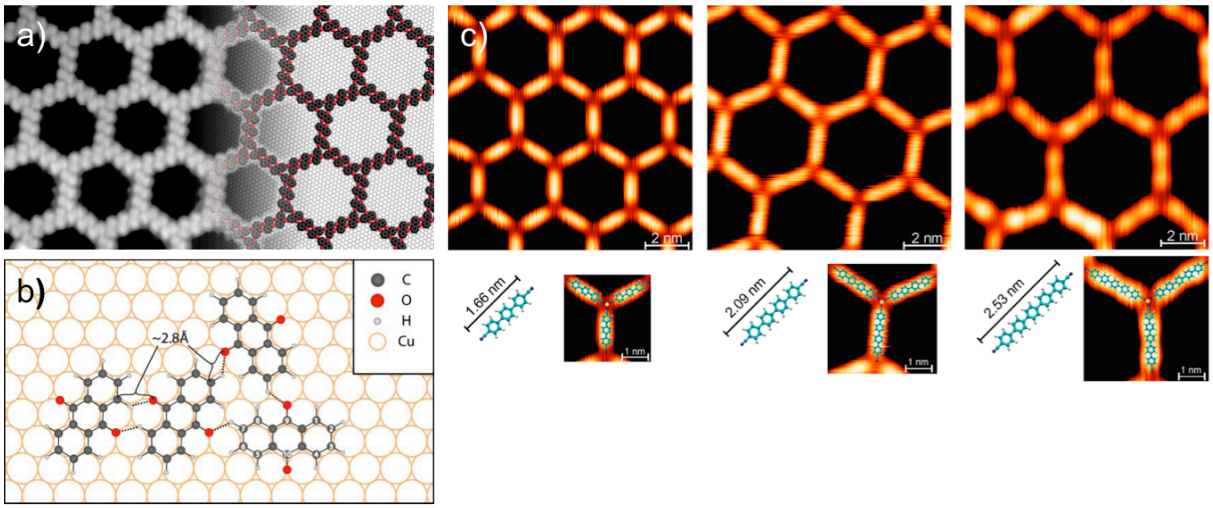

Figure 1.6: a) Anthraquinone molecules form a honeycomb network on a Cu(111) surface with pores of 150 Å by 260 Å, right) unit cell model overlaid. b) Schematic of anthraquinone molecules forming H-bonding. C-H-O distances are indicated. (Image reprinted with permission from ref. [170]. Copyright 2006, Science.) c) Tuning of the pore size by increasing the length of oligo-phenyl linkers by Co-directed self-assembly. below) modeling of oligo-phenyl linkers overlaid on a structural motif from the STM. (Images reprinted with permission from ref. [171]. Copyright 2007, Nano Letters.)

The group of Johannes Barth, building on the unprecedented size of Bartels' pores[170] targeted a self-assembled network that would afford a similarly large cavity, but with greater stability. In order to achieve this they focused on forming 2-D arrays of metal-organic frameworks, as the coordination should be stronger than H-bonding. Initially they investigated oligo-phenyl rods of varying length[171] (see Figure 1.6c) based on a tri-dentate binding motif of Co–Carbonitrile which formed hexagonally symmetric networks over a μm^2 domain on Ag(111) surfaces. The largest pore size of 5.7 nm of the honeycomb network allowed for isolated cases of cavity filling. The deposited rods, caged in by the cavity walls could be switched by manipulation from the STM tip by changing the scan direction or applied bias voltage.

In an attempt to create even larger cavities they synthesized a para-hexaphenyl-dicarbonitrile rod **1.96** (Figure 1.7) by Suzuki coupling[172] which when deposited with cobalt atoms lead to the formation of a 67Å long pore.[173] The honeycomb network was further stabilised by the epitaxial fit of the coordination sites with the underlying Ag(111) substrate which was imaged by STM with atomic resolution. After further investigations in the 70–300K temperature range, the network was found to still be stable without degradation at room temperature, however any uncoordinated rods became highly mobile.

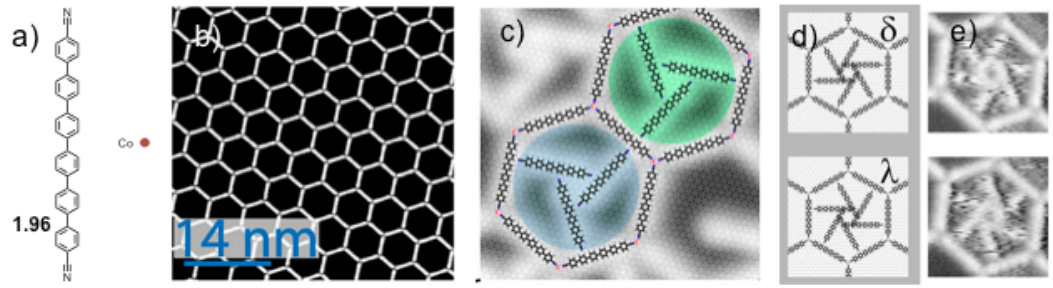

Figure 1.7: a) *para*-Sexiphenyl-dicarbonitrile 1.96 and Cobalt generate b) well defined 2-D coordination honeycomb network on a Ag(111) surface with a cavity of van der Waals radius of 24 nm^2. c) Structure model overlaid on STM images showing two chiral arrangements of trimers. d) The chiral configurations (δ + λ) can be interconverted at 146 K and gives rise to e) rotations seen by STM in the pore. Images reprinted with permission from ref. [174]. Copyright 2010, PNAS.

In order to functionalise the surface further and investigate constitutional dynamics of these uncoordinated rods trapped in the pores Kühne et al.[174] played with the deposition conditions. The ideal stoichiometry of this nanomesh is 3:2 of Rod:Cobalt. If more rods are present they begin to deposit in the network cavities. At a 10% excess of para-hexaphenyl-dicarbonitrile monomers to this ratio, trimers are formed (see Figure 1.7c). These rods are themselves epitaxial with the Ag(111) surface with the nitrogen of the terminal nitriles located at hollow sites on the Ag surface. These trimer guests are found in two enantiomorphous forms which are distinguishable at low temperatures. They performed a series of STM measurements with increasing temperature to investigate the possibility of a dynamer[175] response. They were able to resolve concerted rotational motion of the trimers while maintaing their chirality (see Figure 1.7d). Above 70 K interconversion between the two dynameric enantiomers occurs, removing any chiral signature, demonstrating a rare example of constitutional dynamics inside the nanopores of this self-assembled system.

These examples of progressively more functional cavities raises the prospect of designing such a porous network that allows for even greater control over the rotations of the guest, with the possibility of directionality and addressability by external stimuli, i.e. not limited to thermally induced random rotational motions in a nanopore.

1.3.5 Melamine-PTCDI honeycomb networks

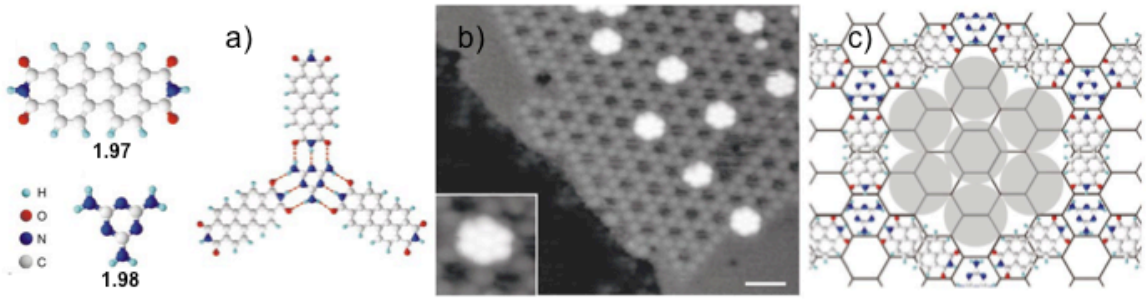

Figure 1.8: Perylene tetra-carboxylic di-imide (PTCDI) 1.97 and melamine 1.98 can a) H-bond to form three coordinate 2-D networks. b) STM image of heptamers of C_{60} filling the cavities of melamine-PTCDI honeycomb network. c) Schematic modeling of the surface network. Image reprinted with permission from ref. [176]. Copyright 2003, Nature.

In a multi-component system there is greater scope for rational design of the surface architecture to encourage formation of porous sites. Theobald et al.[176] explored the formation of a two-component assembly using the strong H-bonding formed between perylene tetra-carboxylic di-imide (PTCDI) and melamine (see Figure 1.8). The conditions of formation must be carefully controlled, otherwise a wide variety of polymorphic domains of the melamine-PTCDI are accessible, with a particular dependence on the annealing temperature.[177] The three-fold symmetry of the melamine allows for the formation of a honeycomb network by annealing at 100°C after a step-wise deposition of the two components, where the network remains commensurate with the underlying Ag/Si(111) surface. Uniquely they were then able to sublime a third molecular component, filling the cavities with heptamers of C_{60}.

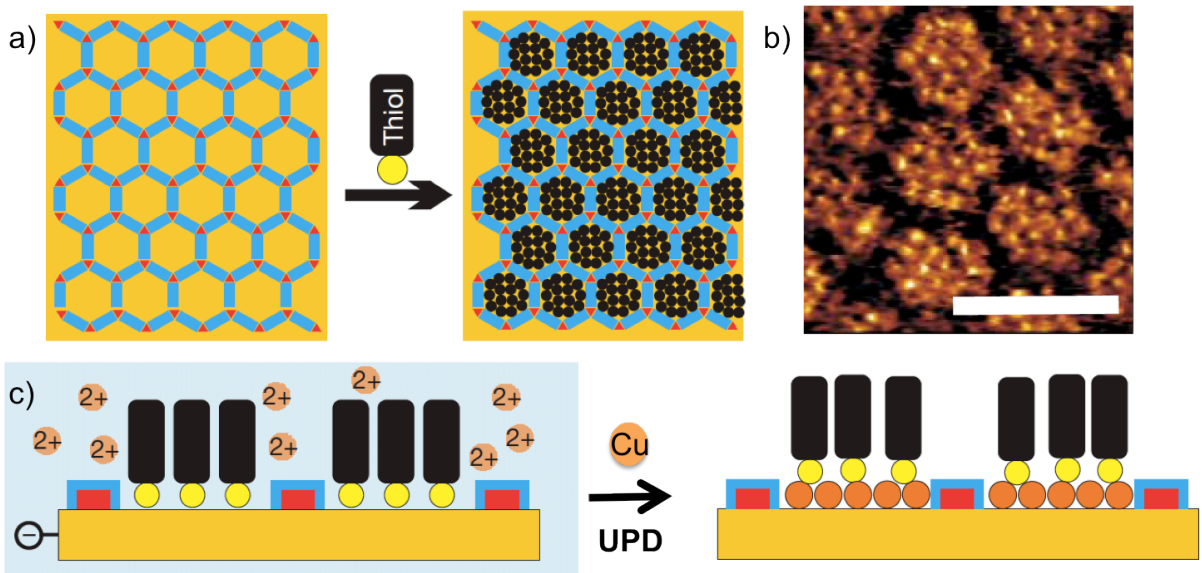

Figure 1.9: a) Schematic of SAM formation in the pores of a melamine-PTCDI network on Au. b) High resolution STM image of a C12SH alkyl thiol SAM framed by the honeycomb network, scale

bar 5nm. c) Illustration of UPD electrochemical Cu deposition in the porous network at the alkane thiol/Au interface. Image reprinted with permission from ref. [149]. Copyright 2008, Nature.

The Buck Group have looked to combine this supramolecular approach to patterning surfaces with the more traditional concept of self-assembled monolayers (SAMs).[178] In the examples above (Figure 1.6 – Figure 1.8), all STM investigations were performed under UHV conditions, which is restricted to molecules which can be easily sublimed. Madueno et al.[149] moved to a solution-based fabrication which additionally allows for the formation of SAMs. They first formed the same melamine-PTCDI network on a Au(111) surface from a solution of DMF which gave higher surface coverage than under UHV conditions (see discussion above[176]). By working on a gold surface they were then able to form SAMs of alkane thiols corralled in the honeycomb cavity (see Figure 1.9a,b). Due to the template control of where the SAMs were formed and the stability of this network, it was even possible to further process the surface. Cu was selectively inserted at the SAM–substrate interface by underpotential deposition[179] (UPD, see Figure 1.9c), thus rendering the thiol-substrate bond even more stable.[180] Notably, the Cu-UPD occurred more readily in this hybrid system than for densely packed uniform SAMs. In later studies it was shown that the melamine-PTCDI hydrogen-bonded network acts as a diffusion barrier to the deposited Cu adatoms, limiting their presence on the surface to the 3.5nm pore.[181]

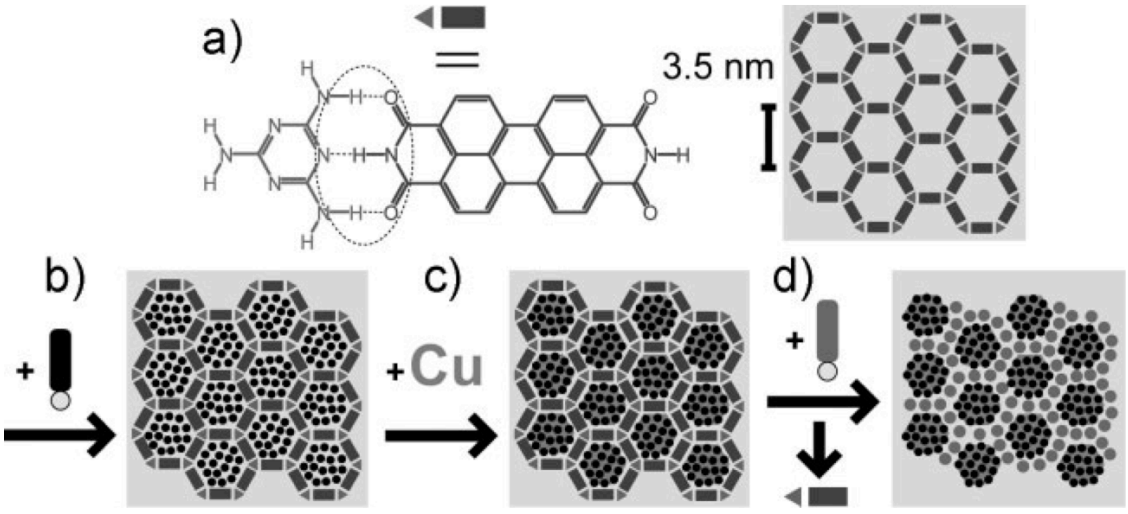

Figure 1.10: a) Three-fold H-bonding of melamine–PTCDI generates a regular hexagonal porous network on Au(111). b) Templated SAM formation of an aromatic-thiol. c) Cu UPD insertion d) addition of a second thiol substitutes the melamine-PTCDI sacrificial network. Image reprinted with permission from ref. [182]. Copyright 2010, Small.

The role of the melamine-PTCDI honeycomb is not just limited to a template. It can also be used as a sacrificial mask to generate binary self-assembled monolayers[182] (see Figure 1.10).

After formation of the network (Figure 1.10a) and templated SAM formation using an aromatic thiol (Figure 1.10b), the stability of the SAM islands was increased by Cu-UDP (Figure 1.10c). This allowed for a subsequent substitution of the network backbone with a second thiol, in this case adamantane-thiol (Figure 1.10d). This high level of processing relies on the stability of the SAM nanoislands in relation to further displacement or lateral diffusion by the second thiol, intimately controlled by the kinetics and thermodynamics of the binary SAM.

Chemical modification of the PTCDI monomers by substitution at the perylene core with adamantane thioether groups[183] results in two enantiomers when adsorbed on the surface.[184] Their statistical arrangement in the bimolecular honeycomb network gives rise to different pore geometries which yields pronouncedly different arrangmements of C_{60} molecules deposited in the cavities. These studies demonstrate the robustness of the triple-hydrgen bonded system and that bulky 3-D substituents can both be deposited and resolved by STM in the honeycomb network.

1.3.6 Outlook for molecules on surfaces

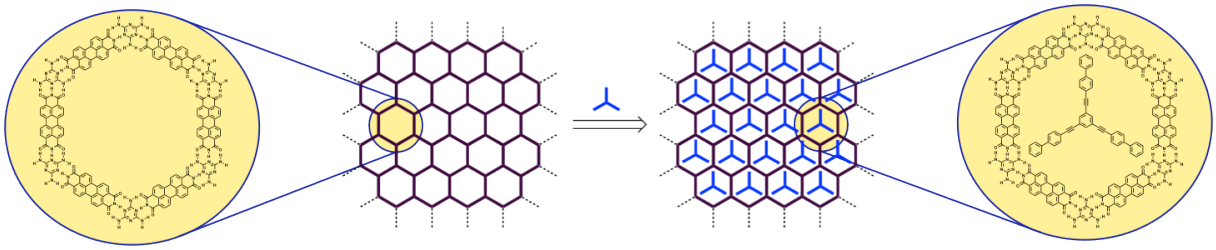

Figure 1.11: Schematic of a melamine-PTCDI honeycomb network with the pores filled with OPE star molecules. Zooms show the proposed molecular arrangement on an Au(111) surface with idealized geometry.

Using advanced techniques in phenyl-acetylene synthesis[185] we are currently investigating a series of star shaped guests for deposition into a melamine-PTCDI honeycomb network (see Figure 1.11). We hope to see rotation of the stars inside the cavities, and even to use the secondary pores formed to host another guest, achieving an unprecedented level of surface patterning and molecular control. By adding H-bonding moieties to the periphery of the star, these guests should influence the relative rate of molecular motion mediated through non-bonding interactions with the honeycomb network.

The selected examples described above highlight some of the latest developments in supramolecular surface science in the past half-decade. They demonstrate the amazing degree of control and precision hierarchical molecular systems have for tailoring the emergent properties of a surface.

In the following chapters we will expand upon these ideas and present examples of molecular systems that reward a careful design in their assembly. The tuning of the structural motif of single molecules in this way allows for the systematic evaluation of new structure-function relationships.

2 Building Blocks for Synthesis

Chapter2 presents in detail what constitutes an ideal building block, with concrete examples for the formation of both aryl and carbazole based molecules. The use of acetylene as a glue to attach them is vital to the methodology. Statistical Sonogashira couplings and their relative advantages are presented. Halide exchange to activate the carbazole reactivity is found to be particularly useful. Finally the chapter closes with a selection of collaborative examples applying the building block ideology to synthesis in the formation of polymers, dimers and a D–π–A systems.

2.1 Building Block Design

In order to design, and synthesize molecules for a particular function, we must have an available supply of building blocks that can be readily attached together. The concept of 'building blocks' as a simple, modular unit is wide spread in many different professions and has its foundations in the industrial revolution. It is the basis of the Henry Ford factory assembly line, in the construction industry it allowed for the fast assembly of pre-fabricated homes and even sky scrappers. Once a method was found for the reliable, fast and efficient formation of repeat units which could be added together, the accelerating effect this had on the rate of economic and societal progress was truly explosive. Perhaps even more importantly the products of this additive model became *more than the sum of their parts*. I believe that the field of organic synthesis is also going through such an upward, accelerating rate of progress from a similar basis. We now know enough about the relative reactivity and compatibility of functional groups to apply the same 'building block' principles to the synthesis of new molecules. The resulting compounds also very quickly take on emergent properties that could not be predicted solely through knowledge of the individual constituents' properties.

In realm of strategies for synthesis, much has been written on the use of protecting groups in organic synthesis, most notably all students of organic chemistry quickly become acquainted with "Greene's Protective Groups in Organic Synthesis, Wiley-VHC" the go to resource. Strategies for the use of PGs in synthesis are also widely discussed, however usually in terms of the particular functional group to be protected. Michael Schelhaas and Herbert Waldmann are notable for having classified PGs based on their lability[70], allowing for a more strategic approach to synthesis. Just as there are ideal properties for selecting protecting groups we can also describe the ideal properties required for the perfect building block.

The ideal building blocks for organic synthesis should be;

1. Scalable
2. Storable
3. Extendable
4. Compatible

Building blocks should be quickly and cheaply synthesised on a large scale, be stable to storage 'on the shelf' for an extended period of time, be modular and extendable to allow for fast branching to multiple targets, using FGs ideally without, but if necessary with suitable PGs that ensure tolerance to a wide variety of reaction conditions. A library of chemicals meeting these requirements can then be assembled to facilitate our ultimate goal, namely design for function, not structure.

The first stage in all the projects that will be covered in this thesis was to ascertain what building blocks do we have in hand, what building blocks might we need, and then to proceed to assemble them together in a modular fashion.

2.1.1 Acetylene as a glue

The phenyl-acetylene bond, as discussed in chapter 1, allows for a directly modular approach for the assembly of macromolecular structures. The acetylene moiety can be quickly and efficiently installed onto a molecule by Sonogashira cross-coupling and using the family of acetylene protecting groups (Figure 2.1) building blocks can be prepared with orthogonal reactivates.

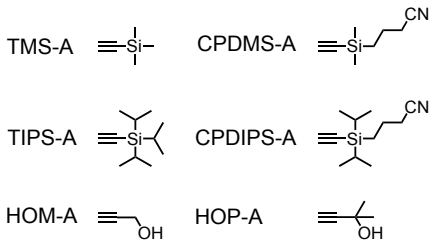

Figure 2.1: All common acetylene PGs used to install –C≡C– onto a building block in this thesis.

In this thesis we will make use of all these commercially available compounds; TMS-A, TIPS-A, HOM-A, and HOP-A. CPDMS-A[91] and CPDIPS-A[96] were both prepared following the literature procedures presented by Sigurd Höger who introduced these two compounds to the community. The yields are fairly consistent over many batches, and the product is quickly isolated by Kugelrohr distillation.

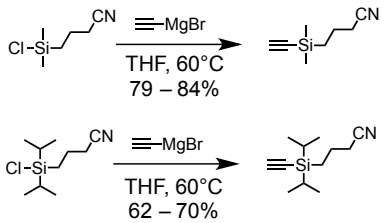

Scheme 2.1: Synthesis of CPDMS-A and CPDIPS-A

The other acetylene PGs discussed in section 1.2.6 from chapter 1, TMG-A and THP-DOPS-A groups were not investigated. THS-A is particularly useful for improving the solubility of compounds with a strong tendency to form π–π stacks, such as porphyrins.[20] Once these protected acetylenes are installed onto a building block they can be cleaved, usually quantitatively to reveal the free –C≡C–H which can be used in a further Sonogashira coupling to connect two complementary building blocks together. In this way the acetylene acts as a 'glue' to attach modular building block units together. As was discussed in section 1.2.2 often the most important consideration is which moiety should bear the Sonogashira leaving group (usually an aryl-halide) and which should have the free acetylene. Examples of this change of disconnection come up time and again in the following chapters. The flexibility to be able to swap the disconnection often means the difference between an impossible synthesis and a trivial one.

2.1.2 Phenyl-acetylenes: the modular approach

The phenyl ring is the most important functional unit in the class of organic materials properties we are interested in. The delocalised ring allows for conjugation between adjacent carbon atoms which gives rise to absorptions in the visible light spectrum, excited states that can relax by photoemission and the carrying of charge through space, either with electrons or holes. The degree of conjugation can be tuned by changing the electronic properties of the ring by the presence of electron-withdrawing (EWG) or electron-donating (EDG) groups. The substitution pattern on a benzene ring also influences the relative strength of these appended functional groups, with the strongest communication across the ring in the *para*-position, and much weaker conjugation in the *meta*- position. We can add alkyl chains directly to the ring in order to increase a molecules' solubility without strongly altering its electronic properties. However, alkyl chains will affect the bulk behaviour of an ensemble of molecules where inter-molecular interactions play a dominant role, such as the melting point, degree of crystallinity, and relative rates of relaxation from an excited state.[162]

The core starting block for extending the π-system of compounds in this thesis is 1,4-dihexyl-2,5-diiodobenzene **2.1** which is synthesised in two steps starting from cheap and widely available 1,4-dichlorobenzene (Scheme 2.2). The first step is a classic Kumada coupling using a nickel catalyst and n-hexyl Grignard. The hexylmagnesium bromide can be generated by stirring hexylbromide with magnesium fillings, or purchased pre-prepared as a 2.0M

solution in Et_2O from Sigma Aldrich. So long as the Grignard is fully formed there is no appreciable change in yield.

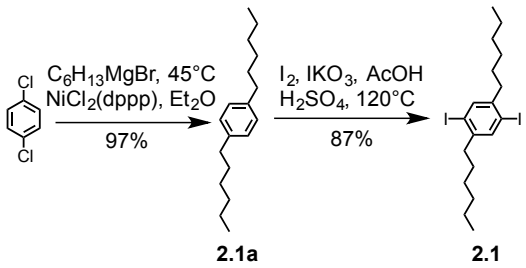

Scheme 2.2: Two step synthesis of 1,4-dihexyl-2,5-diiodobenzene

Different bis-phosphate ligands are available for the Ni(II) catalyst, the main difference is governed by the length of alkyl chain bridging the phosphines which alters the ligand byte angle. For this reaction the best results were obtained with a 1,3-bis(diphenylphosphino)propane (dppp) ligand. The reaction was found to proceed considerably slower with a 1,2-Bis(diphenylphosphino)ethane (dppe) ligand, and results in the formation of a considerable quantity of the mono-substituted product. The iodination to form **2.1** is complete overnight with the addition of sub-equimolar equivalents of IKO_3. Godt and co-workers[65] have reported an extensive study on the formation of mono-iodinated and regio isomers of **2.1**, but these side products can easily be removed by recrystallization.

2.1.3 Statistical coupling of acetylenes

As was discussed in section 1.2.7 the most useful phenyl-acetylene building blocks are asymmetric, allowing for the controlled assembly of different molecules to either end of the block. In this example we will use **2.1**, but the concepts are applicable to any symmetric aromatic building block. The symmetry is best reduced using a 'statistical' Sonogashira coupling procedure with a desired protected acetylene (Figure 2.2). Technically the product of the first coupling changes the reactive species, so the reaction is not truly statistical, but in practise the difference in reactivity is not noticeable, and we can therefore formally treat the reaction as if it were truly statistical in nature. In order to obtain an orthogonally protected building block the reaction can be made either stepwise, pathway A or sequentially, pathway B. The advantage of the one pot reaction, pathway A is that there is only one work-up, however in order to be able to have a chance of isolating the desired, orthogonally protected product, an excess of the second acetylene must be used.

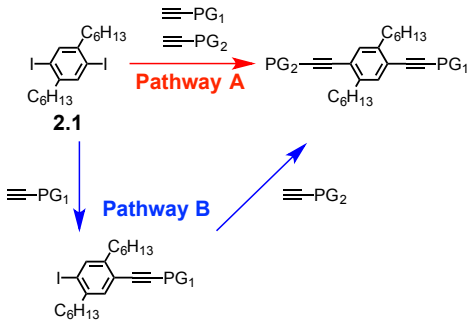

Figure 2.2: Two possible routes to the formation of an orthogonally protected building block by Sonogashira cross-coupling. Pathway A is a one pot, Pathway B is two steps with isolation of the intermediate species.

If this is not the case, then the number of species of mono-reacted compounds quickly exceeds your ability to isolate the separate products by column chromatography. The starting material, in this case **2.1** is consequently entirely used up, Figure 2.3. In the stepwise approach of pathway B, the first step leads to the formation of the same intermediates, but because the products are isolated after this first Sonogashira coupling the unreacted starting material **2.1** can be re-isolated and recycled in further reactions.

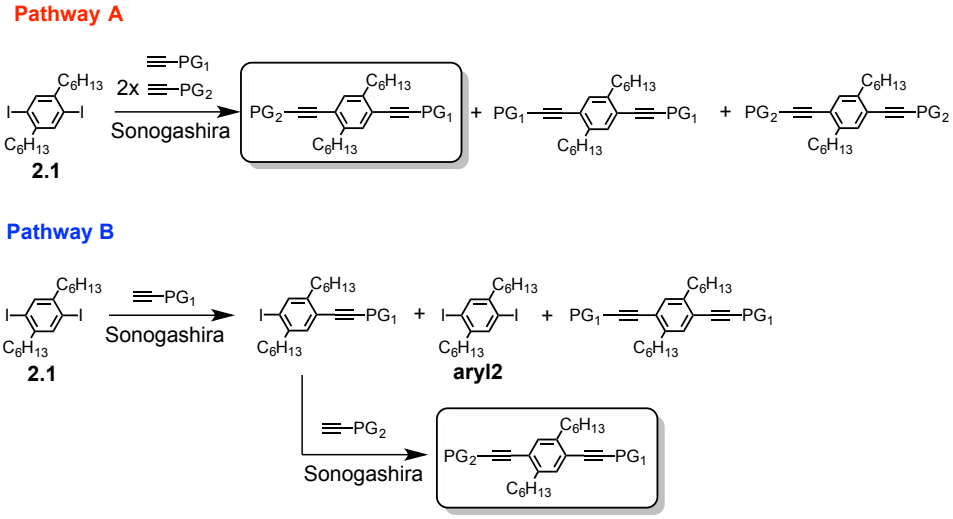

Figure 2.3: The harsh reality of statistical Sonogashira couplings is that you form a number of products which must be isolated. The two pathways have their own relative advantages and disadvantages

If the reagents are used with the corresponding ratio of **2.1** sm : PG_1-A of 1:1, and the reaction is truly statistical in nature, we would expect the product distribution **mono** : **sm** : **di-sub** of this first coupling to be 50:25:25. Experimentally this has been found to be the case, any discrepancies usually only occur when volatile acetylenes are employed such as TMS-A where the reactive species escapes before completion. However greater control of the product distribution can be made by using sub-equimolar equivalents of the acetylene relative to the

starting material. A large excess of the starting material favours the formation of the mono-substituted product. In practise a happy compromise of sm : PG_1-A of 1:0.7 leads to a high yield of the desired mono-substituted product as demonstrated in the formation of **2.2** (Scheme 2.3).

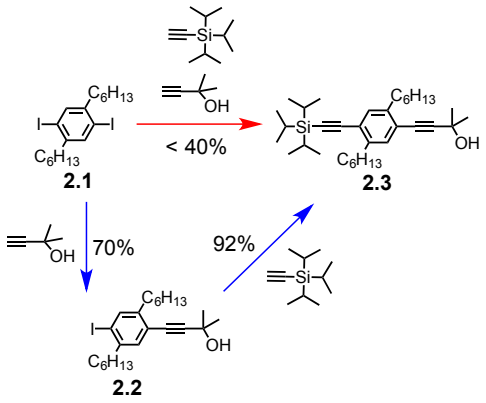

Scheme 2.3: Actual examples of the two pathways. All arrows represent Sonogashira cross-couplings with the following reaction conditions: $PdCl_2(PPh_3)_2$, CuI, DIPA, THF.

In conclusion we see that pathway A leads to a maximum yield of the orthogonally protected building block of < 40%. The stepwise approach of pathway B can lead to overall yields of the same product as high as > 60% over two steps, with the re-isolation of unreacted starting material. Ultimately the decision comes down to the availability of your starting material, and whether the extra time in isolation by column chromatography is paid back with the corresponding increase in yield. For readily available starting materials pathway A should be favoured, for precious starting materials pathway B should be preferred.

2.1.4 Generating a library of aromatic building blocks

Using the statistical Sonogashira coupling approach on 1,4-dihexyl-2,5-diiodobenzene **2.1** it was possible to generate a large library of aromatic building blocks with a range of sequentially labile and orthogonally protected acetylenes. These reactions also lead to the formation of symmetrically protected building blocks (Figure 2.4). The Sonogashira coupling of the whole range of available protected acetylenes was facilitated in this case by using a diiodo benzene moiety, the increased reactivity of iodine limiting the formation of diacetylene side products, as the homo-coupling usually occurs at slower rate. A catalyst system of $PdCl_2(PPh_3)_2$ (< 5 mol%) and finely ground CuI (< 5 mol%) in the presence of a degassed mixture of DIPA and THF for solubility gives complete coupling of the acetylene to the benzene building block.

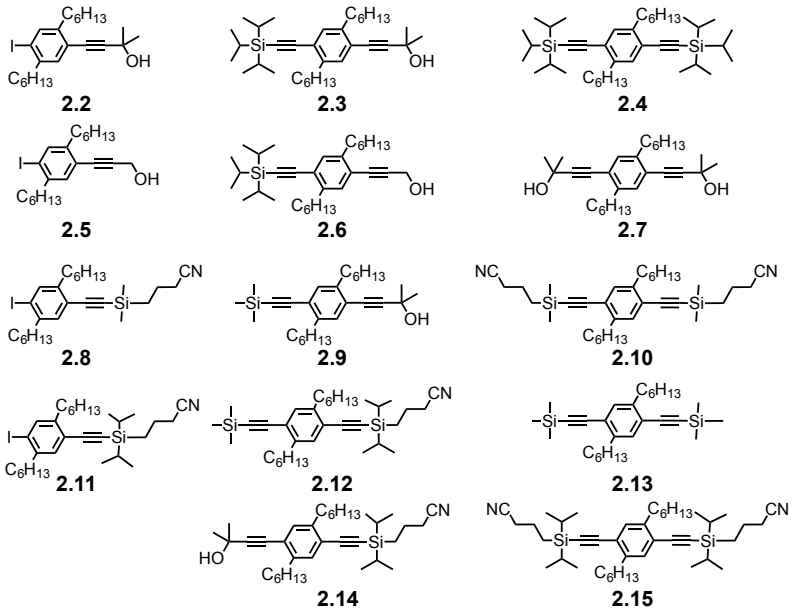

Figure 2.4: Library of building blocks synthesized, demonstrating the broad scope of available products using the statistical Sonogashira coupling procedure with different combinations of protected acetylenes. The left column contains mono-substituted polar acetylenes, the middle column are orthogonally protected and the right column are the corresponding di-substituted homogeneous building blocks. Full synthetic procedures can be found in the experimental chapter.

Applying our criteria for the ideal properties of a modular building block we can see that **2.2**, **2.5**, **2.8** and **2.11** are the most prized compounds in the library as they match well all four of our ideal requirements for the perfect building block. They can be formed in >20g scale, are stable for months on the bench and because of the combination of a free iodine FG and protected acetylene they can be extended in either direction. Lastly the acetylene PGs are also polar, allowing for easy purification of products by column chromatography on silica gel. The orthogonally protected building blocks are particularly useful as the PGs can be selectively removed in the presence of the other in high yield (Scheme 2.4).

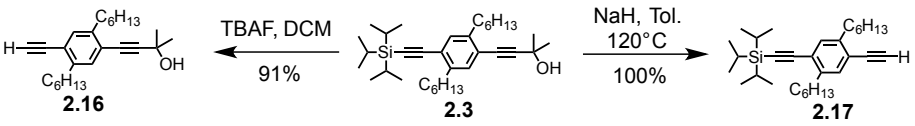

Scheme 2.4: The orthogonally protected building block 2.3 can be selectively deportected using standard conditions, in very high yield, leaving the alternate PG unaffected to afford 2.16 or 2.17.

2.3 can be subjected to either a fluoride source such as TBAF to afford **2.16**, leaving the polar tag HOP protecting group intact, or **2.3** can be treated with NaH in refluxing toluene to afford **2.17**, leaving the TIPS PG unaffected. As was discussed in section 1.2.6 of chapter 1 this concept of true orthogonality is much more powerful in synthetic design then sequential lability.

In the following chapters we will look at how this library of simple aryl monomer building blocks (Figure 2.4) can be applied to the formation of much larger π-extended molecules reaching the length domain of several nanometers.

2.2 Carbazole as a building block

Carbazole was first isolated from coal tar by C. Graebe and C. Glaser in 1872. It is still obtained industrially from coal tar in the thousands of tons per annum scale, or recovered as a side product from the industrial synthesis of anthracene on the 100,000 ton per annum scale, primarily for use in the synthesis of polymer dyes.[186] It has a very low toxicity with an LD_{50} values ranging from 200 mg/kg (mice) to 5000 mg/kg (rats) and it has no known carcinogenicity.[187] The extended π-system in carbazole, while not as strong as competing organic dyes such as porphyrins or phthalocyanines still leads interesting properties to carbazole containing compounds.[188] Carbazoles are widely found in industrial scale products such as polymers in the dye and emerging organic solar cell industry because carbazole is still stable at the elevated temperatures required in industrial process such as spin coating and annealing, a common post treatment for organic dyes.[189] This means carbazole is favoured over NDI and PDI polymer products because of its greater stability, it also much cheaper to synthesize than porphyrins.

2.2.1 Carbazole functionalization

The carbazole molecule can be functionalised at the -9*H* position under basic conditions by S_N2 reaction to give the alkylated product or used as the nucleophile in an S_NAr.[190] The simple alkylation proceeds cleanly in the presence of NaH and a polar solvent such as DMF.

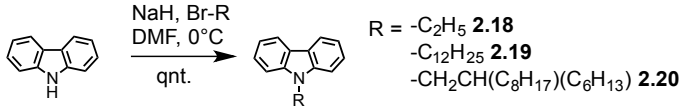

Scheme 2.5: Alkylation of 9*H*-carbazole under S_N2 conditions with NaH as base affords the product in quantitative yield.

Increasing chain length considerably reduces the melting point of the compounds, chains longer than C8 are liquid at room temperature. Branched chains, as found in **2.20**, prevent intermolecular π-π stacking. Some carefully selected alkyl chains have also been used to

engender liquid crystalline properties to the carbazole.[191] It is also possible to perform a 'statistical' alkylation using a di-bromo-alkyl chain such as 1,8-dibromoctane (Scheme 2.6). Using a large excess of the alkyl chain favours the formation of the mono-substituted species **2.21** over the totally doubly substituted chain **2.22**.

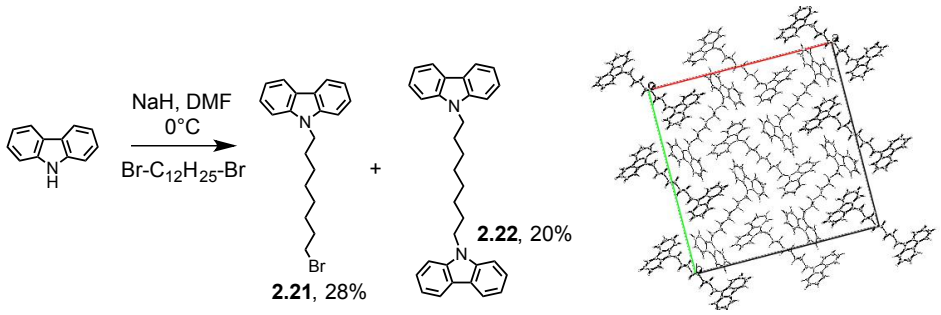

Scheme 2.6: Left: Alkylation by 'statistical' S_N2 substitution of 1,8-dibromoctane. The ratio of 2.21 to 2.22 could be further increased by using a large excess of the alkyl chain. Right: Corresponding crystal structure of 2.22 shows an alternating stack.

Functionalisation of the aromatic rings can be made by electrophilic aromatic substitution ($E_{Ar}S$) however the nitrogen at the centre directs exclusively to the 3,6- positions (Figure 2.5).

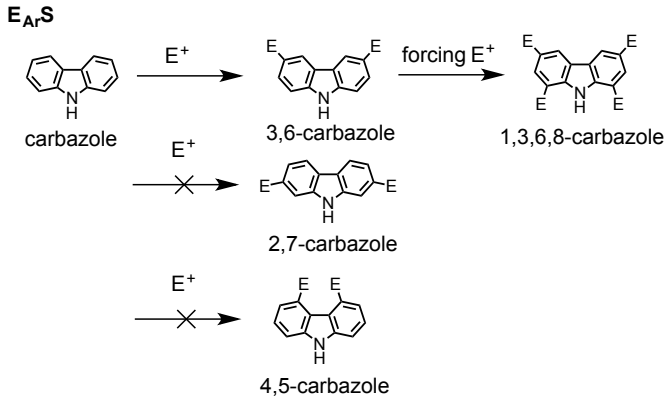

Figure 2.5: $E_{Ar}S$ of carbazole leads exclusively to the 3,6- substituted carbazole. More forcing conditions, usually with a Lewis acid present can give the tetra substituted 1,3,6,8-carbazole. It is not possible to functionalise exclusively the 2,7- positions. 4,5-carbazole is too highly strained to form.

This can be demonstrated using a Friedel-Crafts alkylation. Stirring carbazole with 2-chloro-2-methylpropane with zinc chloride as Lewis acid affords the expected 3,6- di-alkylated carbazole **2.23** (Scheme 2.7).

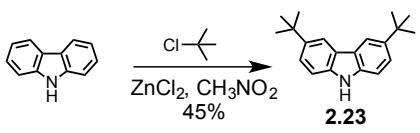

Scheme 2.7: Friedel-Crafts alkylation of carbazole showing the specificity of $E_{Ar}S$ for the 3,6-position

In order to obtain a 2,7- substituted carbazole the nitrogen heterocycle must be formed after the 2,7- substituents are already in place. 4,5- substituted carbazoles are too hindered to be formed, although 1,2,3,4,5,6,7,8-octa-chloro-9*H*-carbazole is catalogued in the Beilstein database from a Russian group from the year 1939. Nucleophilic aromatic substitution (S_NAr) is possible on a carbazole with substituents already in place that you wish to substitute, but it is even more difficult than on a benzene ring as the carbazole rings are already very electron rich, so an activated substrate is required.[192]

The Conjugation of 3,6 vs 2,7 across the biphenyl is quite different (Figure 2.6). 3,6-Carbazoles are *para* substituted with respect to the nitrogen heterocycle, and the predominant conjugation (red) of molecular orbitals therefore passes over the node of nitrogen. 2,7-Carbazoles have a weaker *meta* conjugation to the nitrogen and the molecular orbitals are predominately conjugated along the backbone of the two phenyl rings (green).

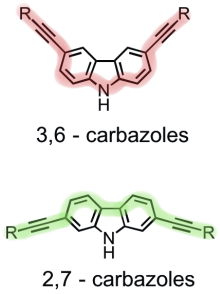

Figure 2.6: difference in conjugation path in 3,6- vs 2,7- carbazoles

This difference in conjugation path has implications for the photophyical properties of 3,6- vs 2,7- substituted carbazoles.[193] Kato et al.[194] have reported that if the substituents are also photo-active species such as thiophenes, the bathochromic shift in absorption and emission can become even further enhanced.

2.2.2 Synthesis of 2,7-substituted carbazoles

Carbazoles with a 2,7- substitution pattern are under represented in the literature, probably owing to the difficulty of their synthesis. However it is worth the extra synthetic effort, as the molar absorptivity of a 2,7-carbazole can be up to double that of the corresponding 3,6 carbazole.[195] All 2,7-carbozoles are made by formation of the nitrogen heterocycle between a biphenyl (Figure 2.7), and within that there are a couple of different approaches, usually on the route to forming carbazole based polymers as employed by Prof. Mario Leclerc,[196] a leader in this field.

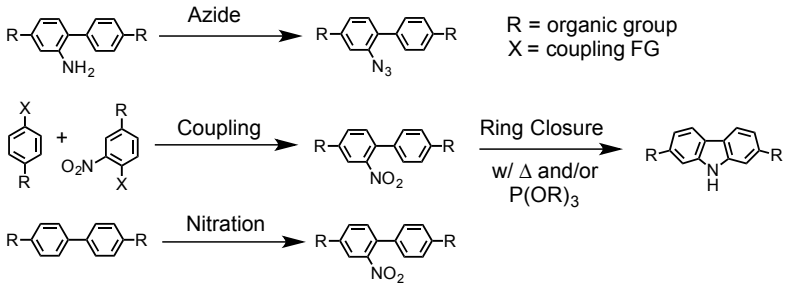

Figure 2.7: Methods towards the formation of 2,7-carbazoles all follow the same pattern, formation of a biphenyl accompanied by ring closure to form the nitrogen heterocycle.

Once a biphenyl is present with an amino group a common transformation is to convert the amine to an azide,[197] followed by heating to form the carbazole ring driven by the loss of $-N_2$.[198] The biphenyl can be formed from coupling reactions that are either palladium or copper catalysed including the common Stille[190] or Sukuki[199] couplings. Direct nitration of a biphenyl ring can also afford the precursor in good yield.[200] The ring closure is then made by reduction of the nitro group using an organo phosphane such as PPh_3 or $P(OEt)_3$.[201] These methods normally afford the symmetric carbazole product.

In order to obtain the most modular building block as an expandable 2,7-carbazole (Scheme 2.8) it is tempting to combine two different aryls in the first step by a copper catalysed Ullmann type cross coupling[202] to form biaryl **2.25**. The carbazole **2.26** can then be formed in a Cadogan ring closing reduction of the nitro group using triethyl phosphate.

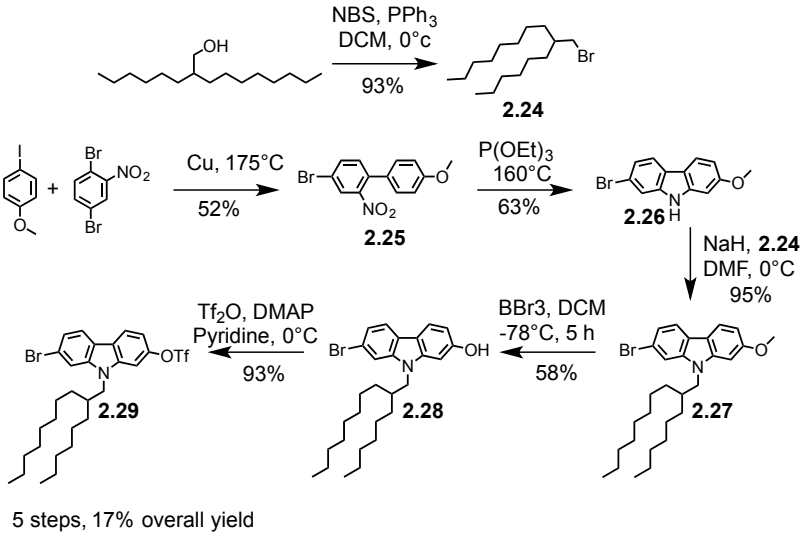

Scheme 2.8: Five step synthesis of asymmetric 2,7-carbazole 2.29.

The -9*H* carbazole **2.26** can then be alkylated using the standard NaH, DMF conditions in good yield. The alkyl chain **2.24** is branched to prevent π-π stacking, and asymmetric to allow for the possibility of forming a glassy or even liquid crystalline phase.[203] The

commercially available alcohol is transformed into a halide leaving group using an Apple reaction.[204] The methoxy group from **2.27** can be removed[205] using BBr_3 as a strong Lewis acid to reveal the free –OH group in **2.28** which can then be transformed into a good leaving group[203] for Sonogashira cross couplings by condensation with trifluoromethanesulfonic anhydride to afford the target asymmetric carbazole **2.29** in five steps with an overall yield of 17%. Kamikawa *et al.*[206] have reported on the difficulty of achieving a selective acetylene coupling of a triflate in the presence of a bromine and this compound was not utilised further.

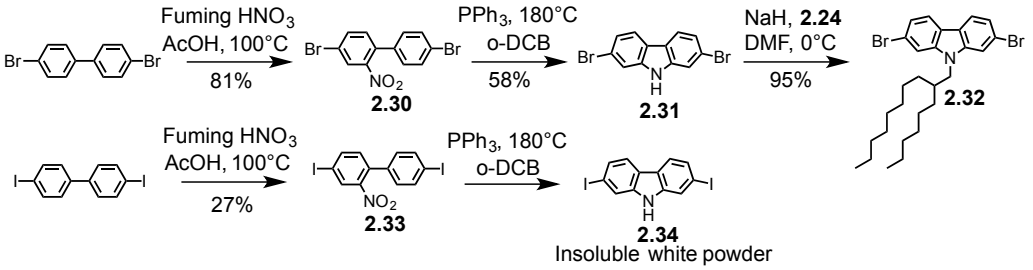

Scheme 2.9: Synthesis of a symmetric carbazole building block 2.32 starting from dibromobenzene. Using diiodobenzene is difficult due to the reduced solubility of the product formed.

An alternative approach to form a suitable carbazole building block is to form a symmetric 2,7-carbazole and then perform a subsequent statistical Sonogashira coupling to break the symmetry of the molecule. The advantage of this approach is that the five steps can be reduced to three, and the reactions can be performed on up to 20 g scale without difficulty (Scheme 2.9).

Starting from dibromobiphenyl nitration with fuming nitric acid affords **2.30** within 30 min.[200] It is important to use such a strong nitric acid, as with the more often used 37% or even 90% nitric acids the yields are very poor. Over nitration on the second ring gives rise to a second spot by TLC but in the subsequent Cadogan ring closing reduction both starting compounds give the same product **2.31**. The formation of the *N*-heterocycle is reported to be most dependant on the temperature of the reaction,[201] using a sand bath and a very high boiling solvent such as *o*-DCB ensures an acceptable yield. Alkylation of **2.31** affords the desired symmetric 2,7-dibromo-9-(2-hexyldecyl)-carbazole **2.32** after three steps in a 45% overall yield, a considerable improvement over the asymmetric route presented above. Attempts at replicating this synthesis with the same conditions using diiodobenzene were frustrated by the very low solubility of the iodinated biphenyl products **2.33** and **2.34**.

2.2.3 Sonogashira coupling to carbazole

With the symmetric carbazole building bock **2.32** in hand, attempts were made to break the symmetry by mono-acetylation using Sonogashira cross couplings. Initially TMS-A was applied using the standard $PdCl_2(PPh_3)_2$, CuI, DIPA catalytic system (Scheme 2.10), however it was not possible to separate the very non-polar products **2.35** and **2.36** from each other, or from unreacted starting material. Moving to the polar protecting group CPDIPS-A after an extended reaction time and elevated temperatures yielded **2.37** in only 7%. The low reactivity of **2.32** under the applied conditions is most probably due to the electron rich π system which disfavours the first oxidative addition of Pd.

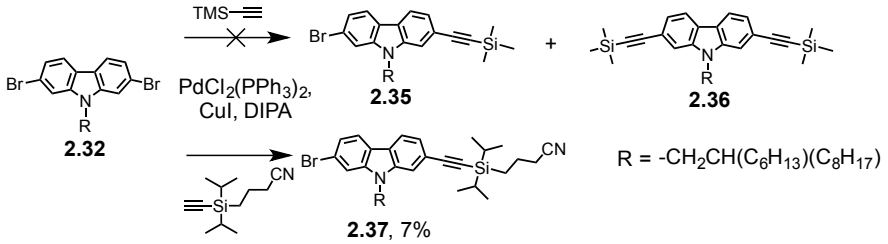

Scheme 2.10: De-symmetrisation of 2,7-dibromo-9-(2-hexyldecyl)-carbazole 2.32 using TMS-A lead to inseparable mixtures of 2.35 and 2.36. Applying the polar CPDIPS-A using the standard catalyst system of $PdCl_2(PPh_3)_2$, CuI, DIPA, THF gave poor yields of 2.37.

Therefore a range of palladium catalyst ligands were investigated. Palladium tetrakis triphenylphosphine $Pd(PPh_3)_4$ gave the best results so long as the reaction was held at 80°C overnight (Scheme 2.11). With these improved conditions the de-symmetrised **2.37** could be isolated in >40% yield. In order to broaden the range of available carbazole building blocks available, other polar protected acetylenes were also investigated.

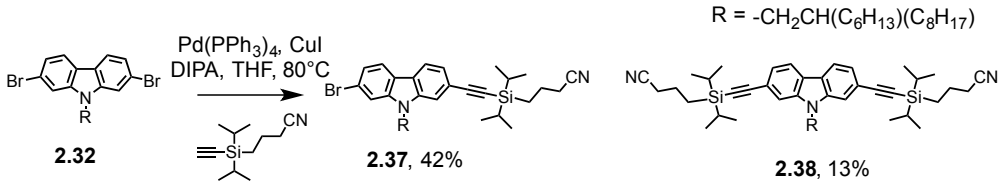

Scheme 2.11: Successfully de-symmerterised 2.37 was achieved by swapping in $Pd(PPh_3)_4$, and elevating the temperature. The di-substituted carbazole 2.38 could also be isolated from the reaction mixture.

HOP-A could also be coupled to **2.32** to give a statistical mixture of mono-substituted carbazole **2.39** in 43% and di-substituted carbazole **2.40** in 27% yield (Scheme 2.12). In order to discover the limits of reactivity of the **2.32** di-bromo building block to Sonogashira cross

couplings, several test reactions to drive the coupling to the di-coupled product were made (Scheme 2.12).

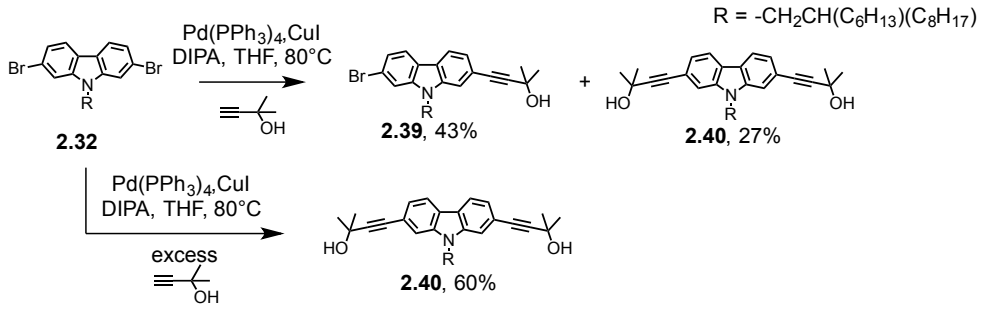

Scheme 2.12: The building block 2.32 could be expanded by coupling with HOP-A.

Under the best conditions still only 60% yield of **2.40** could be achieved, and after extending the reaction time and increased catalyst loadings, the starting material was still recovered with minimal de-halogenation. Performing the cross-coupling under microwave conditions saw no improvement in the yield, although it did reduce the reaction time required.

This would appear to highlight the low reactivity of the carbazole species towards the first oxidative addition step required in the Sonogashira catalytic cycle. An interesting corollary to this hypothesis presented itself when trying to synthesize the asymmetric 2-(ethynyl-HOP)-7-(ethynyl-CPDIPS)-9-(2-hexyldecyl)-carbazole **2.41**. Depending on whether the reaction was made starting with the 2-Bromo-7-(CPDIPS-A) carbazole **2.37** or the 2-Bromo-7-(HOP-A) carbazole **2.39** dramatically different yields of **2.41** are achieved (Scheme 2.13).

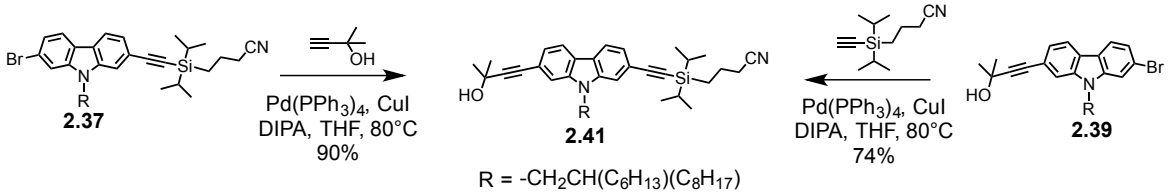

Scheme 2.13: Depending on the approach to synthesise 2.41 a dramatic change in yield is observed.

This nuance would indicate that the acetylene protecting groups are influencing the electronics of the carbazole ring to such an extent that the degree of oxidative addition is altered. The CPDIPS group has an EWG effect which accelerates the rate of oxidative addition by making the Br-Aryl bond more polarised. The HOP group has an EDG effect which supresses the rate of oxidative addition, reducing the expected yield. This ability of the acetylene PG to play a role in the reactivity of a species should be taken into account during the design of synthetic pathways.

2.2.4 Halogen exchange on carbazole building blocks

Another way to increase the yield of Sonogashira cross-couplings is to use a better leaving group. The attempted direct synthesis of 2,7-diiodo carbazole **2.34** was discussed above (Scheme 2.9). Therefore attempts were made to perform halogen exchange on **2.32** from bromine to the more reactive iodine species. Tim Swager and co-workers[207] have reported a successful halogen exchange of a 2,7-dibromo-9-octyl-carbazole by lithium exchange at -78°C with *n*-BuLi quenching with I_2 in a reported yield of 45% after recrystallization. Our target building blocks have much longer alkyl chains to aid the solubility of larger architectures and are therefore liquids, so must be purified exclusively by column chromatography. Due to this limitation the highest yield obtained of **2.42** was only 24%, with mixed fractions of mono-substituted and de-halogenated product, not to mention the difficulty in separating compounds with such similar R_f on silica gel. First quenching the lithiated species with TMS-Cl, followed by treatment with ICl as reported by Dane et al.[208] might allow for an easier purification over two steps.

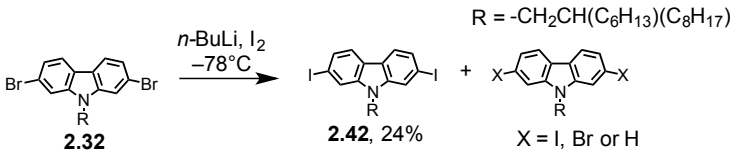

Scheme 2.14: Lithium halogen exchange leads to low yields of the desired diiodo halogen 2.42 due to a mixture of side products obtained.

An alternative method to perform halogen exchange is the well known Finkelstein reaction which is effective for the transformation of alkyl-halides. Buchwald and co-workers[209] reported in 2002 an aromatic version of the Finkelstein reaction using CuI in the presence of a diamine ligand and the corresponding halide salt. Surry et al.[210] have reviewed this aromatic-Finkelstein reaction, concluding that the standard conditions of CuI, NaI and one of three principle amine ligands (listed right hand side of Scheme 2.15) can effect the transformation of Ar-Br to Ar-I in most cases. Occasionally it is necessary to vary the di-amine ligand depending on the substrate to obtain the best results. The reaction appears to be driven by the relative solubility of the Na-halide salt. Using solvents that NaBr is poorly soluble in such as dioxane and avoiding polar solvents such as DMF where it is more soluble, drives the substitution of Ar-Br for Ar-I due to the precipitation of NaBr. The reaction requires elevated temperatures and is usually performed in a sealed tube. The removal of oxygen is vital to ensure that the copper catalyst remains active.

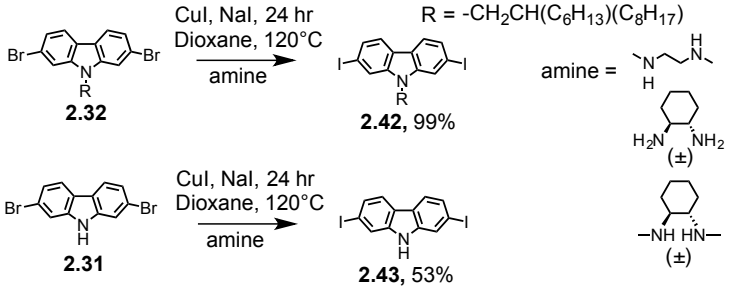

Scheme 2.15: Applying Buchwald-Finkelstein type conditions to our carbazoles affords the diiodo carbazole 2.42 in quantitative yield after only an extraction. The yield of 2.43 is reduced owing to its very low solubility.

In our hands the transformation of dibromo carbazole **2.32** to diiodo carbazole **2.42** could be effected in 99% yield after extraction, and was elemental analysis pure (Scheme 2.15). Applying the same conditions in an attempt to form diiodo-9*H*-carbazole **2.43** yielded the product in 53% yield, principally due to the very low solubility of this compound. This copper catalysed aromatic substitution is a powerful tool to perform halogen exchange and will prove invaluable in the formation of carbazole based nanoscale architectures, as is presented in chapter 4.

2.3 Applying Building Blocks in Synthesis

Below are some selected examples of projects that used the building blocks presented here in short reaction sequences which were made in collaboration with others. They give a flavour for what is possible with the building block approach to synthesis. More involved examples are presented in chapters 3, 4 and 5.

2.3.1 Monomers for Polymer dispersion of SWCNT

Single-walled carbon nanotubes (SWCNTs) are promising additives for opto-electronic devices, however the separation by size and between metallic and semi-metallic tubes is required before they can be applied. Extending the work with our collaborators at Karlsruhe Institute of Technology (KIT)[211–214] we have synthesised a series of monomers for incorporation into fluorene and carbazole based polymers used in the selective dispersion of SWCNTs. The synthesis of polymers from monomer building blocks is perhaps the easiest application of the building block methodology to synthesis.

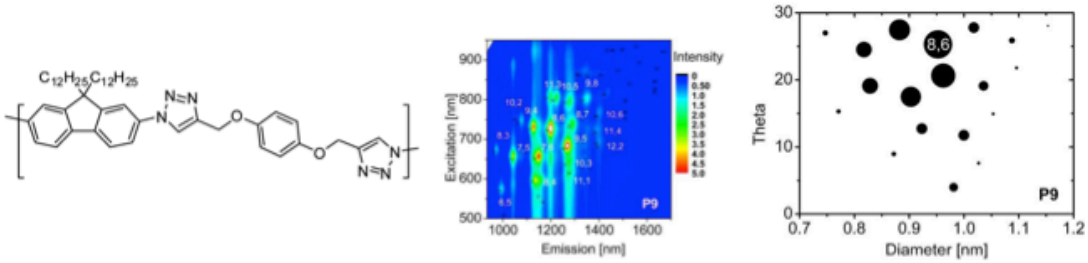

Figure 2.8: A polymer structure investigated (left) was used to disperse SWCNTs in solution. A 2D fluorescence density map (centre) is used to assign the selectivity of the dispersed SWCNTs (right). Images reproduced with permission from ref. [215]. Copyright 2012, Polymer Chemistry.

This work was recently published in Polymer Chemistry[215] where we broadened the synthetic routes available to make such CNT selective polymers. We also looked at the effect of increasing and alternating electron density in the polymer backbone.

The synthesis of monomers containing terminal acetylenes is shown in Scheme 2.16. 1,4-bis(Prop-2-yn-1-yloxy)benzene **2.44** and 1,5-bis(Prop-2-yn-1-yloxy)naphthalene **2.45** were synthesised by reacting hydoquinone and 1,5-dihydroxynapthalene respectively with propargyl bromide under basic conditions of K_2CO_3 in MeCN. 1,4-Diethynyl-2,5-dihexylbenzene **2.56** was synthesised in four steps starting from 1,4-dichlorobenzene following a literature procedure.[216],[217],[218]

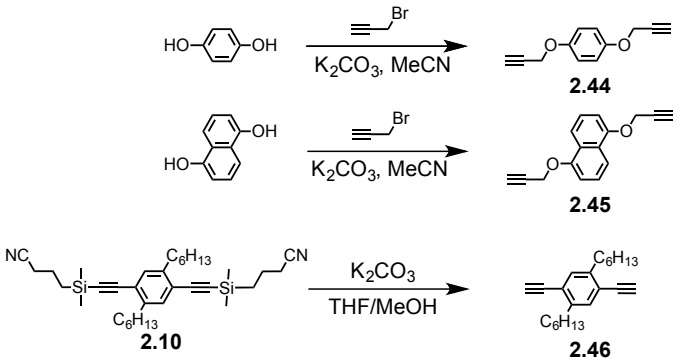

Scheme 2.16: Synthesis of acetylene monomers for use in azide-click polymerisation to form polymers suitable for the dispersion of SWCNTs.

These acetylene monomers were then used by our collaborators in KIT to generate a library of polymers by preforming azide-click polymerisations, as a faster route than the more traditional Suzuki based polymerisations. For the interested reader, the Polymer Chemistry paper is reproduced in full as an appendix to at the end of this thesis.

2.3.2 Push-pull carbazoles in D–π–A systems

In order to investigate conjugated π-systems the 2,7-carbazole building blocks presented in section 2.2.3 were coupled two together to form carbazole dimers. Daniel Ebner, a Wahl Praktikum student under my supervision made an ethyl form of building block **2.41** (Scheme 2.17). Removal of the CPDIPS PG with TBAF and subsequent Sonogashira coupling forms an orthogonally protected asymmetric dimer building block. After a sequence of deprotection and coupling steps this gives access to a series of D–π–A carbazole dimers.

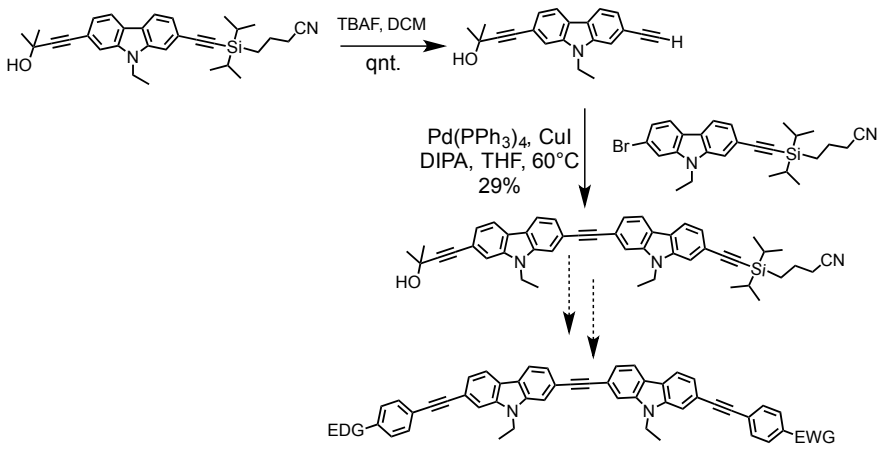

Scheme 2.17: Carbazole dimers synthesized by Daniel Ebner during a Wahlpraktikum in the Mayor group to investigate push pull systems in extended carbazole based dimer rods.

The building block methodology allows for the fast derivatization to form libraries of interesting compounds. Once a library has been synthesised, systematic investigation of the compounds leads to comprehensive insights into the relationship between the underlying molecular structure and its properties.

Structure-property relationships can also be studied on monomers of carbazole. Together with Samuel Egli, a Masters student in the mayor group, we set out to apply the building block methodology to investigate the variations in photophysical properties between 3,6- and 2,7- D–π–A carbazoles in a systemic way. We obtained twelve 2,7-substituted carbazoles and eight 3,6-substituted carbazoles. It was also possible to form a cross-substituted 2,3,6,7-push-pull carbazole (Figure 2.9).

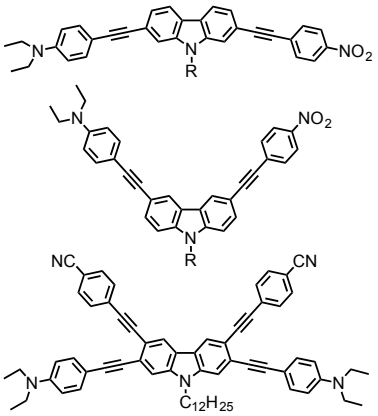

Figure 2.9: Sample of D–π–A carbazoles synthesised by Samuel Egli using the building block approach.

The photo-physical investigations confirmed our hypothesis that the 2,7-substituted carbazoles show a stronger conjugation over 3,6- carbazoles owing to the difference in conjugation path (Figure 2.10). The 2,7- carbazoles are red-shifted in both adsorption and fluorescence compared to the corresponding 3,6- carbazoles. X-ray crystal determinations of two of the ethyl chain carbazoles could also be obtained.

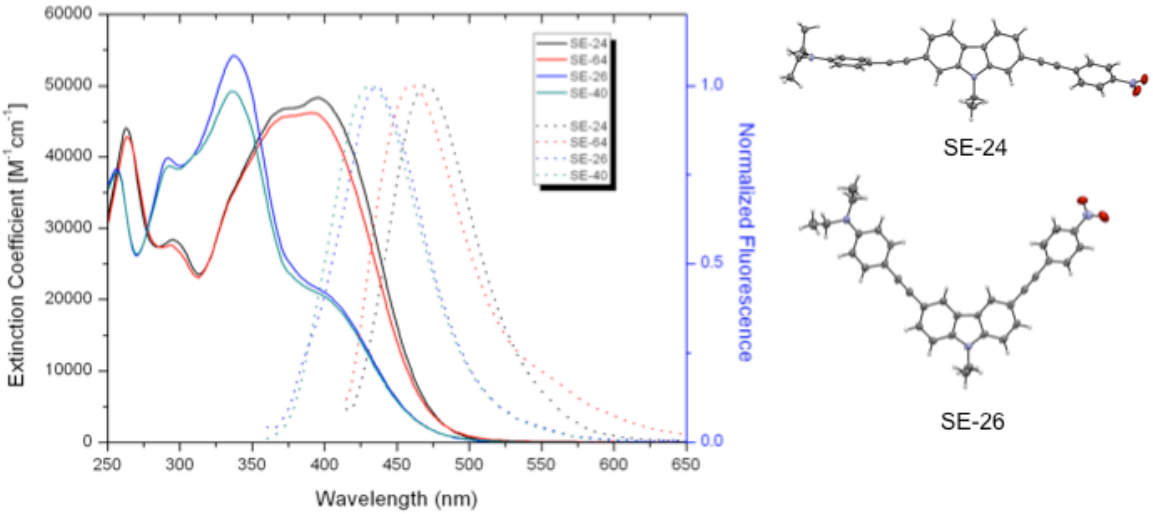

Figure 2.10: Reprints from the masters thesis of Samuel Egli of photophysical studies on 2,7- and 3,6- carbazoles synthesised using the building block approach. Right: crystal structures of carbazoles SE-24 and SE-26 obtained by Dr. Markus Neuberger.

The synthetic details for these compounds can be found in Samuel Egli's Masters thesis. The results demonstrate that using acetylenes attached to suitable building blocks is a viable method to investigate structure-property relationships in small molecules. In the following chapters we turn our attention to the assembly and characterisation of rather larger nanoscale molecules.

2.4 Conclusion and outlook:

The ideal building block for organic synthesis should be scalable, storable, extendable and compatible to the synthetic route. The assembly of nanoscale architectures requires a method for the modular assembly of these building block which can be achieved using phenyl-acetylene and Sonogashira cross-couplings. We have seen that it is possible to de-symmetrise an aryl or carbazole moiety by performing statistical couplings of protected acetylenes. In this way a large library of building blocks can be assembled.

Carbazole is an interesting molecular component for synthesis, and the two substitution patterns have altered electronic properties. The 3,6-carbzoles are accessible via direct electrophilic aromatic substitution, where as 2,7-carbazoles must be formed by Cadogan ring cyclisation. Once an acetylene protecting group is attached to carbazole it was found to influence the electronics of an adjacent aromatic system and has consequences for the yield of Sonogashira cross couplings. Halide exchange from bromide to iodide can greatly increase the reactivity of the carbazole to cross-couplings.

The building block methodology can be applied to access tailored monomers as part of polymer synthesis, leading to our published results on the dispersion of SWCNTs. Dimers and interesting D–π–A carbazoles were also made, allowing for the systematic investigation of the effect structure and substitution pattern has on the observed physical properties. In the next chapters we turn to more involved examples that use the aryl and carbazole building blocks presented above.

3 Molecular Wires: OPE Rods & Stars

Chapter 3 presents the application of the building block method to synthesize functional nanoscale molecules for applications in the field of molecular electronics. Starting with very small aryl-sulphur molecular rods we expand the oligomer length to over 6 nm. The relative advantages of a divergent versus convergent synthetic approach are discussed in detail, before we report the synthesis of a three-armed star for application in a novel three-terminal device, making extensive use of recycling GPC and sophisticated NMR studies for their purification and characterisation.

3.1 Single molecule wires

The field of Molecular Electronics is as broad as it is complex. At the heart of the topic is the meeting of the classical ideas of electrical components and a macroscopic physical picture of their workings, with the microscopic quantum picture of atomic components. It is a multi-disciplinary field requiring the expertise of those trained as physicists to both utilise and develop new physical methods to integrate molecular length scale components with chemists, and increasingly biological scientists, who synthesis the individual components that are at the heart of any measurement.

The contacting of single molecules between electrodes allows for the formation of single-molecule based devices.[219] Initially the field was started with the hypothesis from Aviram and Ratner in 1974 that a single molecule with a D–π–A system with the right HOMO and LUMO levels could act as a single-molecule rectifier.[220] Since then single-molecule devices have been extensively studied,[221] showing both diode[222] and switching[223] behaviour in molecular junctions. Length dependence of alkanethiols has been well reviewed by Frisbie et al. [224][225] Long wires from a surface studied by STM have even been explored with regard to the extent of lateral coupling of π-orbitals to the underlying gold surface,[226] demonstrating the high degree of control that the underlying molecular structure has on the observed physical properties, and therefore function.

It was our aim to further the state of the art from a chemical perspective. This can be done by focusing on single molecule experiments that explore the fundamental nature of the physical processes at work. The Mayor group have previously reported on the direct influence of biphenyl torsion angle on the conductance of an single-molecule rod.[227,228] We set out to synthesis a molecular wire for integration in a novel Aharonov–Bohm effect set-up,[229] where the molecular wire is located in a junction with an applied magnetic field, altering its degree of conductance. We also explored the formation of a three arm molecule to integrate into a novel molecular device.[230]

3.2 Synthetic approaches to an organic single-molecular wire

The most simple organic wire is made from a single bezene molecule with two sulphur groups attached (1,4-benzene-dithiol) in order to have a strong electronic coupling to the Fermi level of gold electrodes. Increasing the length of the rod, or introducing other FGs

affects the degree of conductance.[231] The choice of anchor group has therefore traditionally been sulphur, although other anchor groups are now being widely explored such as isocyanates.[232] In this work we stick with the traditional thiol anchor group in order to allow easy comparison of our results with others reporting in the field.

3.2.1 OPE and OPV rods

In order to lengthen the molecule from 1,4-benzene-dithiol, we can insert acetylene between the benzene core and the sulphur anchor groups by coupling phenyl-acetylenes bearing acetyl protected sulphur anchor groups to 1,4-diiodo-benzene (Scheme 3.1).[56]

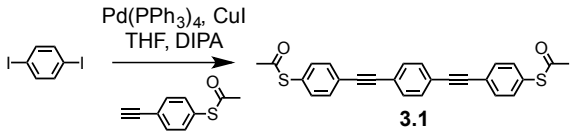

Scheme 3.1: Sonogashira coupling provides a convergent route to form OPE 3.1 by coupling 1,4-diiodobenzene to 4-ethynylphenyl-ethanethioate.

The linear OPE rod **3.1** has been extensively studied in MCBJ setups, and in this case was synthesised and sent to Prof. Bert Hecht, University of Würzburg for investigation together with the complementary OPV rod **3.2**, stored in the group (**Error! Reference source not found.**). The desired anchor group for physical investigation is the free thiol R–SH, and it would therefore be preferable to have in hand the free thiol rods, however in practise this FG is readily oxidised to the dithiol R–S–S–R, and leading here to extensive polymerisation. R–SH rods are therefore commonly stored with an acetyl PG. Molecular break junction measurements have been made directly onto acetyl protected sulphurs,[233] but you can also perform an in situ deprotection of the acetyl to obtain the free thiol in solution. The important thing is that the free thiol is not exposed to oxygen, including that dissolved in the solution used to make the physical investigations with.

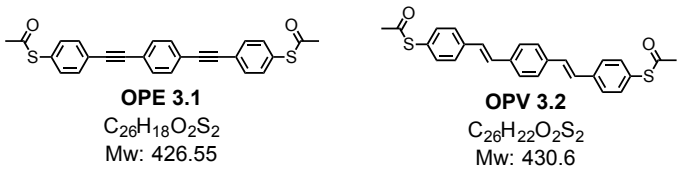

Figure 3.1: OPE 3.1 and OPV 3.2 sent to Prof. Bert Hecht for physical investigation

Insitu Deprotection:

The following protocol is adapted from the available literature and is recommended for in situ deprotection of the thiol acetyl: First dissolve the compound in a suitable solvent ($CHCl_3$,

CH_2Cl_2, or THF are best) which has been purged of oxygen by bubbling argon through the solution for at least 30 min per 500 mL. With less solvent a shorter time is okay, with more, longer. Solvent should be freshly prepared in this way immediately prior to use and not used after storing. Then either;

- For SAM formation (mono-deprotection) treat with 15% by volume degassed Et_3N stirring for 24hr or Bu_4NOH for 40 min (but leads to incorporation of the amine salt to SAM) see Hummelen and co-workers[234] for details and quantities.

- For complete deprotection and/or ligand exchange add 10% aqueous solution of H_4NOH and stir under argon for 24hr. (10 μL of base solution to 2 mL of a 1 mmol solution in THF of the thiol acetyl rod). see Mangold et al.[235]

The two rods, OPE **3.1** and OPV **3.2** sent to Prof. Bert Hecht, University of Würzburg have comparable solubility. Chloroform, dichloromethane and tetrahydrofuran will dissolve the compounds fully, in sufficient dilution. The kinetics of solvation are quite slow and sonication helps to dissolve higher concentrations. We are currently awaiting the results of their investigations.

3.2.2 Bridging larger gaps

These short rods are ideal for study from solution in MCBJ setups, where the junction to be bridged is spontaneously formed in solution, however in order to bridge electrodes that are formed on a device or surface from lithography techniques much longer molecules are required. In collaboration with KIT for the physical measurements in a novel Aharonov-Bohm set-up, we targeted the synthesis of OPE rod **3.3**, to bridge a lithographically obtained junction. They required a linear rod of at least 6 nm for testing in their set-up. The terminal sulfur groups are to be left protected by an acetyl group to ensure the stability of the compound in storage prior to deprotection at the time of the physical measurements.

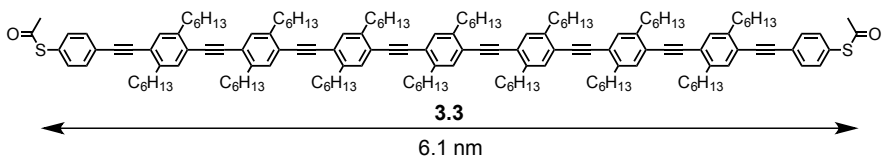

Figure 3.2: OPE rod 3.3 modelled by MM2 to have a length of 6.1nm sulphur–sulphur.

There are two synthetic approaches to build-up such long rods, the Divergent approach or the Convergent approach (see section 1.2.10, chapter 1 for a discussion of their relative advantages and disadvantages). The OPE length will ultimately be limited by its solubility. Formation of 16-mers is reported, but solubility was a major issue at the octomer.[236] The divergent approach is appealing because of the iterative nature which should obtain the target compound **3.3** in a series of deprotection, coupling steps starting from our building block **2.7** introduced in chapter 2 and this route was investigated first (Scheme 3.2).

Quantitative removal of the HOP PG is achieved using the standard conditions of NaH in refluxing toluene to afford **3.4**. The Songashira coupling was performed under standard conditions with the asymmetric building block **2.2**. These steps were repeated three times prior to a final coupling of **3.8** with the protected sulphur building block **3.9** to obtain the target OPE **3.3** in a poor overall yield of 0.47% in a linear sequence of nine steps from commercially available material.

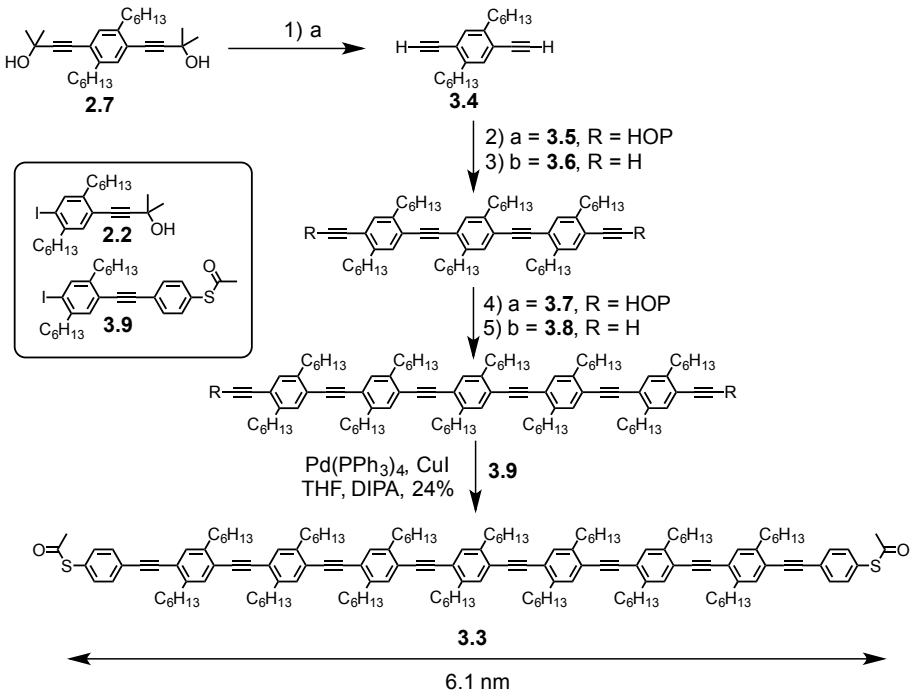

Scheme 3.2: Divergent synthesis of 3.3 through an iterative series of deprotection, coupling steps starting from building block 2.7. Conditions: a) 2.2, $PdCl_2(PPh_3)_2$, CuI, DIPA, THF, rt, 16 hr. b) NaH, Toluene, 120°C, 1 hr. Yields: step 1, 100%. 2, 22%. 3, 100%. 4, 20%. 5, 100%.

This very low overall yield of the divergent route can be explained by the formation of many homo-coupled products giving rise to difficult separations on silica gel and lousy yields of around 20% at each coupling step even after repeating the reactions with a more vigorous freeze-pump-thaw degassing method. The deprotection of the 2-Methyl-3-butyn-2-ol (HOP) appears to proceed in quantitative yield but the di-acetylenes formed are very unstable,

changing colour quickly if left open to air and require purification with degassed solvent on a plug of SiO_2. With these synthetic and purification difficulties found in the divergent approach, we turned our attention to a convergent synthesis.

As the convergent route must begin with the sulphur anchor group on the end of the rod, a ^{t}Bu PG was used by coupling tert-butyl(4-ethynylphenyl)sulfane with building block **2.2** to give **3.10** quantitatively (Scheme 3.3). This PG was chosen because the ^{t}Bu protected sulphur has been found in the Mayor group to be more stable than the corresponding acetyl protected sulphur, giving higher yields under Songashira coupling conditions. A further deprotection and coupling sequence was carried out to extend the rod to three hexyl benzenes in length, **3.15**. This time a microwave reactor was also used for the coupling reactions to speed up the reaction times, although the yields were unchanged from the traditional coupling.

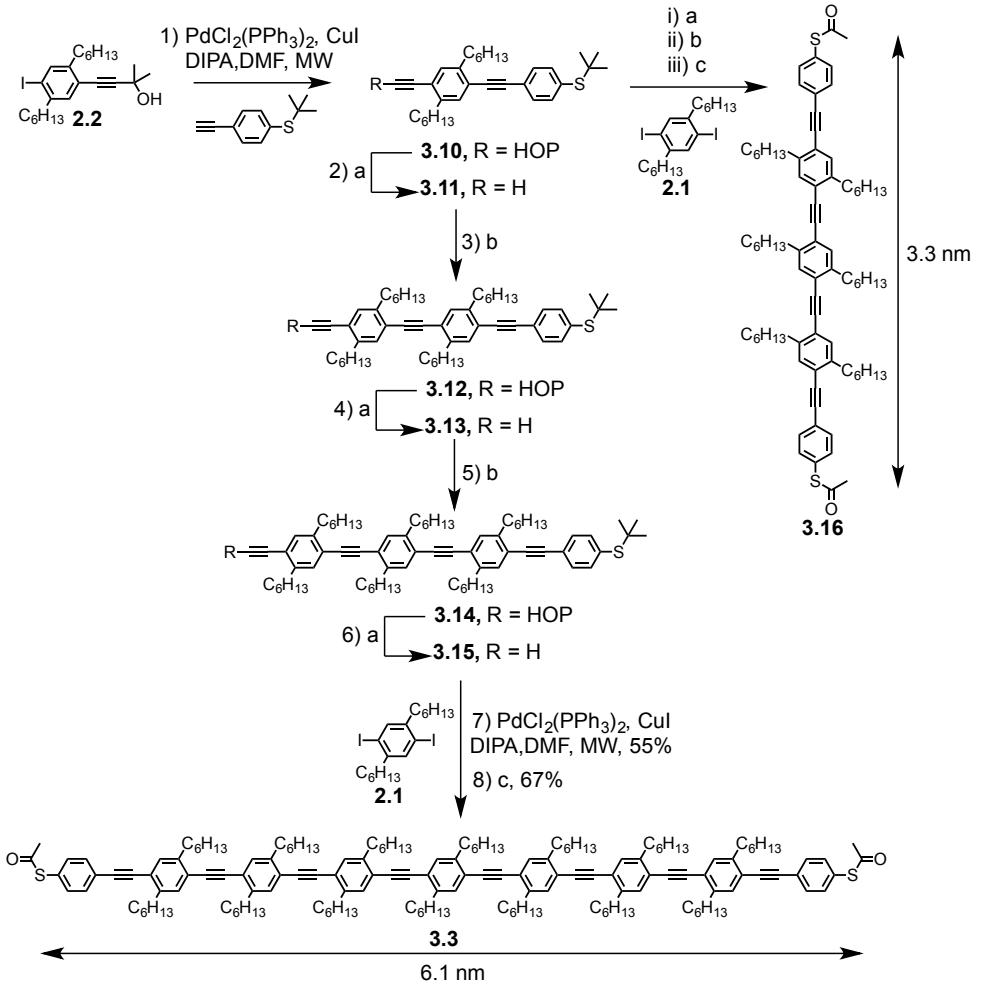

Scheme 3.3: Convergent synthesis to rod4b through an iterative series of deprotection, coupling steps starting from building block 2.2. It was also possible to branch the sequence at 3.10 to synthesize 3.16. Conditions: a) 2.2, $PdCl_2(PPh_3)_2$, CuI, DIPA, DMF, MW, 120°C. b) NaH, Toluene, 110°C, 1 hr. c) DCM, AcCl, BBr_3, 0°C, 1 hr. Yields: step 1, 100%. 2, 100%. 3, 95%. 4, 100%. 5, 83% 6, 100%, i, 100%. ii, 75%. iii, qnt.

What is noticeable is that the convergent sequence has considerably higher isolated yields of the rods after coupling than for the divergent sequence. Starting with **2.2** we obtained the target OPE **3.3** in an overall yield of 18% in a linear sequence of 11 steps from commercially available material. This dramatic improvement over the divergent approach is attributed to the design of the synthetic route and making full use of the polarity of the HOP protected acetylene. In the divergent sequence each rod after coupling has two HOP groups present, but so too do any homocoupled side products. These compounds have the same polar end groups, and only differ slightly in length. However homocoupling in the convergent route would lead to a rod without any HOP group and hence a very different R_f on SiO_2 than the desired product. The final transprotection of the ^{t}Bu protected sulfur on rod **3.15** to the acetyl PG was effected using BBr_3 in a solution of DCM and acetyl chloride (AcCl).

In the first instance this transprotection reaction was tested in the synthesis of OPE **3.16** which could be synthesized by splitting the convergent sequence after the first coupling. This gave **3.16** with an MM2 modeled length of 3.3 nm. Although this rod would seem to be too short for the nano-gaps discussed above, it does demonstrate the versatility of this building block based approach to the assembly of nano-scale molecular architectures. The longer acetyl protected rod **3.3** was sent to KIT for investigation in their physical set-up.

3.3 A single-molecule three-terminal device

The formation of a three terminal, single-molecule device is both incredibly appealing and incredibly challenging. In order to truly mimic the macroscale of silicon based electronic circuits we must find an approach to connect three electrical contacts through one molecule.[237] Molecular wires have been demonstrated to show many of the functions of integrated circuits including wires, diodes, and rectifiers however a functioning single-molecule transistor with three contact points still eludes the community.[11] Naturally a molecular architecture with three distinct anchoring groups that can bridge three isolated electric contacts is required. These electrodes must also have the right geometry and size at the nanoscale so that a synthetically accessible molecule can still be synthesized from the bottom up using readily available building blocks. Prof. Marc Tornow has been working extensively in the field of nano-contact printing (Figure 3.3).

Figure 3.3: Schematic of nano-junctions that can be fabricated in the Tornow group using lithographic techniques. Left, classic two-terminal junction. Center, multiply bridged nano-gap for increased conductance across the junction. Right, hypothesised three-terminal junction bridged by a single molecule. Reprinted with permission from ref. [238]. Copyright 2011, Nanotechnology.

In 2009 his group reported the formation of nano-gaps in the < 10nm regime used to form a molecular junction between three electronically isolated Ti/PdAu contacts.[239] He has since been able to fabricate some nano-gaps in the < 5nm regime where it would even become possible to bridge the junction with a single molecule.

We set out to establish a new collaboration with Prof. Tornow, applying the building block methodology to synthesize a pyramidal molecule with length dimensions of greater than 4 nm for use in the formation of a tri-stable single-molecule junction. The surface deposition is envisaged to be made from solution and the physical studies will be carried out by Marc Tornow of IHT, Technische Universität Braunschweig.

3.3.1 Synthetic target of a three arm star

We want to make a fully conjugated molecule with three contact points to bridge gold surface islands. In order to increase the binding affinity of the star to the surface domains, we envisaged incorporating two sulfur anchor groups to each of the terminal stars' benzene units. We therefore settled on the phenyl-di-benzylic sulfur moiety (). The use of benzylic sulfurs was desired in order to allow the star to sit raised up from the gold nano-islands upon surface deposition.[240] There are two ways to construct such a star; either the OPE arms are pre-formed and attached to a central tri-bromo/iodo benzene in at the last stage, the so called convergent approach, or the OPE rods are constructed iteratively using protection deprotection techniques to sequentially build up the length of the star from its center – the divergent approach.

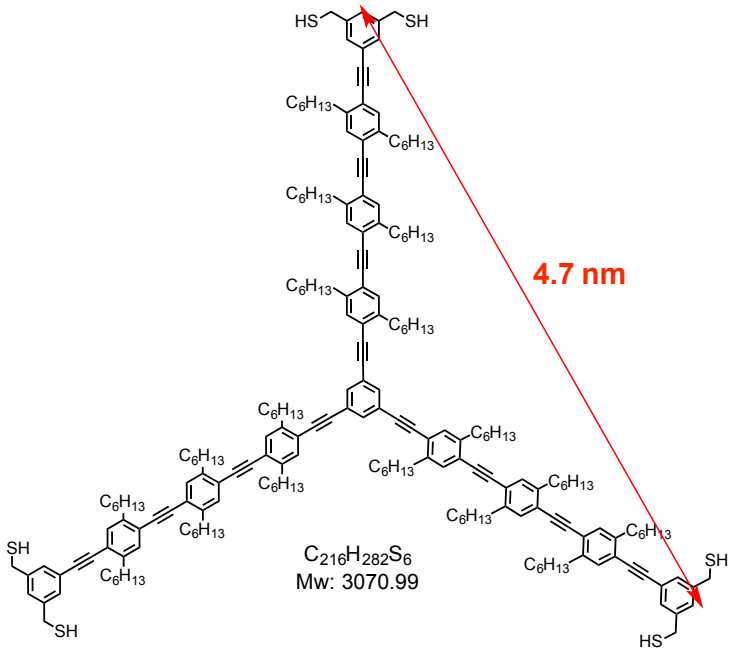

Figure 3.4: Target three arm star for fabrication of three-terminal single molecule device. In red, MM2 modelling of the C-to-C length from the last carbon of each arm.

3.3.2 Divergent approach to synthesize the star

In our initial work on the synthesis of molecular wire OPE rods (described above in section 3.2.2) we found that a divergent approach led to the formation of side-products which were very difficult to remove as they so closely resembled the intended coupled product. However in the synthesis of such a star structure the divergent approach was again investigated as here any homo-coupled side products would have a different number of polar HOP groups present and should be more easily separated without loss of the desired product to mixed fractions during purification.

Starting from 1,3,5-tri-bromobenzene the addition of three acetylenes to the benzene core was achieved by coupling with an excess of TMS-A under standard Sonogashira conditions (Scheme 3.4). Removal of TMS was achieved cleanly using potassium carbonate in a solvent mixture of MeOH/THF. Then a sequential coupling and deprotection sequence was made by coupling asymmetric building block **2.2** three times to the central core star, extending the arms by one benzene ring per coupling. The hexyl chains on the building block increased the solubility of the molecule. The yields for these couplings (Scheme 3.4) at 76%, 68%, and 20% may not seem impressive, but remember that this is actually a three fold reaction so a yield of 68–76% corresponds to a yield of ~90% for each of the individual Sonogashira couplings.

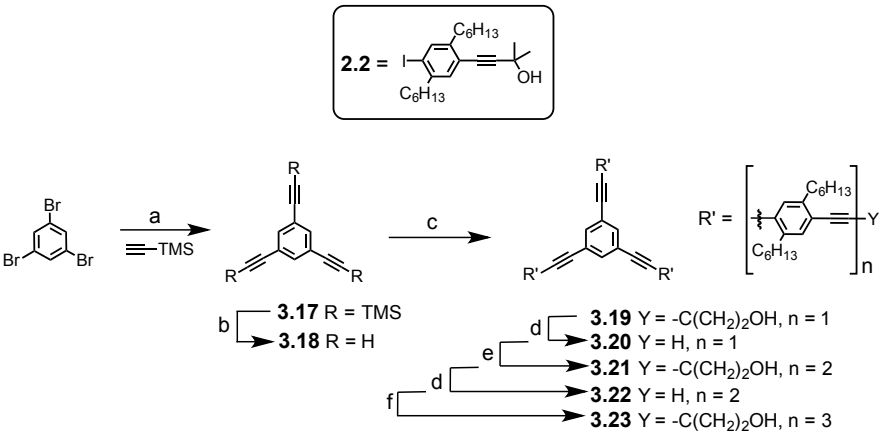

Scheme 3.4: Divergent approach to assembling the star. Reagents and conditions: a) 2.2, $PdCl_2(PPh_3)_2$, DIPA, THF, rt, 88%. b) K_2CO_3, THF/MeOH, 90%. c) 2.2, $PdCl_2(PPh_3)_2$, DIPA, THF, rt, 68%. d) NaH, Toluene, 120°C, qnt. e) 2, $PdCl_2(PPh_3)_2$, DIPA, THF, rt. 76% f) 2.2, $PdCl_2(PPh_3)_2$, DIPA, THF, rt. 20%.

The final coupling performed to obtain star **3.23** required purification by recycling GPC and the much lower isolated yield of 20% for this reaction step reflects that fact. The main impurity was the doubly substituted star, with one terminal acetylene unreacted, perhaps due to the much slower reaction rate as the molecule increased in size due to the lower probability of a collision being of the correct orientation on the molecules reaction surface.

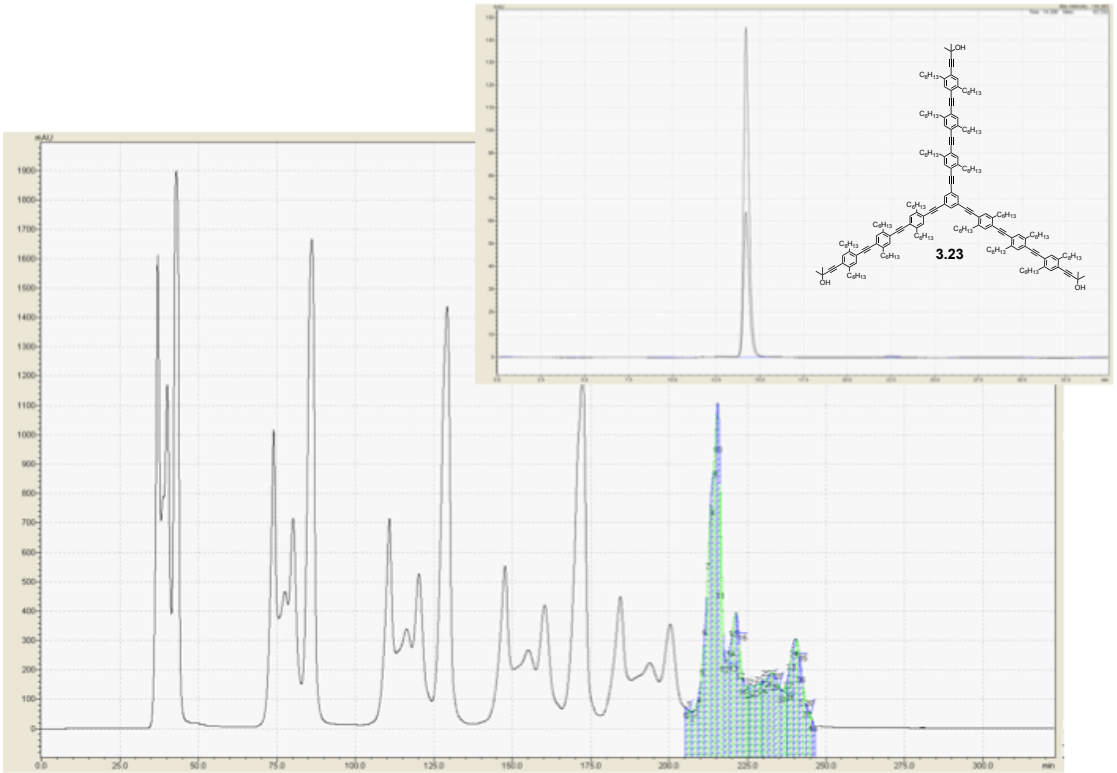

Figure 3.5: Recycling GPC trace for the purification of star 3.23. Inset, clean analytical trace after purification, showing optical purity at both 360 nm and 450 nm.

3.3.3 Convergent approach to synthesize the star

In parallel to the divergent synthesis described above, we were able to synthesize **3.26** on the road to a totally convergent synthesis of the target star. In the same vain as the convergent synthesis to the OPE rods described above (Scheme 3.3), the sulphur groups must be present from the beginning of the synthesis – and therefore contain sufficiently stable protecting groups to allow for clean reactions under the iterative reactions of Sonogashira coupling and base catalysed deprotection. It was felt that the BBr_3 reagent required for the transprotection of ^{t}Bu protected sulphur was rather a harsh treatment to be risked on our laboriously synthesized star, and therefore the triphenylmethyl (trityl) protecting group of the benzyilc thiol was used instead.[241] This PG is removed under acidic conditions of TFA in the presence of a scavenger such as triethylsilane.[242]

The sulphur bearing rod **3.26** was synthesised by employing the trityl protected sulphur building block **3.24** (a building block readily available following the procedures described in the PhD thesis of Torsten Peterle, Mayor Group, Basel) in a Sonogashira coupling with asymmetric building block **2.2** in 91% (Scheme 3.5). Removal of the HOP acetylene PG and performing a statistical coupling with the symmetric building block **2.1** afforded rod **3.27** in 24%, also forming the symmetric di-coupled product **3.28** (Scheme 3.6) in 42% yield.

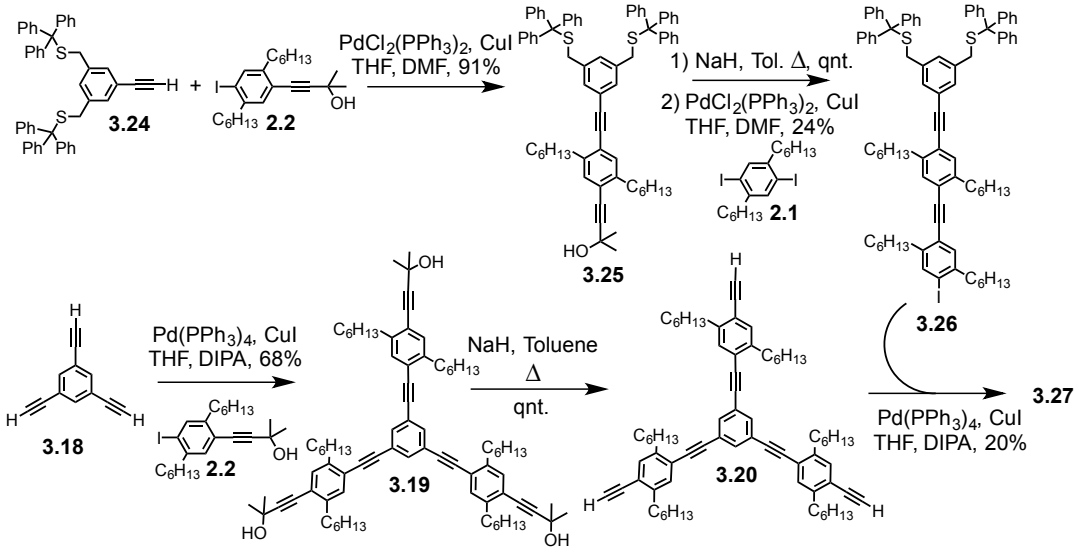

Scheme 3.5: Convergent synthesis to rod

The synthesis of star **3.20** was made in a divergent fashion leading to the final assembly step, coupling the arm **3.26** three times to the stars-core **3.20**. The reaction appeared to go to completion at this stage, and purification by column chromatography on SiO_2 gave a crude of

the desired triyl protected star **3.27**. In order to ensure the purity of this star this crude was passed through the recycling GPC to obtain a single, optically pure species in 20% yield.

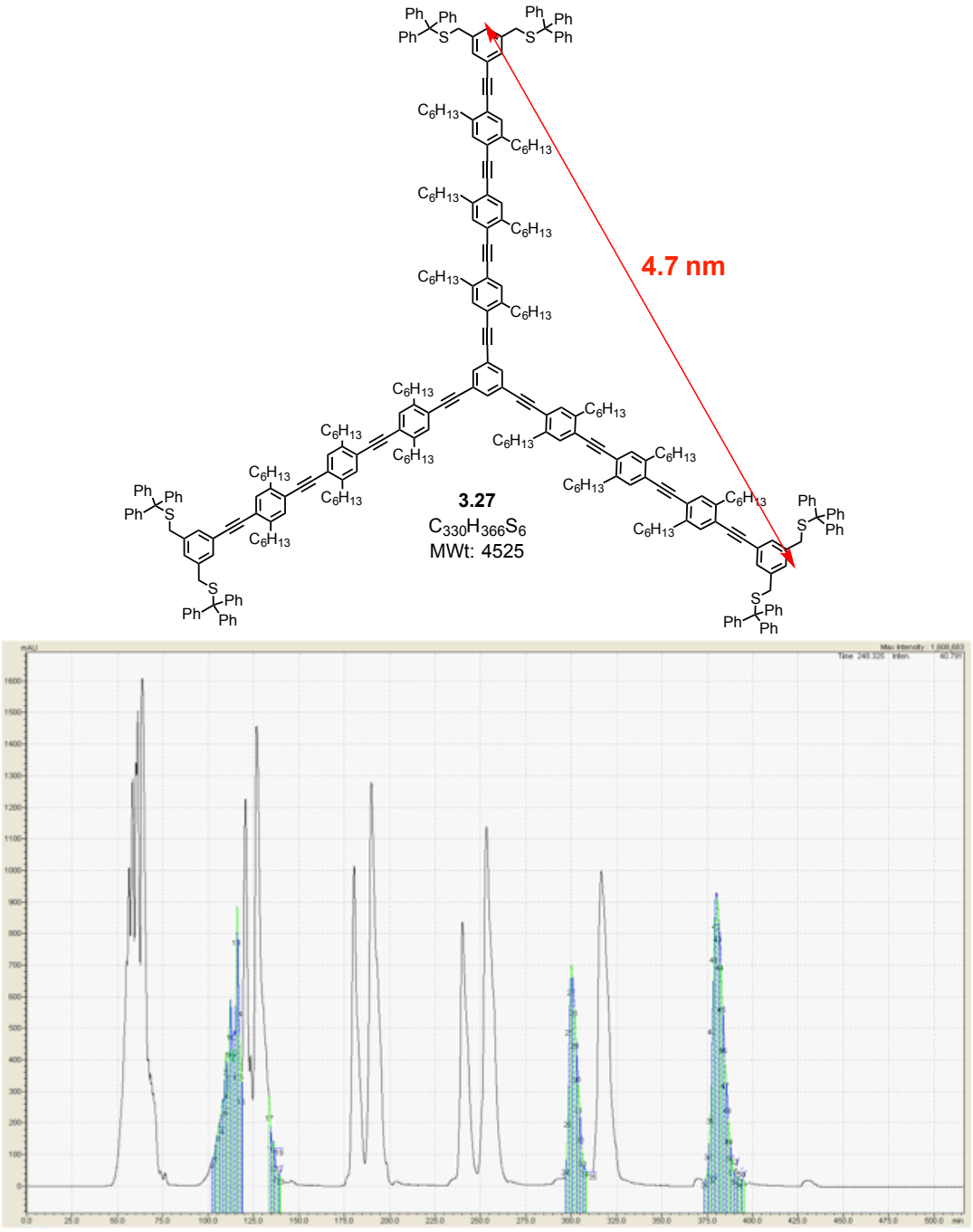

Figure 3.6: Top: trityl protected star 3.27 obtained through a convergent-divergent hybrid approach. Bottom: recycling GPC trace of the isolated star after six runs through the GPC columns.

3.3.4 Three-arm star characterisation

The characterisation of such large single-molecule species is always a challenge, as unlike polymer synthesis which gives rise to mixtures, it should be possible to obtain a single isolated species. In our hands all molecular rods and stars bearing terminal sulphur groups

gave very poor signals by MALDI-Tof. The best matrix material found was trihydroxyacetophenone, but especially for the larger structures no mass signal could be clearly resolved from the background noise. It therefore became incredibly important to characterise the star **3.27** isolated above by other methods.

With the help of Dr. Daniel Häussinger a series of NMR experiments were carried out. Proton ^{1}H spectra were readily obtained, however our attempts to gather a carbon ^{13}C were all unsuccessful, even after a 36 hr data collection on a Bruker 600 MHz NMR. We attribute this to the dynamics of the molecule in solution, and given the similarity and symmetry of the carbon environments that the delay times were too long, and too weak to be resolved. We therefore set out to collect the full range of 2-D NMR experiments of COSY, HMQC, HMBC, NOESY, and DOSY from which it was possible to deduce the carbon chemical shifts (Figure 3.7). A full assignment of all environments is not achievable due to their similarity, giving rise to many multiples of signals with near identical chemical shifts.

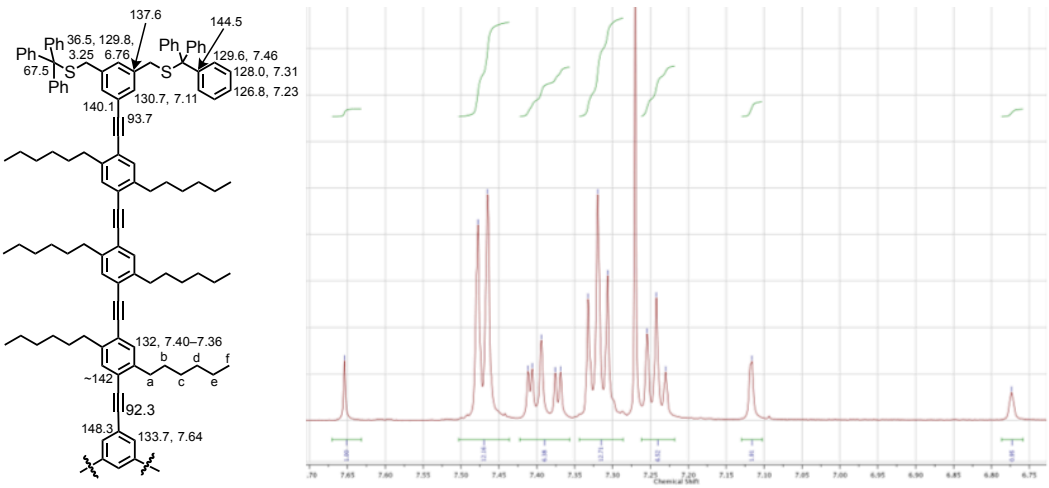

Figure 3.7: Left, 1H and 13C assignment of star 3.27. Right, zoom of the aromatic nmr region showing the high level of purity of the sample by nmr. Purity was also confirmed by GPC.

In order to improve our confidence that the species under investigation really has the identity and regio configuration we ascribe in Figure 3.6, a series of DOSY diffusion coefficient measurement experiments were made. We compared the diffusion coefficients of the precursor rod **3.26** with that of the isolated product **3.27**. What was directly measured was a Pulsed Field Gradient Spin Echo (PFGSE) experiment for both compounds.[243] The entire proton ^{1}H spectrum is collected at varying field strengths, and one peak is plotted on a graph of gradient strength vs the intensity of that peak for each measurement. 32 such spectra were measured, and plotting this shows a sigmoidal curve, by numerically finding a best fit using

the non-spherical form of the Stokes-Einstein equation to the data points.[244] This was done using an iteration program within the TopSpin NMR software.

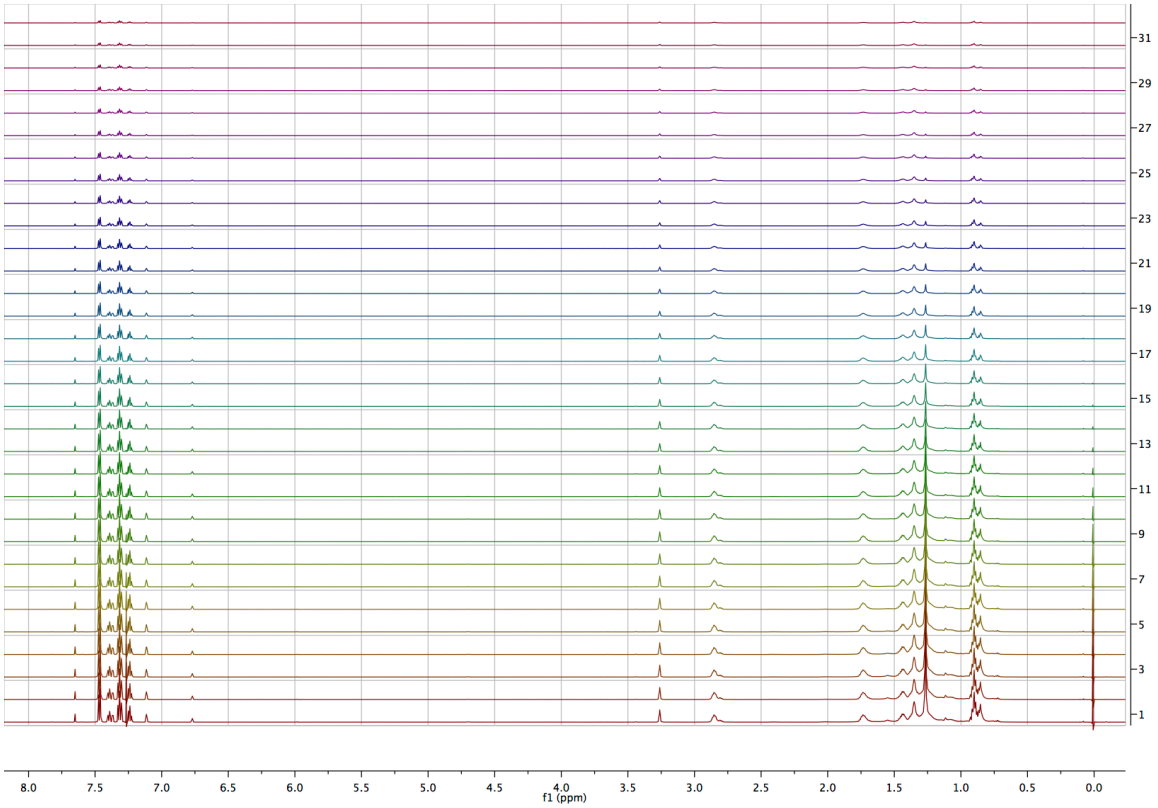

Figure 3.8: Stacked PFGSE spectra from star 3.27. x-axis is the chemical shift, y-axis 32 stacked spectra at varying field strengths. From this data we deduce the diffusion coefficient.

The rod **3.26** found convergence after 40 such iterations, and the star **3.27** after 45 iterations. From this data we can directly read out the attributed 'diffusion coefficient' – as a proxy for the viscosity of the molecule tumbling in the infinitesimal window we approximated from our plot. This gave a diffusion coefficient of 4.63×10^{-10} m^2S^{-1} for the rod sm **3.26** and of 2.75×10^{-10} m^2S^{-1} for the star **3.27**. The ratio between these two compounds is in line with what we would expect with in relation to their relative atomic weights, which we use as a proxy for their non-spherical size.

The UV-vis and fluorescence spectra of star **3.27** were also measured (Figure 3.9). The large cross-section of the UV-spectrum is simply the additive value of having the three side arms together in the same molecule.

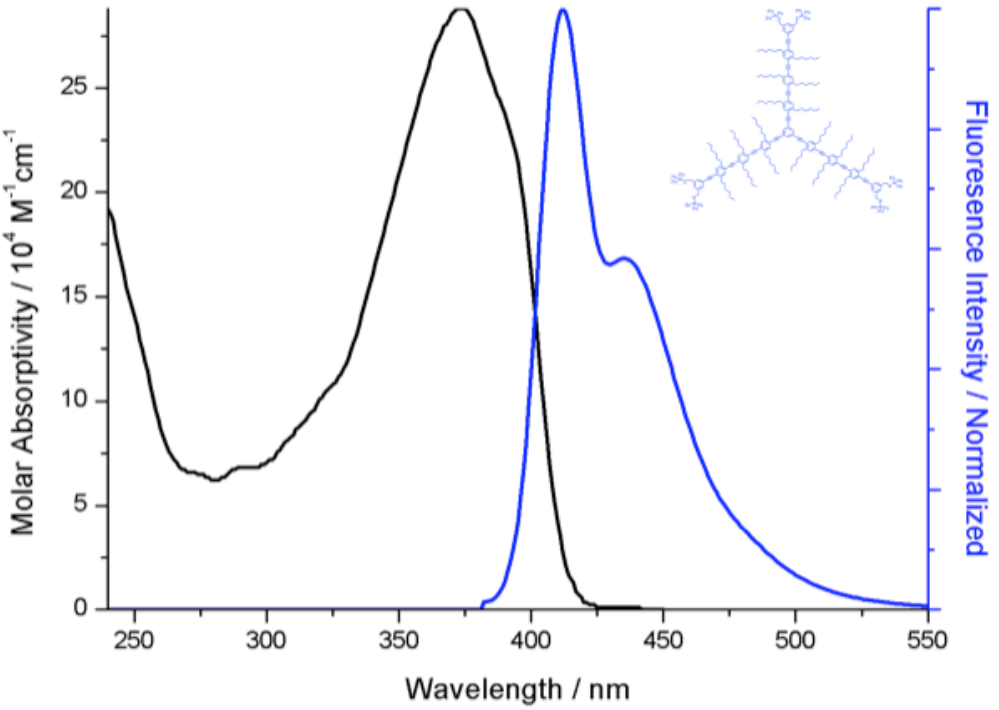

Figure 3.9: Photophysical measurement of star 3.27 (inset). Black trace – UV-vis spectrum. Blue trace –fluorescence emission spectrum normalised to unity. Fluorescence excitation at 374nm.

3.3.5 Removal of thiol protecting groups

In order to ensure that deposition of the star into the Marc Tornow's nano-patterned electrodes it is desirable to characterise the free thiol form of the star. This was we can be confident that all the PG were removed and that the star is able to form a good contact with the electrode. In order to do achieve this the trityl protecting groups on star **3.27** need to be removed. Test reactions were performed on the rod **3.28** isolated as the di-substituted species from the reaction mixture to afford **3.26**. Deprotection of the trityl groups could be achieved for all four thiols to afford **3.29**, in the best case with 35% yield using a solution of 4% TFA in DCM in the presence of triethylsilane to scavenge the trityl carbocation (Scheme 3.6).

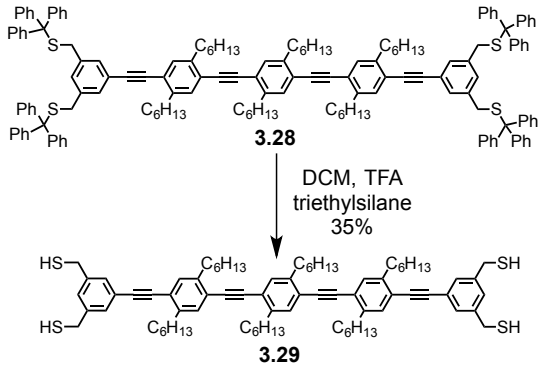

Scheme 3.6: Deprotection of di-substituted rod 3.28 with TFA to afford the deprotected rod 3.29.

Surprisingly the mass spectra of **3.29** could be measured as a weak signal by MALDI. NMR also confirmed the formation of the desired free thiol rod **3.29** in solution. However if the rod is placed under vacuum to dryness it is no longer soluble. The same conditions were applied to star **3.27** but no compound was ever isolated, only an insoluble crust after column chromatography. Instead an insitu deprotection, followed by reprotection with an acetyl group was attempted. This gave promising results on the **3.28** and the same conditions were applied to the star **3.27** (Scheme 3.7). This time the star could be isolated after recycling GPC to afford the hexa-acetyl star **3.30** in 31%.

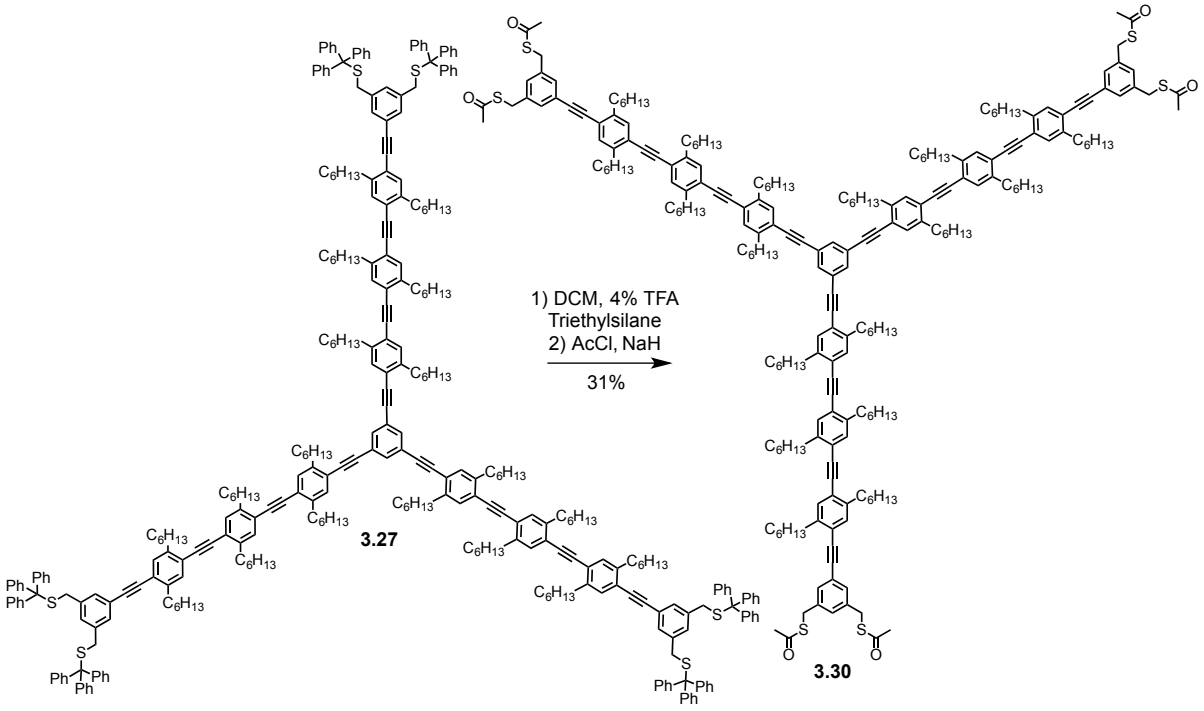

Scheme 3.7: Trans-protection strategy to form the hexa-acetyl star 3.30.

The analytical GPC trace of the target star (Figure 3.10) confirmed the optical purity of the star **3.30**, which was also shown to be pure by NMR. Unfortunately, still no mass spectrum could be obtained for these sulphur containing compounds.

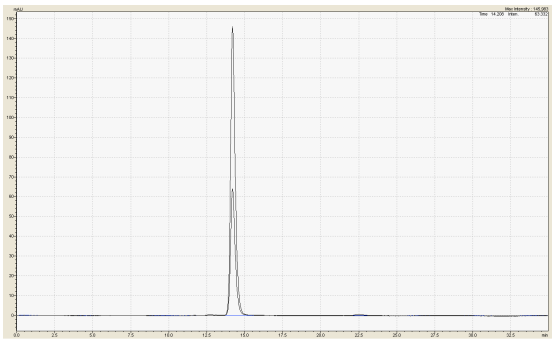

Figure 3.10: Analytical GPC trace confirming the optical purity of star 3.30, measured at both 360 nm and 450 nm.

Overall the target star **3.30** could be synthesised in a yield of 8.1% over 8 linear steps starting from the building blocks **3.24** and **2.2**.

3.4 Conclusion and Outlook:

Appling the building blocks introduced in chapter 2, we explored divergent and convergent strategies to assemble extended OPE rods of over 6 nm. The synthesis of the OPE was most successful with a convergent approach, but required switching of the sulphur protecting group from acetyl to ^{t}Bu. This gave the OPE rod **3.3** in an 18% overall yield.

Turning our attention to a three terminal device the synthesis of a three-arm star bearing trityl protecting groups was reported. The characterisation of the star was difficult and required extensive NMR studies to assign its identity. Diffusion coefficient experiments were carried out to confirm our analysis. The transprotection of the sulphur PG from the trityl to acetyl was made to afford the desired star **3.30** in an 8% overall yield from 8 linear steps. Both the rod **3.3** and star **3.27** have been sent to the group of Prof. Marc Tornow for physical investigation in his nanopatterned set-ups to fabricate a working three-terminal device.

It would be interesting to have in hand a more electron rich rod and asymmetric star arms (Figure 3.11) in order to investigate the effect of electron density on the conductance.

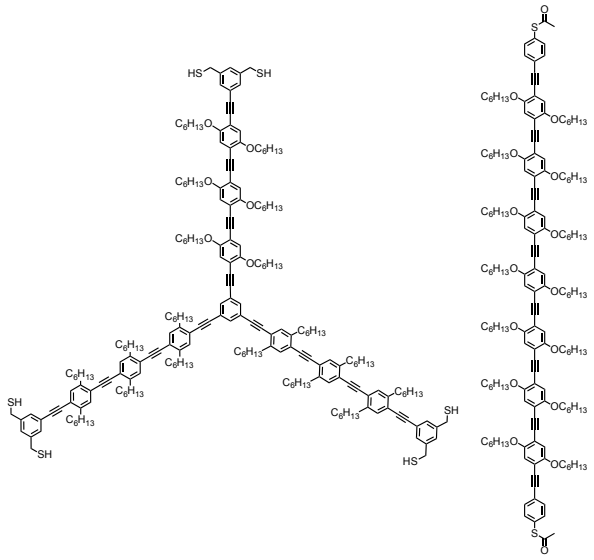

Figure 3.11: Proposed electron rich, asymmetric star and rod

If there is a large enough a difference in conductivity, then by alternating the current across the three terminals of a contacted asymmetric star, we would be able to discern its orientation in the junction.

4 Nano-Scale Carbazole Architectures

Chapter 4 applies the carbazole building blocks methodology towards the synthesis of a giant π-conjugated molecular ring. Such a macroycle is desired in order to explore the limits of electronic conjugation in molecular systems, of particular interest is the search for meta-metallic behaviour from such systems. The synthesis was achieved using all the tools of phenyl-acetylene assembly and is an illustrative example of the power of the building block approach.

4.1 Investigations of a nanoscale carbazole based architecture

Massive fully conjugated cyclic pi-systems are expected to show unique optical and magnetic properties, especially when the induced electronic coupling through the cycle is particularly strong.[245] Cyclic forms of linear chains can show marked differences in their photo-physical properties.[246] Carbazoles in particular are highly luminescent and as they are strong hole transporters, they are widely applied in opto-electronic devices and as such should prove ideal candidates for study. However carbazole based macrocycles reported to date lack efficient pi-conjugation throughout their entire backbone.

Here we present the synthesis of model systems that maximise the conjugation in carbazole oligo-phenyl-ethylene rods and cycles. After establishing new synthetic routes towards carbazole based oligomers by applying the building blocks from chapter 2 we present an approach to the template directed synthesis of a fully conjugated 7 nm diameter carbazole based macrocycle. A range of polar, orthogonal acetylene protecting groups were employed to assemble the macrocyclic structure via palladium catalysed cross-coupling reactions. The carbazole moieties allow insertion of a semi-rigid template, facilitating an efficient cyclisation.

4.1.1 Design of an organic metamaterial

Metameterials were first hypothesised by V. G. Veselago[247] in 1968 and are a class of substances which have unusual physical properties characterised by possessing a negative magnetic permeability (μ) and permittivity (ε) which should give rise to a negative refractive index.[247] Veselago hypothesized that materials simultaneously possessing a negative μ and ε would have a negative refractive index, bending light away from the normal rather than towards it. The proof of concept came, when in 1999 J.B. Pendry *et al.*[248], reported the first material to show a negative magnetic permeability (μ) in the microwave region. This was quickly followed in 2001 by the reporting of the first material to show a negative refractive index by R.A. Shelby *et al*.[249] again in the microwave region. This finding was based on the use of split-ring resonators, a metallic object shaped like a miniature bar magnet which behaves as a magnetic coil with an in built capacitor which produces a large induced dipole moment. When a split-ring resonator is excited at a frequency above its resonance frequency the magnetic permeability becomes negative. Therefore work towards a metamaterial at

wavelengths shorter than the microwave region will require even smaller split-ring resonators than those used by Shelby.

Current research work towards shorter wavelength metamaterials focuses on the use of lithography techniques to print patterned surfaces with smaller and smaller metallic strips shaped to act as split-ring resonators.[250] The difficulty is in reaching high enough precision when forming such small metal rings. A bottom up approach by chemically addressing this problem by forming a ring starting from the atomic scale and building up to larger structures is a more viable approach to obtain such small structures with high precision.

4.1.2 Molecular Requirements

Building on the concept of using a split-ring resonator in order to obtain metametallic behaviour, an analogous organic molecule can be envisaged, principally a macrocyclic structure. The molecule must be suitable for surface deposition; either by sublimation or, with larger molecular weight structures, solution phase deposition. The molecule should be fully conjugated about its circumference in order to allow the build up of ring currents induced by circulating electrons. A *para* substitution pattern would ensure the strongest induced current. Use of aryl-acetylene bonds should be conducive to a successful synthesis of such a macrocycle using suitable acetylene protecting groups. A break in the conjugation, possibly using an acetylene-Pt-acetylene junction[251] would create a split in the macrocycles' conjugation introducing the 'capacitor effect' into the molecule as observed in the metallic split-ring resonators mentioned above.

The diameter of the required macrocycle needs to be large enough that a ring current can be induced by placing the sample in a sufficiently strong magnetic field. The smaller the cycle, the larger the magnetic field (B) required. However the smaller the cycle — assuming a split-ring resonance effect is observed — the shorter the wavelength of light that can be forced to obtain a negative μ and ε.

Mayor *et al.*[245] have reported an initial attempt at the synthesis of a suitable molecule using a thiophene based macrocycle with a calculated diameter of 11.8 nm.[245] The intention was to observe a persistent ring current and then to induce metametalic behaviour, however this molecule was too floppy to lie flat on a surface and was therefore unsuitable for further investigation.

Use of a template to maintain some rigidity in the macrocycle should overcome the problems encountered by Mayor. Covalent templates have also been shown, largely through the work

of Höger and co-workers[252], to greatly improve the yield and synthetic viability of large macrocycles. Müllen and co-workers have shown that insertion of a rigid template to act as a scaffold for shape-persistent macrocycles greatly improves surface deposition.[253],[254] Their macrocycles (Figure 4.1) are based on either a carbazole moiety[253],[255] or a fluorine[254], both substituted in the 2,7 position with a tetra-substituted porphyrin acting as a template connected to the periphery through an ester functionality which allows for easy removal of the template used in their synthesis.

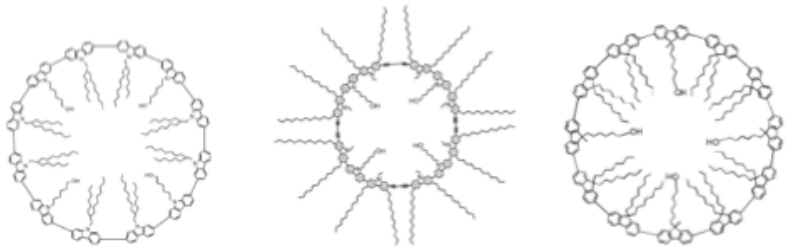

Figure 4.1: Two carbazole[253],[255] and fluorine[254] macrocycles, after template removal, synthesised by Müllen and co-workers.

4.1.3 Target Structure: a novel carbazole macrocycle

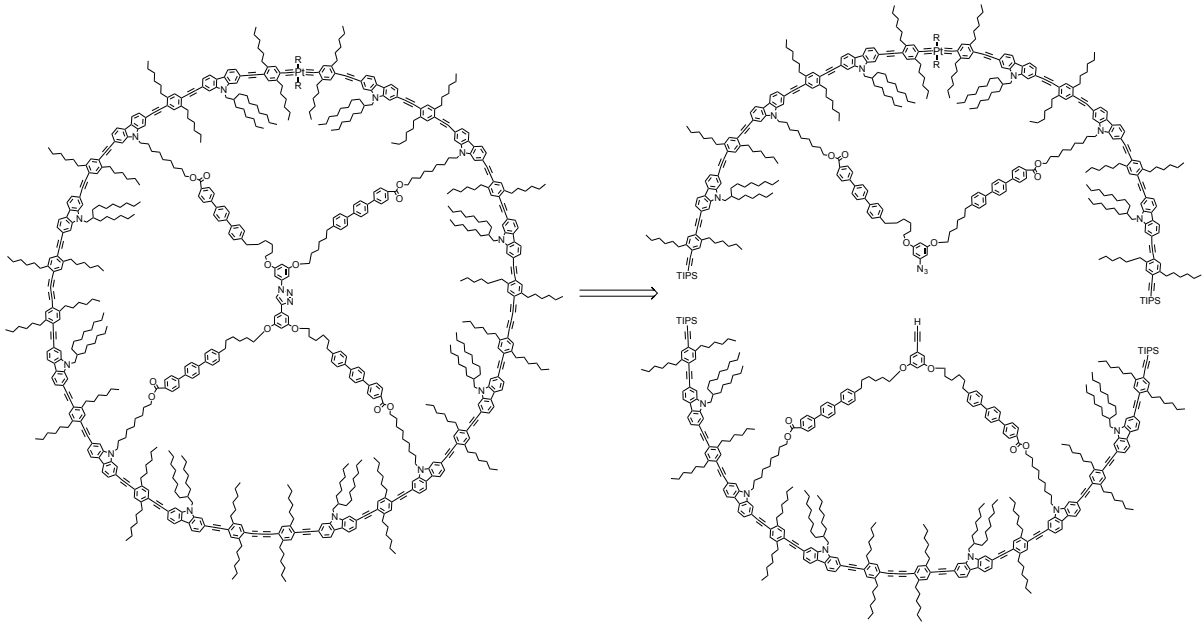

Figure 4.2: Target macrocycle consisting of di-acetylene linkers, an acetylene-Pt-acetylene junction and click chemistry used to combine the two half hemispheres.

A target macrocycle is proposed comprising all of the physical characteristics discussed above. The proposed macrocycle (Figure 4.2) consists of carbazole moieties connected to aryl groups through acetylenes. Alternating carbazoles are connected to a semi-rigid template. The template consists of alkyl chains in order to ensure that any induced ring

currents around the circumference are not disrupted by conjugation to the template. Once the two half hemispheres are fabricated, they can be combined at the template using click chemistry, then deprotection of TIPS protected acetylenes allows for copper mediated di-acetylene cyclisation.

In the first instance a simpler macrocycle is to be synthesised, from which the building blocks and the purification methodologies developed, should allow fast synthesis of the final intended molecule (Figure 4.2). This decision was made in order to facilitate faster synthesis of a very similar macrocycle to test its behaviour upon surface deposition. Such a macrocycle, if suitably deposited, should still allow testing of persistent ring currents, however it would not be expected to demonstrate metametallic behaviour.

The first generation target macrocycle is comprised of four symmetric parts around a central template (Figure 4.3). The quarter cycle can be synthesised from two further symmetric parts prior to connection to the template. This means that the outer rim and template may be synthesised in parallel and connected prior to cyclisation and surface deposition. If the template is bound to the circumference through ester bonds it may be easily removed allowing the possibility for deposition of another molecule in the cavity. The use of hexyl chains at the aryls and $-C_{16}H_{33}$ on eight of the twelve carbazoles should ensure good solubility in organic solvents to aid the synthesis and surface deposition—and may possibly encourage solution phase stacking or liquid crystalline behaviour.

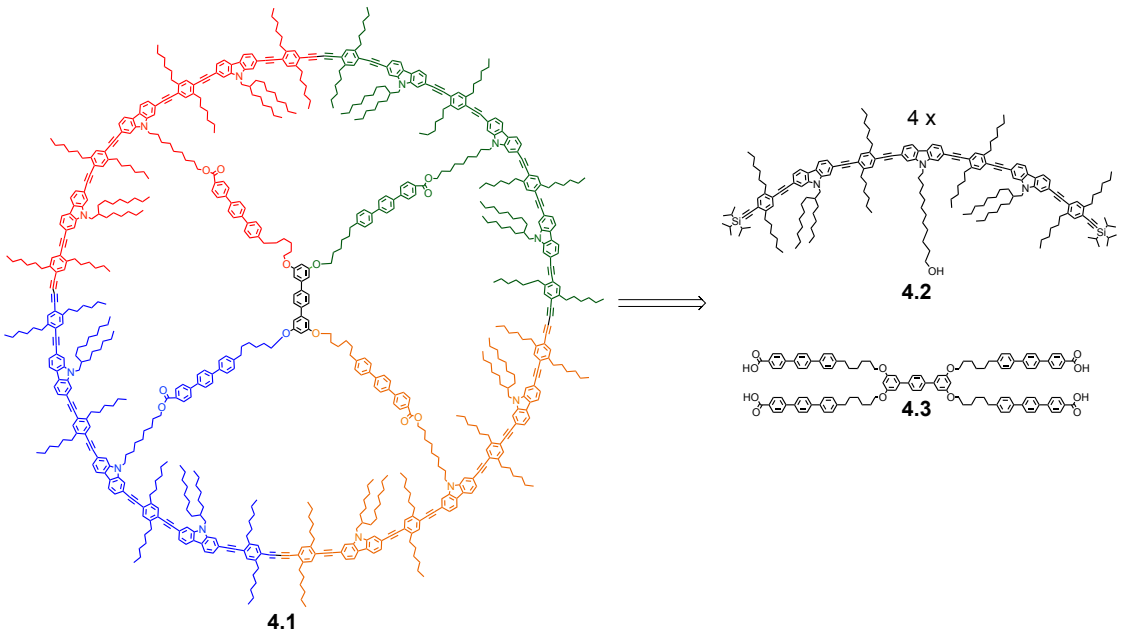

Figure 4.3: First generation macrocycle comprising four symmetric parts bound to a central template through ester bonds and to each other via di-acetylene bonds.

Initial molecular modelling studies on the intended macrocycle indicate that the diameter of the ring would be 7.2 nm with an internal angle at each carbazole moiety after energy minimization of 158°. The intended structure consists of twelve carbazoles, however the internal angle of a dodecagon is 150°. As a consequence of this the acetylene bonds must be significantly bent from the traditional 180° bond angle. This modelling also demonstrated that the template should have arms of at least 3 nm in length. Höger *et al.*[256] have shown that as long as the template is large enough a significant increase in the Glaser coupling cyclisation yield can be expected. If the template is too large improved cyclisation yields are still observed. This length can be achieved using an alkyl chain with a minimum of nine carbons connected to the linking carbazole, with and ester bond to the template, or with a chain of 12 carbons when linked to the acetylene template.

4.1.4 Retrosynthesis of a symmetric carbazole ring

The quarter cycle can be synthesised from two orthogonally protected oligomers **4.4** following selective deprotection of the acetylene and Sonogashira coupling to a third carbazole linker comprising a suitable FG to connect the quarter cycle to the template (Figure 4.4). For example a terminal alcohol would allow bonding to the template structure by esterification in a similar mode to Jung et al.[253]

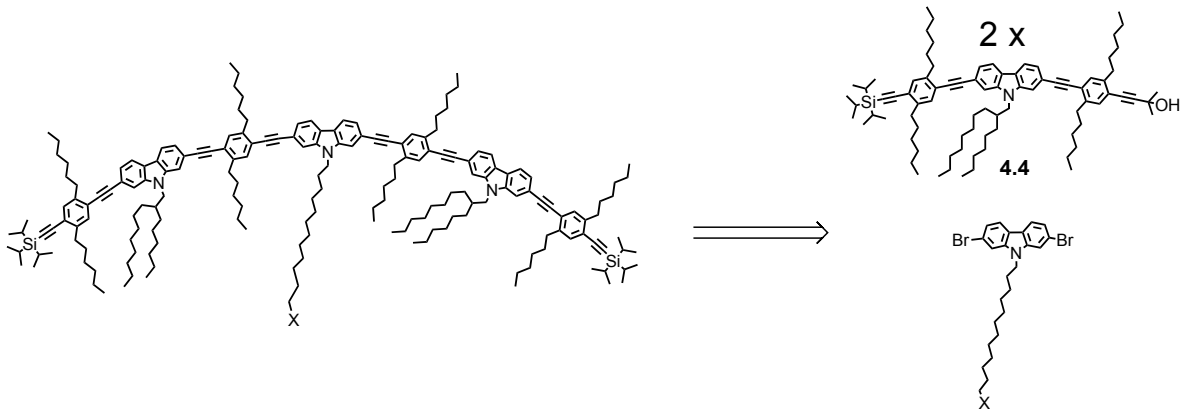

Figure 4.4: Retro-syntheis of the quarter cycle which can be synthesized from an orthogonally protected oligomer comprising 1/8th of the total cycle and a linker carbazole functionalised with a FG x suitable for connection of the quarter cycle to the template.

The TIPS protecting group was chosen to be the final acetylene protecting group to be removed as it is stable to both acidic and basic conditions and is routinely removed in quantitative yields. The final step prior to cyclisation will be the deprotection of eight acetylenes so it is imperative that this reaction operates efficiently. The 2-hydroxyprop-2-yl

protecting group was chosen as it is removed under basic conditions (*c.f.* TIPS protecting group) and the increased polarity on silica gel derived from the alcohol group will allow for easier purification of precursor molecules. This combination of orthogonal protecting groups is widely reported in the chemical literature, an example of which was nicely demonstrated by Jacobsen *et al.*[257] The iterative use of a similar protecting strategy has been reported by Godt and co-wokers.[258]

The orthoganlly protected oligomer **4.4** can be synthesised by statistical Sonogashira coupling to a di-bromo carbazole building block **2.32** and a further orthogonally protected aryl molecule **2.3**, also formed by a statistical coupling to a diiodo aryl unit **2.1** (These building blocks were introduced in chapter 2). The carbazole moiety can be synthesised following the work of Jung *et al.*[253] and **2.1** unit by modification of Rehahn *et al.*[259]

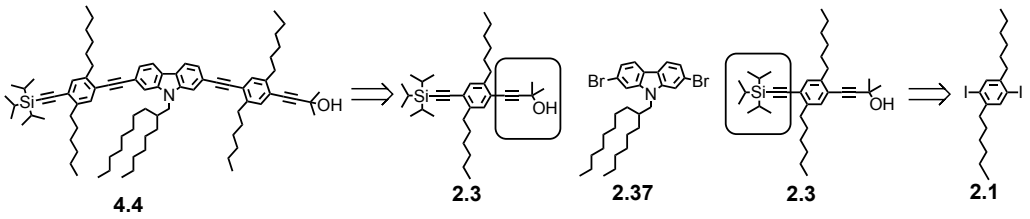

Figure 4.5: Retrosynthesis of carbazole oligomer 4.4 comprising one eighth of the final cycle from two consecutive statistical Sonogashira couplings using orthogonal acetylene protecting groups.

These statistical coupling steps are the price of achieving orthogonal protection of the acetylene functional groups. Symmetric couplings could be achieved, but this would then require statistical deprotection of the protecting group in order to achieve monomer products. In theory greater control can be achieved with statistical couplings over statistical deprotections by varying the concentration of reactants. Ziener and Godt[236] have reported the synthesis and subsequent iterative Sonogashira coupling of an asymmetric aryl unit — but the material cost of avoiding the statistical coupling step seems too high.

The target template structure **4.3** can be synthesised in parallel to the outer ring **4.2**, with the two combined by an ester condensation prior to cyclisation. The template should consist of four symmetric arms bound together at the centre with a tri-phenyl aromat. The arms are to consist of a conjugated aromatic tri-phenyl system in order to provide some rigidity and increased electron density to aid in surface deposition, but also to contain alkyl chains to disrupt electronic conjugation through the template.

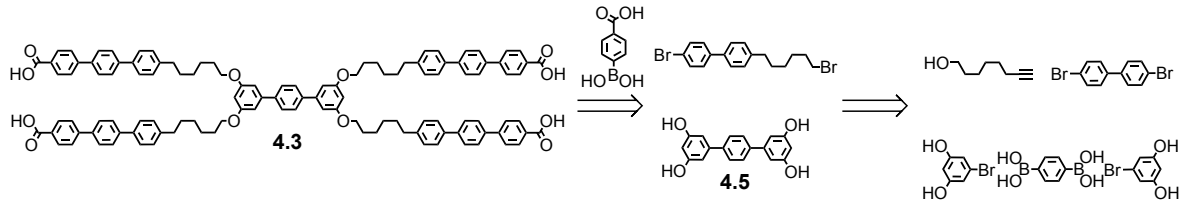

Figure 4.6: Retrosynthesis of the template 4.1 which can be formed in two parts, one central aromat 4.5 achieved by Suzuki coupling and an alkylated biphenyl which, after an S_N2 substitution and a final Suzuki coupling to a *para*-substituted carboxylic acid, will afford 4.3

4.2 Synthetic approaches to assemble the macrocycle

Following our retrosynthetic analysis described above, the synthetic path to build up a massive, fully conjugated ring can be broken down into three distinct parts. The outer rim can be assembled by combing the aryl and carbazole building blocks described in chapter 2 to form a carbazole based rod. These rods can be stitched together with a linker used to attach the outer rim carbazole rods to the template prior to the final cyclisation step The template can be built up from aromatic rings in a convergent manner.

4.2.1 Synthesis of the 1/8th cycle rim from bromo-carbazoles

The initial approach to assemble suitable carbazole rods was to insert acetylenes onto the carbazole directly, placing these low yielding steps as early as possible in the linear synthetic sequence, see section 2.2.3 for discussion of the low reactivity of 2,7-dibromo-9*H*-carbaoles. Starting with carbazole building block **2.41** (for a reminder of the synthesis see Scheme 2.13) with two orthogonal protecting groups allows for asymmetric growth of the rod in both directions (Scheme 4.1). Deprotection of HOP using standard conditions of NaH in refluxing toluene afforded **4.6** in 71%. Sonogashira coupling of **4.6** with aryl building block **2.2** afforded **4.7** in 47% yield. The yield was reduced due to the formation of a large amount of di-acetylene homocoupled product **4.8**.

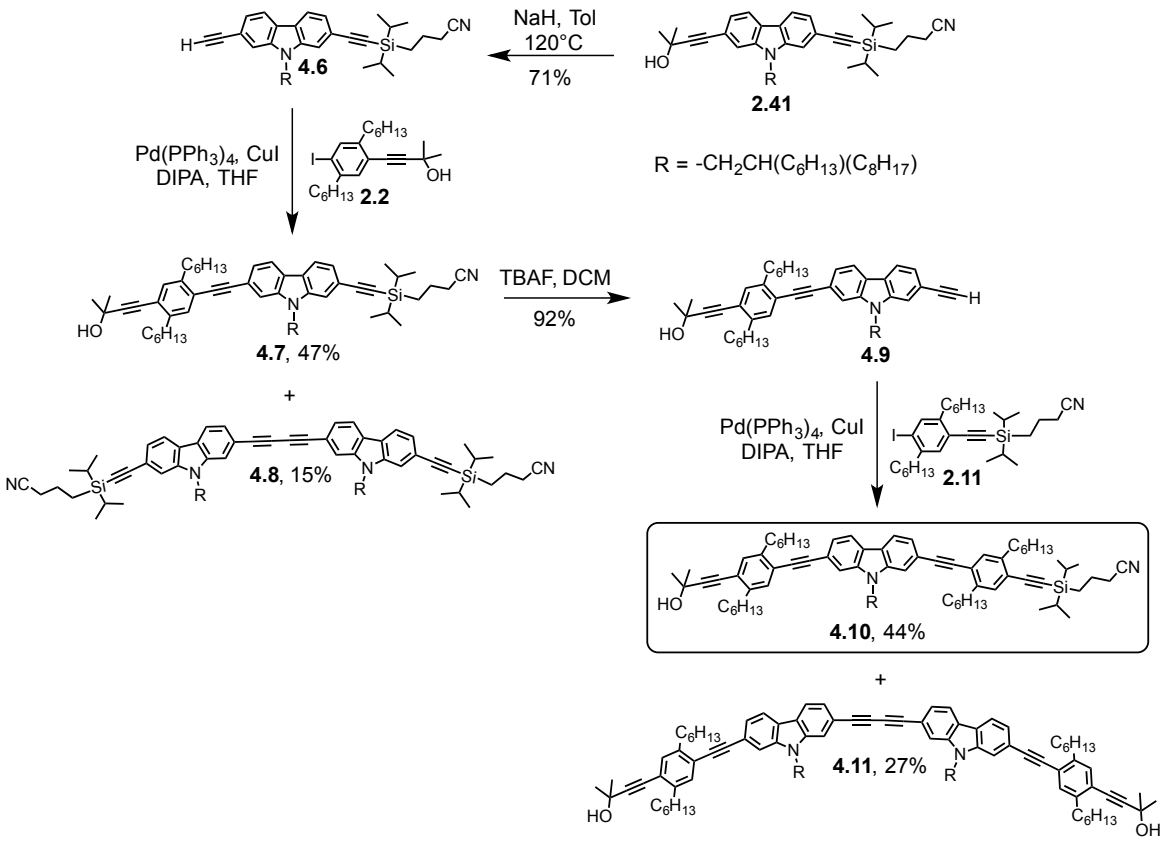

Scheme 4.1: Linear sequence for the synthesis of rod 4.10 starting from the orthogonally protected acetylated carbazole building block 2.41. The formation of di-acetylene homocoupled carbazoles 4.8 and 4.11 was particularly disappointing. This route affords 4.10 in only 2.62% yield over nine steps.

Extending the rod from the other direction by removal of the CPDIPS PG with TBAF afforded **4.9** in 92%. Coupling of **4.9** to **2.11** afforded **4.10** in 44%, again the yield reduced due to the formation of the di-acetylene homocoupled product **4.11**. This sequence yielded carbazole rod **4.10**, 1/8th of the macrocycle rim in an appalling 2.62% yield over the total nine step linear sequence. Attempts at performing the Sonogashira reactions under 'copper free conditions' lead to no conversion. The carbazole rods **4.6** and **4.9** are perhaps more prone to the formation of the Glauser coupled product due to the very electron rich nature of the carbazole unit.

An alternative approach was therefor investigated starting from the mono-substituted building block, 2-bromo-7-(ethynyl-CPDIPS)-9-(2-hexyldecyl)-carbazole **2.39**. The coupling of **2.39** with aryl-acetylene **2.16** gave a lousy 7% yield of **4.7**, Scheme 4.2.

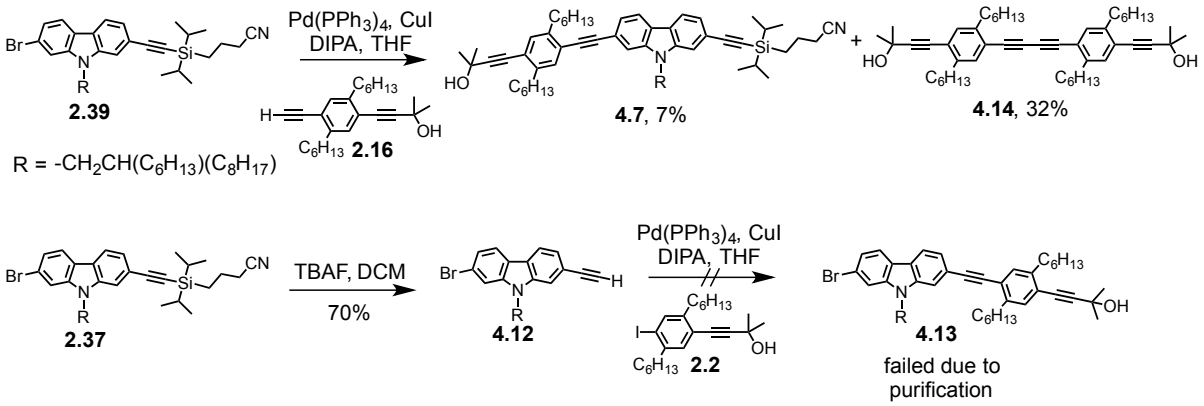

Scheme 4.2: Shifting the acetylene disconnection back using building block 2.39 made for a lousy reaction sequence in attempts to form 4.7. A selective Sonogashira coupling of iodine from 2.2 in the presence of bromine on 4.12 led to an inseparable mixture of sm and the product 4.13.

In order to find an alternative route, the selectivity of iodine over bromine in Sonogashira couplings was employed lower sequence, Scheme 4.2. **2.37** was deprotected with TBAF to yield **4.12** in 70%. Palladium catalyzed coupling conditions were applied to **4.12** with **2.2** to form **4.13**. However during purification it become apparent that the R_f values of the starting material **2.2** and the product **4.13** were too close to be separated from each other on SiO_2. This is due to the dominance of the -OH functional group on the polarity of these otherwise apolar molecules.

In an attempt to improve on the yields shown in Scheme 4.1, and avoid the wasteful di-acetylene formation, the acetylene disconnection was completely removed from the carbazole (Scheme 4.3). Building block 2,7-dibromo-9-(2-hexyldecyl)-carbazole **2.32** was subjected to a statistical coupling with aryl-building block **2.16** which afforded **4.13** in 24% yield. Only trace quantitates of the homocoupled aryl **4.14** were observed, in contrast to the large amount seen formed in the reaction with **2.37** described above.

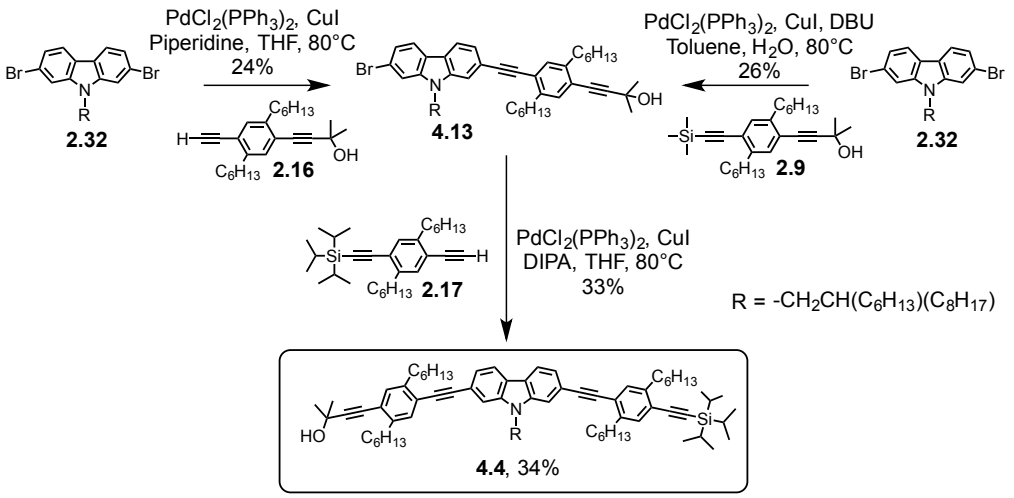

Scheme 4.3: Starting from building block 2.32 quickly leads to the formation of rod 4.4, 1/8th of the intended macrocycle target. 4.13 can be synthesized by a statistical coupling of 2.16 or by an in situ deprotection/coupling procedure under standard Sonogashira conditions with 2.9. The subsequent coupling of 4.13 with 2.17 afford 4.4 in an overall yield of 4.5% over five linear steps.

The mono-substituted carbazole **4.13** could also be formed by performing an in situ deprotection and coupling procedure as reported by Mio et al.[112] with a modestly improved yield of 26%. **2.32** was reacted with **2.9** in the presence of the normal Sonogashira catalyst, but with the addition of DBU and stoichiometric quantities of H_2O in order to remove the TMS PG from **2.9**. With **4.13** in hand it could be coupled with **2.17** to afford **4.4** in 34% yield. This route reduced the number of linear steps from nine down to five with an overall yield of 4.5% for an orthogonally protected 1/8th cycle, a marginal improvement than when starting with the di-acetylene carbazole **2.41**, and a much preferred route given the reduction in the number of linear steps. However a more drastic improvement is required in order to obtain sufficient quantities of the 1/8th cycle to complete the macrocyle synthesis. This can be made by performing a halogen exchange on the carbazole moiety from bromine to the more reactive iodine species, as presented below.

4.2.2 Synthesis of the linker to make quarter cycle rim

With a working route to the 1/8th cycle in place, the next disconnection calls for the synthesis of a linker to combine two molecules of the 1/8th cycle rod and attach this extended rod to a central template. 2,7-9*H*-carbazoles have three reactive sites, and seem the obvious choice to use given the supply of building blocks already available. Because the 1/8th rods **4.4** and **4.10** are already asymmetric, differing only in their silyl protecting groups, the linker can be symmetric and used to attach two rods together with a stoichiometry of 1:2.

2,7-9*H*-carbazole **2.31** was alkylated following the standard procedure presented in section 2.2.1, of chapter 2, using an excess of 1,12-dibromododecane (Scheme 4.4). This yielded a majority of the desired alkylated carbazole **4.15**, and a small quantity of the di-substituted alkyl chain **4.16**. This di-substituted product **4.16** was used in test reactions to investigate conditions to ensure an efficient coupling of acetylene groups to the carbazole core. This four-fold coupling required extended reaction times, extensive heating and additional catalyst loadings to drive the reaction to completion yielding **4.17** in only 15% with the most favorable reaction conditions.

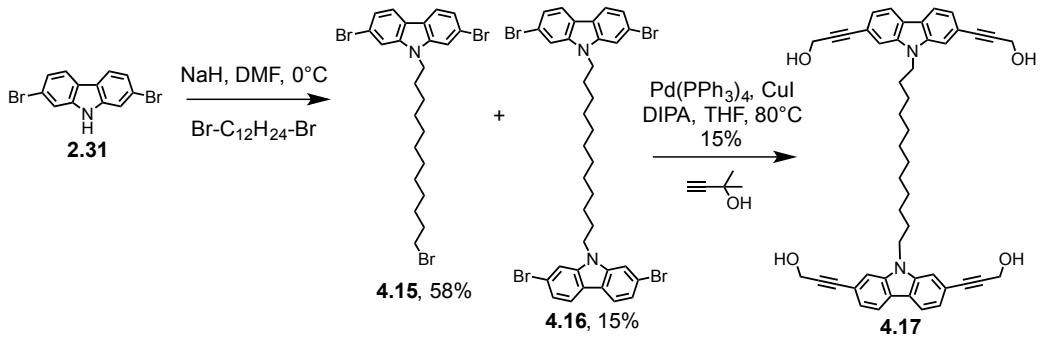

Scheme 4.4: Synthesis of linker carbazole by alkylation of building block 2.31. The reactivity of the carbazole towards Sonogashira coupling was tested by reacting 4.16 with HOP-A to afford 4.17.

In order to overcome the low reactivity of the di-bromo compounds a method of performing a halogen exchange was investigated. Taking inspiration from Müllen and co-workers,[260][261] a palladium catalyzed borylation was performed on **4.15**, yielding the bis-borylated product **4.18** in 65% (Scheme 4.5). Treatment of **4.18** with Chloramine-T and NaI successfully replaced the boron species with iodine, however a scrambling of the alkyl-halide was also observed giving a 'clean' mixture. The nmr showed a clean aromatic region, but both alkyl species could be observed in a rough ration of 2:1. This was corroborated by mass spectrometry which indicated the presence of both species **4.19** and **4.20**. Attempts at a Finkelstein substitution in DMF to isolate a single molecular species led to the somewhat unanticipated formation of the alkyl formate **4.21** due to decomposition of the DMF at the elevated temperatures employed. Fortunately the formate group in **4.21** could be efficiently converted to the primary alcohol **4.22** using strong acid in refluxing EtOH.

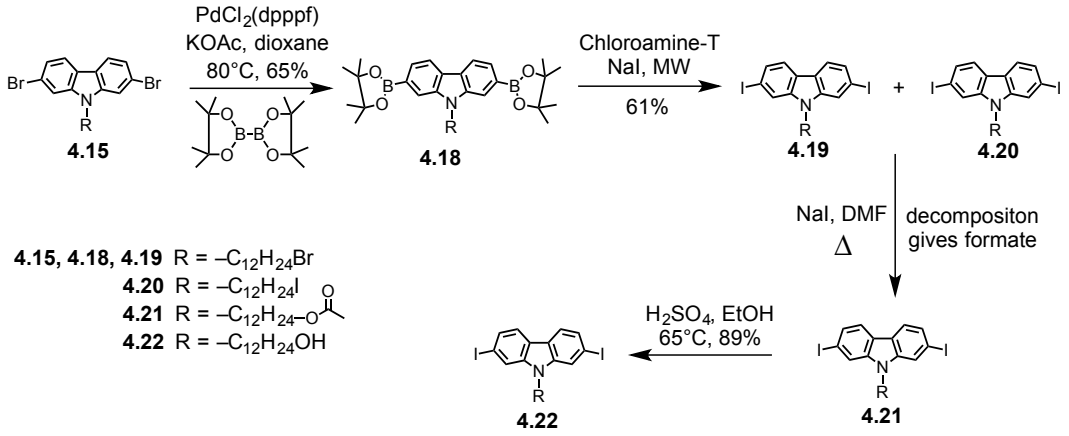

Scheme 4.5: Transformation of the di-bromo linker 4.14 into the diiodo linker 4.22, also shifting from a bromo-alkyl group in 4.14 to a primary alcohol in 4.22.

A more efficient and smarter way to perform the halogen exchange of a bromo-carbazole to an iodo-carbazole was presented in section 2.2.4 in chapter 2. In order to profit from this more efficient aromatic-Finkelstein type reaction **2.31** was alkylated with 12-Bromo-1-dodecanol using K_2CO_3 as base yielded **4.23** in 55% (Scheme 4.6). Then a halogen exchange was performed using the Buchwald conditions[209] to afford the symmetric iodo-carbazole **4.22** in 96%.

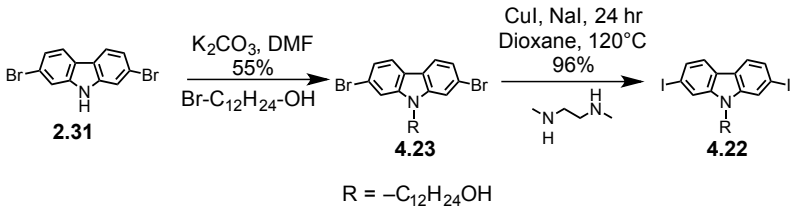

Scheme 4.6: Efficient synthesis of linker 4.22 by alkylation of building block 2.31, followed by a copper catalysed halogen exchange.

With this linker in hand the next step on our path to the target macrocycle is to attach two 1/8th cycle rims to linker building block **4.22**. It also becomes tempting, with this efficient halogen exchange method, to enhance our existing synthesis of the 1/8th cycle.

4.2.3 Synthesis of the 1/8th cycle rim accelerated with iodo-carbazoles

In section 2.2.4 of chapter 2, we saw how halogen exchange on carbazoles could be performed in quantitative yield after only an extraction using a CuI/NaI mixture. The diiodo carbazole **2.42** was applied following the five step linear sequence described in section 4.2.1 above. A statistical coupling of **2.42** with **2.16** afforded **4.24** in an acceptable 40% yield, and

19% yield of the di-substituted compound **4.25**, already indicating the greatly increased reactivity of the iodo-species.

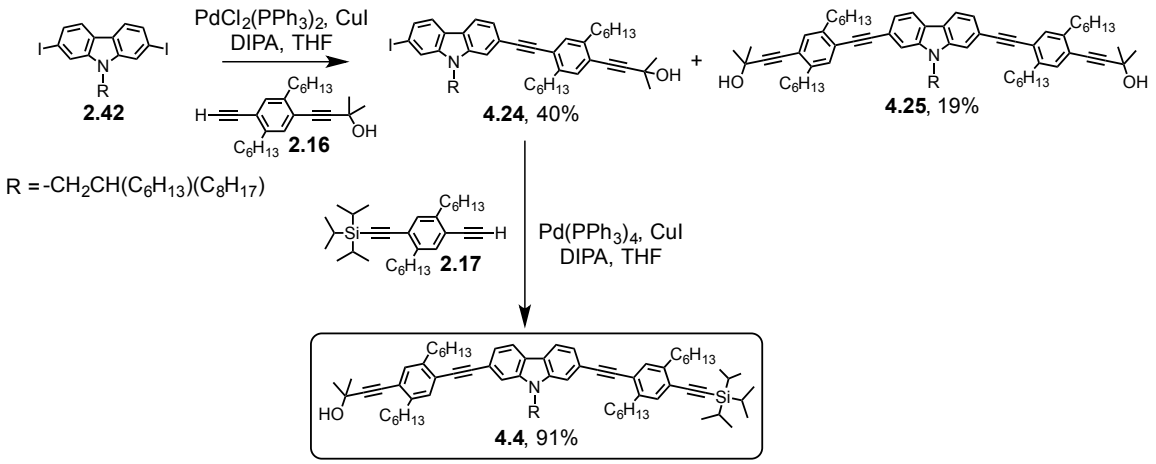

Scheme 4.7: Improved synthetic route to 1/8th cycle 4.4 using the increased reactivity of iodo-carbazole to Sonogashira cross-couplings.

A second Sonogashira coupling of **4.24** with **2.17** afforded the target 1/8th rod **4.4** in an amazing 91% yield. This is almost three times the yield observed for the same reaction carried out with the bromo-species **4.13**. Overall this route has a linear sequence of six steps with an overall yield of 18.5%, the main loss occurring at the statistical reaction step, but the recovered starting material can be recycled, so the route is actually less wasteful than the overall yield would suggest.

4.2.4 Assembly of the quarter cycle and characterisation

With an efficient route to the synthesis of the 1/8th cycle rod bearing orthogonal protecting groups **4.4** and **4.10**, the next step is to couple them with the di-iodo linkers described above. In order to 'load the deck' in our favor, it is proposed that the HOP protecting group, which requires refluxing toluene and NaH to deprotect, is removed from the 1/8th rod. The silyl group left in place can be cleaved under the more mild conditions of TBAF at RT, leaving it as the only PG present in the resulting quarter cycle. Initially the polar silyl PG, CPDIPS from **4.10** was investigated over the TIPS from **4.4** because it was hopped that its extra polarity would make the purification of the target compound **4.27** on silica easier.

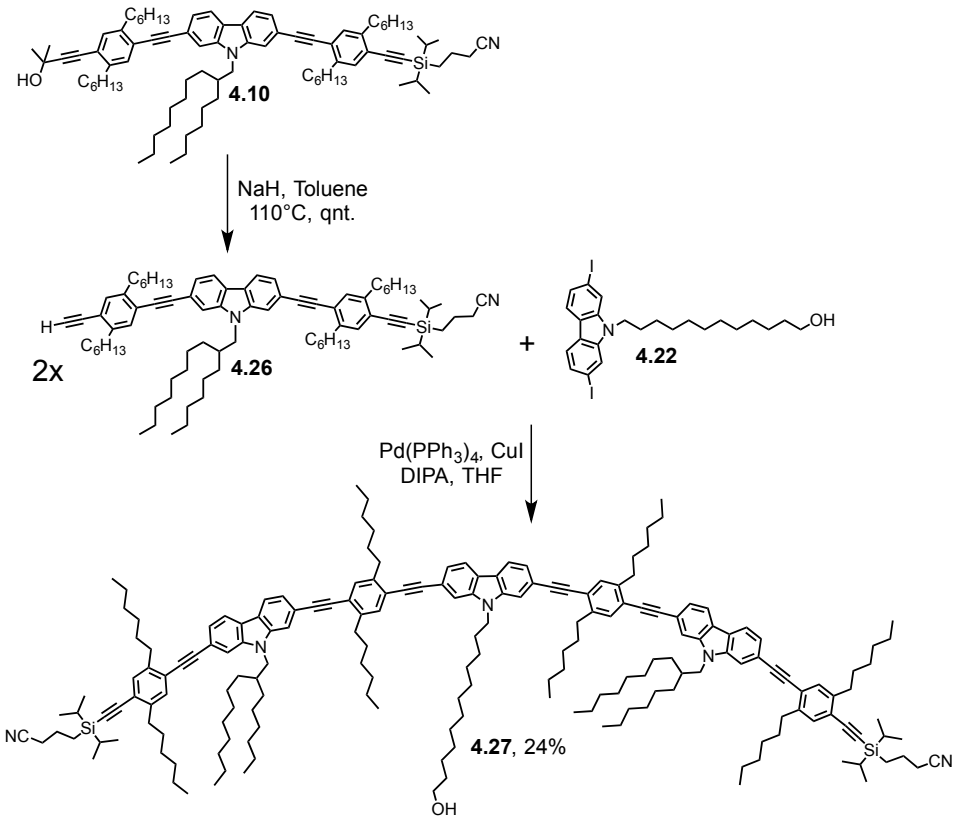

Scheme 4.8: Synthesis of quarter cycle 4.27. Deprotection of the HOP group from 1/8th cycle rod 4.10 afforded 4.26 quantitatively. Sonogashira coupling of 4.26 with 4.22 afforded the quarter cycle 4.27 in 24% yield after purification.

The deprotection of the HOP group from **4.10** using the standard conditions afforded **4.26** quantitatively (Scheme 4.8), however it required several hours to be complete by TLC, in contrast to the usual 1 hr at reflux for other HOP protected aceetylenes. This extended reaction time is likely due to the reduced reaction site to molecule ratio, meaning that more collisions are required before the correct reaction geometry is obtained in solution. After characterization of **4.26** by MALDI-TOF of the reaction, this compound was worked up and used directly in a Songashira coupling with **4.22** as the stability of this free acetylene was not known. The coupling using $Pd(PPh_3)_4$, CuI in a mixture of DIPA and THF afforded the target quarter cycle compound **4.27** in 24% yield after purification. After extraction the crude was passed through a column of SiO_2 running a gradient of cyclohexane:DCM. Some starting material could be recovered, however a second column was required to remove the homo-coupled side-product and afford the quarter cycle **4.27** NMR pure.

The full assignment of **4.27** was made using a Bruker 600 MHz NMR and extensive 2-D experiments with the help of Dr. Daniel Häussinger, the departmental NMR expert. Using deuterated chloroform as solvent the following experiments were made; proton ^{1}H, carbon ^{13}C, COSY, HMQC, HMBC, NOESY, TOCSY and DOSY. The diffusion coefficient was

determined to be 3.03 x 10^{-10} m^2S^{-1}. See section 3.3.4, of chapter 3, for a discussion on how the diffusion coefficient can be calculated from a DOSY spectrum, Figure 4.7 (top) shows the curve fitting. The proton ^1H assignment is depicted graphically in Figure 4.7.

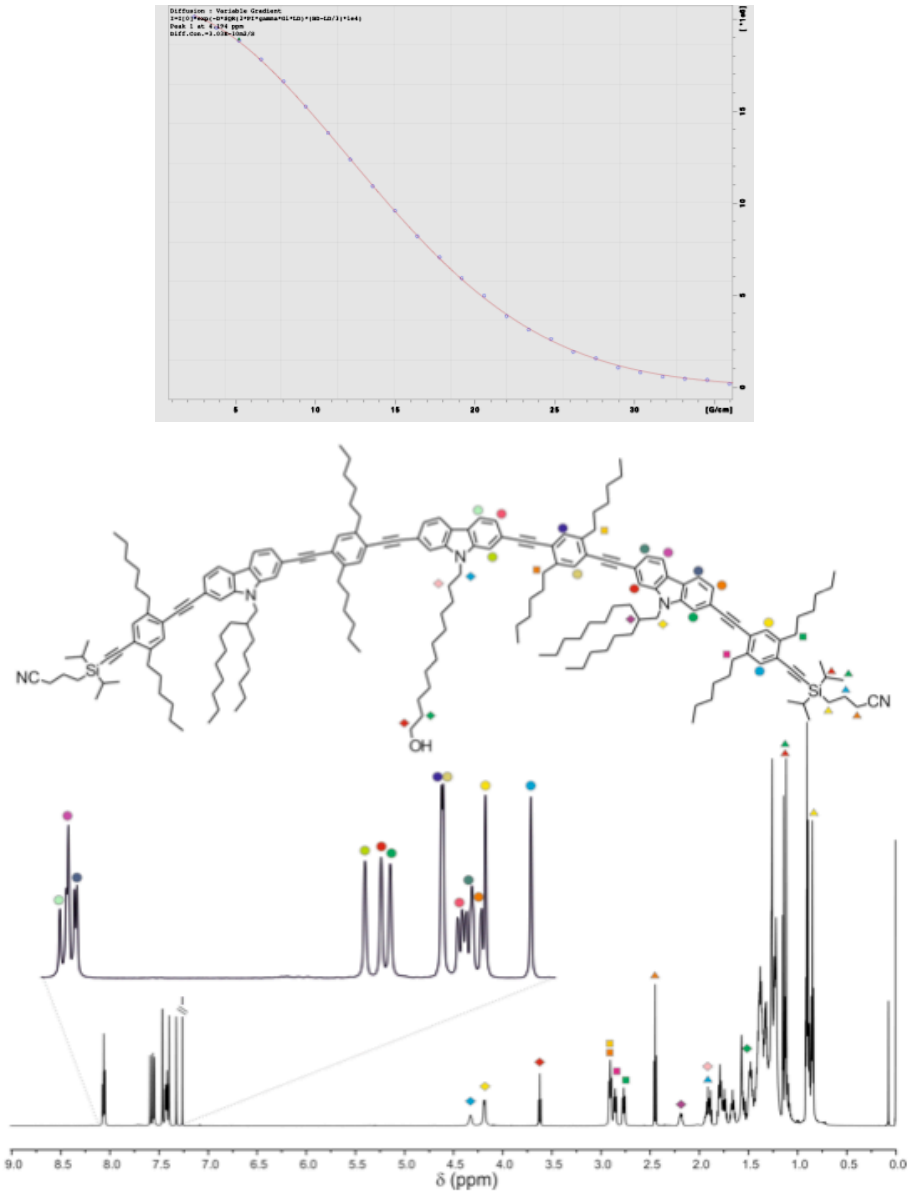

Figure 4.7: Top: curve fitting to the PGSE experiment. Bottom: ^1H NMR (600 MHz, $CDCl_3$) full spectral assignment of quarter cycle 4.27 was made using a combination of 2D experiments (^1H, ^{13}C, COSY, HMQC, HMBC, NOESY and TOCSY). The diffusion coefficient was determined to be 3.03x10-$^{10}m^2s^{-1}$.

The photophysical properties of the rods **2.41**, 1/8th cycle **4.10** and quarter cycle **4.27** were also investigated. This shows a marked bathochromic shift in absorption and fluorescence, exactly as would be expected with the increase in conjugation length. The increase in absorption cross-section indicates a reduction in the size of the HOMO – LUMO gap. For the quarter cycle **4.27**, excitation at either absorption band 274 nm or 395 nm gives rise to an

identical emission band, with lower intensity. This indicates that the transition arises form the same excited state species, despite the excitation being on a different molecular band.

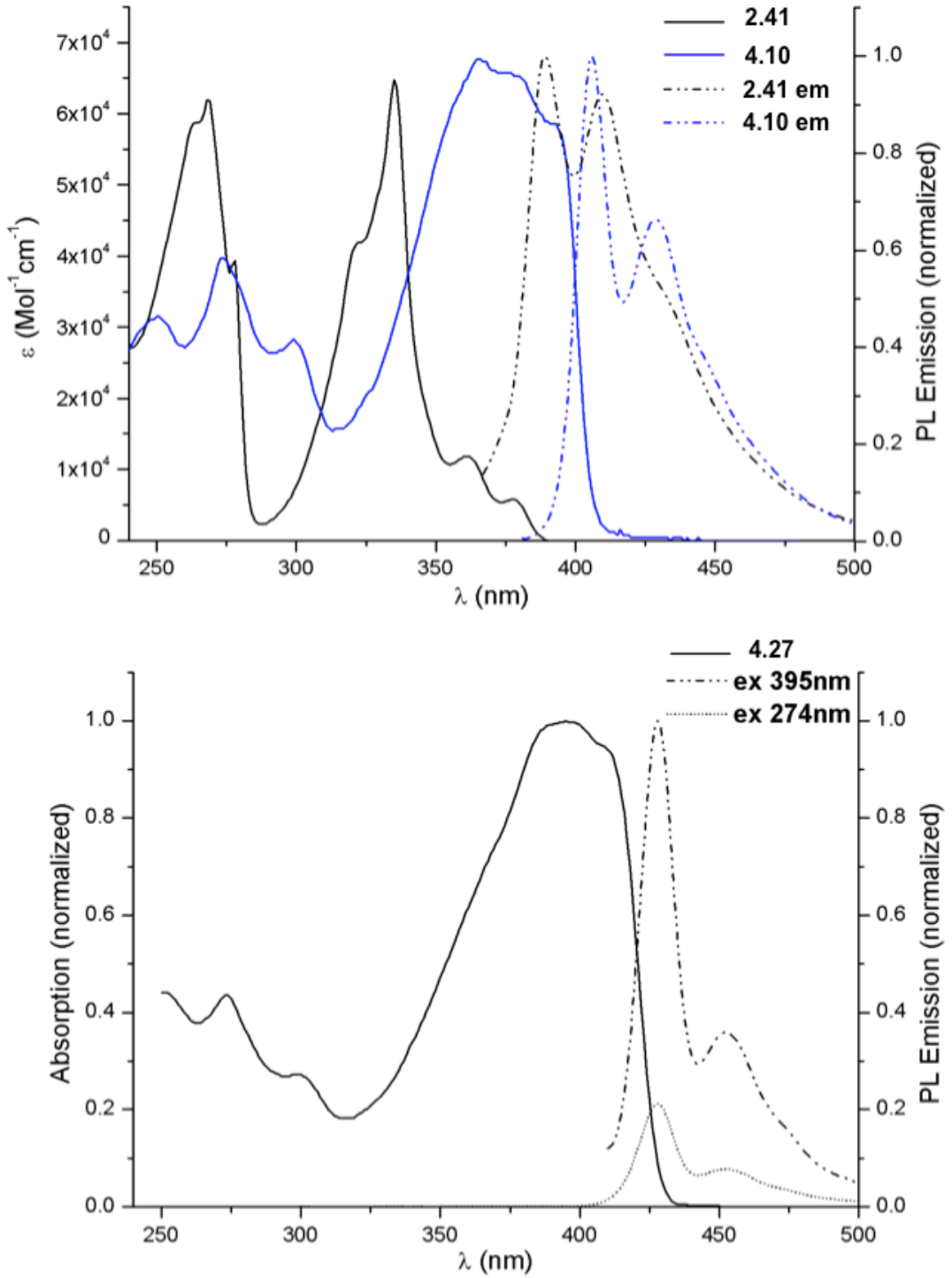

Figure 4.8: Photo-physical investigations were made in CHCl3 at room temperature. Top: Fluorescence excitation 2.41: 330 nm, 4.10: 365 nm. Bottom: respective adsorption and emissions are shown with normalised intensity.

These photo-physical properties are in line with expectations and demonstrate the broad scope for applying these carbazole compounds in opto-electronic devices.

4.2.5 Synthetic approaches to suitable template scaffolds

In order to promote an efficient cyclisation reaction to afford the desired macrocylic structure a template is vital. A covalent template, which is not conjugated with the outer ring is desirable in order to ensure that any electronic effects are confined to the ring itself, without interference from the template so a less rigid structure with alkyl chains is desired. The use of biphenyl or terphenyl moieties is desired to aid with physisorption of the marocylce to a surface by increasing the interaction strength between molecule and surface. For the template synthesis a convergent approach was desired, in order to limit the number of 4-fold reaction steps required.

In order to have four reactive sites from which the template can reach out to attach to four molecules of the quarter cycle, forming a four-mer type dendron a tetrahydroxy terphenyl **4.5** was envisaged, with a very similar structure and synthesis to that reported by Roberti et al.[262] (Scheme 4.9)

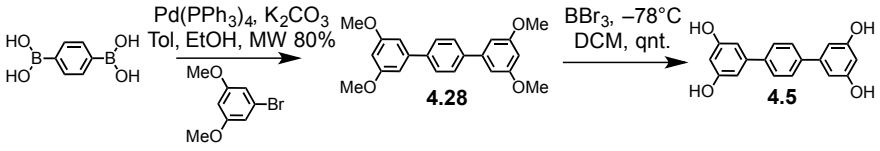

Scheme 4.9: Synthesis of terphenyl 4.28 was achieved by Suzuki coupling. The methoxy groups could be cleaved quantitatively using an excess of boron tribromide to afford the tetrahydroxy 4.5.

A palladium catalyzed Suzuki coupling of Benzene-1,4-diboronic acid in a solvent mixture of toluene/EtOH, with commercially available 1-Bromo-3,5-dimethoxybenzene afforded terphenyl **4.28** in 80% yield. The reaction time could be reduced and the corresponding yield improved by subjecting the coupling to microwave irradiation with complete conversion after just 45 min. Removal of the $–CH_3$ groups to reveal the free –OH could be made quantitatively by treating **4.28** with BBr_3 at –78°C to afford the desired terphenyl **4.5**.

With the template core in hand, we now turn our attention to the template arms. From the synthetic strategy outlined above in section 4.1.4 the arms of the template can be built up from 4,4'-dibromobiphenyl **4.29** in a modular way to allow for incorporation of different end functional groups to investigate for their potential to link the template with the outer quarter cycle rod. Starting with a statistical Sonogashira coupling of **4.29** with 5-Hexyn-1-ol afforded biphenyl **4.30** in up to 77% yield by using an excess of the alkyl-acetylene, with only small quantities of the di-substiuted biphenyl **4.31** formed (Scheme 4.10). An Apple reaction using PPh_3 and NBS in a 1:1 mixture of MeCN:Et_2O transformed the –OH group in **4.30** into an alkyl-bromide **4.32** in up to 95% yield.

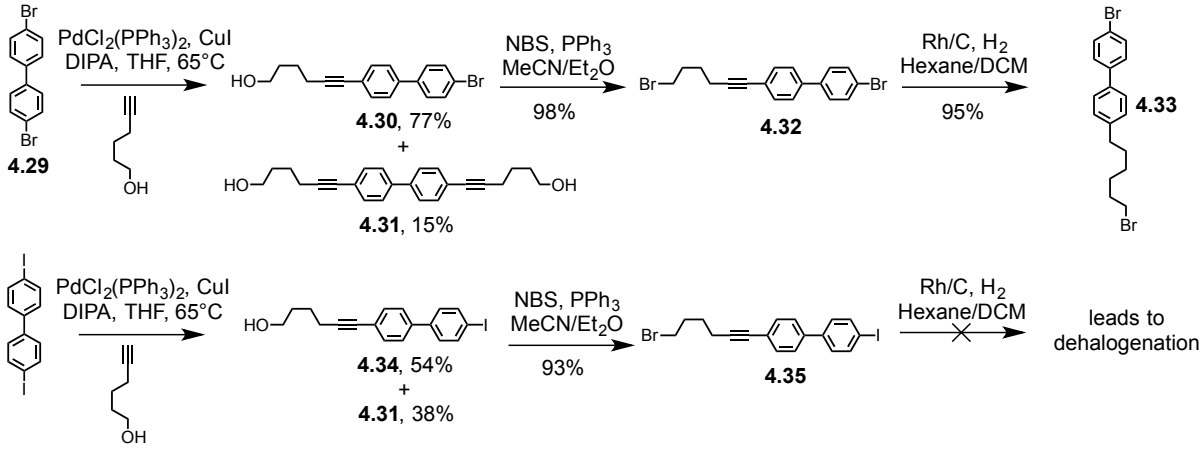

Scheme 4.10: Synthesis of template arms bearing an Ar-X for FGI to allow for connection to the quarter cycle linker. Statistical coupling of di-halo biphenyls gave 4.30 and 4.34. An Apple reaction converted the –OH group to alkyl-halogens into 4.32 and 4.35. Reduction of acetylene FG with a rhodium catalyst and 10 bar H_2 gave 4.33 in high yield. Subjecting 4.35 to the same conditions failed as dehalogenation occurred.

At this stage, many attempts were made to reduce the acetylene FG in **4.32** as it was thought that it may make the final compounds less thermally and optically stable, as it is well reported that activated acetylenes can undergo numerous reactions.[7] Hydride reduction with a Pd(0) catalyst was investigated in the reduction of **4.32** to **4.33**. However very inconsistent results were obtained. Occasional the reaction worked as desired, but more often there was no conversion seen. Varying the catalyst loading, switching from Pd/charcoal to Pd/carbon and varying the applied pressure of H_2 facilitated the dehalogenation of the Ar-Br. After consulting the literature, a rhodium catalyzed reduction was attempted. Adapting the literature procedure of et al.[263], Rh on carbon was used with 10 bar H_2 and afforded the reduced biphenyl **4.33** reliably in up to 95% yield.

Another template arm **4.35** bearing an Ar-I was also synthesized (Scheme 4.10 lower) in an analogous fashion to the Ar-Br arm, simply substituting the starting biphenyl for 4,4'-diiodobiphenyl. However in this case, moving to the iodo-species actually resulted in poorer yields. This can be attributed to the low solubility of the iodo-biphenyl species, which is markedly lower than the corresponding brom-biphenyls. Applying Pd catalyzed reducing conditions to **4.35** lead to dehalogenation, perhaps not unexpectedly owing to increased reactivity of Ar-I to palladium. Applying the rhodium conditions from et al.[263] described above still resulted in isolation of the dehalogenated species, and this synthetic route was not investigated further.

With these template arms in hand, the next step was to attach them to the template core **4.5** (Scheme 4.11). The S_N2 substitution of the alykyl-bromide in **4.33** was very slow. In order to

accelerate the reaction and drive it completion the addition of KI was required to act as nucleophilic catalyst. Stirring the core **4.5** with **4.33** in DMF with K_2CO_3, and KI for four days gave the desired tetra-substituted template **4.36** in 70% yield after purification. Although a mass signal for temp11 could not be observed despite numerous efforts, 2-D NMR studies allowed for a full assignment of the spectrum, corroborating the structural identity of **4.36**. Elemental analysis with a surprisingly good agreement could also be obtained.

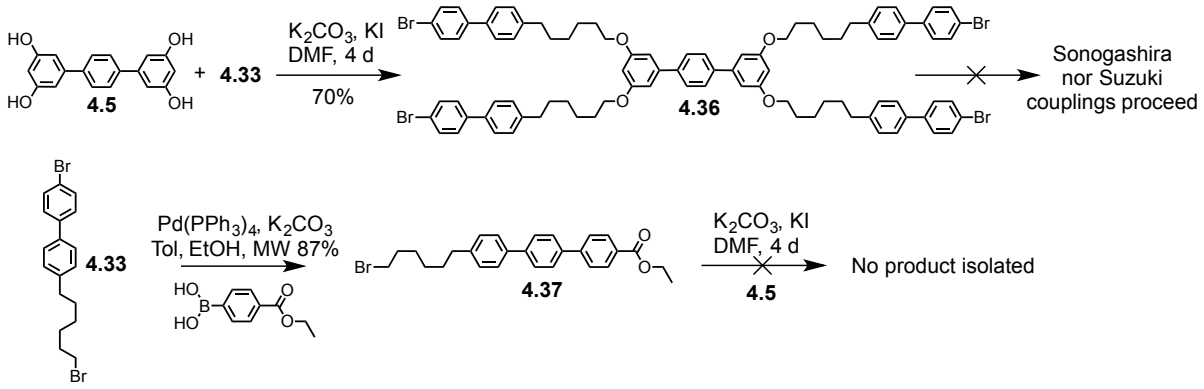

Scheme 4.11: Template assembly by S_N2 substitution. The identity of 4.36 was confirmed with extensive 2-D NMR studies. Attempts at functionalising the Ar-Br groups failed. Therefore the coupling was first performed on 4.33 to afford 4.37 with a suitable FG to use for connecting to the quarter cycle. Unfortunately attaching 4.37 to the core 4.5 could not be achieved.

Further functionalization of **4.36** by palladium coupling to the Ar-Br present was desired. Initially **4.36** was subjected to standard Sonogashira coupling with TIPS-A using a range of palladium catalysts, however no product could ever be isolated. Pushing the reaction with higher catalyst loadings lead to the formation of the fourfold-dehalogened compound. This would indicate that oxidative addition was being achieved, and it was rather the transmetalation step which was the problem. Moving to a Suzuki cross coupling using the commercially available 4-ethoxycarbonylphenylboronic acid still failed to lead to a reaction, and only wild mixtures were observed, even after purification of what was a single spot by TLC. With these difficulties in mind, other synthetic routes were explored.

After storage of template arm **4.32** it was determined that the acetylene was sufficiently stable to be left in place. Therefore **4.32** was functionalised with two desired FGs that would be appropriate to use in connecting the template to the outer cycle rims (Scheme 4.12). **4.32** was used in a Sonogashira coupling with TIPS-A to afford **4.38** in good yield. Suzuki coupling conditions were applied to **4.32** to afford **4.39**, again in good yield.

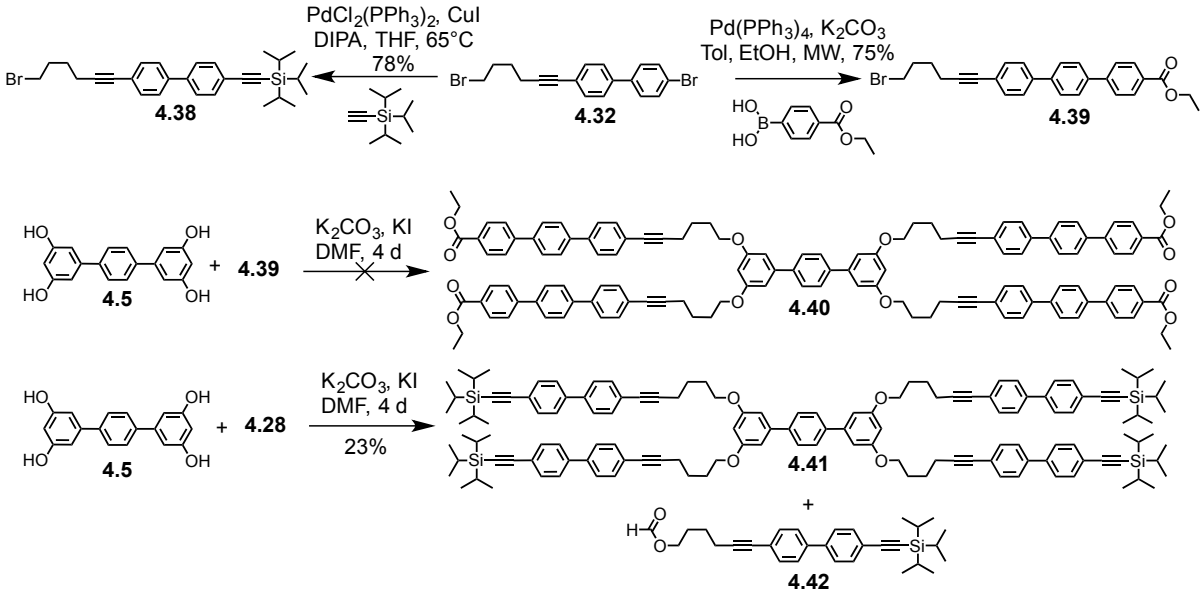

Scheme 4.12: Synthesis of template rods and their assembly as precursors to the desired template 4.3. The building block 4.32 was derivatized to two different functional groups, an acetylene 4.38 and a carboxylic acid 4.39. Assembly by S_N2 substitution only succeeded in the isolation of 4.41.

The assembly of the template using both arms **2.38** and **2.39** respectively, was then attempted using the best of the screened conditions in the formation of **2.36**. Unfortunately after stirring the core **4.5** with **2.39** no product could be isolated. After heating and extending the reaction time new species were seen by TLC, but were only mixtures once isolated by column chromatography. Some mixtures showed weak MALDI mass signals that would fit with the presence of one or more free carboxylic acids. Therefore the mixtures were treated to hydrolyzing conditions but the free carboxylic acid analogue of **4.40** could not be identified. After performing the same hydrozing conditions directly to template arm **4.39**, the resulting free carboxylic acid compound could also not be isolated. Fortunately subjecting **4.5** and **4.38** to the same conditions did result in formation of the desired template **4.41**, after heating for four days and purification by recycling GPC. The yield of the reaction at 23% is quite low, but this can be attributed to the formation of the formate compound **4.42** which was isolated from the reaction mixture. It was likely formed by the decomposition of DMF at elevated temperature for an extended period of time. By GPC the main side products were attributed to be the mono-, di- and tri-arm substituted forms of **4.41**. A test reaction to ensure that the TIPS PGs could be removed cleanly was performed (Scheme 4.13).

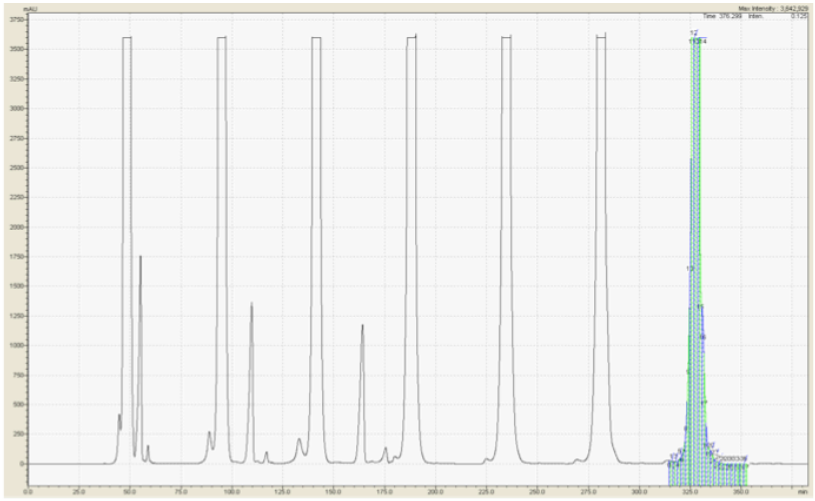

Figure 4.9: Reccyling GPC trace, showing the purification of the TIPS protected template 4.41.

Under dry conditions, template **4.41** was dissolved in DCM and an excess of TBAF (1M in THF) added. The desired fully deprotected template **4.43** could be isolated quantitatively, provided the reaction was left for stirring for several hours.

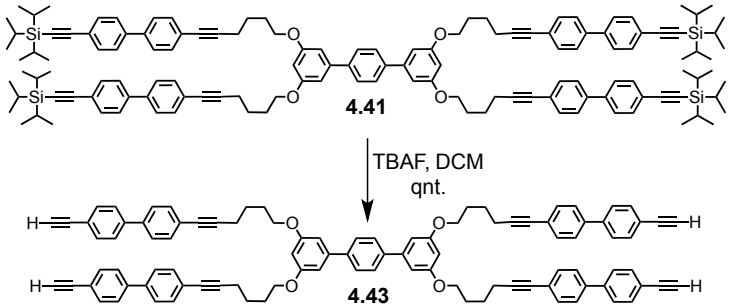

Scheme 4.13: Quantitative deprotection of template 4.41 using TBAF afforded the free acetylene template 4.43 ready for an azide click reaction to connect four molecules of the quarter cycle rim.

The successful synthesis of template compound **4.43** was achieved over seven steps in an overall yield of 45.6% from commercial starting materials, using one statistical reaction. The next challenge is to use this template to connect four molecules of a quarter cycle rod, as the last step prior to forming the target macrocycle.

4.2.6 Connecting the template to the quarter cycle rim

With the template and quarter cycle in hand, we are well on the way to our target macrocycle. An ideal method to connect the outer rim to the inner template would be by a click reaction of an azide to the terminal acetylene of **4.43**. In order to hedge ourselves once again, the linker **4.44** was made as a model compound for use in test reactions for the assembly of the outer rim to the template (template synthesis described above in section 4.2.5) Compound

4.44 (Scheme 4.14) was envisaged as a proxy for quarter cycle **4.27**, as it bears the same CPDIPS PGs. The coupling of **4.15** with CPDIPS-A was made to be able to test azide formation with the shortest route to a test compound with the library of building blocks in hand at that time. The coupling reaction is surprisingly high yielding at 89%, given that it is performed on a di-bromo carbazole, and in marked contrast to the HOP-A coupling to form **2.40** discussed in section 2.2.3, chapter 2. This is perhaps another example of the CPDIPS groups' electron withdrawing power over HOP being able to accelerate the rate of oxidative addition of palladium during Sonogashira coupling.

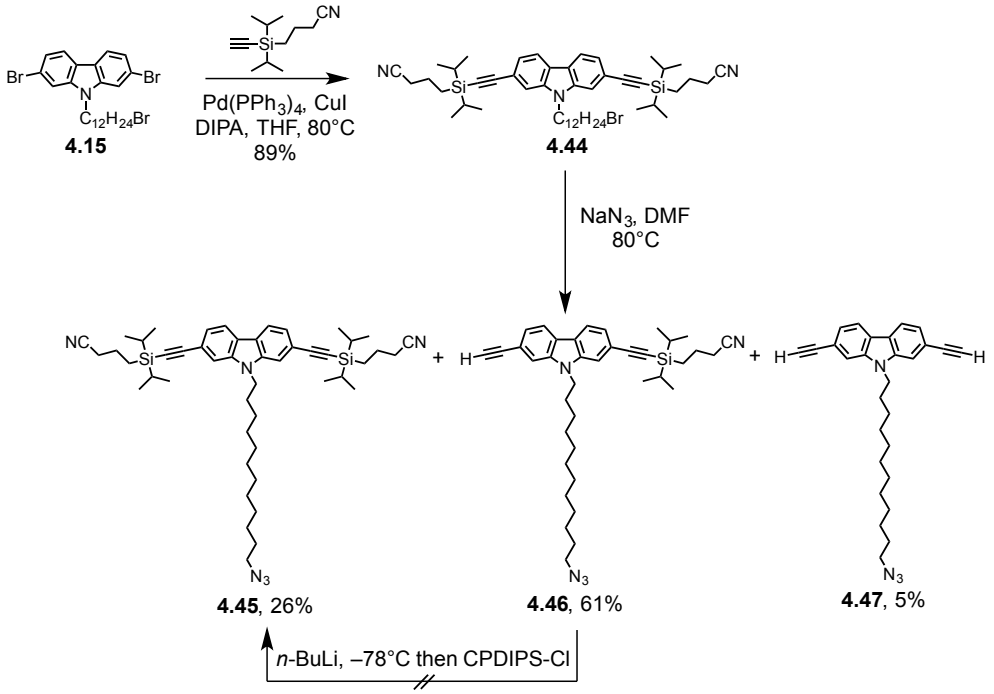

Scheme 4.14: Test compound 4.44 was synthesized as a test compound for azide formation. The coupling of CPDIPS-A to 4.15 gives a high yield of 4.44. Substitution of the alkyl-bromide in 4.44 leads to the unexpected deprotection of CDPISPS giving a mixture of products. Conversion of 4.46 into the desired 4.45 via the acetylide gives an inseparable mixture.

During the attempt at a clean reaction of the azide substitution of the alkyl-bomide in **4.44** using sodium azide in DMF at 80°C the sudden and unexpected deprotecton of the CPDIPS occurred to give a mixture of **4.45**, **4.46**, and **4.47**. Disaster. The only saving grace was that there was clean substitution of the alkyl-bromide in all products. The $N_3^{\ominus}$ anion is obviously a strong enough, and small enough nucleophile to be able to deprotect the CPDIPS group. Looking at the ratio of products of this unintended deportection, it is tempting to conclude that the azide is selective for formation of the mono-deprotected compound **4.46**, a curious insight. However it is more likely that the product ratio is actually due to the equivalence of azide present being used up, which halted the deprotection reaction. An attempt was made to

convert **4.46** into **4.45** using *n*-BuLi at –78°C to form the acetylide and quenching with 3-Cyanopropyldiisopropylchlorosilane (CPDIPDS-Cl), however the reaction did not proceed cleanly and the mixture was abandoned.

This result rules out the use of quarter cycle **4.27** in an azide coupling to a template. Another test compound, **4.48** this time bearing two TIPS protecting groups was synthesized by coupling **4.23** with TIPS-A under standard Sonogashira conditions (Scheme 4.15).

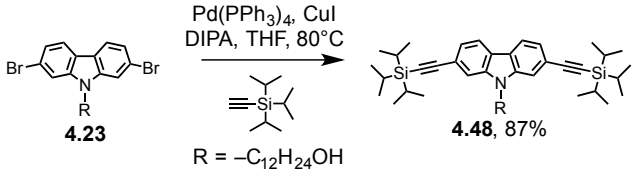

Scheme 4.15: A different model compound 4.48 bearing two TIPS protecting groups was synthesised by Sonogashira coupling of building block 4.23 with TIPS-A.

Stirring **4.48** with sodium azide in DMF at 80°C led to total recovery of the starting material, indicating that the additional steric bulk of a third isopropyl group was sufficient to prevent deprotection. With this insight in mind, a second quarter cycle **4.2** was synthesized in analogous fashion to **4.27** using the TIPS protected analogues (Scheme 4.16).

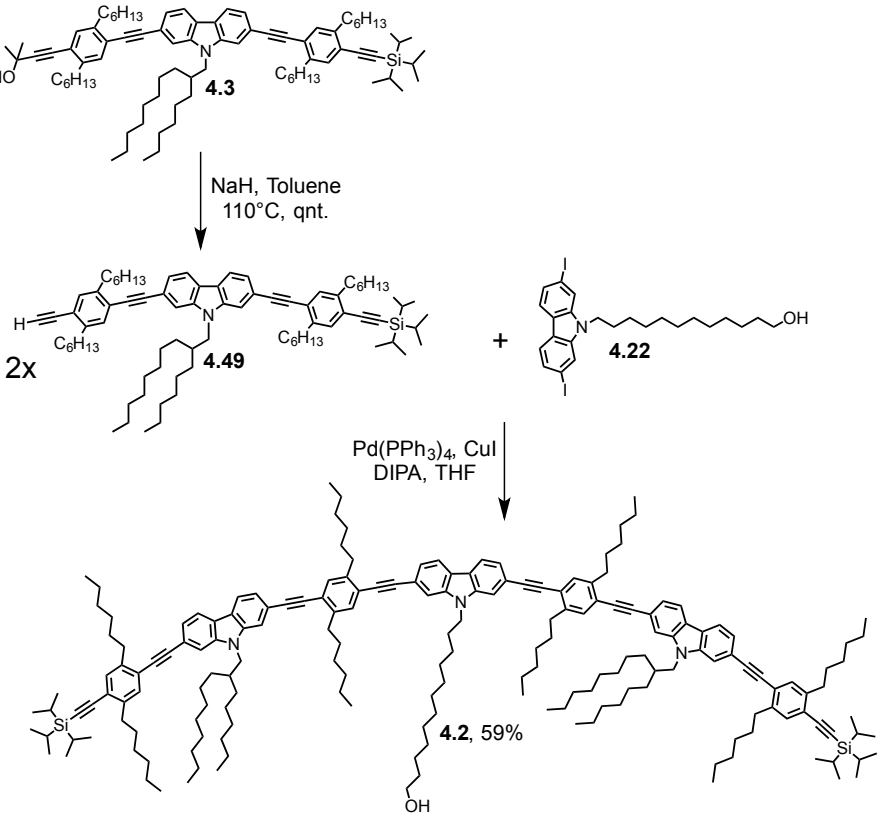

Scheme 4.16: Synthesis of quarter cycle 4.2 using TIPS protecting groups. The HOP PG of 1/8th cycle rod 4.3 could be deprotected in 93% to 4.49. Sonogashira coupling of 4.49 with 4.22 afforded the quarter cycle 4.2 in 59% yield after purification by GPC.

Starting from 1/8th cycle rod **4.3**, treatment with NaH in refluxing toluene afforded **4.49** in 93% after purification by column chromatography to ensure the subsequent reaction was not contaminated with any side products carried over. Sonogashira coupling of **4.49** with **4.22** in a stoichiometric ratio of 2:1 lead to very clean conversion to quarter cycle **4.2** bearing two TIPS protecting groups after purification by recycling GPC.

By using the shortest route to the quarter cycle, employing iodo groups in all Sonogashira couplings meant that quarter cycle **4.2** was synthesized in an overall yield of 2.62% over a total of 16 steps from commercial compounds in a non-linear sequence. Importantly the yields of the later steps in the sequence are considerably higher yielding and scalable than the first routes investigated.

4.2.7 Attempts at cyclisation

In order to try and short-cut the route towards monodispersed macrocyle the di-HOP 1/8th cycle rod **4.25** was deportected with NaH and the free acetylene **4.50** was reacted under oxidative coupling conditions. Anderson and co-workers[264] have demonstrated that using I_2 as a additive promotes the formation of di-acetylenes.

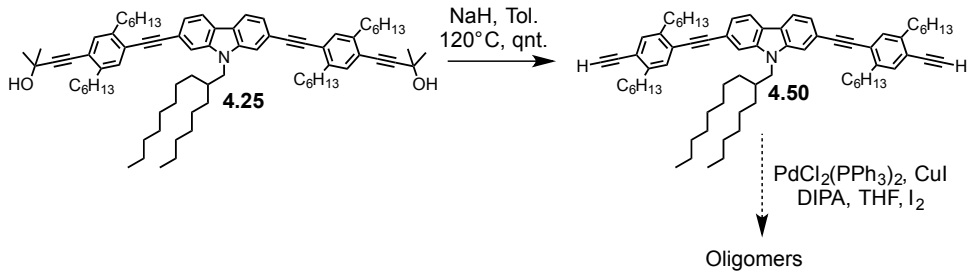

Scheme 4.17: Deprotection of the side product 4.25 gave access to the free-acetylene rod 4.50. Attempts at oligomer formation, or even cyclisation were made using modified Glaer-Hay conditions of Pd(II), CuI in the presence of an oxidant.

High dilution conditions of $>10^{-4}$ molar were used as this is reported to favor the formation of cyclic over linear oligomers.[265] From the recycling GPC trace (Figure 4.10) we can identify the formation of oligomers, but not in sufficient qunatities to be able to identify them. The dimer species was the main signal by MALDI-Tof experiments.

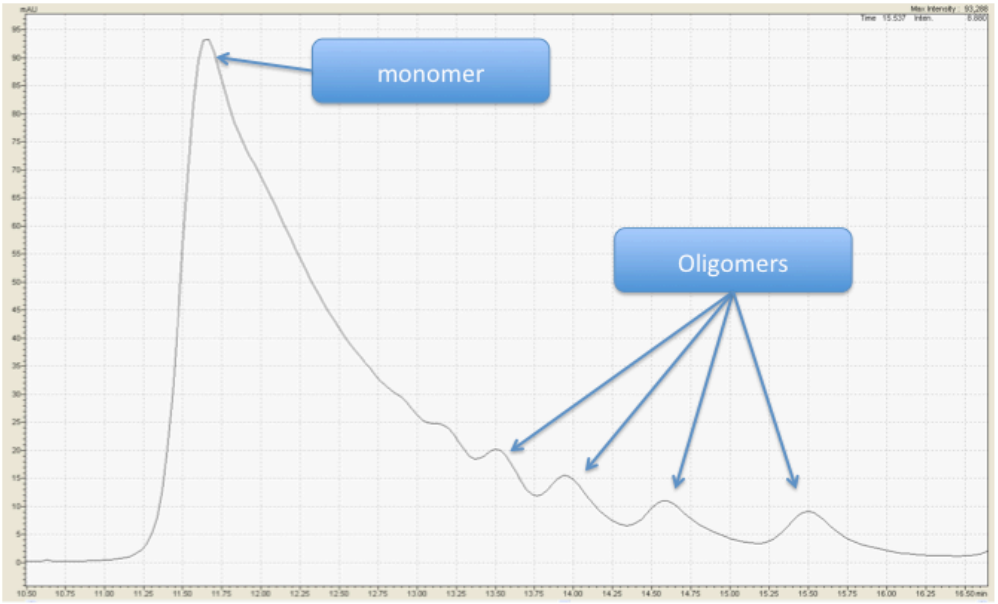

Figure 4.10: Analytical recycling GPC trace of the oligomers formed by the oxidative coupling of the acetylene rod 4.50.

It remains to be seen whether the target cycle **4.1** can be made with this much shorter approach, however the initial investigations favor the afore mentioned stepwise synthetic sequence as the most viable approach.

4.3 Conclusions and outlook

The route towards a giant fully conjugated carbazole based macrocycle was presented. Although the target structure **4.1** was not elucidated, considerable progress was made in proving the synthetic route. The successful synthesis can now be achieved in just 27 steps. The application of shifts in disconnection afforded the quarter cycle rod in as few as 16 total steps in a highly convergent synthesis. By reducing the linearity of the sequence it was possible to increase the scale of the synthesis from sub-ten milligrams up to hundreds of milligrams. This 5.8 nm rod with a molecular weight of 2663 was fully characterized by NMR and UV. Two promising templates were synthesized, and the outer cycle rod adapted to better match the needs of linking the template with the quarter cycle.

5 Supramolecular Architectures

Chapter 5 focuses on the synthesis of star shaped molecules and their investigation on surfaces in hydrogen bonded porous networks. Bottom-up approaches to achieve this surface functionalisation have been achieved by intercalating the porous network from solution onto a Au(111) surface with a series of phenyl-acetylene based stars. Tuning of the chemical structure allows for controlled molecular motion to be observed in the pores, pushing the limits of emergent function by design.

Supramolecular chemistry presents a short cut to the assembly of nanoscale architectures. Instead of the synthetic chemist needing to build up and place every bond and interaction to hold a structure together, the principles of self-assembly can be employed to take over. In Section 1.3 of chapter 1, we covered a series of examples of nanopatterning using such systems. We were introduced to the PTCDI–melamine hydrogen bonded network and its ability to spontaneously form hexagonal honeycomb patterns on a surface.[266]

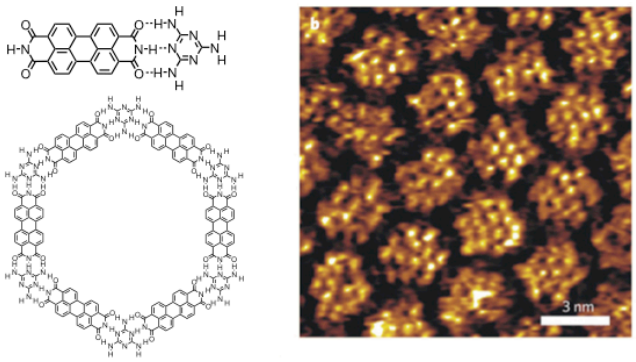

Figure 5.1: Left: H-bonding between Perylene tetra-carboxylic di-imide (PTCDI) and melamine spontaneously forms three coordinate, hexagonal networks on a gold surface. Right: STM image of SAM formation of the network on Au, reprinted with permission from ref. [149]. Copyright 2008, Nature.

Manfred Buck, at the University of St Andrews has pioneered the further functionalisation of this supramolecular system and made extensive studies of it by STM.[149] We set out to investigate the possibilities to use the honeycomb pore as a host for a phenyl-acetylene based stars in collaboration with the Buck group (Figure 5.2).

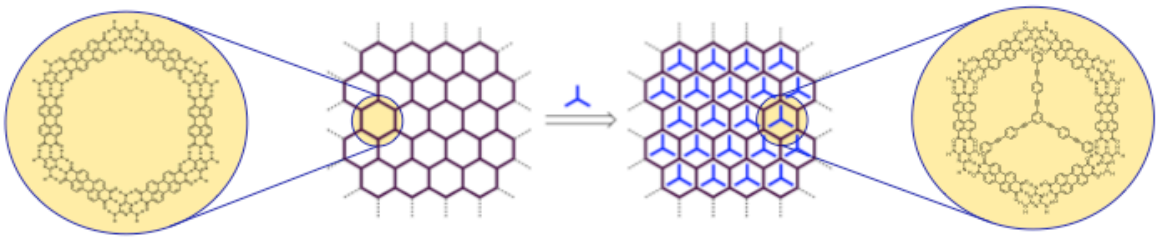

Figure 5.2: Proposed schematic of OPE stars deposited in the PTCDI-melamine honeycomb lattice

It is clear that functionalised surfaces require precise control of substituent architecture and surface morphology. Using bottom-up approaches to achieve such surface functionalisation we set out to use the PTCDI–melamine based hydrogen-bonded porous network as a template to intercalating and host single-molecule rods, and test the limits of control that we as architects can exert on the system by design. All STM studies were carried out by the Buck group at the University of St. Andrews.

5.1 Initial studies – probing the size of the pore

5.1.1 Phenyl-acetylene star synthesis

At the outset we made some inital modeling of the pore in chem-3D, concluding that a three arm, phenyl-acetylene Mercedes type star such as **5.1** should fill the cavity. It was postulated that if the intermolecular interactions were sufficiently weak, and the adsorption of the compound to the underlying gold surface was sufficiently mobile, that the star **5.1** may be mobile within the cavity.

The retro-synthesis of star **5.1** could be achieved by either a convergent or divergent approach. Both were investigated, as each has its own merits. The convergent route (Scheme 5.1) allows for a fast synthesis in just three steps, and only one reaction that must be completed three fold on a single molecular species. The divergent approach (Scheme 5.2) may be easier to purify as the typical side reaction of Sonogashira couplings, the homocoupled di-acetylene compounds, should be separable from the product.

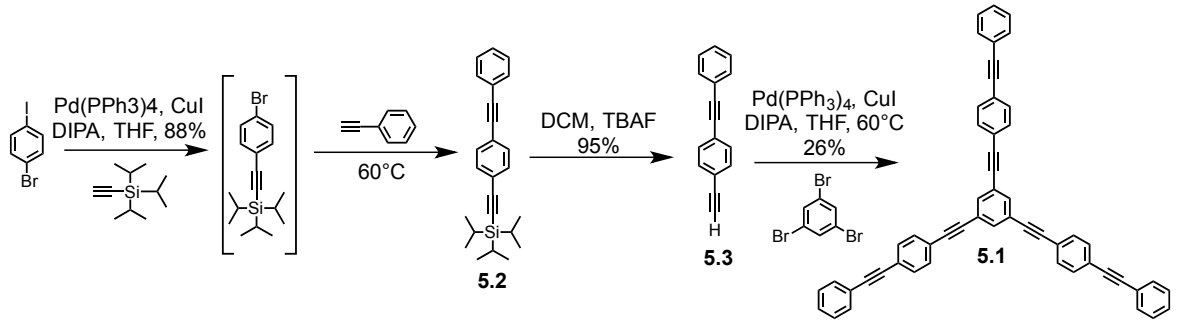

Scheme 5.1: Convergent approach to the assembly of star 5.1. The arms of 5.1 are made in a one-pot, sequential Sonogashira coupling, followed by deprotection with TBAF to give the free acetylene rod 5.2. After deprotection, the final coupling afford 5.2 after a laborious purification.

The arms of the star were assembled using a one-pot, two fold Sonogashira coupling. Using the selective reactivity of iodide over bromide. Stirring 1-bromo-4-iodobenzene with 1 eq of TIPS-A under standard Sonogashira conditions formed the intermediate rod in solution. Later an excess of phenyl-acetylene was added and the reaction stirred for a further time to afford the arm building block **5.2** in 88% yield after purification by column chromatography. Removal of the TIPS PG using TBAF afforded the free acetylene arm **5.3** in 95%. The final coupling to 1,3,5-tribrombenzene afforded the target star **5.1** in 26% yield. However this was only the best yield obtained. The reaction had to be performed multiple times before a suitable purification method could be found involving two columns on SiO_2 and two passes

through size exclusion columns with Bio Beads of different cross-linkings (SX-1 and SX-8). The convergent approach yielded **5.1** in an overall yield of 22%, but with an onerous purification which was made incredibly difficult by side reactions leading to homo-coupled acetylenes and also possibly a cyclo-addition reaction.

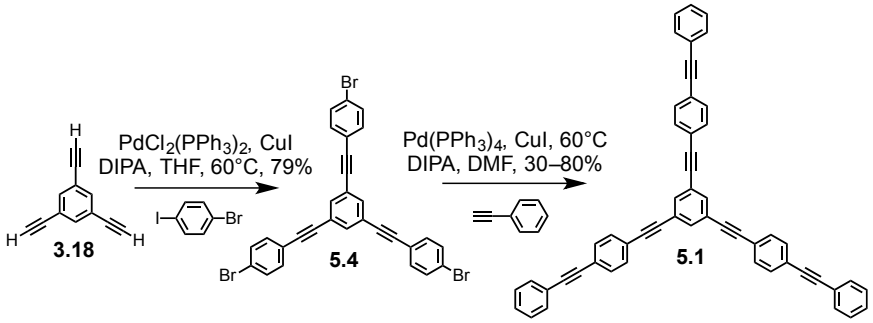

Scheme 5.2: Divergent reaction sequence to the target star 5.1, using the building block 3.18 from chapter 3 in an iodo-selective coupling. The final coupling yield can be increased by using a large excess of phenyl-acetylene.

The divergent approach is a four step sequence, using the building block 1,3,5-triethynylbenzene **3.18**, presented in chapter 3. A selective Sonogashira coupling of **3.18** with the iodide from 1-bromo-4-iodobenzene yields **5.4** in 79% yield. The final coupling of phenyl-acetylene to **5.4** affords the target star **5.1** in up to 80% yield when the reaction is made with a large excess of phenyl-acetylene. The main side product is the doubly reacted star. The divergent sequence affords the **5.1** in 50% overall yield, and despite every reaction having to be made at three reaction sites per molecule.

5.1.2 Phenyl-acetylene star characterisation

The phenyl-acetylene star **5.1** was sent to St. Andrews for initial studies by STM. The first investigations were deposition of this star on a gold Au(111) surface, in order to find the right conditions, solvents and annealing temperatures to work with the compound (left, Figure 5.3). The star could also be crystallised by dissolving in a minimum quantity of DCM and layering hexane on top, to allow for a slow diffusion of hexane into the saturated solution. This gave very thin, fine needles that with some encouragement could be measured by x-ray diffraction. Because of the delicate nature of the crystals, they were sent to Olaf Fuhr at KIT as the in house x-ray source here in Basel could not achieve sufficient intensity to resolve a clear diffraction pattern (right, Figure 5.3).

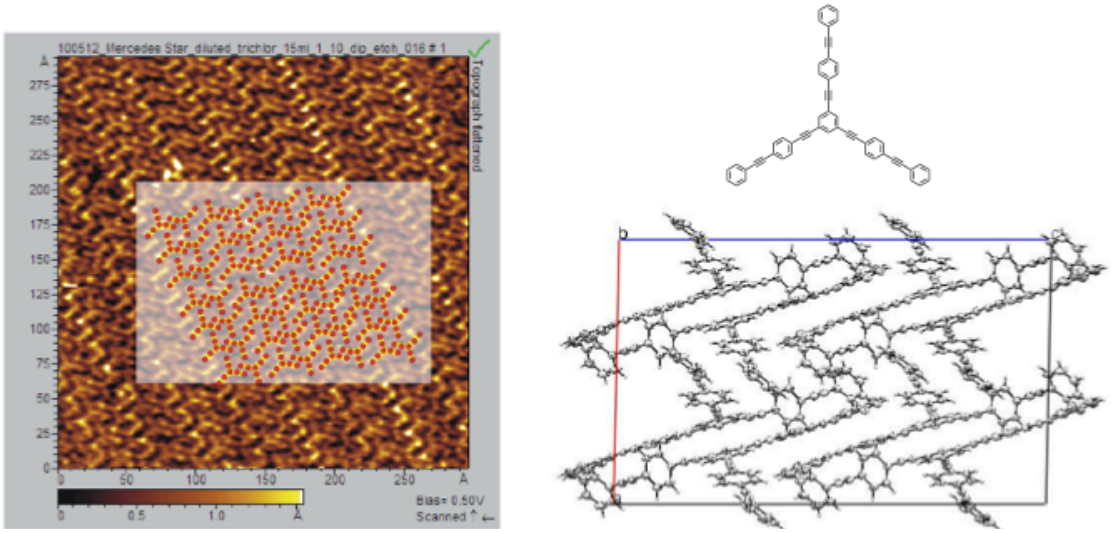

Figure 5.3: Left: STM picture (bias 0.5 V) of 5.1 deposited on a Au(111) surface. Overlaid is a modelling of the packing of the stars. The colour shading denotes the height above the surface in Å. Right: X-ray structure packing of 5.1. The view shown down the z-axis is a direct match of the 2-D assembled molecules depicted in by STM.

The crystal structure data has a relatively high R-value owing to the low quality of the crystals for diffraction. Figure 5.3 shows that the STM picture of the molecules in a 2-D monolayer and the 3-D crystal packing have a good match with each other. The gaps formed in the 2-D arrangement may allow for the intercalation of metal adatoms at these interstitial sites.

After these initial investigations demonstrated that the Buck group could resolve the star **5.1** well by STM, the next step was to deposit the star onto a preformed layer of the PTCDI–Melamine honeycomb network (left, Figure 5.4). From the STM image one can clearly resolve the PTCDI-melamine honeycomb network, however wherever a star shape is present the honeycomb lattice has been 'broken open'. More detailed molecular modelling carried out by the Buck group (right, Figure 5.4) shows that the star **5.1** is slightly too large to fit inside the hexagonal cavity. With these findings coming from St Andrews, we set about the designing the synthesis of slightly smaller stars that should be able to fit inside the honeycomb cavity.

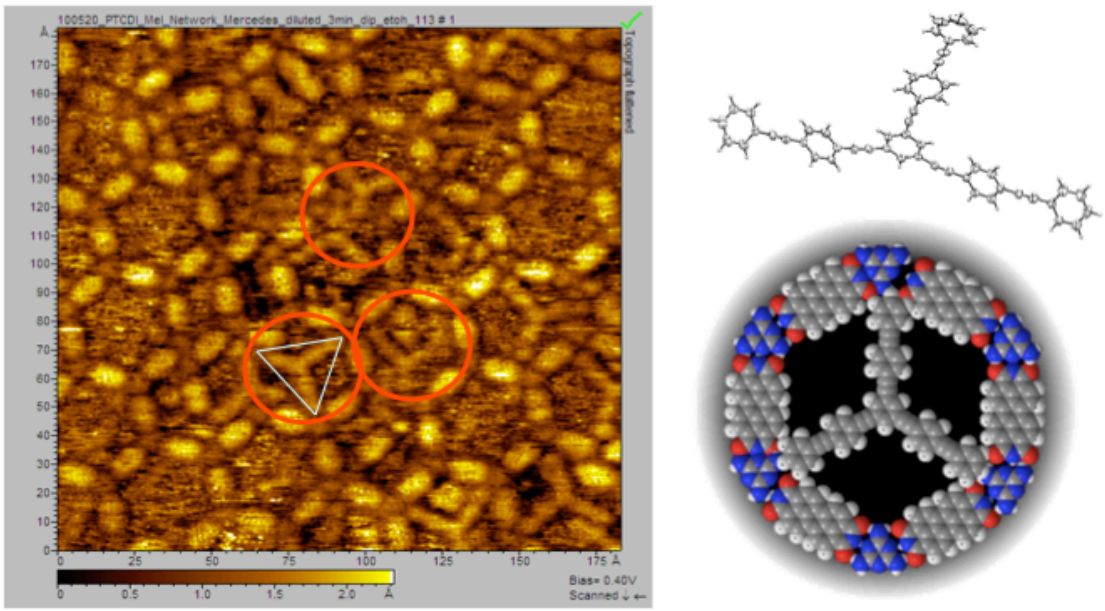

Figure 5.4: Left: STM picture (bias 0.4 V) of 5.1 deposited in the cavities of PTCDI-melamine on a Au(111) surface. The colour shading denotes the height above the surface in Å. Circled in red are regions where the stars are clearly resolved, but have 'broken-out' of the hexagonal network. Right: Above is the Ortep projection of 5.1 shown at the 50% probability level. Below is more detailed molecular modelling carried out by Manfred Buck showing that 5.1 is slightly too large to fit inside the cavity.

5.1.3 Biphenyl and a stilbene star synthesis

Compound **5.1** was found to be too large to fit inside the cavity it was designed for, 'breaking-out' from the hydrogen bonded network upon deposition. Therefore a biphenyl based, three arm star **5.5** and a stilbene based, three arm star **5.6** were envisaged to be small enough to avoid this complication. The assembly of these stars followed the same divergent strategy explored above. The 4-iodo-1,1'-biphenyl **5.7** was prepared following a one-pot Sandmeyer procedure.[267] The stilbene arm **5.8** was prepared by David Muñoz. He prepared a phosphonium ylide from 1-bromomethyl-4-iodobenzene and made a Wittig reaction with benzaldehyde. The arm **5.8** could be isomerised to give exclusively the (*E*)-isomer by first stirring the arm in refluxing toluene with a couple crystals of iodine.

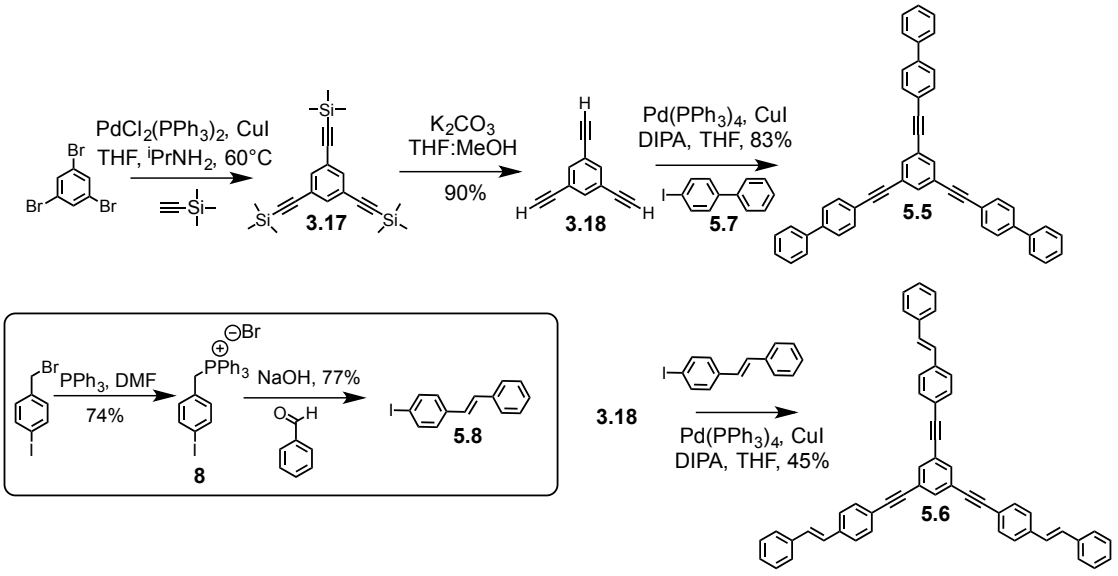

Scheme 5.3: Divergent assembly of biphenyl star 5.5 and stilbene star 5.6. Inside the box is the synthesis of the stilbene arm 5.8, carried out by David Muñoz. The difference in yield of the final coupling is due to the difficult purification of 5.6, which required extensive chromatography.

The biphenyl star **5.5** could be synthesized in an overall yield of 47% over four steps. The stilbene star **5.6** was synthesized in 27% yield over three steps.

5.1.4 Biphenyl and stilbene star characterisation

After the stars **5.5** and **5.6** were received in St. Andrews, STM investigations could be made. This time we moved directly to the honeycomb-porous network. Unfortunately the stilbene star gave only poorly resolved images and further molecular modelling by the Buck group indicated that it too is still every so slightly too large to fit nicely inside the cavity. The biphenyl star however gave nicely resolved STM pictures, where the arms of the star could be clearly observed (Figure 5.5). However the majority of cavities were filled with what appear to be 'six-arm' stars. As it was possible to obtain an x-ray crystal structure of **5.5** we were secure in its identity. From the height profile above the surface, we can rule out the possibility of two stars being co-deposited on top of each other. The only explanation remaining is that we are observing rotational dynamics of the biphenyl star inside the pore, which is occurring at a faster rate than the scanning speed of the STM (Figure 5.6).

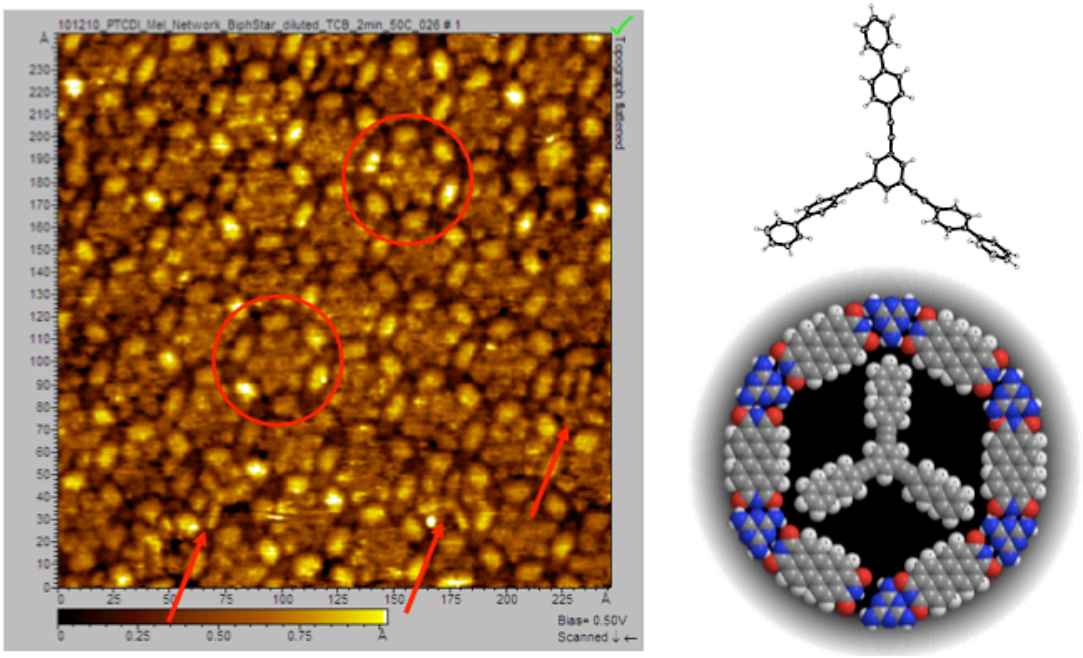

Figure 5.5: Left: STM picture (bias 0.5 V) of 5.5 deposited in the cavities of PTCDI-melamine on a Au(111) surface. The colour shading denotes the height above the surface in Å. Circles mark some of the pores where six protrusions are seen. This would indicate dynamics in the pore, 5.5 flips between two equivalent configurations and this happens so quickly that we see the average. The arrows indicate trapping of the star, where some additional entity must be in the pore to pin the molecule to one position. Right: Above is the Ortep projection of 5.5 shown at the 50% probability level from the x-ray crystal data. Below is a molecular modelling of 5.5 showing the star fitting nicely inside the pore.

In order to investigate the constutional dynamics of the rotation we brain stormed on how to obtain a greater level of control over the system. Because the STM set-up in St Andrews is at the solid liquid interface, cooling of the set-up is difficult. Instead we proposed to introduce functional groups at the end of the stars' arms that could increase the interaction enthalpy with the hydrogen-bonded supramolecular network.

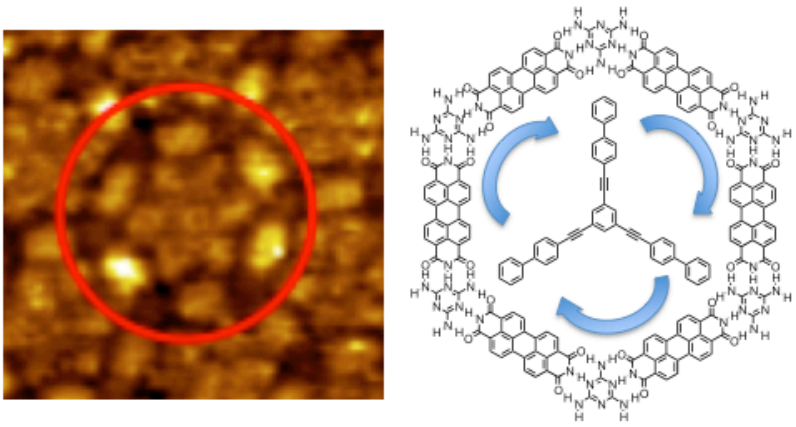

Figure 5.6: Left: zoom of region of the STM picture shown in Figure 5.5 depicting the 'six-arms' which we attribute to be rotations of the biphenyl star 5.5 in the pore. Right: Molecular drawing of the PTCDI-Melamine hexagonal pore with a rotating star 5.5 inside. Note it is not possible to discern the direction of rotation.

5.2 Molecular dynamics in the pore

The STM images obtained from the biphenyl star **5.5** indicated that the PTCDI-melamine honeycomb network was able to host star shaped guests of the correct size. This induced fit was sufficient to allow for apparent rotations of the star inside the pore. In order to investigate the limits of control that we could exert on the system we proposed introducing -OH hydroxyl groups to the ends of the star in hopes of changing the interaction energy of the rotation in the cavity.

5.2.1 Tri-hydroxy biphenyl star synthesis

In order to add pendant hydroxy groups to the ends of the biphenyl star, we again followed a divergent strategy. We settled to initially investigate a three-hydroxy star **5.9**, as it was worried that any more hydroxyl groups may interfere too much with the hydrogenbonding of the underlying PTCDI-melamine network. Therefore **5.9** was synthesised using building block **5.4** described above, in a Suzuki coupling with 3-hydroxyphenyl-boronic acid (Scheme 5.4).

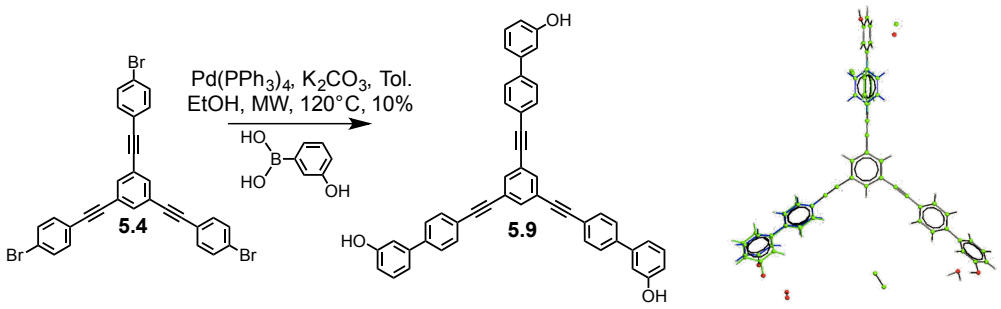

Scheme 5.4: Left: Suzuki coupling to afford tri-hydroxy biphenyl star 5.9 in a divergent synthesis. Right: X-ray crystal structure under refinement due to a high degree of disorder in the unit cell, with solvent molecules shown. The structural assignment is unambiguous, but the unit cell has still to be determined.

The solubility of **5.9** was quite low in normal solvents, which hindered its purification. In order to obtain a pure sample, mixed fractions after column chromatography on silica gel were dissolved in $CHCl_3$ and passed through the recycling GPC. However due to the products low solubility in chlorinated solvents only a 10% isolated yield of clean product could be achieved. Several attempts were made at growing crystals suitable for x-ray diffraction however only long fibrous needles were obtained. Some needles were placed in the x-ray diffractometer, only to be too weak to even stand in the flow of nitrogen used to cool the

sample. Our efforts were rewarded with one set of needles grown from a saturated solution of MeOH to which TBME was allowed to slowly diffuse. A diffraction pattern could be obtained, however the crystal is highly disordered, requiring heavy refinement using an iterative approach to approximate a fit to the pattern collected (right, Scheme 5.4).

5.2.2 Surface investigations on the tri-hydroxy biphenyl star

After the tri-hydrox biphenyl star **5.9** was received in St. Andrews, it was investigated in an analogous fashion to the other stars. Deposition of the star in the honeycomb cavity gave STM images with a wave like appearance. This wave structure comes from the underlying gold surface, demonstrating the high quality of the underlying substrate (left, Figure 5.7). The Buck group were able to perform a Fourier Transform or "diffraction image" of this image, shown centre, Figure 5.7. The back transformation of the filtered image, shown right, Figure 5.7 where only bright spots were selected for back transformation gives a representative image of what the substrate looks like on the average, not just after a single line scan.

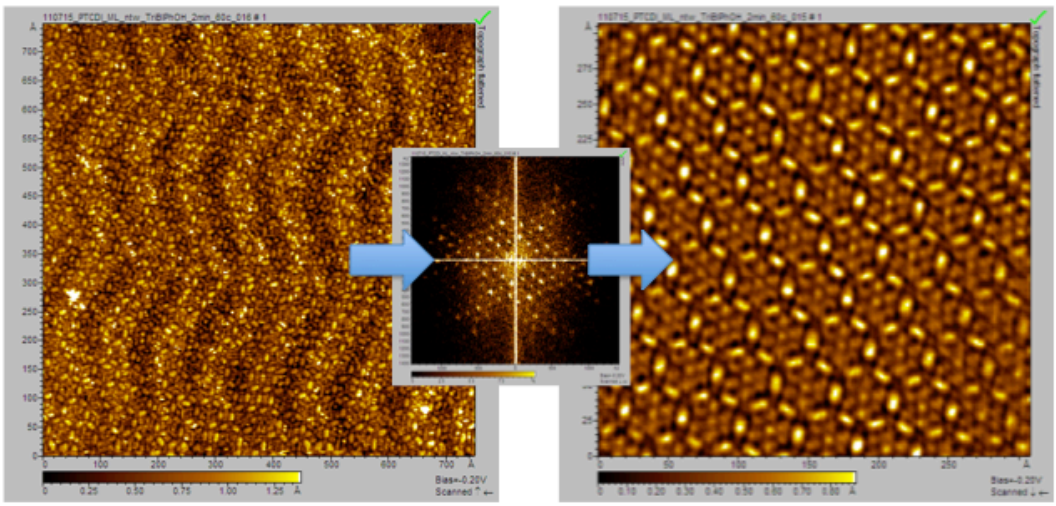

Figure 5.7: Tri-hydroxy biphenyl star 5.9. Left: STM image (bias 0.5 V) of PTCDI-melamine network with 5.9 deposited on a Au(111) surface. The colour shading denotes the height above the surface in Å. Center: Fourier transform of the image to obtain a 'diffraction pattern'. Right: Reprocessed back transformation showing the surface as it looks on the average. Here we see clearly that the star 5.9 is present uniformly across the surface with equal distribution of orientations inside the pore.

In the following high resolution STM image we can see the network close up (Figure 5.8). Here it is apparent that many more of the stars are stationary inside the pore, and from the Fourier transform image, deduce that there is a uniform distribution of orientations of the star across the whole surface.

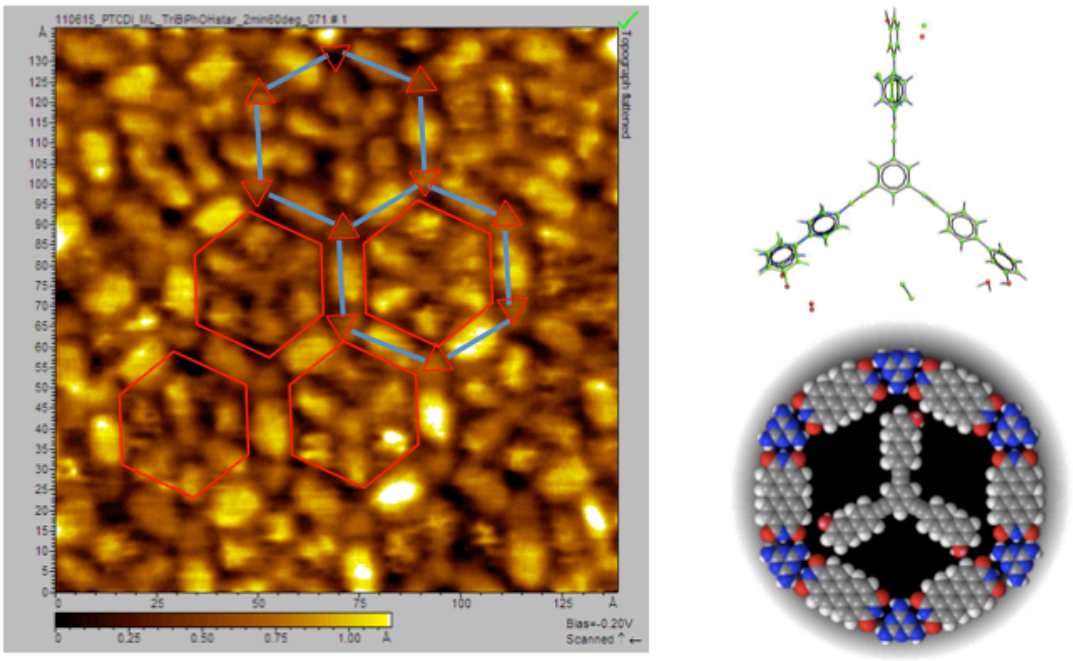

Figure 5.8: Left: High resolution STM image (Bias –0.2 V) of 5.9 in the honeycomb network. The colour shading denotes the height above the surface in Å. Right: Above x-ray crystal structure refinement of the tri-hydroxy biphenyl star. Below modelling of the star fitting nicely inside the cavity. Note that it is not possible to assign the precise configuration of the –OH groups.

In the close up image of the surface, we see that there are also some sites that still show apparent conformational changes of the star in the pore at, or faster than the timescale of an STM scan. We therefore decided to up the ante, and increase the number of hydroxy groups on the end of the star to further push the limits of the interaction presented below.

5.3 Controlled motion of stars inside the pore

5.3.1 Templating of the network using C_{60}

Buck and co-workers have been able to use the PTCDI-melamine honeycomb network as a host for Buckminsterfullerene C_{60}.[184] Modelling of the tri-hydroxy star **5.9** carried out by the Buck group showed that three C_{60} balls would fit in the empty space between the arms of the star in the pore, compared to seven in an unoccupied pore. In a further experiment, C_{60} was deposited onto an annealed substrate of the PTCDI-melamine network hosting our star **5.9**. In this way they obtained a template effect with-in a template, demonstrating an unprecedented level of control over the system (Figure 5.9).

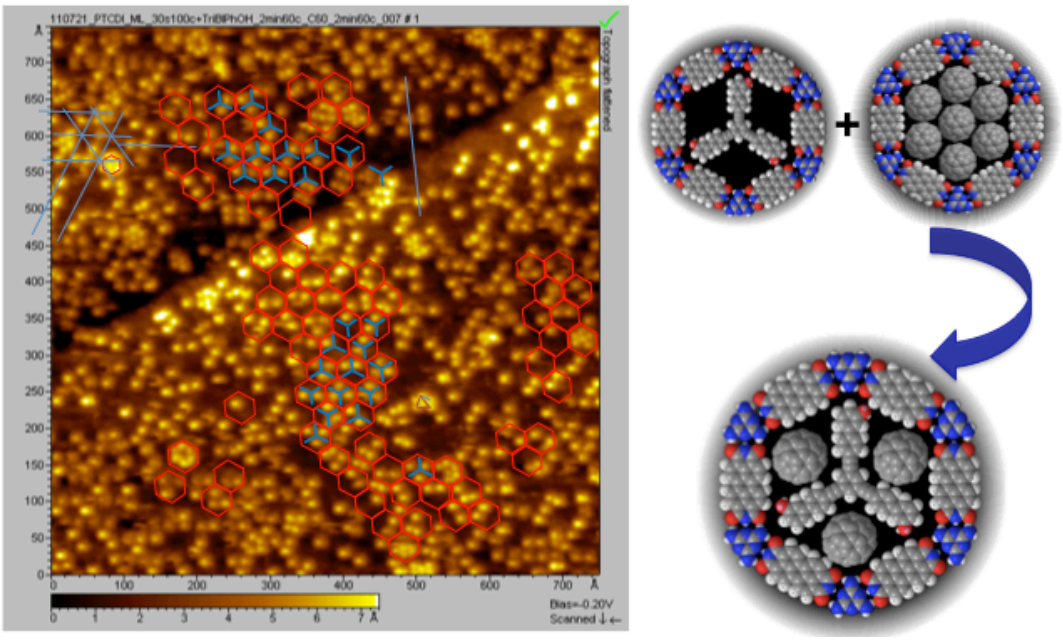

Figure 5.9: Left: STM image (Bias –0.2 V) of 5.9 in the honeycomb network. The colour shading denotes the height above the surface in Å, the overlaid with models. Right: Schematic modelling of the approach. Instead of using the pores to host either 5.9 or C_{60}, by combing the two molecules on one surface, the rotation of the star can be stopped, and the C_{60} precisely patterned (see discussion below).

First the honeycomb monolayer of PTCDI-melamine is fabricated, then the star **5.9** is deposited from solution, locating itself as a guest inside the pores leaving space fore up to three Bucky balls. Finally C_{60} is deposited and sits in the space left. From the STM imagine shown in Figure 5.9 we can see that there are indeed some pores that fit the modelling shown to the right. However more often than not the interstitial sites are only partially filled with C_{60}, and in many cases the star appears to have been knocked out of the hexagonal honeycomb and up to seven C_{60}s can be seen, but the density of packing is not uniform.

Our next approach was to further increase the interaction enthalpy of the star with the honeycomb network by increasing the number of hydroxy groups at the periphery of the arms.

5.3.2 Hexa- and octa- hydroxy star synthesis

We proposed doubling the number of hydroxy groups to six by placing two hydroxy groups at the end of each arm of the star to give **5.10** modelled in Figure 5.10, left. We also proposed introducing a fourth arm to the core of the star, thus increasing the number of hydroxy groups to eight, **5.11** but also lowering the symmetry of the star Figure 5.10, right. In this way we hoped that the increased interaction enthalpy would be enough to fix the stars' orientation

inside the pore, possibly being able to manipulate its orientation by stimulation from the STM tip itself. The reduced symmetry in a four arm star is vital for such an experiment, as we would now be able to differentiate the direction of rotation.

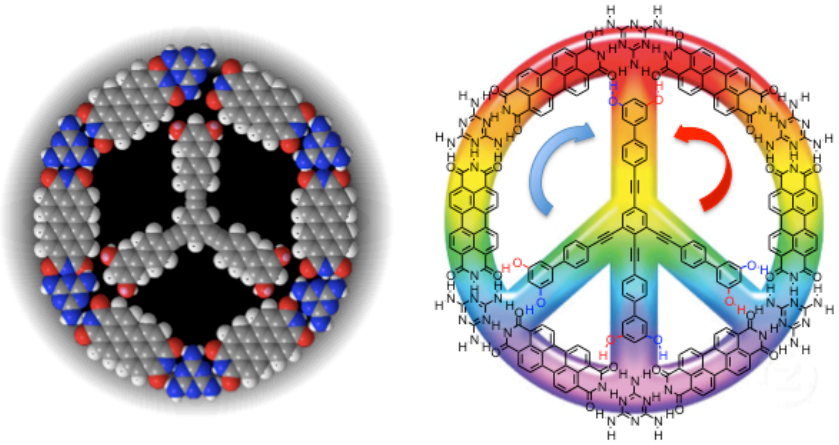

Figure 5.10: Modelling of target stars with six hydroxy groups 5.10 (left) and four arms with eight hydroxy groups 5.11 (right) able to form H-bonds to the honeycomb network.

Again we followed the favoured divergent route to synthesize these stars. Initially David Muñoz made a methoxy protected version of **5.10** by making a Suzuki coupling of **5.4** with the commercially available 3,5-dimethoxyphenyl boronic acid, however attempted removal of the methyl groups to reveal six free hydroxy groups with BBr_3 gave a mixture of products, the main impurities being the partially deprotected stars which were impossible to separate from the desired product.

Therefore an alternative strategy was considered akin to the synthetic route to the biphenyl star **5.5**. First the iodo-biphenyl **5.12** building block had to be prepared. Initially we attempted a statistical Suzuki coupling to 1,4-diiodo benzene with 3,5-dimethoxyphenyl boronic acid followed by removal of the methyl groups, however the formation of the di-substituted product dominated. The insertion of the first methoxy ring appeared to accelerate the insertion of the second ring to give this slanted product distribution. With these 'fast' routes ruled out we set out to build up the arm stepwise (Scheme 5.5). Starting from 4-iodoaniline the amine FG was masked with di-ethyl triazine **5.13**. Suzuki coupling of **5.13** with 3,5-dimethoxyphenyl boronic acid under microwave conditions afforded **5.14** in 56%. The yield was reduced principally by loss of the triazine functional group.

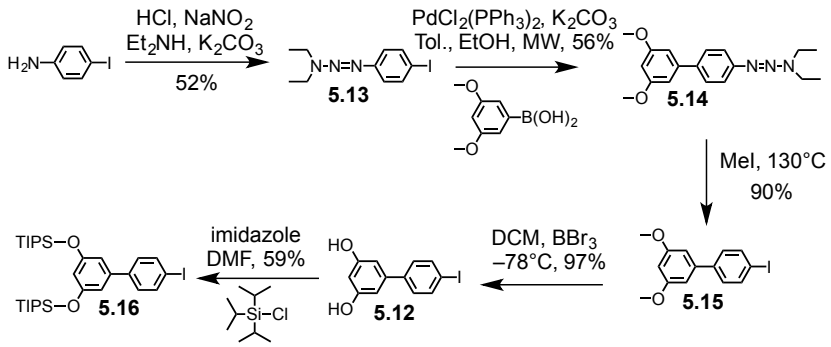

Scheme 5.5: Syntheis of di-hydrox biphenyl arm 5.12 by a stepwise approach.

Functional group interconversion of the triazine to iodine was made by heating **5.14** in super heated MeI in a sealed tube to give the building block **5.15**. Removal of the methoxy groups to give the free hydroxy groups was made quantitatively using BBr_3. At this stage with **5.12** in hand, the hydroxy groups were silyl protected, with an easily removed PG **5.16** in order to avoid the difficult purification of the subsequent star formed bearing six hydroxy groups. Our experience with the three-hydroxy star **5.9** was the cause for this abundance of caution.

The assembly to the final star was made by coupling **5.16** with building block **3.18** to afford the star **5.10**. However this compound was still not easy to purify by traditional column chromatography techniques on silica, and was only finally isolated pure after preparative TLC. Removal of the TIPS PG groups using TBAF, formed the target six hydroxy star. While the target star **5.10** was made by this route, it could not be separated from the tetra-butylammonium salt coming from the TBAF deprotecting agent employed due to the high polarity of **5.10** and the similarity of the solubility of the star verses the salt. Instead the free hydroxy arm **5.12** was Sonogashira coupled directly to the core **3.18**. Surprisingly the purification and work up of this reaction proved easy, as the additional hydroxy groups greatly improved the solubility of the star in polar solvents compared to the three hydroxy star **5.9**. The only issue was that a gel or semi-crystaline lattice was formed from **5.10** in EtOAc which could only be disrupted by the addition of MeOH. In order to remove all traces EtOAc solvent as seen by NMR, the compound had to be passed through a reverse-phased column (C18, 40-60Å) in MeOH, removal of the solvent to afford the star solvent free.

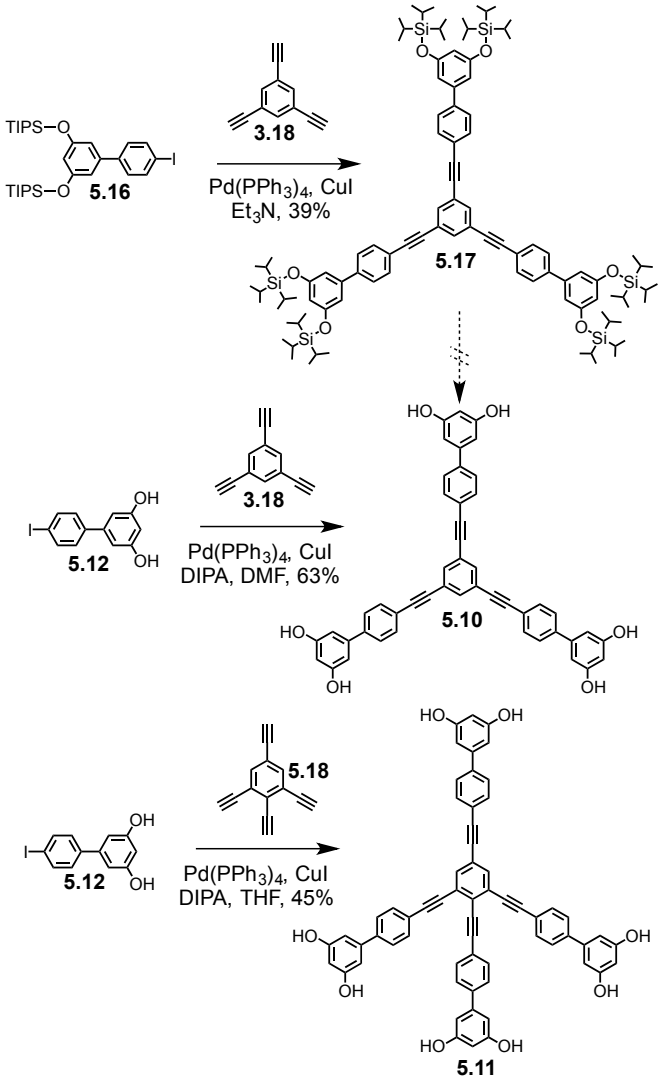

Scheme 5.6: Final assembly of building blocks to afford the target stars 5.10 and 5.11 by Sonogashira cross-coupling.

The four arm star **5.11** required coupling to a four acetylene benzene **5.18** synthesized by David Muñoz to afford star **5.11**. This star had excellent solubility in polar solvents, both MeOH and EtOAc and could be purified by passing twice through a reversed phase column (C18, 40-60Å). The stars **5.10** and **5.11** were then sent to St. Andrews for the surface investigations, with the hope that we would see stars fixed in their orientation inside the PTCDI-melamine cavity.

5.3.3 Surface investigations of the three and four arm biphenyl stars

Surface investigations on the stars **5.10** and **5.11** were conducted to push the limits of our ability to exert control on the supramolecular system stemming from the underlying structure of the compound.

Deposition of the six hydroxy star **5.10** into the porous PTCDI-melamine network gave qualitatively identical findings to the three hydroxy star **5.9**. We attribute this to the positioning of the biphenyl at the end of the arm, the inherent twist of the biphenyl prevents both hydroxy groups from laying commensurate to the surface. Synthesis of a star with the acetylene placed before the final hydroxy phenyl may change the interaction.

Owing to the difference in solubility of the four arm star **5.11** compared to the other stars it was initially deposited onto a clean gold surface (Figure 5.11).

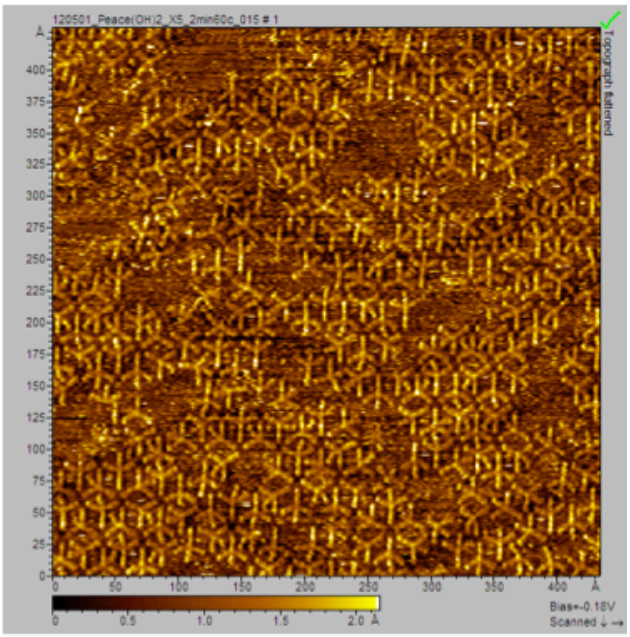

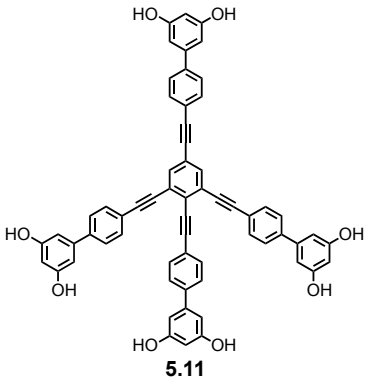

5.11

Figure 5.11: STM image (bias -0.16 V) of the four arm star 5.11 (right) adsorbed from DMF at 60°C. In the image we see that the stars are interdigitated with each other, with localised domains of high density packing.

Having found the required conditions of deposition using DMF at 60°C the next experiment was to deposit the four-arm star **5.11** into the pores of a PTCDI-melamine hexagonal network. In the STM image we see that many pores are filled, with four protrusions shown, indicating that the star goes easily into the pore (Figure 5.12). Some rotations can still be resolved but they appear much slower than for any of the other stars, indicating that **5.11** is enthalpically stabilised with a greatly reduced rate or even no rotations inside the pore as we have lost the hexagonal symmetry seen for the other rotating stars. A subsequent scan of the STM tip across the same region after 75 seconds shows that some of the stars fixed in position rotate by one position, predominately towards the scan direction, possibly by the star being drawn to the tip as it approaches, but more studies of the system are required before any conclusions can be drawn.

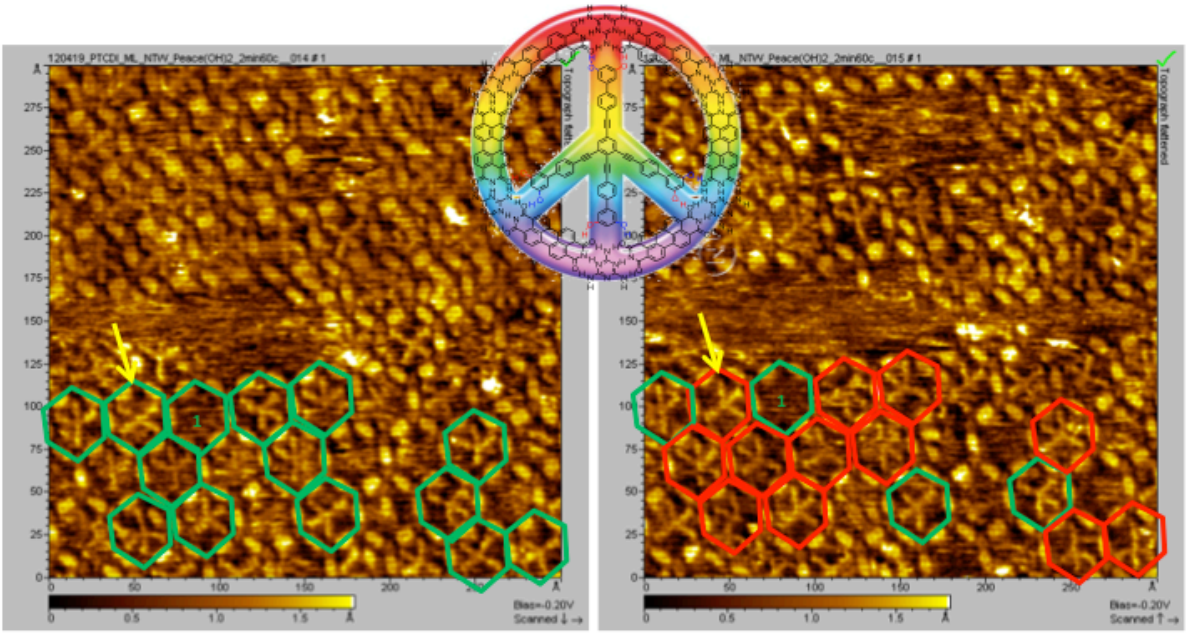

Figure 5.12: Two subsequent images (75s apart) of the peace star 5.11: STM images (bias –20 V), green overlay of the PTCDI-melamine network. The right image (collected 75s later) those molecules which have rotated are marked in red. Those in green remain unchanged from their configuration in the first image. The yellow arrow marks the same cell between the two images.

With the inclusion of a fourth arm and a total of eight hydroxy groups we have shown the way that organic synthesis can exert control on the emergent properties of the stars on a gold surface, and from the family investigated, that the lower symmetry of the four arm star **5.11** allows us to obtain much more information about the constitutional dynamics of guests in a PTCDI-melamine network.

5.4 Conclusion and Outlook

We set out to explore the limits that substituent architecture plays in the control of a functionalised surface. Using a bottom-up approach to achieve this surface functionalisation we intercalated a PTCDI-melamine based hydrogen-bonded porous network from solution (Figure 5.13). The synthesis of the stars was achieved by applying a divergent approach combing suitable building blocks to extend the acetylene scaffold in a modular fashion.

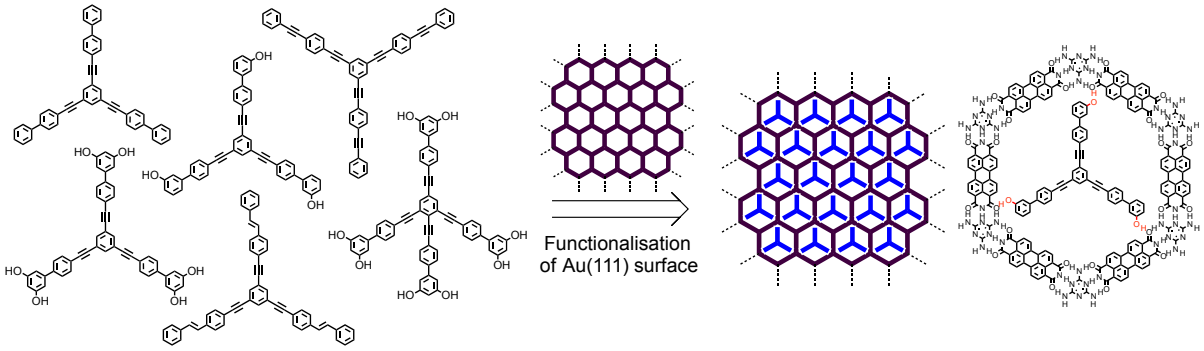

Figure 5.13: A family of phenyl-acetylene stars were synthesised and their deposition into a porous hexagonal network of PTCDI-melamine supramolcular network was investigated by STM.

We reported the synthesis, crystal structure determination and Scanning Tunneling Microscopy (STM) investigations of this family of star shaped molecular rods demonstrating single molecule organisation in an extended array with implications for the future directed assembly of molecules in precise patterns on a surface. Further intercalation of C_{60} led to a secondary templating effect. Controlled switching of the four arm star was observed on the gold surface by STM.

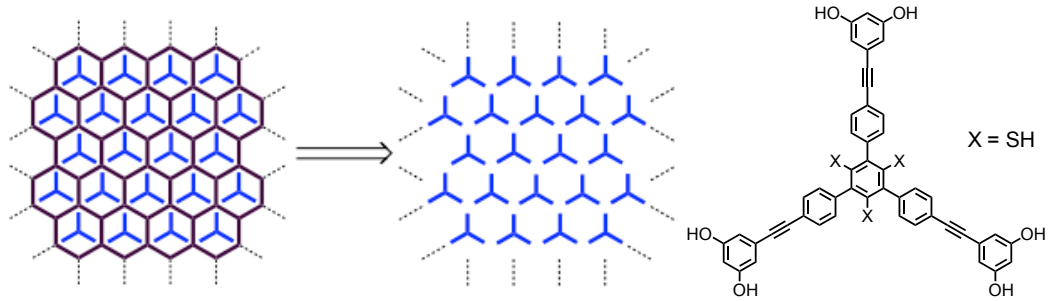

Figure 5.14: Removal of the template PTCDI-melamine network would leave the guests organised with long range order in an extended array. Right: proposed star with the acetylene positon moved to allow both –OH groups to interact with the template. X functional groups such as SH or anther reactive group would allow for the star to be chemisorbed to the underlying gold substrate.

A future direction for this project could be the subsequent removal of the underlying PTCDI-melamine network to reveal the stars with an organisation on the surface dictated by the template (Figure 5.14). The Buck group have already been able to achieve removal of the hexagonal network by substitution with copper under potential deposition (Cu UPD) followed by substitution with alkyl thiols (see section 1.3.5 for discussion and references).
In order to ensure that the stars stay in this extended ordered array, pendant groups such as -SH at the core of the star are required to allow for chemisorption to the underlying gold substrate and prevent migration of the molecular stars across the surface.

6 Conclusion

In this thesis we validated a building block approach to the assembly of nanoscale molecular architectures, and illustrated the approach in the synthesis of three key areas of nanotechnology.

In chapter 2 we presented the ideal characteristics and synthesis of phenyl-acetylene based building blocks. The high degree of modularity achievable using Sonogashira cross-couplings was demonstrated with three examples. Monomers used for polymer synthesis in the dispersion of SWCNTs, dimers of 2,7-carbazoles and in a systematic study of D–π–A carbazole libraries.

In Chapter 3 we applied the aryl-building blocks to the field of molecular electronics. A 6nm OPE rod for use as a molecular wire was synthesised with a convergent approach in 18% overall yield in 11 steps. A three-armed, 4.7 nm star architecture was synthesized in 8% overall yield over 14 steps and sent to our collaborators. The trityl protected star was fully characterised by NMR, and diffusion experiments confirmed the macromolecular properties of this system.

In chapter 4 the 27 step synthetic sequence towards a 7.2 nm fully π-conjugated, 2,7-carbazole based macrocycle was presented. The quarter cycle was synthesized bearing either CPDIPS or TIPS protecting groups. Several routes to a covalent template were explored, and a viable, terminal acetylene based template was fully characterised. The synthetic routes were made possible by maintaining a high level of adaptability and applying tenacity to the whole range of possible synthetic couplings.

In chapter 5, we reported the synthesis, crystal structure determination and STM investigations of a family of tailored phenyl-acetylene star molecules. In close collaboration with the group of Manfred Buck, the stars' architecture was tuned with close feed-back from the physical investigations made by STM. We were able to show single-molecule organisation in an extended array. Using the PTCDI-melamine supramolecular network as a host, we also tailored the molecular dynamics of the stars in the pores.

The future of this methodology probably lies in combing the approaches presented in chapters 4 and 5. Supramolecular chemistry and the self-assembly of molecular systems that it drives is becoming a reliable tool in synthesis. A non-covalent template driven self-assembly of a giant macrocycle, as demonstrated by Anderson and co-workers,[268] could see a rapid expansion in the number of nanoscale, single-molecule architectures.

The outlook for a phenyl-acetylene building block approach is bright. With the right choice of disconnection, and combing tailored building blocks by convergent-divergent approaches a new wave of truly nanoscale single-molecule objects awaits. The areas explored in this thesis demonstrate the broad scope and wide applicability of the approach.

7 Experimental Section

Experimental details;

The manipulation of all air/water sensitive compounds was carried under using standard high vacuum techniques. Commercially purchased reagent grade solvents were degassed with argon prior to use. Chemicals were obtained from commercial sources or following literature procedures. Analytical thin layer chromatography (TLC) was carried out on *Merk® silicagel 60 F_{254}* glass TLC plates visualizing with UV light at 254 nm and 366 nm. Column chromatography was performed using silica gel 60 (230-240 mesh), except were stated otherwise.

NMR spectra were recorded at ambient prope temperature using a *Bruker DPX-NMR* (400 MHz), unless otherwise stated. Chemical shifts (δ) are quoted in parts per million (ppm) relative to the residual solvent proton peak ($CDCl_3$: 7.26 ppm) and solvent residual carbon peak ($CDCl_3$, δ = 77.16.) Multiplicities are denoted; singlet (s), doublet (d), triplet (t), multiple (m) and doublet of doublets (dd). Mass spectra were obtained by GC-MS, EI (70eV, measured by Dr. H. Nadig on a *Finnigan* MAT 95Q), ESI (measured on a *Bruker Esquire* 3000) and MALDI-Tof (on an *Applied Bio Systems Voyager-De*). Molecular ions are denoted and only the major peak reported. Elemental analyses were measured by W. Kirsch on a *Perkin-Elmer Analysator 240* and the values are given in percent. Melting points (mp) were determined with a *Stuart SMP3* apparatus and are uncorrected.

The compounds are organised in relation to their order of appearance in the text, numbered by chapter as **1.23** – to denote the 23rd compound in Chapter 1.

7.1 Compounds from Chapter 2

[(3-Cyanopropyl)dimethylsilyl]acetylene (CPDMS-A)

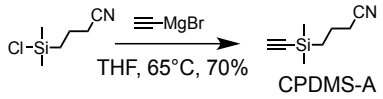

Following a procedure from Höger et al.[218] An oven dried 500 mL three neck flask with reflux condenser was charged with (3-cyanopropyl)dimethylsilyl chloride (8.4 g, 8.5 mL, 52 mmol) dissolved in dry THF (40 mL). Then ethynlmagnesium bromide (0.5 mol in THF, 177 mL, 88.3 mmol) was added dropwise by cannula. The reaction mixture was then heated to reflux for 20 hr. After cooling, the reaction mixture was diluted with Et_2O (150 mL) and quenched with water (80 mL) and then 2M HCl (20 mL). The organic layer was extracted with Et_2O, washed with water, then brine, ensuring the aqueous phase was mildly acidic. The organic phase was dried over $MgSO_4$ and solvent removed. The crude product was distilled by Kugelrohr (95 °C / 0.35 mbar) to afford **CPDMS-A** as a colourless oil (5.5 g, 70%). **bp** 95 °C / 0.35 mbar (lit.[218] bp 65 °C / 1 mbar). **^{1}H NMR** (400 MHz, $CDCl_3$): δ_H = 2.24–2.16 (m, 3H), 1.65–1.52 (m, 2H), 0.66–0.53 (m, 2H), 0.0 (s, 6H). **^{13}C NMR** (101 MHz, $CDCl_3$): δ_C = 119.7 (s), 94.6, 88.2, 20.6 (t, CH_2), 20.6 (t, CH_2), 15.5 (t, CH_2), -2.0 (2 q, 2 CH_3). **MS** (EI +, 70 eV) *m*/*z* $C_8H_{13}NSi$ = 136.1 $[M–Me]^{+}$. **GC-MS** *m*/*z*; 14.0 min, 136 $[M–Me]^{+}$. **Anal.** Calcd for $C_8H_{13}NSi$: C, 63.52; H, 8.66; N, 9.26. Found: C, 63.38; H, 8.43; N, 9.10.

[(3-Cyanopropyl)diisopropylsilyl]acetylene (CPDIPS-A)

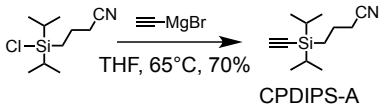

Following a procedure from Gaefke et al.[269] a 500 mL three neck round bottom flask with reflux condenser and dropping funnel were heated out under vaccum (30 min) and charged with (3-cyanopropyl)diisopropylsilyl chloride (CPDIPS-Cl, 10.2 mL, 45.4 mmol) dissolved in a solution of THF (30 mL). Then ethynlmagnesium bromide (O.5 mol in THF, 100 mL, 49.9 mmol) was transferred from a 100 mL Aldrich bottle to a dropping funnel via cannula. The solution was then added dropwise to the CPDIPS-Cl solution over 1 hr. The reaction mixture was then heated to reflux overnight. After cooling, Et_2O (150 mL) was added and H_2O (80 mL) and a small amount of 1M HCl (aq) until the aqueous phase was mildly acidic. The organic layer was extracted with Et_2O and washed with H_2O (3x 50 mL) and then Brine

(1x 50 mL) and dried over $MgSO_4$. The solvent was removed leaving a black oil which was distilled by Kugelrohr to afford **CPDIPS-A** as a colourless oil (7.87 g, 84%). **^{1}H NMR** (500 MHz, $CDCl_3$): δ_H = 2.46 (s, 1H), 2.45 (d, J = 4.9 Hz, 2H), 1.90–1.81 (m, 2H), 1.16–1.00 (m, 14H), 0.85–0.76 (m, 2H). **^{13}C NMR** (101 MHz, $CDCl_3$): δ_C = 119.8, 95.9, 85.4, 21.2, 20.9, 18.1, 17.9, 11.5, 9.5. **MS** (EI +, 70 eV) *m/z* (%) = $[M–C(CH_3)_2]^{+}$ 164.2 (100), 165.2 (16), 166.2 (4) . **Anal.** Calcd for $C_{12}H_{21}NSi$: C, 69.50; H, 10.21; N, 6.75. Found: C, 69.49; H, 9.96; N, 6.64.

1,4-Dihexylbenzene (2.1a)

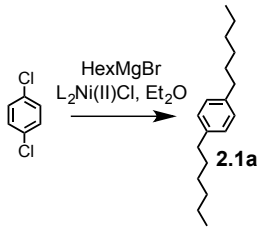

A procedure from Rehahn et al.[217] was adapted as follows: A 500 mL two neck round bottom flask with a reflux condenser attached was dried in vacuo and charged with 1,4-dichlorobenzene (10.90 g, 74.1 mmol) and $NiCl_2$(dppp) (120 mg, 0.222 mmol). Then anhydrous Et_20 (60 mL) was added and the flask placed under argon. This mixture was cooled to 0°C and then Hexylmagnesium bromide (100 mL, 200 mmol) was added dropwise via cannula. A colour change from red to yellow occurred. The reaction mixture was then heated to reflux and left stirring for 16 hr. Then the reaction mixture was cooled to 0°C and slowly quenched with DI water (20 mL) followed by 6M HCl (aq, 40 mL). The aqueous phase was washed with Et_2O (3 x 50 mL). The combined organic fractions were then washed with brine and dried over Na_2SO_4 and the solvent removed under reduced pressure. The yellow oil obtained was then distilled with a Kugelrohr to afford **2.1a** as a colourless oil (18.4 g, 100%). **bp** 120°C/0.4 mbar. **^{1}H NMR** (400 MHz, $CDCl_3$): δ_H = 7.09 (s, 4H), 2.56 (t, J = 8.0 Hz, 4H), 1.65–1.52 (m, 4H), 1.39–1.23 (m, 12H), 0.88 (t, J = 6.7 Hz, 6H). **^{13}C NMR** (100 MHz, $CDCl_3$): δ_C = 140.2, 128.4, 35.7, 31.9, 31.7, 29.2, 22.8, 14.3.

1,4-Dihexyl-2,5-diiodobenzene (2.1)

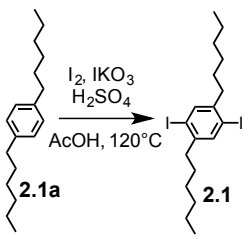

Following a procedure from Kukula et al.[216] a 500 mL round bottom flask was charged with **2.1a** (18.3 g, 74.3 mmol) dissolved in glacial AcOH (250 mL). Then I_2 (20.1 g, 81.7 mmol), KIO_3 (7.95 g, 37.1 mmol) H_2SO_4 (98%, 16.6 mL) and H_2O (3 mL) were added. The reaction mixture was heated to reflux for 20 hr, after which time the solvent was reduced to 1/3rd its initial volume by distillation. The mixture was cooled with an ice bath and filtered. The dark brown solid was passed through a short column (SiO_2, Cyclohexane) and recrystalised twice from ethanol to afford **2.1** as white needles (27.8 g, 75%). $\mathbf{R_f}$ = 0.60 (SiO_2; cyclohexane). **^{1}H NMR** (400 MHz, $CDCl_3$): δ_H = 7.59 (s, 2H), 2.59 (t, J = 8.0 Hz, 4H), 1.60–1.47 (m, 4H), 1.43–1.27 (m, 12H), 0.90 (t, J = 6.7 Hz, 6H). **^{13}C NMR** (100 MHz, $CDCl_3$): δ_C = 145.0, 139.4, 100.5, 40.0, 31.8, 30.3, 29.2, 22.7, 14.2.

4-(2,5-Dihexyl-4-iodophenyl)-2-methylbut-3-yn-2-ol (2.2)

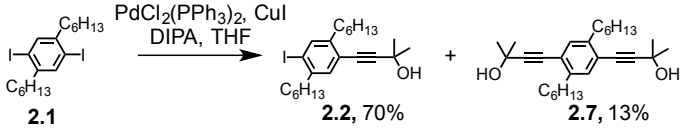

2.1 **2.2,** 70% **2.7,** 13%

A two neck round bottom flask was charged with **2.1** (5 g, 10.0 mmol) and the catalytic system $Pd(PPh_3)_2Cl_2$ (71.2 mg, 0.100 mmol), and CuI (38.2 mg, 0.201 mmol) were dissolved in dry THF (50 mL) and diisopropylamine (10 mL) and the solution bubble purged with Argon for 20 min. Then 2-methylbut-3-yn-2-ol (0.657 mL, 6.72 mmol) was added via syringe and the reaction mixture stirred under argon for 20 hr. When the reaction was deemed complete by TLC (DCM), TBME and water were added and the organic layer was extracted, washed with 2M HCl (aq), Brine and then dried over $MgSO_4$. The Products were isolated by column chromatography on SiO_2 (DCM, then 25% EtOAc in DCM to remove third spot which requires recrystalisation to purify), fractions evaporated to afford **2.2** as a yellow oil. (2.14g, 70%). $\mathbf{R_f}$ = 0.45 (SiO_2; DCM). **^{1}H NMR** (400 MHz, $CDCl_3$): δ_H = 7.62 (s, 1H), 7.19 (s, 1H), 2.73–2.51 (m, 4H), 1.99 (s, 1H), 1.62 (s, 6H), 1.61–1.50 (m, 4H), 1.44–1.23 (m, 12H), 0.99–0.82 (m, 6H). **^{13}C NMR** (100 MHz, $CDCl_3$): δ_C = 144.5, 143.1, 139.8, 132.7, 122.5, 101.3, 98.2, 80.9, 66.2, 40.6, 34.2, 32.1, 32.1, 31.9, 31.0, 30.6, 29.6, 29.4, 23.0, 23.0, 14.5. **MS** (EI +, 70 eV) m/z = 454.2 [M^+]. **Anal.** Calcd for $C_{23}H_{35}IO$: C, 60.79; H, 7.76. Found: C, 60.68; H, 7.52.

4,4'-(2,5-dihexyl-1,4-phenylene)bis(2-methylbut-3-yn-2-ol) (2.7)

Isolated from the reaction mixture above by column chromatography. The orange solid can be recrystallized in DCM layered with cyclohexane to give **2.7** as a white crystalline solid. (0.36 g, 13%). **mp** 94.5 °C. $\mathbf{R_f}$ = 0.12 (SiO_2; DCM). $\mathbf{R_f}$ = 0.64 (SiO_2; DCM/EtOAc 3:1). **^{1}H NMR** (400 MHz, $CDCl_3$): δ_H = 7.19 (s, 2H), 2.64 (m, 4H), 2.20 (s, 2H), 1.62 (s, 12H), 1.60–1.51 (m, 4H), 1.41–1.21 (m, 12H), 0.88 (t, J = 6.7 Hz, 6H). **^{13}C NMR** (101 MHz, $CDCl_3$): δ_C = 142.2, 132.4, 122.1, 98.3, 81.1, 65.9, 34.2, 31.9, 31.6, 30.7, 29.4, 22.7, 14.2. **MS** (EI +, 70 eV) m/z = 410.3 [M^+]. **Anal.** Calcd for $C_{28}H_{42}O_2$: C, 81.90; H, 10.31. Found: C, 81.84; H, 10.34.

4-(2,5-Dihexyl-4-((triisopropylsilyl)ethynyl)phenyl)-2-methylbut-3-yn-2-ol (2.3)

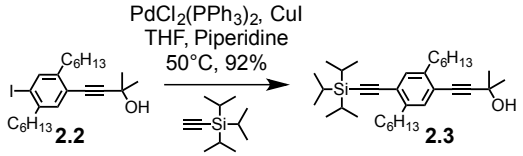

The catalytic system of $PdCl_2(PPh_3)_2$ (21.8 mg, 30.8 µmol), CuI (11.7 mg, 61.6 µmol) and **2.2** (1.40g, 3.08 mmol) were dissolved in dry THF (16 mL) and piperidine (4 mL) and the solution bubbled purged with argon for 30 min. Then (Triisopropylsilyl)acetylene (0.83 mL, 3.7 mmol) was added and the reaction mixture stirred at 50°C for 17 hr. When deemed complete by TLC, the mixture was diluted with TBME and water. The combined organic layers were washed with 2M HCL(aq), brine, and dried over Na_2SO_4. The product was purified by flash chromatography on SiO_2 (DCM), fractions combined and evaporated to afford **2.3** as a yellow oil (1.45 g, 92%). $\mathbf{R_f}$ = 0.56 (SiO_2; DCM). **^{1}H NMR** (400 MHz, $CDCl_3$): δ_H = 7.24 (s, 1H), 7.20 (s, 1H), 2.77–2.61 (m, 4H), 2.01 (s, 1H), 1.68–1.56 (m, 11H), 1.39–1.23 (m, 12H), 1.14 (s, 20H), 0.93–0.83 (m, 6H). **^{13}C NMR** (101 MHz, $CDCl_3$): δ_C = 142.9, 142.5, 133.3, 132.7, 123.2, 122.3, 106.0, 98.5, 95.5, 81.5, 66.2, 34.8, 34.5, 32.2, 32.2, 31.9, 31.3, 31.1, 29.7, 23.0, 19.1, 14.5, 11.8.

The desired product **2.3** can also be formed in a one pot procedure starting from **2.1**, but this leads to the formation of a considerable amount of **2.4**.

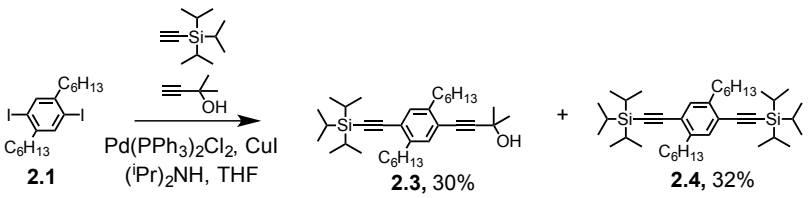

A round bottom flask was charged with $PdCl_2(PPh_3)_2$ (65.9 mg, 93 μmol), CuI (17.7 mg, 93 μmol), and **2.1** (390 mg, 0.78 mmol). To this flask was added THF (2 mL) and diisopropylamine (1 mL) and the solution degassed with Argon for 20 min. Then (Triisopropylsilyl)acetylene (176 μL, 0.78 mmol) was added via syringe and 5 hr later 2-Methyl-3-butyn-2-ol (153 μL, 1.57 mmol). The solution was stirred for 17 hr under Argon. When the reaction was deemed complete by TLC, the solvent was removed and the reaction mixture treated with water (2 mL) and extracted with DCM. The organic layer was washed successively with water, brine and dried over Na_2SO_4, solvent removed and the crude passed through a column of SiO_2 (DCM, then ramp of 1:5 Ethyl acetate:DCM, stripping column with neat Ethyl acetate)to afford **2.3** as a yellow wax (123.2 mg, 30%), and **2.4** as a yellow oil (150 mg, 32%).

((2,5-dihexyl-1,4-phenylene)bis(ethyne-2,1-diyl))bis(triisopropylsilane) (2.4)

^{1}H NMR (400 MHz, $CDCl_3$): δ_H = 7.28 (s, 2H), 2.83–2.66 (m, 4H), 1.72–1.55 (m, 4H), 1.45–1.26 (m, 12H), 1.17 (s, 36H), 1.13 (s, 6H), 1.01–0.82 (m, 6H). **^{13}C NMR** (101 MHz, $CDCl_3$): δ_C = 142.6, 133.0, 122.9, 105.8, 95.2, 34.6, 32.0, 31.1, 29.6, 22.8, 18.9, 18.7, 14.2, 11.5.

3-(2,5-dihexyl-4-((triisopropylsilyl)ethynyl)phenyl)prop-2-yn-1-ol (2.6)

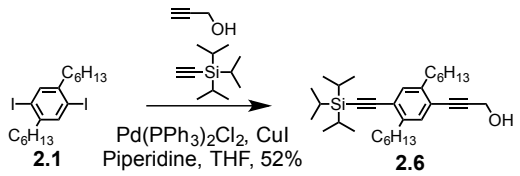

A round bottom flask was charged with **2.1** (1.00 g, 2.01 mmol) and the catalytic system of $Pd(PPh_3)_2Cl_2$ (14.2 mg, 20.1 μmol), and CuI (7.7mg, 40.1 μmol) were dissolved in dry THF (10 mL) and piperidine (2 mL) and the solution bubbled with Argon for 20 min. Then propargyl alcohol (83 μL, 1.4 mmol) was added dropwise via syringe and the reaction mixture stirred under argon for 20hr. Then (Triisopropylsilyl)acetylene (0.55 mL, 2.41 mmol) was added and the mixture stirred for a further 20 hr. The reaction mixture was then diluted with TBME and water. The aquous layer was extracted with TBME, The combined organic layers were washed with 2M HCL(aq), brine, and dried over Na_2SO_4. The crude product was purified by flash chromatography on SiO2 (Hexane/DCM 1:1), fractions evaporated to afford **2.6** as a yellow oil (353 mg, 52%). **^{1}H NMR** (400 MHz, $CDCl_3$): δ_H = 7.63 (s, 1H), 7.22 (s, 1H), 4.52 (t, J = 6.7 Hz, 4H), 2.81–2.54 (m, 7H), 1.71–1.49 (m, 10H), 1.33 (d, J = 13.7 Hz,

21H), 1.13 (s, 18H), 1.00–0.78 (m, 6H). **^{13}C NMR** (101 MHz, $CDCl_3$): δ_C = 139.5, 132.7, 51.9, 40.3, 34.5, 33.7, 31.8, 30.6, 30.3, 29.1, 22.7, 18.8, 14.2, 11.5.

4-(((2,5-dihexyl-4-iodophenyl)ethynyl)dimethylsilyl)butanenitrile (2.8)

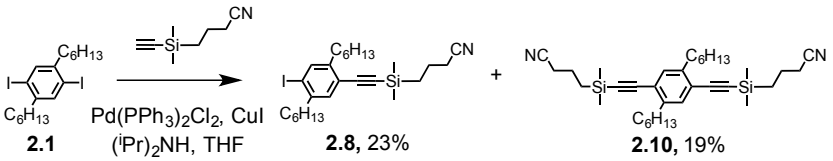

This reaction was performed by nano student Simon Zihlmann. A 500 mL two neck round bottom flask was charge with **2.1** (6.55 g, 13.14 mmol), the catalytic system of $PdCl_2(PPh_3)_2$ (184 mg, 0.26 mmol), CuI (75 mg, 0.39 mmol) dissolved in THF (150 mL) and DIPA (40 mL). The reaction mixture was degassed by bubble purging with argon for 20 min. Finally CPDMS-A (1.39 g, 9.20 mmol) was added dropwise by syringe. The reaction mixture was stirred under argon for 20 hr, becoming a dark brown in colour. Water was added and extracted with TBME. The organic layer was washed successively with 2M HCl (aq), brine and dried over $MgSO_4$. The crude was passed through a column of SiO_2 (1:1 cyclohexane:DCM), fractions combined to afford **2.8** as an orange oil (1.6 g, 23%). $\mathbf{R_f}$ = 0.33 (SiO_2; cyclohexane/DCM 1:1). **^{1}H NMR** (400 MHz, $CDCl_3$): δ_H = 7.63 (s, 1H), 7.23 (s, 1H), 2.69–2.56 (m, 4H), 2.42 (t, *J* = 7.0 Hz, 2H), 1.88–1.77 (m, 2H), 1.63–1.50 (m, 4H), 1.43–1.25 (m, 12H), 0.96–0.80 (m, 8H), 0.26 (s, 6H). **^{13}C NMR** (101 MHz, $CDCl_3$): δ_C = 180.1, 144.6, 142.9, 139.6, 132.7, 122.3, 119.7, 104.8, 101.6, 96.4, 40.3, 34.0, 31.8, 31.8, 30.7, 30.3, 29.4, 29.2, 22.8, 22.7, 20.8, 20.7, 15.9, 14.2, 14.2, -1.7. **MS** (EI +, 70 eV) *m*/*z* (%) = 521.2 (100%) [M^+]. **Anal.** Calcd for $C_{26}H_{40}INSi$: C, 59.87; H, 7.73; N, 2.69. Found: C, 59.98; H, 7.60; N, 2.90.

4,4'-(((2,5-dihexyl-1,4-phenylene)bis(ethyne-2,1-diyl))bis(dimethylsilanediyl))dibutanenitrile (2.10)

as an orange oil (1.3 g, 19%). $\mathbf{R_f}$ = 0.06 (SiO_2; cyclohexane/DCM 1:1). **^{1}H NMR** (400 MHz, $CDCl_3$): δ_H = 7.24 (s, 2H), 2.71–2.64 (m, 4H), 2.42 (t, *J* = 7.0 Hz, 4H), 1.90–1.76 (m, 4H), 1.67–1.55 (m, 4H), 1.40–1.26 (m, 12H), 0.95 – 0.81 (m, 10H), 0.26 (s, 12H). **^{13}C NMR** (101 MHz, $CDCl_3$): δ_C = 142.8, 132.8, 122.6, 119.8, 105.3, 101.8, 97.0, 34.3, 31.9, 30.7, 29.4, 22.8, 20.8, 20.7, 15.9, 14.2, -1.7. **MS** (EI +, 70 eV) *m*/*z* (%) = 544.4 ()100% [M^+]. **Anal.** Calcd for $C_{34}H_{52}N_2Si_2$: C, 74.94; H, 9.62; N, 5.14. Found: C, 74.82; H, 9.31; N, 4.91.

4-(2,5-dihexyl-4-((trimethylsilyl)ethynyl)phenyl)-2-methylbut-3-yn-2-ol (2.9)

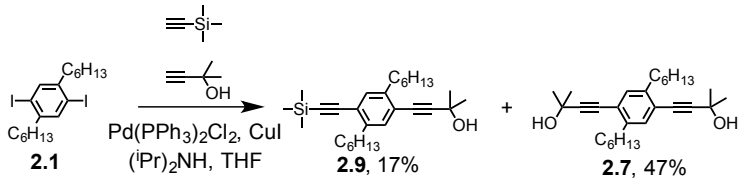

A round bottom flask was charged with $PdCl_2(PPh_3)_2$ (74.1 mg, 0.104 mmol), CuI (39.8 mg, 0.209 mmol), and **2.1** (1.04 g, 2.09 mmol). To this flask was added THF (8 mL) and $(^iPr)_2NH$ (1.5 mL) and the solution degassed with Argon for 15 min. Then ethynyltrimethylsilane (0.212 mL, 1.46 mmol) was added via syringe and after 16.5 hr, 2-Methyl-3-butyn-2-ol (0.265 mL, 2.72 mmol) was added. The solution was stirred for a further 17hr under Argon. When the reaction was deemed complete by TLC, the rxn mixture was treated with water (2 mL) and extracted with DCM. The organic layer was washed successively with water, 2M HCl(aq), brine and dried over Na_2SO_4, solvent removed and the crude passed through a colum on SiO_2 (2:1 cyclohex:DCM) to afford **2.9** as a yellow oil (150mg, 17%). **^{1}H NMR** (400 MHz, $CDCl_3$): δ_H = 7.24 (s, 1H), 7.19 (s, 1H), 2.74–2.60 (m, 4H), 2.05 (s, 1H), 1.62 (d, *J* = 5.7 Hz, 6H), 1.58 (dd, *J* = 7.2, 2.0 Hz, 4H), 1.40–1.22 (m, 12H), 0.95–0.80 (m, 6H), 0.28–0.20 (m, 9H). **^{13}C NMR** (126 MHz, $CDCl_3$): δ_C = 142.8, 142.2, 132.6, 132.4, 122.5, 122.2, 104.0, 98.9, 98.3, 81.1, 65.9, 34.2, 34.2, 31.9, 31.9, 31.6, 30.7, 29.4, 22.8, 14.2, 0.1. **MS** (MALDI-TOF) *m*/*z*: $[M+H]^+$ calcd for $C_{28}H_{44}OSi$, 424.32; found 424.31.

4-(2,5-dihexyl-4-[(3-Cyanopropyl)dimethylsilyl]ethynyl]-phenyl (2.11)

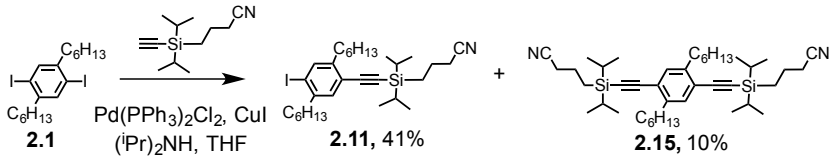

A two neck round bottom flask was charged with **2.1** (6.95 g, 14.0 mmol) and CuI (53 mg, 279 µmol) and $Pd(PPh_3)_2Cl_2$ (196 mg, 279 µmol) and dried under vaccum for 30 min. Then DIPA (40 mL) and dry THF (40 mL) were added and the resulting solution bubble purged with argon for 20 min. Then CPDIPS-A was added via syringe (from a distillation flask and washed out with 5 mL dry, degassed THF). The reaction mixture was then stirred overnight at RT. The reaction mixture was extracted with H_2O and TBME, the organic layer washed with 2M HCl (aq), brine and dried over $MgSO_4$. The crude was passed through a column of SiO_2 (1:1 cyclohexane:DCM), fractions combined and solvent removed to afford **2.11** as a dark oil (2.22 g, 41%). $\mathbf{R}_f$ = 0.53 (SiO_2; cyclohexane/DCM #:#). **^{1}H NMR** (400 MHz,

$CDCl_3$): δ_H = 7.64 (s, 1H), 7.23 (s, 1H), 2.71–2.58 (m, 4H), 2.42 (t, *J* = 6.9 Hz, 2H), 1.92–1.79 (m, 2H), 1.65–1.50 (m, 4H), 1.45–1.22 (m, 12H), 1.17–1.00 (m, 14H), 0.97–0.77 (m, 8H). **^{13}C NMR** (101 MHz, $CDCl_3$): δ_C = 144.5, 143.0, 139.6, 132.9, 122.5, 119.8, 106.0, 101.5, 93.6, 40.3, 34.2, 31.9, 31.8, 30.9, 30.4, 29.4, 29.2, 22.8, 21.5, 21.0, 21.0, 18.4, 18.1, 14.2, 11.9, 9.8. **MS** (EI +, 70 eV) *m/z* (%) = 577.3 (1%) [M^+], 534.3 (100%) [M–^{i}Pr]$^+$. **Anal.** Calcd for $C_{30}H_{48}INSi$: C, 62.37; H, 8.37; N, 2.42. Found: C, 62.39; H, 8.15; N, 2.58.

1,4-bis[2-[(3-Cyanopropyl)dimethylsilyl]ethynyl]-2,5-dihexylbenzene (2.15)

Isolated from the above reaction procedure when trying to form aryl14 in a statistical manner. **2.15** was then isolated by column chromatography as a dark oil (1.24 g, 10%). $\mathbf{R_f}$ = 0.05 (SiO_2; cyclohexane/DCM 1:1). **^{1}H NMR** (400 MHz, $CDCl_3$): δ_H = 7.25 (s, 2H), 2.70 (m, 4H), 2.43 (t, *J* = 6.9 Hz, 4H), 1.93–1.81 (m, 4H), 1.64–1.55 (m, 4H), 1.39–1.26 (m, 12H), 1.16–1.06 (m, 28H), 0.91–0.80 (m, 10H). **^{13}C NMR** (101 MHz, $CDCl_3$): δ_C = 142.7, 133.0, 122.7, 119.8, 106.5, 94.2, 34.5, 31.9, 31.0, 29.5, 22.8, 21.5, 21.0, 18.4, 18.1, 14.2, 11.9, 9.9. **MS** (MALDI-TOF) *m/z*: [M-C_3H_5]$^{\square+}$ calcd for $C_{39}H_{62}N_2Si_2$, 614.4; found 614.3, [M+Na]$^+$ calcd for $C_{42}H_{68}N_2Si_2Na$, 679.48; found 679.41, [M+K]$^+$ calcd for $C_{42}H_{68}N_2Si_2K$, 695.46; found 695.40.

4-(((2,5-dihexyl-4-((trimethylsilyl)ethynyl)phenyl)CPDIPS (2.12)

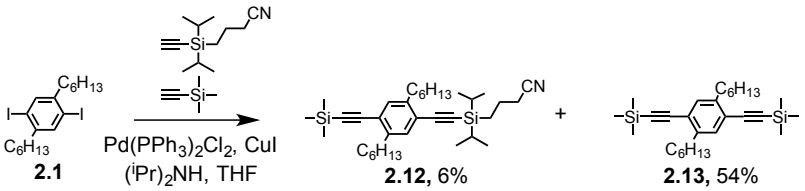

$PdCl_2(PPh_3)_2$ (70.5 mg, 99.5 μmol), CuI (37.9 mg, 0.199 mmol), and **2.1** (991 mg, 1.99 mmol). To this flask was added THF (8 mL) and (^{i}Pr)$_2$NH (1.5 mL) and the solution degassed with Argon for 15 min. Then CPDIPS-A (0.289 g, 1.39 mmol) was added via syringe, and after 16.5 hr trimethylsilylacetylene (0.376 mL, 2.59 mmol). The solution was stirred for a further 17 hr under Argon. When the reaction was deemed complete by TLC (DCM), the reaction mixture was treated with water (2 mL) and extracted with TBME. The organic layer was washed successively with water, 2M HCl(aq), brine and dried over Na_2SO_4, solvent removed and the crude passed through a column on SiO2 (3:2 cyclohexane:DCM, then ramp of 1:1 cyclohexane:DCM, stripping column with neat ethyl acetate to afford **2.12** as a yellow oil. (49 mg, 6%). **^{1}H NMR** (400 MHz, $CDCl_3$): δ_H = 7.25 (s, 1H), 7.23 (s, 1H), 2.69 (dt, *J* =

8.5, 2.7 Hz, 4H), 2.42 (t, J = 6.9 Hz, 2H), 1.94–1.80 (m, 2H), 1.69–1.52 (m, 4H), 1.41–1.24 (m, 12H), 1.17–1.05 (m, 14H), 0.95–0.80 (m, 8H), 0.30–0.22 (m, 9H). **^{13}C NMR** (101 MHz, $CDCl_3$): δ_C = 142.9, 142.6, 133.0, 132.6, 122.9, 122.5, 119.8, 106.6, 103.9, 99.2, 94.0, 34.4, 34.3, 31.9, 31.8, 30.9, 30.8, 29.5, 29.5, 22.8, 22.8, 21.5, 21.0, 18.4, 18.1, 14.2, 11.9, 9.9, 0.1.

((2,5-dihexyl-1,4-phenylene)bis(ethyne-2,1-diyl))bis(trimethylsilane) (2.13)

Isolated from the above reaction mixture in the attempted formation of **2.13** as a yellow oil (476 mg, 54%). **^{1}H NMR** (400 MHz, $CDCl_3$): δ_H = 7.24 (s, 2H), 2.74–2.62 (m, 4H), 1.69–1.54 (m, 4H), 1.31 (s, 12H), 0.88 (t, J = 6.6 Hz, 6H), 0.24 (s, 18H). **MS** (MALDI-TOF) m/z: $[M+H]^+$ calcd for $C_{28}H_{46}Si_2$, 438.3; found 438.6.

4-(((2,5-dihexyl-4-(3-hydroxy-3-methylbut-1-yn-1-yl)phenyl)ethynyl)diisopropylsilyl)butanenitrile (2.14)

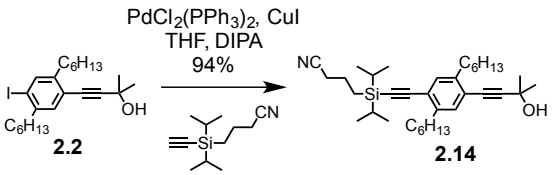

The catalytic system of $PdCl_2(PPh_3)_2$ (182 mg, 257 µmol), CuI (25 mg, 257 µmol) and **2.2** (2.92 g, 6.43 mmol) were dissolved in dry THF (16 mL) and DIPA (4 mL) and the solution bubbled purged with argon for 30 min. Then CPDIP-A (1.87 g, 9.0 mmol) was added and the reaction mixture stirred at 50°C for 17 hr. When deemed complete by TLC, the mixture was diluted with TBME and water. The combined organic layers were washed with 2M HCL(aq), brine, and dried over Na_2SO_4. The product was purified by flash chromatography on SiO_2 (DCM), fractions combined and evaporated to afford **2.14** as a yellow oil (3.24 g, 94%). **^{1}H NMR** (400 MHz, $CDCl_3$): δ_H = 7.24 (s, 1H), 7.21 (s, 1H), 2.74–2.62 (m, 4H), 2.42 (t, J = 6.9 Hz, 2H), 1.99 (s, 1H), 1.95–1.80 (m, 2H), 1.66–1.54 (m, 10H), 1.40–1.25 (m, 10H), 1.15–1.03 (m, 16H), 0.92–0.80 (m, 8H).

4-(4-Ethynyl-2,5-dihexylphenyl)-2-methylbut-3-yn-2-ol (2.16)

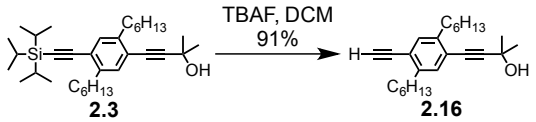

A round bottom flask was charged with **2.3** (530 mg, 1.04 mmol) dissolved in degassed THF (4 mL). Tetrabutylammonium fluoride (1M solution in THF, 1.56 mL) was added dropwise. After 30 min the reaction mixture was passed through a SiO_2 plug (DCM) fractions combined to afford **2.16** as a colourless oil. (335 mg, 91%). $\mathbf{R_f}$ = 0.53 (SiO_2; DCM). **^{1}H NMR** (250 MHz, $CDCl_3$): δ_H = 7.30 (s, 1H), 7.25 (s, 1H), 3.30 (s, 1H), 2.82–2.63 (m, 4H), 2.08 (s, 1H), 1.73–1.55 (m, 10H), 1.47–1.26 (m, 12H), 0.91 (t, *J* = 6.7 Hz, 6H). **^{13}C NMR** (101 MHz, $CDCl_3$): δ_C = 143.1, 142.5, 133.4, 132.7, 122.9, 121.8, 98.7, 82.8, 81.7, 81.3, 66.2, 34.4, 34.2, 32.2, 32.1, 31.9, 30.9, 30.9, 29.6, 29.5, 23.0, 23.0, 14.5.

((4-ethynyl-2,5-dihexylphenyl)ethynyl)triisopropylsilane (2.17)

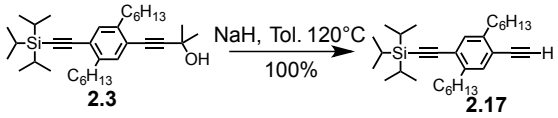

An oven heated 25mL two neck flask was charged with **2.3** (206 mg, 405 μmol) dissolved in dry DMF () and cooled to 0°C with an ice bath. Then NaH (60% dispersion in mineral oil 24.3 mg, 607 μmol) was added and the reaction allowed to warm to RT overnight. After the reaction was deemed complete by TLC the mixture was passed through a short plug, fractins combined to afford **2.17** as an oil (182 mg, 100%). **^{1}H NMR** (500 MHz, $CDCl_3$): δ_H = 7.28 (s, 1H), 7.26 (s, 1H), 3.27 (s, 1H), 2.71 (td, *J* = 10.5, 8.1 Hz, 4H), 1.67–1.54 (m, 4H), 1.43–1.23 (m, 12H), 1.20–1.09 (m, 21H), 0.95–0.82 (m, *J* = 6.8 Hz, 6H). **^{13}C NMR** (126 MHz, $CDCl_3$): δ_C = 142.8, 142.6, 133.1, 133.0, 123.5, 121.5, 105.6, 95.5, 82.6, 81.4, 34.5, 34.0, 31.9, 31.8, 30.9, 30.8, 29.5, 29.3, 22.8, 22.8, 18.8, 14.2, 11.5. **MS** (MALDI-TOF) *m*/*z*: [M–C_3H_7]$^{\square+}$ calcd for $C_{28}H_{44}O_{Si}{}^{\square+}$, 408.31; found 408.68.

9-Dodecyl-9H-carbazole (2.19)

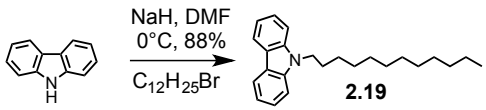

Adapting a procedure reported by Dierschke et al.[200] NaH (60% w/w suspension in mineral oil) (359 mg, 8.97 mmol) was slowly added to a stirred solution of carbazole (1 g, 5.98 mmol) in DMF (20 mL) at 0°C under argon. After 1 hr 1-Bromdodecan (1.64 g, 6.58 mmol) was added by syringe and the reaction stirred under argon for a further 20 hr at RT. The reaction was quenched by the dropwise addition of water and the aqueous phase extracted with DCM. The combined organic fractions were washed with 2M HCl (aq), brine and dried over $MgSO_4$, solvent removed under reduced pressure. The product was purified by

column chromatography on SiO_2 (cylohexane),fractions evaporated to afford **2.19** as a colourless oil (1.76 g, 88%). **^{1}H NMR** (400 MHz, $CDCl_3$): δ_H = 8.03 (dt, J = 7.8, 0.9 Hz, 2H), 7.39 (ddd, J = 8.2, 7.0, 1.2 Hz, 2H), 7.35–7.30 (m, 2H), 7.15 (ddd, J = 7.9, 7.0, 1.1 Hz, 2H), 4.22 (t, J = 7.3 Hz, 2H), 1.79 (p, J = 7.3 Hz, 2H), 1.37–1.07 (m, 18H), 0.80 (t, J = 6.9 Hz, 3H). **^{13}C NMR** (101 MHz, $CDCl_3$): δ_C = 140.6, 125.7, 122.9, 120.5, 118.8, 108.8, 77.2, 43.2, 32.1, 29.8, 29.7, 29.7, 29.7, 29.6, 29.5, 29.1, 27.5, 22.8, 14.3.

9-(2-hexyldecyl)-9H-carbazole (2.20)

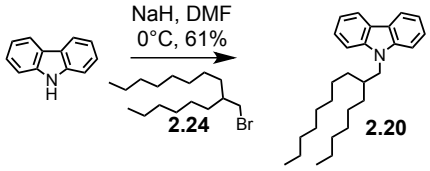

Adapting a procedure reported by Dierschke et al.[200] NaH (60% w/w suspension in mineral oil) (179 mg, 4.49 mmol) was slowly added to a stirred solution of carbazole (500 mg, 2.99 mmol) in DMF (10 mL) at 0°C under argon. Then the branched alkyl chain **2.24** (1.178 g, 3.86 mmol) was added by syringe and the reaction stirred under argon for a further 20 hr at RT. The reaction was quenched by the dropwise addition of water and the aqueous phase extracted with DCM. The combined organic fractions were washed with 2M HCl (aq), brine and dried over $MgSO_4$, solvent removed under reduced pressure. The product was purified by column chromatography on SiO_2 (cylohexane),fractions evaporated to afford **2.20** as a colourless oil (709 mg, 61%). **^{1}H NMR** (400 MHz, $CDCl_3$): δ_H = 8.02 (d, J = 7.8 Hz, 2H), 7.38 (ddd, J = 8.1, 7.1, 1.1 Hz, 2H), 7.31 (d, J = 8.2 Hz, 2H), 7.19–7.10 (m, 2H), 4.08 (d, J = 7.5 Hz, 2H), 2.06 (dt, J = 11.8, 6.3 Hz, 1H), 1.35–1.06 (m, 24H), 0.79 (dt, J = 9.2, 6.9 Hz, 6H). **^{13}C NMR** (101 MHz, $CDCl_3$): δ_C = 141.1, 125.6, 122.9, 120.4, 118.8, 109.1, 77.2, 47.9, 38.1, 32.1, 32.1, 32.0, 31.9, 30.1, 29.8, 29.7, 29.4, 26.7, 22.8, 22.7, 14.3, 14.2.

9-(8-bromooctyl)-9*H*-carbazole (2.21)

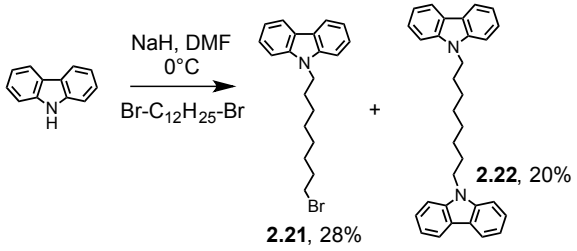

Adapting a procedure reported by Dierschke et al.[200] NaH (60% w/w suspension in mineral oil) (718 mg, 17.9 mmol) was slowly added to a stirred solution of carbazole (2.00 g,

12.0 mmol) in DMF (40 mL) at 0°C under argon. Then 1,8-Dibromoctane (6.51 g, 23.9 mmol) was added by syringe and the reaction stirred under argon for a further 20 hr at RT. The reaction was quenched by the dropwise addition of water and the aqueous phase extracted with DCM. The combined organic fractions were washed with 2M HCl (aq), brine and dried over $MgSO_4$, solvent removed under reduced pressure. The product was purified by column chromatography on SiO_2 (cylohexane),fractions evaporated to afford **2.21** as a colourless oil (1.21 g, 28%). **^{1}H NMR** (400 MHz, $CDCl_3$): δ_H = 8.06–7.99 (m, 2H), 7.43–7.34 (m, 2H), 7.36–7.29 (m, 2H), 7.17–7.10 (m, 2H), 4.22 (t, *J* = 7.2 Hz, 2H), 3.29 (t, *J* = 6.8 Hz, 2H), 1.79 (dt, *J* = 12.3, 6.0 Hz, 2H), 1.75 – 1.66 (m, 2H), 1.37 – 1.12 (m, 8H). **^{13}C NMR** (101 MHz, $CDCl_3$): δ_C = 140.5, 125.7, 122.9, 120.5, 118.8, 108.8, 43.2, 34.1, 32.8, 29.3, 29.1, 28.7, 28.2, 27.3.

1,8-di(9*H*-carbazol-9-yl)octane (2.22)

From the reaction mixture of the procedure described above **2.22** was isolated after column chromatography as white needles (521 mg, 20%). **^{1}H NMR** (400 MHz, $CDCl_3$): δ_H = 8.13 (dt, *J* = 7.8, 0.8 Hz, 4H), 7.48 (ddd, *J* = 8.2, 7.1, 1.2 Hz, 4H), 7.41 (d, *J* = 8.2 Hz, 4H), 7.25 (ddd, *J* = 7.9, 7.2, 1.0 Hz, 4H), 4.29 (t, *J* = 7.2 Hz, 4H), 1.85 (p, *J* = 7.3 Hz, 4H), 1.39–1.27 (m, 8H). **^{13}C NMR** (101 MHz, $CDCl_3$): δ_C = 140.5, 125.7, 122.9, 120.5, 118.8, 108.8, 43.1, 29.3, 29.0, 27.3.
See also the Crystal structure data!!

3,6-Di-tert-butyl-9H-carbazole (2.23)

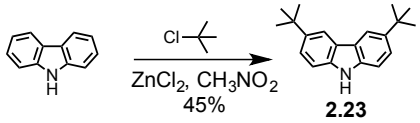

2.23

Following a literature procedure,[270] a two neck 100 mL round bottom was charged with carbazole (2.00 g, 11.4 mmol) dried under vacuum. Then under N_2 $ZnCl_2$ (511 mg, 3.75 mmol) was added and dissolved in nitromethane (50 mL). Finally (3.75 mL, 34.1 mmol) was added dropwise and the reaction left to stir under N_2. After formation of an orange precipitate the reaction was deemed complete by TLC (4:1 cyclohexan:DCM). The reaction was quenched by the slow addition of water, and extracted with TBME. The organic phase was washed with 2M HCl (aq), brine and dried over $MgSO_4$. The crude was passed through a column of SiO_2, fractions combined and solvent removed to afford **2.23** as a white solid

(1.43 g, 45%). **^{1}H NMR** (400 MHz, $CDCl_3$): δ_H = 8.10 (d, J = 1.8 Hz, 2H), 7.81 (s, 1H), 7.48 (dd, J = 8.5, 1.9 Hz, 2H), 7.33 (d, J = 8.5 Hz, 2H), 1.48 (s, 18H). **^{13}C NMR** (101 MHz, $CDCl_3$): δ_C = 142.4, 138.2, 123.7, 123.5, 116.3, 110.1, 34.8, 32.2 as lit.

7-(Bromomethyl)pentadecane (2.24)

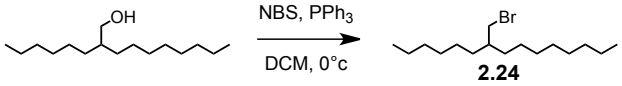

Adapting a procedure reported by Kastler et al.[204] a 100 mL round bottom flask containing PPh_3 (24.9 g, 94.8 mmol) and 7-(hydroxymethyl)pentadecane (15 g, 60 mmol) dissolved in DCM (45 mL) was bubble purged with Argon and cooled to 0◦C with an Ice bath. N-Bromosuccinimide (16.5 g, 92.4 mmol) was added stepwise over 20 min and the reaction mixture left stirring at RT for 15 hr. Then the solvent was removed and the resulting black residue redissolved in hexane and passed through a short silica plug (SiO_2, hexane), fractions evaporated under reduced pressure to afford **2.24** as a colourless oil (17.1 g, 93%). **^{1}H NMR** (400 MHz, $CDCl_3$): δ_H = 3.45 (d, J = 4.8 Hz, 2H), 1.59 (m, 1H), 1.41–1.16 (m, 24H), 0.89 (m, 6H). **^{13}C NMR** (100 MHz, $CDCl_3$): δ_C = 40.2, 39.9, 33.0, 33.0, 32.3, 32.2, 30.2, 30.0, 29.9, 29.7, 27.0, 26.9, 23.1, 23.1, 14.5, 14.5.

2-Bromo-7-hydroxy-9-(2-hexyldecyl)-carbazole (2.28)

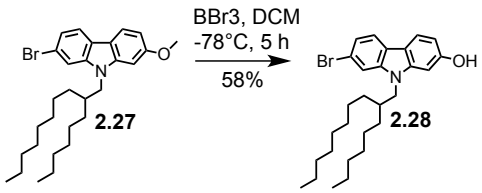

This compound **2.28** was prepared by adapting a literature procedure.[205] A solution of BBr_3 (1 M in DCM, 1.92 mL) was added dropwise to a solution of **2.27** (500 mg, 0.99 mmol) dissolved in DCM (25 mL) pre-cooled to –78°C under Argon. The reaction mixture was allowed to slowly warm to 0°C and stirred for 5 hr. The reaction mixture was then cooled to –78°C and quenched with saturated $NaHCO_3$(aq) (20 mL) and diluted with EtOAc (20 mL). The aqueous layer was extracted with EtOAc (3 x 10 mL) and the combined organic layers were washed with brine (10 mL) and dried over anhydrous Na_2SO_4, filtered and solvent removed. The crude product was purified by flash chromatography on SiO_2 (EtOAc/hexane 1:2), fractions combined and solvent removed to afford **2.28** as a light sensitive, white low melting point solid (284 mg, 58%). $\mathbf{R}_f$ = 0.70 (SiO_2; hexane/EtOAc 2:1). $\mathbf{R}_f$ = 0.56 (SiO_2; DCM). **^{1}H NMR** (400 MHz, $CDCl_3$): δ_H = 7.86 (d, J = 8.3 Hz, 1H), 7.80 (d, J = 8.2 Hz, 1H),

7.44 (d, *J* = 1.6 Hz, 1H), 7.28 (dd, *J* = 8.2, 1.7 Hz, 1H), 6.80 (d, *J* = 2.1 Hz, 1H), 6.73 (dd, *J* = 8.3, 2.2 Hz, 1H), 4.91 (br. s, 1H), 4.01 (d, *J* = 7.6 Hz, 2H), 2.14–1.99 (m, 1H), 1.43–1.15 (m, 24H), 0.92–0.81 (m, 6H). **^{13}C NMR** (101 MHz, $CDCl_3$): δ_C = 155.0, 142.7, 142.2, 122.1, 121.3, 120.6, 118.0, 116.6, 112.0, 108.5, 95.7, 48.1, 37.8, 32.0, 31.9, 30.1, 29.8, 29.6, 29.4, 26.6, 22.8, 22.8, 14.3, 14.2.

2-Bromo-7-(trifluoromethanesulfonate)-9-(2-hexyldecyl)-carbazole (2.29)

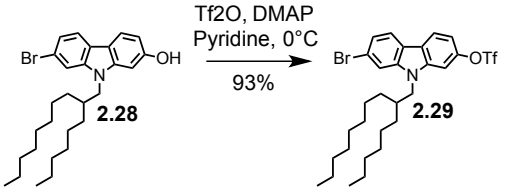

2.29 was prepared by adapting a literature procedure.[203] **2.28** (258 mg, 0.530 mmol) and DMAP (68 mg, 0.557 mmol) were dissolved in pyridine (2mL) degassed with Argon and cooled to 0°C. Trifluoromethanesulfonic anhydride (0.176 mL, 1.06 mmol) was added dropwise to this stirred solution. The reaction mixture was stirred at 0°C under Argon for 2 hr and then left stirring under Argon at RT for a further 17 hr. After this time the excess anhydride was quenched by the slow addition of DI water (1mL) and extracted with Et_2O. The orgainc fraction was washed successively with water, $CuSO_4$ 0.1M, water and brine, dried over Na_2SO_4, filtered and solvent removed and dried under vacuum to afford **2.29** as a yellow oil (306 mg, 93%). $\mathbf{R_f}$ = 69 (SiO_2; cyclohexane/DCM 1:1). **^{1}H NMR** (400 MHz, CD_3CN): δ_H = 8.20 (d, *J* = 8.6 Hz, 1H), 8.06 (d, *J* = 8.3 Hz, 1H), 7.74 (d, *J* = 1.4 Hz, 1H), 7.52 (d, *J* = 2.1 Hz, 1H), 7.40 (dd, *J* = 8.3, 1.6 Hz, 1H), 7.22 (dd, *J* = 8.6, 2.1 Hz, 1H), 4.20 (d, *J* = 7.7 Hz, 2H), 2.10–1.99 (m, 1H), 1.39–1.05 (m, 24H), 0.90–0.74 (m, 6H). **MS** (ESI, *m*/*z*): 618.4 $[M+H]^+$ 100%, requires 618.2. **HPLC** C_{18} isocratic $CNCH_3$, run time 32.59 min, >99%.

4,4'-Dibromo-2-nitro-1,1'-biphenyl (2.30)

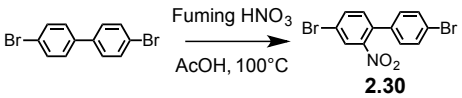

A procedure from Dierschke et al.[200] was adapted as follows: a two necked flask with reflux condenser attached was charged with a solution of 4,4'-dibromo- biphenyl (2.00 g, 6.41 mmol) dissolved in glacial AcOH (30 mL) at 100°C. To this was slowly added fuming HNO_3 (100%, 9.25 mL) and H_2O (0.75 mL) to give a red solution. The reaction mixture was stirred at 100°C for 30 min and then allowed to cool to RT. Then water was slowly added,

using DCM to extract the precipitate. The organic layer was then washed successively with water until a neutral pH was obtained then brine and dried over Na_2SO_4, solvent removed under reduced pressure to afford **2.30** as a yellow solid (1.86 g, 81%). **mp** 126 °C (lit.[200] mp 125–127 °C). $\mathbf{R_f}$ = 0.54 (SiO_2; hexane/CH_2Cl_2 1:1). **^{1}H NMR** (400 MHz, $CDCl_3$): δ_H = 8.03 (d, *J* = 2.0 Hz, 1H), 7.75 (dd, *J* = 8.2, 2.0 Hz, 1H), 7.59–7.53 (m, 2H), 7.29 (d, *J* = 8.2 Hz, 1H), 7.18–7.13 (m, 2H). **^{13}C NMR** (100 MHz, $CDCl_3$): δ_C = 149.7, 136.0, 135.7, 134.5, 133.4, 132.4, 129.8, 127.7, 123.5, 122.2 as Lit.[200]

2,7-Dibromocarbazole (2.31)

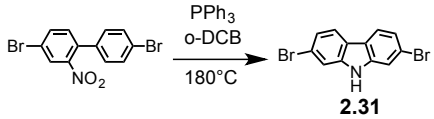

2.31

Following a procedure reported by Freeman et al.[201] 4,4'-dibromo-2-nitro-1,1'- biphenyl **2.30** (12.00 g, 33.6 mmol) and PPh_3 (22.00 g, 84.0 mmol) were dissolved in *o*-DCB (70 mL) under argon and heated to reflux at 180°C for 23 hr. After allowing to cool, the solvent was removed by Kugelrohr distilation. Then the black residue was passed through a plug of SiO_2 (1:1 Hexane:DCM) to remove O=PPh_3 and then the crude was passed through a column on SiO_2 (1:1 Hexane:DCM). After recrystalisation from DCM/Hexane **2.31** was obtained as white crystals (6.38 g, 58%). $\mathbf{R_f}$ = 0.37 (SiO_2; Hexane/DCM 1:1). **^{1}H NMR** (400 MHz, $CDCl_3$): δ_H = 8.06 (s, 1H), 7.88 (d, *J* = 8.3 Hz, 2H), 7.58 (d, *J* = 1.6 Hz, 2H), 7.36(dd, *J* = 8.3, 1.6 Hz, 2H). **^{13}C NMR** (100 MHz, $CDCl_3$): δ_C = 140.4, 123.4, 121.9, 121.6, 119.9, 114.0. **MS** (ESI, *m/z*): 323.7 $[M–H]^-$ 100%, requires 323.9. **Anal.** Calcd for $C_{12}H_7Br_2N$: C, 44.35; H, 2.17; N, 4.31. Found: C, 44.26; H, 2.24; N, 4.37.

2,7-Dibromo-9-(2-hexyldecyl)-carbazole (2.32)

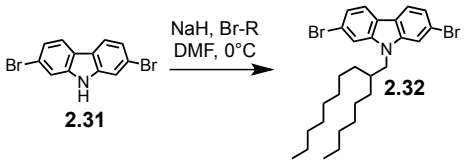

2.31 **2.32**

Adapting a procedure reported by Dierschke et al.[200] NaH (60% w/w suspension in mineral oil) (865 mg, 21.6 mmol) was slowly added to a stirred solution of 2,7-dibromocarbazole **2.31** (5.00 g, 15.4 mmol) in DMF (50 mL) at 0◦C under argon. After 1 hr 7-(bromomethyl)pentadecane **2.24** (6.11 g, 20 mmol) was added by syringe and the reaction stirred under argon for a further 20 hr at RT. The reaction was quenched by the dropwise addition of water and the aqueous phase extracted with DCM three times. The combined

organic fractions were washed with brine and dried over Na_2SO_4, solvent removed under reduced pressure. The product was purified by column chromatography on SiO_2 (Hexane ramping to DCM) fractions evaporated to afford **2.32** as a colourless oil (8.05 g, 95%). $\mathbf{R}_f$ = 0.65 (SiO_2; Hexane/DCM 1:1). **^{1}H NMR** (400 MHz, $CDCl_3$): δ_H = 7.88 (d, *J* = 8.3 Hz, 2H), 7.50 (d, *J* = 1.5 Hz, 2H), 7.33 (dd, *J* = 8.3, 1.6 Hz, 2H), 4.05 (d, *J* = 7.6 Hz, 2H), 2.13–2.02 (m, 1H), 1.42–1.14 (m, 24H), 0.93–0.80 (m, 6H). **^{13}C NMR** (100 MHz, $CDCl_3$): δ_C = 142.0, 122.7, 121.6, 121.4, 119.8, 112.5, 48.0, 37.7, 32.0, 31.9, 31.8, 31.8, 30.0, 29.7, 29.6, 29.4, 26.5, 26.5, 22.8, 22.8, 14.3, 14.2. **MS** (ESI, *m*/*z*): 572 $[M+Na]^+$ 100%, requires 572.1.

4,4'-diiodo-2-nitro-1,1'-biphenyl (2.33)

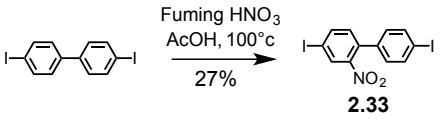

To a 250 mL two necked flask with reflux condenser and wash bottles containing a solution of $Na_2S_2O_3$ was charged with a solution of diiodo-biphenyl (2.00 g, 4.88 mmol) dissolved in glacial AcoH (30 mL) at 100°C was slowly added fuming HNO_3 (100%, 9.25 mL) and water (0.75 mL). The reaction mixture was stirred at 100°C for 30 min and then allowed to cool to RT before further cooling with an ice bath. Then water was added and DCM. The water was extracted with DCM and the orgainc layer washed successively with; water, $Na_2S_2O_3$ (10%, aq), brine, dried over Na_2SO_4 and solvent removed. This crude was passed through a column of SiO_2 (1:1 cyclohexane:DCM) fractions combined to afford **2.33** as a yellow solid (603 mg, 27%). **^{1}H NMR** (400 MHz, $CDCl_3$): δ_H = 8.19 (d, *J* = 0.7 Hz, 1H), 7.94 (dd, *J* = 8.1, 0.9 Hz, 1H), 7.76 (d, *J* = 8.2 Hz, 2H), 7.13 (d, *J* = 8.1 Hz, 1H), 7.02 (d, *J* = 8.2 Hz, 2H). **^{13}C NMR** (101 MHz, $CDCl_3$): δ_C = 149.3, 141.6, 138.1, 136.1, 134.9, 133.2, 133.0, 129.6, 94.9, 92.4. **MS** (EI +, 70 eV) *m*/*z* (%) = 450.9 (100%) $[M^+]$. **Anal.** Calcd for $C_{12}H_7I_2NO_2$: C, 31.96; H, 1.56; N, 3.11. Found: C, 31.69; H, 1.61; N, 3.18.

2-Bromo-7-(ethynyl-CPDIPS)-9-(2-hexyldecyl)-carbazole (2.37)

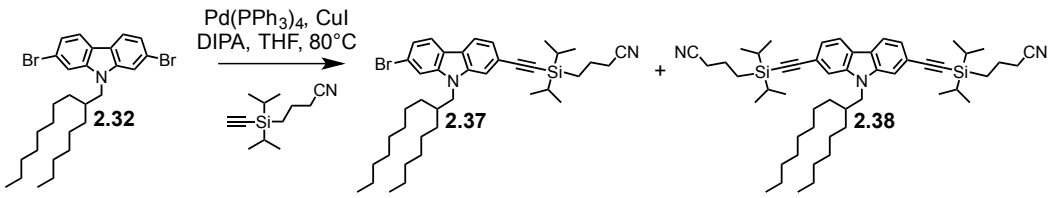

2.32 (4.34 g, 7.9 mmol) was placed in a 500mL round bottom flask and dissolved in THF (150 mL) and DIPA (100 mL) and the solution bubble purged with argon for 15 min. Then

$Pd(PPh_3)_4$ (456 mg, 0.395 mmol) and CuI (75.2 mg, 0.395 mmol) were added followed by CPDIPS-A from a weighed syringe (1.15 g, 5.53 mmol) dropwise. Then the reaction mixture was heated to 80°C and left stirring under argon overnight. The reaction mixture was extracted with Et_2O and H_2O, the organic fraction washed with 2M HCl (aq), brine and dried over $MgSO_4$. The crude was passed through a column on SiO_2 (1:1 cyclohexane:DCM) and **2.37** was isolated as a yellow oil (260 mg, 42%). $\mathbf{R_f}$ = 0.29 (SiO_2; cyclohexane/DCM 1:1). **^{1}H NMR** (500 MHz, $CDCl_3$): δ_H = 7.96 (d, *J* = 7.9 Hz, 1H), 7.89 (d, *J* = 8.2 Hz, 1H), 7.49 (d, *J* = 22.0 Hz, 2H), 7.34 (t, *J* = 9.3 Hz, 2H), 4.09 (d, *J* = 7.3 Hz, 2H), 2.46 (t, *J* = 6.8 Hz, 2H), 2.10 (s, 1H), 1.99–1.86 (m, 2H), 1.50–1.03 (m, 40H), 0.95–0.79 (m, 6H). **^{13}C NMR** (126 MHz, $CDCl_3$): δ_C = 142.5, 140.6, 123.6, 122.7, 122.5, 121.8, 121.4, 120.2, 120.2, 120.0, 119.9, 112.9, 112.4, 109.3, 89.0, 47.9, 37.8, 32.0, 31.9, 31.8, 30.0, 29.7, 29.6, 29.4, 26.6, 26.5, 22.8, 22.7, 21.5, 20.9, 18.4, 18.2, 14.3, 14.2, 12.0, 9.8. **MS** (ESI, *m*/*z*): 699.6 $[M+Na]^+$ 100%, requires 699.3. **MS** (MALDI-TOF) *m*/*z*: $[M+H]^+$ calcd for $C_{40}H_{60}BrN_2Si$, 675.36; found 675.43.

2,7-bis-(ethynyl-CPDIPS)-9-(2-hexyldecyl)-carbazole (2.38)

Isolated as the symmetric, doubly substituted product from the statistical coupling performed above. **2.38** was isolated by column chromatography on SiO2 as a yellow oil (96 mg, 13%). **^{1}H NMR** (400 MHz, $CDCl_3$): δ_H = 7.99 (d, *J* = 8.0 Hz, 2H), 7.49 (s, 2H), 7.35 (d, *J* = 8.0 Hz, 2H), 4.15 (d, *J* = 7.4 Hz, 2H), 2.46 (t, *J* = 6.9 Hz, 4H), 2.13 (s, 1H), 2.03-1.82 (m, 4H), 1.47–1.03 (m, 56H), 0.98–0.75 (m, 6H). **^{13}C NMR** (101 MHz, $CDCl_3$): δ_C = 132.1, 128.7, 128.4, 123.1, 119.8, 108.0, 89.3, 21.4, 20.8, 18.3, 18.0, 11.8, 9.7. **MS** (MALDI-TOF) *m*/*z*: $[M^+]$ calcd for $C_{52}H_{79}N_3Si_2$, 801.58; found 801.35.

2-Bromo-7-(ethynyl-HOP)-9-(2-hexyldecyl)-carbazole (2.39)

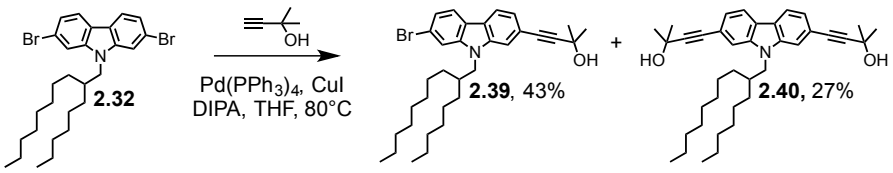

A two neck round bottom flask was charged with **2.32** (1.07 g, 1.95 mmol) and the catylytic system of CuI (18.5 mg, 97.4 μmol) and $Pd(PPh_3)_4$ (113 mg, 97.4 μmol) dissolved in THF (20 mL) and DIPA (10 mL) degassed by bubble purging with argon. Then HOP-A (0.76 ml, 7.79 mmol) was added by syringe and the reaction mixture heated to 80°C under argon. After

16 hr the reaction was deemed complete by TLC and the crude passed through a column of SiO_2 (DCM). Fractions combined and solvent evaporated to afford **2.39** as a yellow oil (466 mg, 43%). **^{1}H NMR** (400 MHz, $CDCl_3$): δ_H = 7.95 (d, *J* = 8.0 Hz, 1H), 7.89 (d, *J* = 8.3 Hz, 1H), 7.50 (d, *J* = 1.5 Hz, 1H), 7.42 (s, 1H), 7.32 (dd, *J* = 8.3, 1.6 Hz, 1H), 7.29 (dd, *J* = 8.0, 1.2 Hz, 1H), 4.08 (d, *J* = 7.6 Hz, 2H), 2.15 – 2.07 (m, 1H), 2.05 (s, 1H), 1.67 (s, 6H), 1.42 – 1.15 (m, 24H), 0.86 (q, *J* = 6.9 Hz, 6H). **^{13}C NMR** (101 MHz, $CDCl_3$): δ_C = 142.5, 140.7, 123.2, 122.4, 121.7, 121.5, 120.2, 120.0, 119.9, 112.6, 112.4, 93.6, 83.4, 65.9, 48.0, 37.8, 32.0, 31.9, 31.8, 31.8, 31.7, 30.1, 29.7, 29.6, 29.4, 26.6, 26.5, 22.8, 22.8, 14.3, 14.2. **Anal.** Calcd for $C_{33}H_{46}BrNO$: C, 71.72; H, 8.39; N, 2.53. Found: C, 71.73; H, 8.49; N, 2.65.

2,7-bis(ethynyl-HOP)-9-(2-hexyldecyl)-carbazole (2.40)

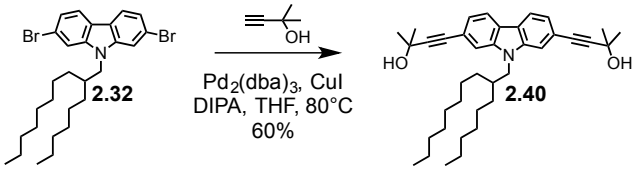

A 250 ml two neck flask was charged with **2.32** (1.00 g, 1.82 mmol). Then CuI (34.7 mg, 182 umol) and Pd2(dba)2 (87.0 mg, 95 umol) and PPh3 (96 mg, 360 umol) were added and the flask dried in vaccuo for 30 min. Then DIPA (60 mL) was added and pump purged back filling with argon x3. Then HOP-A (0.71 mL, 7.3 mmol) was added dropwise and the resulting solution stirred under argon at 80°C overnight. Extraction with DCM, water, 2M HCl (aq), brine dried over $MgSO_4$. The crude was passed through a column SiO_2, 10:1 dcm:EtOAc, fractions combined and solvent removed to afford **2.40** as a white solid (0.61 g, 60%). **^{1}H NMR** (400 MHz, $CDCl_3$): δ_H = 7.95 (d, *J* = 8.0 Hz, 2H), 7.42 (s, 2H), 7.27 (dd, *J* = 8.1, 1.1 Hz, 2H), 4.08 (d, *J* = 7.6 Hz, 2H), 2.12 (s, 3H), 1.67 (s, 12H), 1.40 – 1.14 (m, 24H), 0.86 (q, *J* = 6.9 Hz, 6H). **^{13}C NMR** (101 MHz, $CDCl_3$): δ_C = 141.2, 123.0, 122.6, 120.4, 120.0, 112.5, 93.5, 83.5, 65.9, 48.0, 37.8, 32.0, 31.9, 31.9, 31.8, 31.7, 30.1, 29.7, 29.6, 29.4, 26.6, 26.5, 22.8, 22.7, 14.3, 14.2. **MS** (EI +, 70 eV) *m/z* (%) = 555.4 [M^+]. **MS** (MALDI-TOF) *m/z*: $[M+H]^+$ calcd for $C_{38}H_{54}NO_2$, 556.41; found 556.34. **Anal.** Calcd for $C_{38}H_{53}NO_2$: C, 82.11; H, 9.61; N, 2.52. Found: C, 82.03; H, 9.68; N, 2.70.

2- (ethynyl-HOP)-7-(ethynyl-CPDIPS)-9-(2-hexyldecyl)-carbazole (2.41)

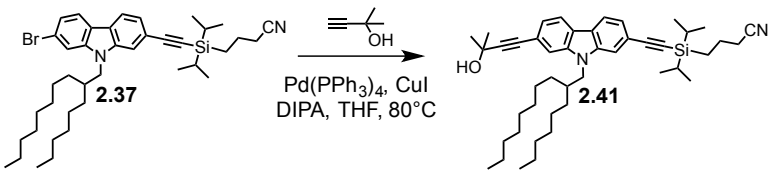

A two neck 50ml round bottom flask with reflux condenser was charged with **2.37** (240 mg, 355 umol), $Pd(PPh_3)_4$ (21 mg, 17.8 µmol), CuI (3.4 mg, 17.8 µmol) and dried in vaccuo for 20 min. Then dry THF (10 mL) and DIPA (5 mL) were added and bubble purged with argon for 15 min. Then HOP-A (104 µL, 1.07 mmol) was added and the reaction heated to reflux overnight. When no more starting material was present by TLC, the reaction was worked up with H_2O, extract with TBME and the organic layer washed with 2M HCl (aq), brine, dried over $MgSO_4$. The crude was passed through a column of SiO_2 (1:1 cyclohexane:DCM) fractions combined and solvent removed to afford **2.41** as a yellow oil (217 mg, 90%). **^{1}H NMR** (400 MHz, $CDCl_3$): δ_H = 7.98 (d, *J* = 2.7 Hz, 1H), 7.96 (d, *J* = 2.7 Hz, 1H), 7.46 (s, 1H), 7.44 (s, 1H), 7.33 (dd, *J* = 8.0, 0.9 Hz, 1H), 7.29 (dd, *J* = 8.1, 0.9 Hz, 1H), 4.12 (d, *J* = 7.5 Hz, 2H), 2.46 (t, *J* = 7.0 Hz, 2H), 2.16-2.08 (m, 1H), 2.06 (s, 1H), 1.96–1.87 (m, 2H), 1.67 (s, 6H), 1.42–1.08 (m, 40H), 0.87 (dt, *J* = 13.6, 6.1 Hz, 6H). **^{13}C NMR** (101 MHz, $CDCl_3$): δ_C = 141.3, 141.0, 123.4, 123.0, 122.9, 122.5, 120.5, 120.4, 120.2, 119.9, 112.8, 112.5, 109.4, 93.6, 89.0, 83.4, 65.9, 47.9, 37.8, 32.0, 31.9, 31.9, 31.8, 31.7, 30.0, 29.7, 29.6, 29.4, 26.6, 26.5, 22.8, 22.7, 21.4, 20.9, 18.4, 18.1, 14.2, 14.2, 12.0, 9.8. **MS** (MALDI-TOF) *m*/*z*: $[M+H]^+$ calcd for $C_{45}H_{67}N_2OSi$, 679.49; found 679.12. **Anal.** Calcd for $C_{45}H_{66}N_2OSi$: C, 79.59; H, 9.80; N, 4.13. Found: C, 79.53; H, 9.60; N, 4.10.

The same compound **2.41** can also be formed in the following reaction, however the yield was found to be much lower at 74%.

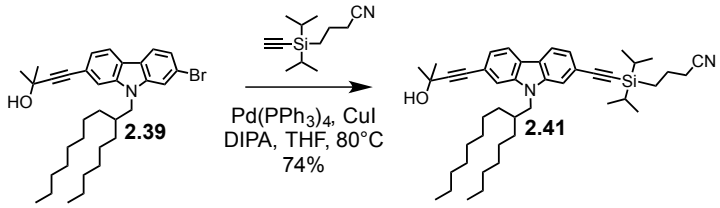

2,7-Diiodo-9-(2-hexyldecyl)-carbazole (2.42)

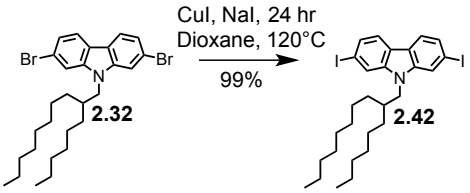

Adapting a literature procedure,[209] 2,7-dibromo-9-(2-hexyldecyl)-carbazole **2.32** (568 mg, 1.03 mmol) was placed in a 5 mL microwave vial that can be pressure sealed. Then CuI (19.7 mg, 0.103 mmol) and NaI (620 mg, 4.14 mmol) were added and the vial sealed and placed under vaccum for 30 min. Then dry Dioxane (1.5 mL) was added under N_2 followed

by N,N'-dimethylethylendiamine (26.2 µL, 0.207 mmol) the vial sealed and heated to 120°C, left stirring for 24 hr. The resulting sludge was diluted with 30% Ammonia (aq) and water, extracted with DCM. The organic layer was washed with brine and dried over $MgSO_4$, solvent removed to afford **2.42** directly as a colourless oil (657 mg, 99%). **^{1}H NMR** (400 MHz, $CDCl_3$): δ_H = 7.74 (d, *J* = 8.2 Hz, 2H), 7.68 (d, *J* = 1.1 Hz, 2H), 7.51 (dd, *J* = 8.2, 1.3 Hz, 2H), 3.98 (d, *J* = 7.5 Hz, 2H), 2.05 (br. s., 1H), 1.42 – 1.14 (m, 24H), 0.95 – 0.79 (m, 6H). **^{13}C NMR** (101 MHz, $CDCl_3$): δ_C = 141.8, 128.3, 121.9, 121.8, 118.4, 90.9, 47.8, 37.6, 32.0, 31.9, 31.7, 30.0, 29.7, 29.7, 29.4, 26.5, 26.4, 22.8, 22.8, 14.3, 14.3. **MS** (EI +, 70 eV) *m*/*z* (%) = 643.1 (100%) [M^+]. **Anal.** Calcd for $C_{28}H_{39}I_2N$: C, 52.27; H, 6.11; N, 2.18. Found: C, 52.50; H, 6.10; N, 2.32.

2,7-Diiodo-9H-carbazole (2.43)

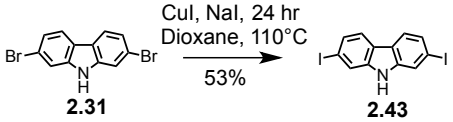

2.31 **2.43**

By adapting a literature procedure,[209] 2,7-dibromo-9H-carbazole **2.31** (509 mg, 1.57 mmol) was placed in a 5 mL microwave vial. Then CuI (29.8 mg, 0.157 mmol) and NaI (939 mg, 6.265 mmol) were added and the vial sealed and placed under vaccum for 30 min. Then dry Dioxane (2.0 mL) was added under N_2 followed by N,N'-dimethylethylendiamine (39.7 µL, 0.313 mmol) and the vial sealed and heated to 110°C, left stirring for >24 hr. The resulting sludge was diluted with 30% Ammonia (aq) and water, extracted with DCM. The organic layer was washed with brine and dried over $MgSO_4$, solvent removed to afford **2.43** directly as a colourless oil (350 mg, 53%). **^{1}H NMR** (400 MHz, $CDCl_3$): δ_H = 8.03 (s, 1H), 7.79 (dd, *J* = 1.5, 0.5 Hz, 2H), 7.77 (dt, *J* = 8.2, 0.7 Hz, 2H), 7.54 (dd, *J* = 8.2, 1.5 Hz, 2H). The Product was not soluble enough to obtain a clearly resolved carbon spectrum.

1,4-bis(Prop-2-yn-1-yloxy)benzene (2.44)

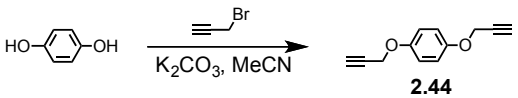

2.44

Hydroquinone (1.00 g, 9.08 mmol) and K_2CO_3 (3.17 g, 22.7 mmol) were dissolved in MeCN (20 mL), then while stirring at RT propargyl bromide solution (80% wt in toluene, 2.95 mL, 27.2 mmol) was added dropwise. After 14 hr H_2O (50 mL) was added and the aqueous layer washed with TBME (2x 50 mL). The organic layer was neutralised with 2M aqueous HCl, washed with brine and dried over $MgSO_4$. The solvent was removed and the crude passed

through a column of SiO_2 (1:1 cyclohexane:DCM), fractions combined and solvent removed under reduced pressure to afford 1,4-bis(prop-2-yn-1-yloxy)benzene **2.44** as a white solid (1.13 g, 67%). **mp**: 49.1°C. $\mathbf{R_f}$ = 0.33 (1:1 cyclohexane:DCM). **^{1}H NMR** (400 MHz, $CDCl_3$): δ_H 6.93 (s, 4H, Ar H), 4.65 (d, *J* = 2.4 Hz, 4H, –OC*H*$_2$C≡C), 2.51 (t, *J* = 2.4 Hz, 2H, acetylene H). **^{13}C NMR** (101 MHz, $CDCl_3$): δ_C 152.6 (Cq), 116.2 (Ct), 78.9 (Ct), 75.5 (Ct), 56.7 (Cs). **GC–MS** *m/z*: 186 (M^+). **Anal.** Calcd for $C_{12}H_{10}O_2$: C, 77.40; H, 5.41. Found: C, 77.25; H, 5.51.

1,5-bis(Prop-2-yn-1-yloxy)naphthalene (2.45)

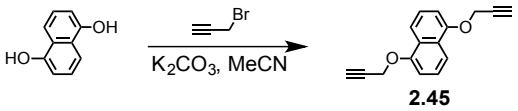

2.45

1,5-Dihydroxynaphthalene (1.00 g, 6.24 mmol) and K_2CO_3 (2.18 g, 15.6 mmol) were dissolved in MeCN (10 mL), then while stirring at RT propargyl bromide solution (80% wt in toluene, 2.02 mL, 18.7 mmol) was added dropwise. After 14 hr the reaction mixture was diluted with H_2O (50mL) and the aqueous layer washed with TBME (2x 50 mL). The organic layer was neutralised with 2M aqueous HCl, washed with brine and dried over $MgSO_4$. The solvent was removed and the crude passed through a column of SiO_2 (1:1 cyclohexane:DCM), fractions combined and solvent removed under reduced pressure to afford 1,5-bis(prop-2-yn-1-yloxy)naphthalene **2.45** as a white solid (0.31 g, 21%). **mp** 146.3°C. $\mathbf{R_f}$= 0.42 (1:1 cyclohexane:DCM). **^{1}H NMR** (400 MHz, $CDCl_3$): δ_H 7.91 (d, *J* = 8.6 Hz, 2H), 7.39 (dd, *J* = 8.3, 7.7 Hz, 2H), 6.98 (d, *J* = 7.7 Hz, 2H), 4.89 (d, *J* = 2.4 Hz, 4H, –OC*H*$_2$C≡C), 2.55 (t, *J* = 2.4 Hz, 2H, acetylene H). **^{13}C NMR** (101 MHz, $CDCl_3$): δ_C 153.3 (Cq), 126.9 (Cq), 125.3 (Ct), 115.4 (Ct), 106.5 (Ct), 78.7 (Ct), 75.7 (Ct), 56.3 (Cs). **GC-MS** *m/z*: 236 (M^+). **Anal.** Calcd for $C_{16}H_{12}O_2$: C, 81.34; H, 5.12. Found: C, 81.08; H, 5.17.

1,4-Diethynyl-2,5-dihexylbenzene (2.46)

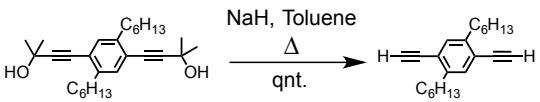

2.7 **2.46**

A 50 mL round bottom flask with reflux condenser attached was charged with **2.7** (665 g, 1.62 mmol) and dried under vacuum for 30 min. Then dry toluene (40 mL) was added and bubble purged with argon for 15 min. Finally NaH (60% w/w suspension in mineral oil) (50.5 mg, 2.11 mmol) was added and the resulting suspension heated to reflux for 1.5 hr,

when the reaction was deemed complete by TLC (cyclohexane). The reaction mixture was loaded directly onto a plug of silica in cylcohexane, UV active fraction collected and solvent removed to afford **2.46** as a yellow oil (477 mg, 100%). $\mathbf{R_f}$ = 0.43 (cyclohexane). **^{1}H NMR** (400 MHz, $CDCl_3$): δ_H 7.29 (s, 2H, Ar H), 3.28 (s, 2H, acetylene H), 2.74 – 2.68 (m, 4H), 1.65 – 1.56 (m, 4H), 1.39 – 1.25 (m, 12H), 0.89 (t, *J* = 6.9 Hz, 6H). **^{13}C NMR** (101 MHz, $CDCl_3$): δ_C 142.9 (Cq), 133.1 (Ct), 122.1 (Cq), 82.4 (Ct), 81.7 (Ct), 33.9 (Cs), 31.8 (Cs), 30.6 (Cs), 29.2 (Cs), 22.7 (Cs), 14.2 (Cp). **MS** (EI 70eV) *m/z*: M^+ 294.2.

1,4-Diethynyl-2,5-dihexylbenzene **2.46** can also be prepared in starting from **2.10**:

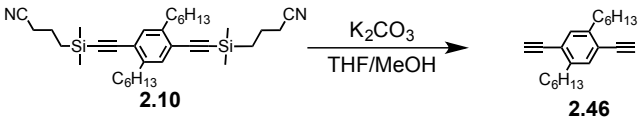

2.10 **2.46**

1,4-bis[2-[(3-Cyanopropyl)dimethylsilyl]ethynyl]-2,5-dihexylbenzene[218] **2.10** (500 mg, 0.92 mmol) was dissolved in an argon degassed 1:1 mixture of THF:MeOH (8 mL: 8mL), then finely ground K_2CO_3 (512 mg, 3.67 mmol) was added. After 30 min the reaction was complete by TLC (1:1 cyclohexane:DCM) and was quenched with H_2O, extracted with TBME, neutralised with 2M aqueous HCl and dried over $MgSO_4$. The solvent was removed and the crude passed through a column of SiO_2 (cyclohexane) fractions combined and solvent removed under reduced pressure to afford 1,4-diethynyl-2,5-dihexylbenzene **2.46** as a yellow oil (122 mg, 45%).

7.2 Compounds from Chapter 3

S,S'-((1,4-phenylenebis(ethyne-2,1-diyl))bis(4,1-phenylene)) diethanethioate (3.1)

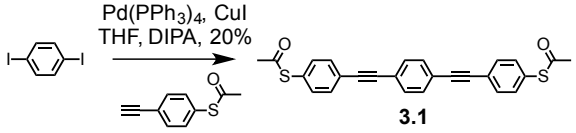

3.1

A round bottom flask was charged with 1,4-diiodobenzene (350 mg, 1.06 mmol) and the catalytic system of $Pd(PPh_3)_4$ (123 mg, 106 µmol), and CuI (20.2 mg, 106 µmol) were dissolved in dry THF (10 mL) and piperidine (2 mL) and the solution bubbled with Argon for 20 min. Then S-(4-ethynylphenyl) ethanethioate (411 mg, 2.33 mmol) dissolved in THF (mL) was added dropwise via syringe and the reaction mixture stirred under argon for 20 hr. when the reaction was deemed complete by TLC it was then diluted with TBME and water. The aquous layer was extracted with TBME, The combined organic layers were washed with 2M HCL(aq), brine, and dried over Na_2SO_4. The crude product was purified by flash

chromatography on SiO2 (cyclohexane:EtOAc 5:1), fractions evaporated to afford **3.1** as a yellow wax (216 mg, 48%). **^{1}H NMR** (400 MHz, $CDCl_3$): δ_H = 7.58 – 7.54 (m, 4H), 7.52 (s, 4H), 7.43 – 7.38 (m, 4H), 2.44 (s, 6H). **^{13}C NMR** (101 MHz, $CDCl_3$): δ_C = 193.5, 134.4, 132.3, 131.8, 128.5, 124.4, 123.2, 90.8, 90.7, 30.4.

4,4'-(((2,5-Dihexyl-1,4-phenylene)bis(ethyne-2,1-diyl))bis(2,5-dihexyl-4,1-phenylene))bis(2-methylbut-3-yn-2-ol) (3.5)

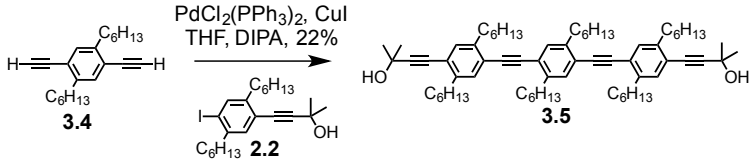

A 100 mL two neck round bottom flask was charged with **2.2** (486 mg, 1.07 mmol), CuI (4.85 mg, 25.5 µmol) and $PdCl_2(PPh_3)_2$ (17.9 mg, 25.5 µmol) and dried under vacuum. The mixture was dissolved in DIPA (15 mL) and bubble purged with argon. Finally **3.4** (150 mg, 509 µmol) was added by syringe from a solution of THF (30 mL) The reaction mixture was left stirring at RT overnight. When TLC (DCM) shows that sm had been consumed, water was added and extracted with TBME. The organic phase was washed with 2M HCl (aq), brine and dried over $MgSO_4$. The crude was passed through a column of SiO_2 (1:1 cyclohex:DCM ramping DCM), fractions combined to afford **3.5** as a yellow wax (104 mg, 22%). **^{1}H NMR** (400 MHz, $CDCl_3$): δ_H = 7.35 (s, 2H), 7.32 (s, 2H), 7.26 (s, 2H), 2.80 (dd, *J* = 15.8, 9.0 Hz, 8H), 2.75 – 2.66 (m, 4H), 2.06 (s, 2H), 1.75 – 1.58 (m, 24H), 1.45 – 1.27 (m, 36H), 0.96 – 0.81 (m, 18H). **^{13}C NMR** (101 MHz, $CDCl_3$): δ_C = 142.4, 142.0, 142.0, 132.6, 132.5, 132.5, 122.9, 122.9, 122.1, 98.4, 93.0, 93.0, 81.2, 65.9, 34.3, 34.3, 32.0, 31.9, 31.7, 30.8, 30.8, 30.8, 29.4, 29.4, 29.4, 22.8, 22.8, 22.8, 14.2, 0.1. **MS** (MALDI-TOF) *m*/*z*: $[M–H]^-$ calcd for $C_{68}H_{97}O_2$, 945.76; found 945.71.

5,5'-((2,5-Dihexyl-1,4-phenylene)bis(ethyne-2,1-diyl))bis(2-ethynyl-1,4-dihexylbenzene) (3.6)

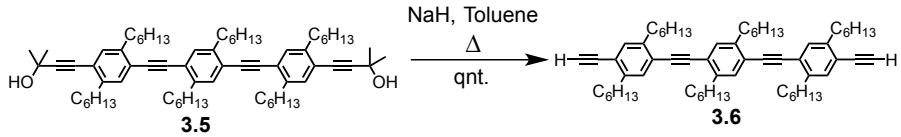

A 50 mL round bottom flask with reflux condenser attached was charged with **3.5** (0.331 g, 349 µmol) and dried under vacuum for 30 min. Then dry toluene (10 mL) was added and bubble purged with argon for 15 min. Finally NaH (60% w/w suspension in mineral oil) (30.7 mg, 767 µmol) was added and the resulting suspension heated to reflux for 1.5 hr, when

the reaction was deemed complete by TLC (cyclohexane). The reaction mixture was loaded directly onto a plug of silica in cylcohexane, UV active fraction collected and solvent removed to afford **3.6** as a yellow wax (0.29 g, 100%). **^{1}H NMR** (500 MHz, $CDCl_3$): δ_H = 7.36 (s, 2H), 7.33 (s, 4H), 3.30 (s, 2H), 2.81 (dd, *J* = 15.7, 8.1 Hz, 8H), 2.77 – 2.70 (m, 4H), 1.74 – 1.60 (m, 12H), 1.45 – 1.28 (m, 36H), 0.93 – 0.82 (m, 18H). **^{13}C NMR** (126 MHz, $CDCl_3$): δ_C = 143.0, 142.1, 142.0, 133.2, 132.6, 132.5, 123.5, 121.5, 107.9, 93.2, 92.9, 82.6, 81.6, 34.3, 34.2, 34.0, 32.0, 32.0, 31.8, 30.9, 30.8, 30.7, 29.4, 29.4, 29.3, 22.8, 22.8, 22.8, 14.3. **MS** (MALDI-TOF) *m*/*z*: $[M]^+$ calcd for $C_{62}H_{86}$, 830.67; found 830.39.

4,4'-(((((2,5-Dihexyl-1,4-phenylene)bis(ethyne-2,1-diyl))bis(2,5-dihexyl-4,1-phenylene))bis(ethyne-2,1-diyl))bis(2,5-dihexyl-4,1-phenylene))bis(2-methylbut-3-yn-2-ol) (3.7)

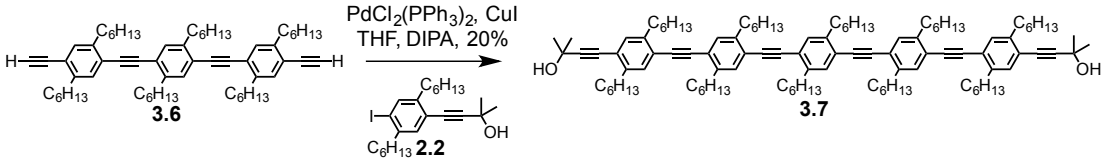

A 100 mL two neck round bottom flask was charged with **2.2** (325 mg, 700 µmol), CuI (3.3 mg, 174 µmol) and $PdCl_2(PPh_3)_2$ (12.3 mg, 174 µmol) and dried under vacuum. The mixture was dissolved in a mix of DIPA (10 mL), THF (5 mL) and bubble purged with argon. Finally **3.6** (290 mg, 349 µmol) was added by syringe from a solution of THF (30 mL) The reaction mixture was left stirring at RT overnight. When TLC (DCM) shows that sm had been consumed, water was added and extracted with TBME. The organic phase was washed with 2M HCl (aq), brine and dried over $MgSO_4$. The crude was passed through a column of SiO_2 (1:1 cyclohex:DCM ramping DCM), fractions combined to afford **3.7** as a yellow wax (101 mg, 20%). **^{1}H NMR** (500 MHz, $CDCl_3$): δ_H = 7.38 (s, 2H), 7.37 (s, 2H), 7.36 (s, 2H), 7.32 (s, 2H), 7.26 (s, 2H), 2.87 – 2.77 (m, 16H), 2.74 – 2.67 (m, 4H), 2.03 (s, 2H), 1.77 – 1.60 (m, 32H), 1.46 – 1.27 (m, 60H), 0.89 (dt, *J* = 6.8, 5.6 Hz, 30H). **^{13}C NMR** (126 MHz, $CDCl_3$): δ_C = 142.4, 142.1, 142.1, 142.0, 132.6, 132.6, 132.5, 132.5, 122.9, 122.9, 122.9, 122.1, 98.4, 93.2, 93.1, 93.0, 81.2, 78.4, 65.9, 34.4, 34.3, 34.3, 32.0, 32.0, 31.9, 31.7, 30.9, 30.8, 30.8, 29.5, 29.4, 29.4, 22.8, 22.8, 22.8, 14.3. **MS** (MALDI-TOF) *m*/*z*: $[M–H]^-$ calcd for $C_{108}H_{153}O_2$, 1482.19; found 1482.50.

1,3,5-tris((trimethylsilyl)ethynyl)benzene (3.17)

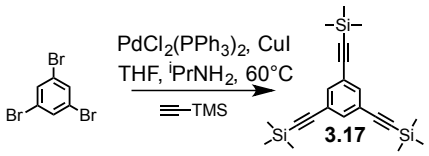

Tribromobenzene (500 mg, 1.56 mmol), $PdCl_2(PPh_3)_2$ (33.1 mg, 46.7 µmol), and CuI (14.8 mg, 77.8 µmol) were placed into an oven dried 25 mL schlenk tube and placed under vacuum for 20 min. Then THF (10 mL) and $^{i}Pr_2NH$ (2 mL) were added and the mixture was degassed with inert gas. Then Ethynyltrimethylsilane (0.89 mL, 6.23 mL) was added and the solution further degassed. The mixture was then heated to 60°C overnight. The reaction was quenched with water and extracted with DCM. The organic layer was washed with 1M HCl (aq), brine and dried over $MgSO_4$. The crude was columned on SiO_2 (cyclohexane) fractions evaporated to afford **3.17** as off white crystals (504 mg, 88%). **mp** 76–78 °C (lit.[271] mp 79–80 °C). $\mathbf{R}_f$ = 0.6 (SiO_2; cyclohexane). **^{1}H NMR** (500 MHz, $CDCl_3$): δ_H = 7.49 (s, 3H), 0.24 (s, 27H). **^{13}C NMR** (126 MHz, $CDCl_3$): δ_C = 135.1, 123.8, 103.3, 95.7, -0.0. **MS** (EI +, 70 eV) *m*/*z* = 366.2 [M^+], 351.2 [M–CH_3]$^{\bullet+}$. **MS** (MALDI-TOF) *m*/*z*: [M]$^+$ calcd for $C_{21}H_{30}Si_3$, 366.2; found 366.16. **Anal.** Calcd for $C_{21}H_{30}Si_3$: C, 68.78; H, 8.25. Found: C, 68.79; H, 8.23.

1,3,5-triethynylbenzene (3.18)

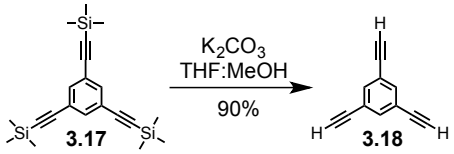

A round bottom flask was charged with **3.17** (500 mg, 1.36 mmol) dissolved in a 1:1 mixture of THF:MeOH to make up a 10 mL solution, this solution was bubble purged with argon for 20 min before K_2CO_3 (952 mg, 6.82 mmol) was added and the mixture stirred at RT for 3 hr, after which time it was passed through a short-plug of SiO_2 (DCM), solvent removed to afford **3.18** as a white, low vapor pressure solid (184 mg, 90%). **^{1}H NMR** (400 MHz, $CDCl_3$): δ_H = 7.57 (s, 3H), 3.10 (s, 3H).**^{13}C NMR** (101 MHz, $CDCl_3$): δ_C = 135.8, 123.1, 81.7, 78.8. **MS** (EI +, 70 eV) *m*/*z* (%) = 150.0 (100) [M^+].

2,2',2''-(((benzene-1,3,5-triyltris(ethyne-2,1-diyl))tris(2,5-dihexylbenzene-4,1-diyl))tris(ethyne-2,1-diyl))tris(propan-2-ol) (3.19)

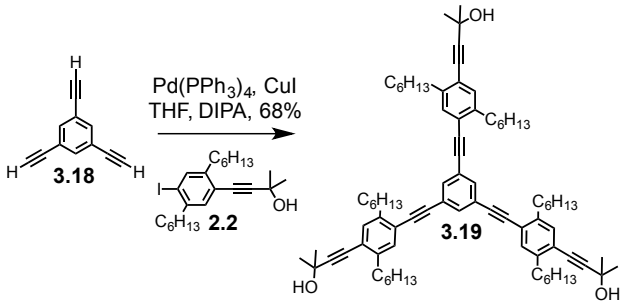

A two neck round bottom flask was charged with **2.2** (2.02 g, 4.45 mmol), CuI (12.8 mg, 67.4 µmol) and $Pd(PPh_3)_4$ (77.9 mg, 67.4 µmol) and placed under vacuum. The mixture was dissolved in a mix of DIPA (5 mL), THF (10 mL) and bubble purged with argon. Finally **3.18** (202 mg, 1.35 mmol) was added. The reaction mixture was left stirring at RT overnight. When TLC (DCM) shows that sm had been consumed, water was added and extracted with TBME. The organic phase was washed with 2M HCl (aq), brine and dried over $MgSO_4$. The crude was passed through a column of SiO_2 (10:1 DCM:EtOAc), fractions combined to afford **3.19** as a yellow wax (1.03 g, 68%). **^{1}H NMR** (400 MHz, $CDCl_3$): δ_H = 7.59 (s, 3H), 7.32 (s, 3H), 7.26 (s, 3H), 2.78 (t, *J* = 7.6 Hz, 6H), 2.70 (t, *J* = 7.7 Hz, 6H), 2.00 (s, 3H), 1.74 – 1.57 (m, 30H), 1.46 – 1.25 (m, 36H), 0.94 – 0.81 (m, 18H). **^{13}C NMR** (101 MHz, $CDCl_3$): δ_C = 1 42.5, 142.4, 133.8, 132.6, 132.5, 124.4, 122.5, 122.1, 98.6, 92.2, 89.7, 81.1, 65.9, 34.2, 34.2, 31.9, 31.9, 31.7, 30.8, 30.7, 29.4, 29.3, 22.8, 22.8, 14.3, 14.2. **MS** (MALDI-TOF) *m*/*z*: $[M–H]^-$ calcd for $C_{81}H_{107}O_3$1127.8; found 1127.05. **Anal.** Calcd for $C_{81}H_{108}O_3$: C, 86.12; H, 9.64. Found: C, 86.11; H, 9.86.

1,3,5-tris((4-ethynyl-2,5-dihexylphenyl)ethynyl)benzene (3.20)

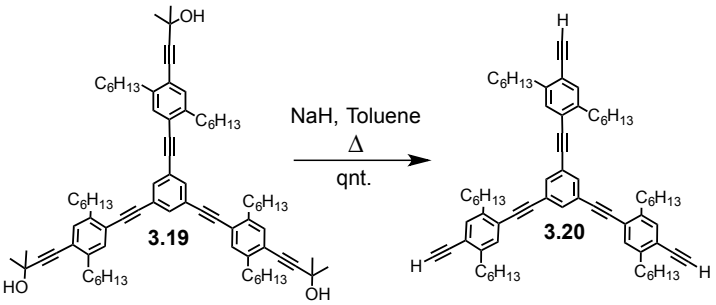

A round bottom flask with reflux condenser attached was charged with **3.19** (460 mg, 407 µmol) and dried under vacuum for 30 min. Then dry toluene (10 mL) was added and bubble purged with argon for 15 min. Finally NaH (60% w/w suspension in mineral oil) (53.7 mg, 1.34 mmol) was added and the resulting suspension heated to reflux for 1.5 hr, when the reaction was deemed complete by TLC (cyclohexane). The reaction mixture was loaded directly onto a plug of silica in cylcohexane, UV active fraction collected and solvent

removed to afford **3.20** as a yellow wax (390 mg, 100%). **^{1}H NMR** (500 MHz, $CDCl_3$): δ_H = 7.60 (s, 3H), 7.34 (s, 6H), 3.31 (s, 3H), 2.85 – 2.69 (m, 12H), 1.76 – 1.58 (m, 12H), 1.48 – 1.28 (m, 36H), 0.98 – 0.79 (m, 18H). **^{13}C NMR** (126 MHz, $CDCl_3$): δ_C = 143.0, 142.5, 133.9, 133.2, 132.5, 124.4, 122.6, 122.0, 92.4, 89.6, 82.5, 81.8, 34.2, 34.0, 31.9, 31.8, 30.7, 30.6, 29.3, 29.3, 22.8, 22.7, 14.3, 14.3. **MS** (MALDI-TOF) *m*/*z*: $[M]^+$ calcd for $C_{72}H_{90}$, 954.70; found 954.57.

4,4',4''-((((benzene-1,3,5-triyltris(ethyne-2,1-diyl))tris(2,5-dihexylbenzene-4,1-diyl))tris(ethyne-2,1-diyl))tris(2,5-dihexylbenzene-4,1-diyl))tris(2-methylbut-3-yn-2-ol) (3.21)

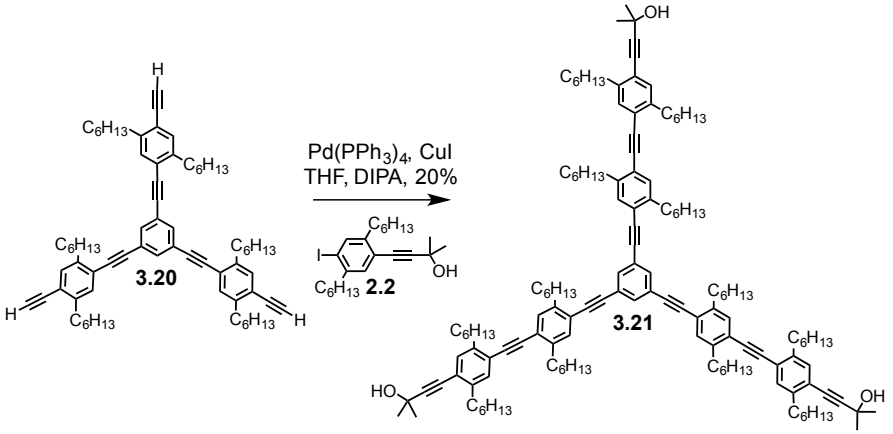

A two neck round bottom flask was charged with **2.2** (590 mg, 1.3 mmol), CuI (3.75 mg, 19.7 µmol) and $Pd(PPh_3)_4$ (22.7 mg, 19.7 µmol) and placed under vacuum. The mixture was dissolved in a mix of DIPA/THF and bubble purged with argon. Finally **3.20** (376 mg, 394 µmol) was added from a solution of degassed THF. The reaction mixture was left stirring at RT overnight. When TLC (DCM) shows that all the sm had been consumed, water was added and extracted with TBME. The organic phase was washed with 2M HCl (aq), brine and dried over $MgSO_4$. The crude was passed through a column of SiO_2 (DCM), fractions combined to afford **3.21** as a yellow wax (0.58 g, 76%). **^{1}H NMR** (500 MHz, $CDCl_3$): δ_H = 7.63 (s, 3H), 7.38 (s, 3H), 7.37 (s, 3H), 7.32 (s, 3H), 7.27 (s, 3H), 2.81 (dt, *J* = 15.3, 7.8 Hz, 18H), 2.74 – 2.61 (m, 6H), 2.02 (s, 3H), 1.79 – 1.58 (m, 42H), 1.48 – 1.24 (m, 72H), 0.89 (q, *J* = 6.8 Hz, 36H). **^{13}C NMR** (126 MHz, $CDCl_3$): δ_C = 142.6, 142.4, 142.1, 142.0, 133.8, 132.7, 132.6, 132.6, 132.5, 124.5, 123.4, 122.9, 122.1, 122.1, 120.4, 98.4, 93.3, 92.9, 89.9, 81.2, 65.9, 34.3, 32.0, 31.9, 31.7, 30.8, 30.8, 30.8, 29.4, 29.4, 29.4, 22.8, 22.8, 14.3, 14.3. **MS** (MALDI-TOF) *m*/*z*: $[M]^+$ calcd for $C_{141}H_{192}O_3$, 1934.5; found 1935.0.

1,3,5-tris((4-((4-ethynyl-2,5-dihexylphenyl)ethynyl)-2,5-dihexylphenyl)ethynyl)benzene (3.22)

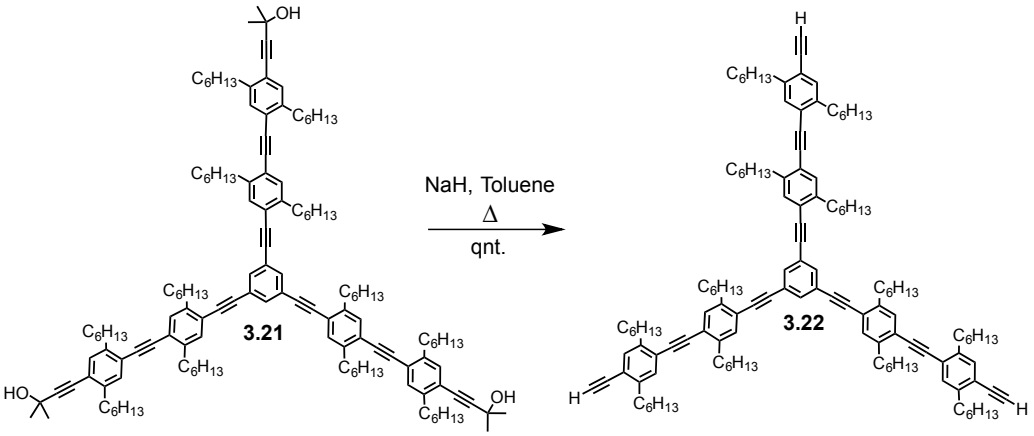

A round bottom flask with reflux condenser attached was charged with **3.21** (463 mg, 291 μmol) and dried under vacuum for 30 min. Then dry toluene (10 mL) was added and bubble purged with argon for 15 min. Finally NaH (60% w/w suspension in mineral oil) (38.4 mg, 960 μmol) was added and the resulting suspension heated to reflux for 1.5 hr, when the reaction was deemed complete by TLC (cyclohexane). The reaction mixture was loaded directly onto a plug of silica in cylcohexane, UV active fraction collected and solvent removed to afford **3.22** as a yellow wax (513 mg, 100%). **^{1}H NMR** (500 MHz, $CDCl_3$): δ_H = 7.63 (s, 3H), 7.38 (s, 3H), 7.37 (s, 3H), 7.34 (s, 6H), 3.31 (s, 3H), 2.86 – 2.78 (m, 18H), 2.77 – 2.72 (m, 6H), 1.77 – 1.60 (m, 24H), 1.48 – 1.28 (m, 72H), 0.89 (q, J = 6.9 Hz, 36H). **^{13}C NMR** (126 MHz, $CDCl_3$): δ_C = 143.0, 142.6, 142.1, 142.0, 133.9, 133.2, 132.7, 132.6, 132.5, 124.5, 123.4, 123.3, 122.2, 121.6, 93.1, 93.1, 92.4, 89.9, 82.6, 81.6, 34.3, 34.3, 34.3, 34.3, 34.2, 34.2, 34.0, 32.0, 32.0, 31.9, 31.8, 30.8, 30.8, 30.8, 30.7, 29.4, 29.4, 29.3, 22.8, 22.8, 22.8, 14.3, 14.3. **MS** (MALDI-TOF) *m*/*z*: $[M–H]^-$ calcd for $C_{132}H_{173}$, 1758.36; found 1758.41.

2,2',2''-(((((((benzene-1,3,5-triyltris(ethyne-2,1-diyl))tris(2,5-dihexylbenzene-4,1-diyl))tris(ethyne-2,1-diyl))tris(2,5-dihexylbenzene-4,1-diyl))tris(ethyne-2,1-diyl))tris(2,5-dihexylbenzene-4,1-diyl))tris(ethyne-2,1-diyl))tris(propan-2-ol) (3.23)

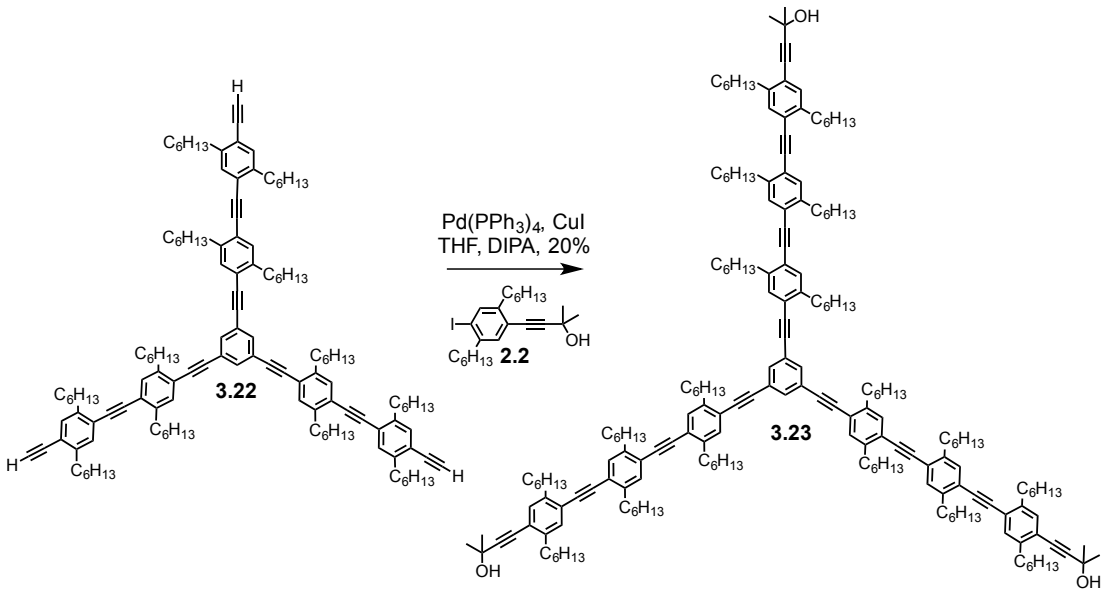

A 100 mL two-necked round bottom flask was charged with **2.2** (530 mg, 1.17 mmol), CuI (2.77 mg, 14.μ umol) and $Pd(PPh_3)_4$ (16.8 mg, 14.6 μmol) and dried under vacuum. Then DIPA (5 mL) and dry THF (5 mL) were added and the resulting solution bubble purged with argon for 20 min. Finally **3.22** (513 mg, 291 μmol) was dissolved in dry-predegassed THF (15 mL total in three washings) and added dropwise. The the reaction was left stirring at RT for 24 hr, as the reaction was not complete by TLC, it was heated to 60°C and left stirring for a further 24 hr. Then water was added and extracted with DCM. The organic phase was washed with 2M HCl (aq), brine and dried over $MgSO_4$. The crude was passed through a column of SiO_2 (8:1 cyclohexane:DCM), the main fraction had solvent removed and the 350 mg of crude was redissolved in $CHCl_3$ and passed through the recycling GPC, fractions combined to afford **3.23** as a yellow wax (159 mg, 20%). **^{1}H NMR** (400 MHz, $CDCl_3$): δ_H = 7.63 (d, J = 3.7 Hz, 3H), 7.39 (d, J = 3.1 Hz, 9H), 7.37 (d, J = 3.7 Hz, 6H), 7.32 (s, 3H), 2.88 – 2.67 (m, 36H), 1.77 – 1.61 (m, 54H), 1.47 – 1.27 (m, 111H), 0.96 – 0.81 (m, 54H). **MS** (MALDI-TOF) m/z: $[M]^+$ calcd for $C_{201}H_{276}O_3$, 2740.15; found 2739.99.

Tritel protected, Three arm molecular junction star, (3.27)

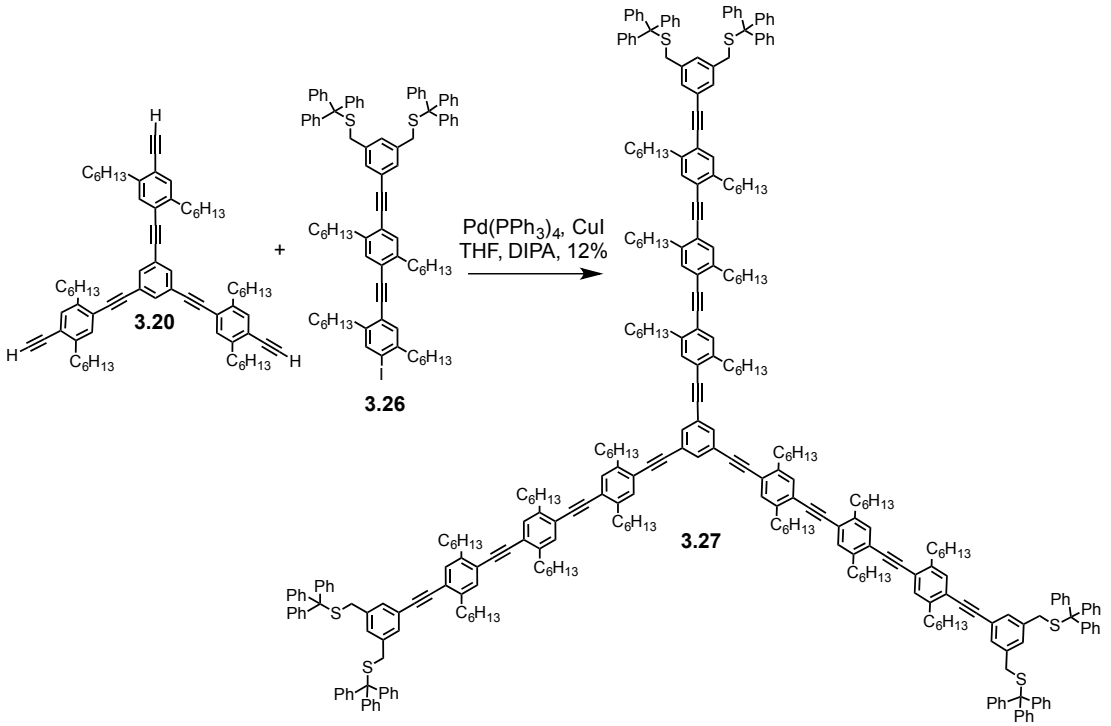

A 50 mL pear shaped flask containing **3.26** (313 mg, 238 µmol) was charged with CuI (1.37 mg, 7.2 µmol) and $Pd(PPh_3)_4$ (16.6 mg, 14.4 µmol). After drying under vacuum for 30 min, These was dissolved in dry THF (4mL) and DIPA (2 mL) and the solution degassed by bubble purging with argon. Finally **3.20** (69 mg, 72 µmol) dissolved in degassed THF (4 mL) was added dropwise. The Reaction was left stirring under argon for 24 hr. Then water was added and extracted with DCM. The organic layer was washed with 2M HCl (aq), brine and dried over $MgSO_4$. The crude was passed through a column of SiO_2 (4:1 cyclohexane:DCM) to remove unreacted sm. The fraction assumed to contain product gave 47 mg of a yellow wax. This was dissolved in $CHCl_3$ and passed twice through the recycling GPC, fractions combined and solvent removed to afford **3.27** as a yellow wax (64.8 mg, 20%).

See chapter 3 for further NMR details and discussion, together with full assignment.

Acetyl protected, Three arm molecular junction star (3.30)

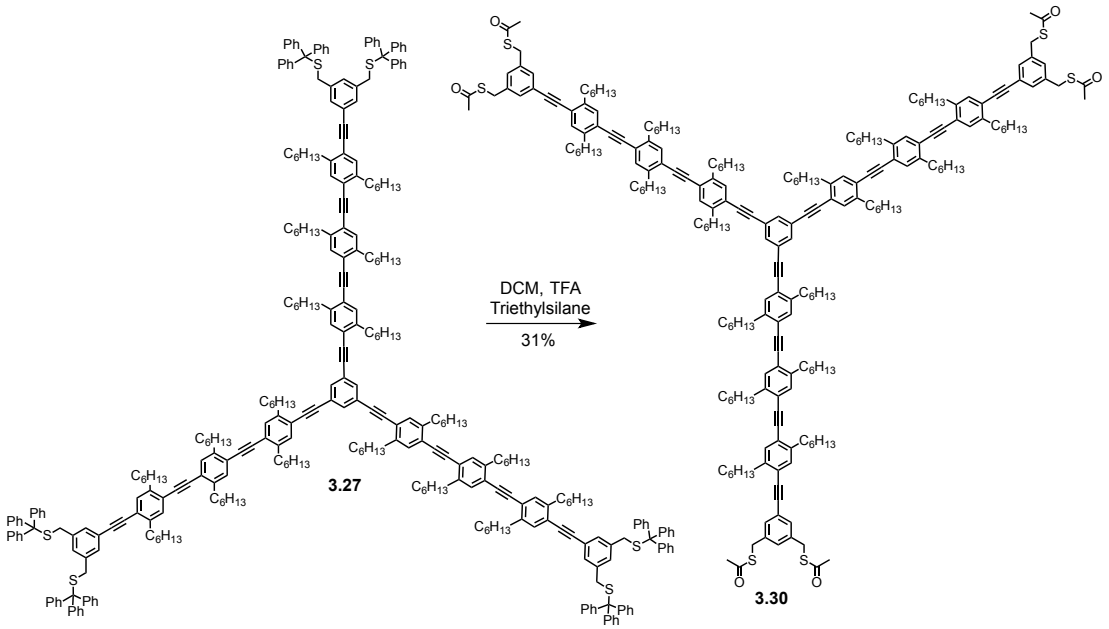

A 10 mL round bottom flask was charged with **3.27** (30 mg, 6.63 µmol) dissolved in 1mL of dry DCM. Then triethylsilyl (13 µL, 80 µmol) was added and 4% TFA was added dropwise. The crude was passed through a size exclusion column (Sx8 Bio Beads), fractions combined to give 21.5 mg of crude. The crude was passed twice through the recycling GPC, fractions combined to afford **3.30** as a yellow wax (6.8 mg, 31%). **^{1}H NMR** (500 MHz, $CDCl_3$): δ_H = 7.66 (s, 3H), 7.40 (td, *J* = 7.7, 6.9, 2.7 Hz, 18H), 7.35 (d, *J* = 1.6 Hz, 6H), 7.20 (s, 3H), 4.11 (s, 12H), 2.90 – 2.80 (m, 36H), 2.40 (s, 18H), 1.73 (dt, *J* = 14.5, 7.6 Hz, 36H), 1.49 – 1.25 (m, 108H), 0.91 (ddd, *J* = 8.5, 5.0, 1.8 Hz, 54H). **^{13}C NMR** (126 MHz, $CDCl_3$): δ_C = 195.0, 142.6, 142.5, 142.1, 142.1, 142.1, 138.6, 132.7, 132.6, 130.8, 34.4, 34.3, 34.3, 34.3, 33.1, 32.0, 31.9, 31.9, 30.9, 30.9, 30.8, 30.8, 30.8, 30.8, 30.5, 29.9, 29.9, 29.8, 29.5, 29.5, 29.5, 29.4, 29.4, 22.8, 22.8, 22.8, 14.3, 14.3, 14.3, 14.3.

7.3 Compounds from Chapter 4

12-(2,7-Bis((4-((7-((2,5-dihexyl-4-((triisopropylsilyl)ethynyl)phenyl)ethynyl)-9-(2-hexyldecyl)-9H-carbazol-2-yl)ethynyl)-2,5-dihexylphenyl)ethynyl)-9H-carbazol-9-yl)dodecan-1-ol (4.2)

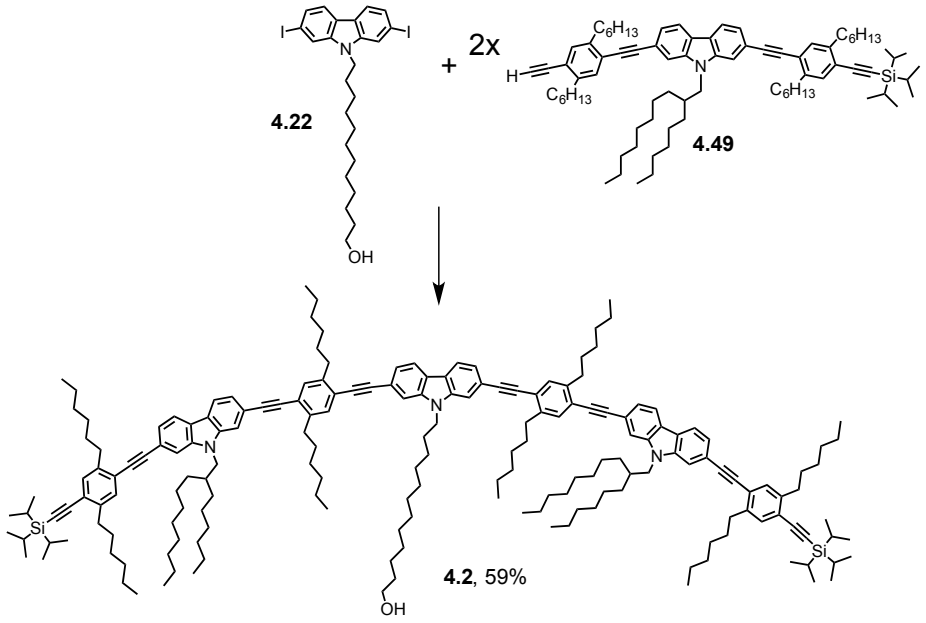

^{1}H NMR (500 MHz, $CDCl_3$): δ_H = 8.12 – 8.05 (m, 6H), 7.65 – 7.56 (m, 6H), 7.51 (d, *J* = 1.4 Hz, 4H), 7.50 – 7.41 (m, 8H), 7.37 (s, 2H), 4.38 – 4.31 (m, 2H), 4.20 (d, *J* = 7.7 Hz, 4H), 3.65 (t, *J* = 6.6 Hz, 2H), 3.00 – 2.80 (m, 16H), 2.23 (dt, *J* = 8.7, 5.4 Hz, 2H), 1.99 – 1.92 (m, 2H), 1.88 – 1.13 (m, 166H), 1.00 – 0.81 (m, 42H). **^{13}C NMR** (126 MHz, $CDCl_3$): δ_C = 142.8, 142.4, 142.4, 142.3, 141.4, 140.9, 133.1, 132.4, 132.4, 132.3, 123.0, 122.9, 122.8, 122.7, 122.7, 122.7, 120.8, 120.6, 120.6, 120.5, 112.3, 111.9, 95.6, 95.5, 95.5, 95.3, 88.7, 88.6, 88.6, 63.2, 38.0, 34.6, 34.5, 34.4, 33.0, 32.9, 32.0, 32.0, 32.0, 32.0, 32.0, 32.0, 32.0, 31.9, 31.1, 30.9, 30.9, 30.9, 30.1, 29.8, 29.8, 29.8, 29.7, 29.7, 29.7, 29.7, 29.7, 29.6, 29.6, 29.6, 29.5, 29.5, 29.4, 29.2, 27.5, 27.1, 27.1, 26.7, 26.7, 25.9, 22.8, 22.8, 22.8, 22.8, 22.8, 22.8, 18.9, 18.9, 18.9, 18.9, 18.8, 18.3, 14.3, 14.3, 14.3, 14.3, 14.3, 14.3, 14.3, 14.3, 14.3, 14.2, 11.6, 11.5, 11.3. **MS** (MALDI-TOF) *m/z*: $[M]^+$ calcd for $C_{186}H_{263}N_3OSi_2$, 2613.02; found 2613.47. See chapter 4 for further characterisation details.

2-[4-(Ethynyl-2,5-dihexylphenyl)-2-methylbut-3-yn-2-ol]-7-(4-{(2,5-dihexyl-4-((triisopropylsilyl)ethynyl)phenyl)ethynyl)}-9-(2-hexyldecyl)-carbazole (4.3)

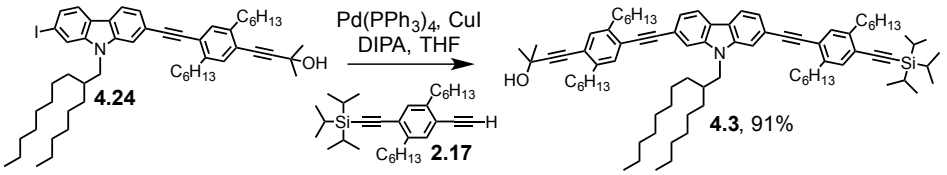

A round bottom flask was charged with **4.24** (357 mg, 0.411 mmol) dissolved in DIPA (7 mL) and THF (3 mL). Then the catalytic system of $Pd(PPh_3)_4$ (23.8 mg, 20.6 µmol) and

CuI (4.0 mg, 20.6 μmol) was added and the solution degassed with argon. Finally the acteylene **2.17** (371 mg, 0.823 mmol) dissolved in pre-degassed THF (20mL) was added slowly. After complete addition the reaction mixture was left stirring at RT overnight. When the reaction was deemed complete by TLC water was added and extracted with DCM. The organic fraction was washed with 2M HCl (aq), brine and dried over $MgSO_4$. The crude was passed through a column of SiO_2 (1:1 cyclohexane:DCM moving to DCM to remove the final spot), fractions combined and solvent evaporated to afford **4.3** as a yellow oil (447 mg, 91%). **^{1}H NMR** (500 MHz, $CDCl_3$): δ_H = 8.04 (d, J = 8.1 Hz, 2H), 7.53 (s, 2H), 7.43–7.36 (m, 4H), 7.30 (d, J = 17.5 Hz, 2H), 4.17 (d, J = 7.5 Hz, 2H), 2.89–2.80 (m, 4H), 2.82–2.73 (m, 2H), 2.77–2.68 (m, 2H), 2.21–2.15 (m, 1H), 1.99 (s, 1H), 1.77–1.61 (m, 14H), 1.49–1.11 (m, 65H), 0.94–0.79 (m, 20H). **^{13}C NMR** (126 MHz, $CDCl_3$): δ_C = 142.8, 142.4, 142.3, 142.3, 141.4, 141.4, 133.1, 132.5, 132.3, 132.3, 123.0, 123.0, 122.9, 122.9, 122.8, 122.7, 122.7, 122.0, 120.9, 120.8, 120.6, 112.3, 105.9, 98.3, 95.4, 95.3, 88.6, 88.4, 81.3, 65.9, 48.0, 38.0, 34.6, 34.4, 34.4, 34.3, 32.0, 31.9, 31.7, 31.1, 30.9, 30.8, 30.8, 30.1, 29.9, 29.8, 29.7, 29.5, 29.4, 29.4, 26.7, 26.6, 22.8, 22.8, 22.8, 22.8, 22.7, 18.9, 14.3, 14.3, 14.2, 14.2, 11.5. **MS** (MALDI-TOF) *m*/*z*: $[M–H]^-$ calcd for $C_{84}H_{122}NOSi$, 1188.94; found 1188.97.

1,4-Bis(2,5-dihexyl-4-((triisopropylsilyl)ethynyl)phenyl)buta-1,3-diyne

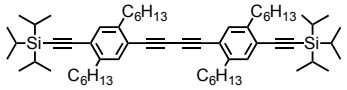

This compound was isolated from the above reaction mixture by column chromatography as a minor impurity. **^{1}H NMR** (500 MHz, $CDCl_3$): δ_H = 7.32 (s, 2H), 7.27 (s, 2H), 2.73 (t, J = 7.8 Hz, 4H), 1.68 – 1.57 (m, 8H), 1.45 – 1.21 (m, 34H), 1.17 – 1.09 (m, 36H), 0.93 – 0.81 (m, 12H). **^{13}C NMR** (126 MHz, $CDCl_3$): δ_C = 143.7, 142.8, 133.4, 133.1, 123.8, 121.3, 105.6, 96.3, 81.8, 78.3, 34.5, 34.1, 31.9, 31.8, 30.9, 30.8, 29.9, 29.4, 29.2, 27.1, 22.8, 18.9, 14.3, 14.2, 11.5. **MS** (MALDI-TOF) *m*/*z*: $[M]^+$ calcd for $C_{62}H_{98}Si_2$, 898.72; found 898.26.

[1,1':4',1''-Terphenyl]-3,3'',5,5''-tetraol (4.5)

Adapting a literature procedure from et al.[262] A 100 mL three neck flask was charged with **4.28** (605 mg, 1.73 mmol) and dried under vacuum for 30 min, then a series of three gas bottles were attached using a T-junction, the first empty, second containing sat. solution of

$Na_2S_2O_3$ and the third containing 1M NaOH (aq). Then dry DCM (20 mL) was added and the solution cooled to –78°C with an acetone/CO_2 bath. Under a positive pressure of Argon, Boron tribromide (1M BBr_3 in DCM, 8 mL) was added to the vigorously stirred solution. After 1 hr a further 5.8 mL of BBr_3 solution was added. The resulting solution was allowed to warm up overnight. The reaction was quenched with the slow addition of H_2O (20 mL) and diluted with DCM (40 mL). The emulsion was poured onto a glass frit under suction. The collected precipitate was dissolved in MeOH and adsorbed to silica, passed through a plug of SiO_2 (EtOAc), fractions combined to afford **4.5** as a white powder (510 mg, 100%). **^{1}H NMR** (400 MHz, CD_3OD): δ_H = 7.59 (d, *J* = 0.9 Hz, 4H), 6.59 (dd, *J* = 2.2, 0.9 Hz, 4H), 6.28 (dd, *J* = 2.6, 1.7 Hz, 2H). **^{1}H NMR** (500 MHz, DMSO-d_6): δ_H = 9.37 (s, 1H), 7.57 (s, 1H), 6.50 (d, *J* = 2.2 Hz, 1H), 6.23 (t, *J* = 2.2 Hz, 1H). **^{13}C NMR** (126 MHz, DMSO-d_6): δ_C = 158.8, 141.6, 139.5, 126.8, 104.7, 101.8, 48.6. **MS** (EI +, 70 eV) *m*/*z* (%) = 294.1 (100) [M^+].

2-(ethynyl-H)-7-(ethynyl-CPDIPS)-9-(2-hexyldecyl)-carbazole (4.6)

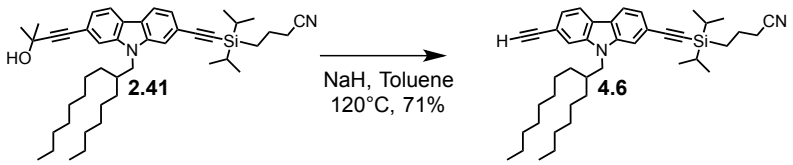

A round bottom flask was charged with **2.41** (212 mg, 0.312 mmol) dissolved in toluene (10 mL) and bubble purged with argon. Then NaH (dispersion of NaH 60% mineral oil, 37.5 mg, 0.937 mmol) and heated to 110°C for 1.5 hr until complete by TLC (DCM). Then the reaction mixture was passed through a plug of SiO_2 (DCM). collect the main fraction to afford **4.6** as a yellow oil (138 mg, 71%). **^{1}H NMR** (400 MHz, $CDCl_3$): δ_H = 7.99 (dd, *J* = 8.0, 5.3 Hz, 2H), 7.52 (s, 1H), 7.47 (s, 1H), 7.39–7.31 (m, 2H), 4.13 (d, *J* = 7.5 Hz, 2H), 3.15 (s, 1H), 2.46 (t, *J* = 7.0 Hz, 2H), 2.16–2.06 (m, 1H), 1.97–1.86 (m, 2H), 1.43–1.05 (m, 40H), 0.94–0.78 (m, 6H). **^{13}C NMR** (101 MHz, $CDCl_3$): δ_C = 141.2, 141.2, 123.5, 123.3, 123.0, 122.8, 120.6, 120.5, 120.4, 119.9, 119.4, 113.2, 112.9, 109.4, 89.2, 85.0, 47.9, 37.9, 32.0, 31.9, 31.9, 31.9, 30.0, 29.9, 29.7, 29.6, 29.4, 26.6, 26.6, 22.8, 22.7, 21.5, 21.0, 18.4, 18.2, 14.3, 14.2, 12.0, 9.9. **MS** (MALDI-TOF) *m*/*z*: $[M+H]^+$ calcd for $C_{42}H_{61}N_2Si$, 621.45; found 621.04.

2-[4-ethynyl-2,5-dihexylphenyl)-2-methylbut-3-yn-2-ol]-7-(ethynyl-CPDIPS)-9-(2-hexyldecyl)-carbazole (4.7)

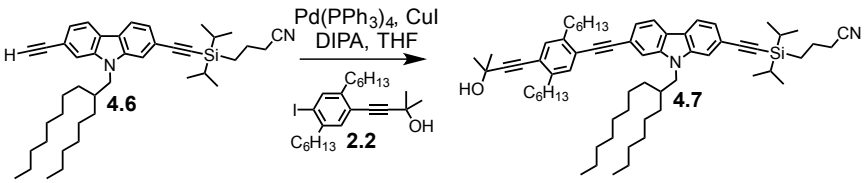

A two neck 50 mL round bottom flask was charged with **2.2** (100 mg, 0.222 mmol), CuI (2.12 mg, 11.1 μmol) and $Pd(PPh_3)_4$ (12.8 mg, 11.1 μmol) and dried under vacuum for 30 min. Then dry THF (5 mL) and DIPA (5 mL) were added and degassed with argon. Finally **4.6** (138 mg, 0.222 mmol) dissolved in degassed THF was added dropwise to the reaction mixture. After 16 hr the reaction was deemed complete by TLC and worked up with H2O, extracted with TBME. The organic layer was washed with 2M HCl (aq), brine and dried over $MgSO_4$. The crude was passed through a column of SiO_2 (3:1 DCM:cyclohexane), fractions combined and solvent removed to afford **4.7** as a yellow oil (99 mg, 47%). **^{1}H NMR** (400 MHz, $CDCl_3$): δ_H = 8.02 (d, *J* = 8.1 Hz, 1H), 7.99 (d, *J* = 8.0 Hz, 1H), 7.53 (s, 1H), 7.48 (s, 1H), 7.41–7.36 (m, 2H), 7.34 (dd, *J* = 8.0, 1.1 Hz, 1H), 7.27 (s, 1H), 4.15 (d, *J* = 7.5 Hz, 2H), 2.88–2.78 (m, 2H), 2.77–2.67 (m, 2H), 2.45 (t, *J* = 7.0 Hz, 2H), 2.20–2.09 (m, 1H), 2.05 (s, 1H), 1.97–1.86 (m, 2H), 1.78–1.59 (m, 10H), 1.41 (s, 12H), 1.38–1.06 (m, 40H), 0.95–0.78 (m, 12H). **^{13}C NMR** (101 MHz, $CDCl_3$): δ_C = 142.4, 142.3, 141.4, 141.2, 132.5, 132.3, 123.5, 123.0, 122.9, 122.9, 122.6, 122.0, 120.9, 120.6, 120.4, 120.2, 119.9, 112.9, 112.3, 109.5, 98.4, 95.3, 89.1, 88.4, 81.2, 65.9, 47.9, 38.0, 34.3, 34.3, 32.0, 31.9, 31.9, 31.9, 31.7, 30.8, 30.8, 30.1, 29.7, 29.6, 29.4, 29.4, 27.1, 26.7, 26.6, 22.8, 22.7, 21.5, 20.9, 18.4, 18.2, 14.3, 14.2, 14.2, 14.2, 12.0, 9.9. **MS** (MALDI-TOF) *m*/*z*: $[M]^+$ calcd for $C_{65}H_{94}N_2OSi$, 946.71; found 946.79.

Homo Dimer 2-(ethynyl-[2-(ethynyl)-7-(ethynyl-CPDIPS)-9-(2-hexyldecyl)-carbazole])-7-(ethynyl-CPDIPS)-9-(2-hexyldecyl)-carbazole (4.8)

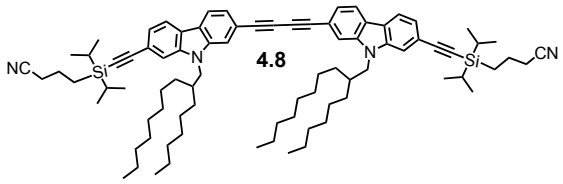

The diacetylene homocoupled product **4.8** was isolated by column chromatography from the reaction mixture from the above procedure as a yellow wax (40 mg, 15%). **^{1}H NMR** (400 MHz, $CDCl_3$): δ_H = 8.01 (d, *J* = 8.1 Hz, 2H), 7.98 (d, *J* = 8.1 Hz, 2H), 7.58 (s, 2H), 7.48 (s, 2H), 7.41 (dd, *J* = 8.1, 1.1 Hz, 2H), 7.35 (dd, *J* = 8.1, 1.1 Hz, 2H), 4.13 (d, *J* = 7.5 Hz, 4H), 2.46 (t, *J* = 7.0 Hz, 4H), 2.17–2.07 (m, 2H), 1.96–1.87 (m, 4H), 1.45–1.08 (m, 80H),

0.93–0.81 (m, 6H). **^{13}C NMR** (101 MHz, $CDCl_3$): δ_C = 141.3, 141.2, 123.7, 123.6, 123.3, 122.8, 120.7, 120.6, 120.6, 119.9, 119.1, 113.6, 112.9, 109.3, 89.4, 83.4, 74.2, 48.0, 38.0, 32.0, 31.9, 30.1, 29.7, 29.6, 29.4, 27.1, 26.6, 26.6, 22.8, 22.8, 21.5, 20.9, 18.4, 18.2, 14.3, 14.2, 12.0, 9.9. **MS** (MALDI-TOF) *m*/*z*: $[M+H]^+$ calcd for $C_{84}H_{119}N_4Si_2$, 1240.89; found 1240.19.

2-(ethynyl-H)-7-[(4-ethynyl-2,5-dihexylphenyl)-2-methylbut-3-yn-2-ol]-9-(2-hexyldecyl)-carbazole (4.9)

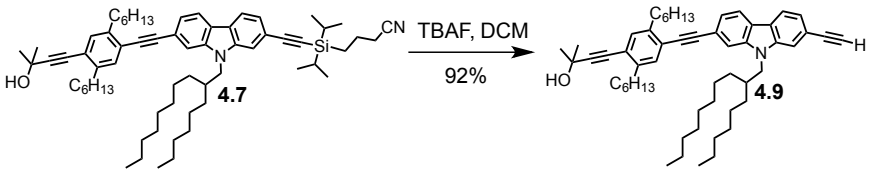

A round bottom flask was charged with **4.7** (99mg, 104 µmol) dissolved in DCM (2 mL) and bubble purged with argon. Then TBAF (1M in THF, 5% H_2O, 160 µL, 160 µmol). After 15 min reaction was complete by TLC (DCM). Then the reaction mixture was passed through a plug of SiO_2 (DCM), the main fraction collected to afford **4.9** as a yellow oil (74 mg, 92%). **^{1}H NMR** (400 MHz, $CDCl_3$): δ_H = 8.00 (t, *J* = 8.4 Hz, 2H), 7.52 (s, 2H), 7.41–7.34 (m, 3H), 7.27 (s, 1H), 4.12 (d, *J* = 7.5 Hz, 2H), 3.16 (s, 1H), 2.87–2.78 (m, 2H), 2.76–2.66 (m, 2H), 2.19–2.06 (m, 1H), 2.03 (s, 1H), 1.77–1.59 (m, 10H), 1.47–1.12 (m, 36H), 0.95–0.78 (m, 12H). **^{13}C NMR** (101 MHz, $CDCl_3$): δ_C = 142.4, 142.3, 141.4, 141.1, 132.5, 132.3, 123.4, 123.1, 123.0, 122.9, 122.5, 122.0, 121.0, 120.6, 120.5, 119.3, 113.2, 112.3, 98.4, 95.3, 88.4, 85.1, 81.3, 77.0, 65.9, 48.0, 37.9, 34.3, 34.3, 32.0, 31.9, 31.9, 31.7, 30.8, 30.8, 30.1, 29.8, 29.6, 29.4, 29.4, 26.6, 26.6, 22.8, 22.8, 22.7, 14.3, 14.3, 14.2, 14.2. **MS** (MALDI-TOF) *m*/*z*: $[M]^+$ calcd for $C_{55}H_{75}NO$, 765.58; found 765.87.

2-[4-ethynyl-2,5-dihexylphenyl)-2-methylbut-3-yn-2-ol]-7-(4-{2,5-dihexyl-4-[(3-Cyanopropyl)dimethylsilyl]ethynyl}-phenyl)-9-(2-hexyldecyl)-carbazole (4.10)

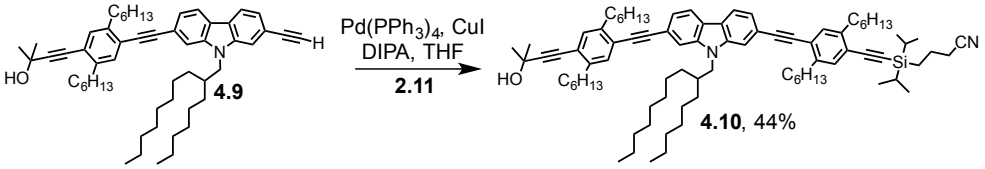

A two-neck 500 mL round bottom flask was charged with **2.11** (55.7 mg, 96.4 µmol) and CuI (0.92 mg, 4.82 µmol) and $Pd_2(dba)_2$ (4.42 mg, 2.82 µmol) and PPh_3 (5.06 mg, 19.3 µmol) dissolved in THF and DIPA. The solution was degassed by bubbling through with argon. Finally acetylene **4.9** (73.9 mg, 96.4 µmol) was added dropwise by syringe from degassed

solution of THF. When the reaction was deemed complete by TLC it was worked up with H_2O, extracted with TBME. The organic layer was washed with 2M HCl (aq), brine and dried over $MgSO_4$. The crude was passed though a coloumn of SiO_2 (DCM), fractions combined and solvent removed to afford **4.10** as a yellow oil (50.1 mg, 45%). **^{1}H NMR** (500 MHz, $CDCl_3$): δ_H = 8.04 (s, 1H), 8.03 (s, 1H), 7.53 (s, 2H), 7.41 (t, *J* = 1.2 Hz, 1H), 7.40–7.37 (m, 3H), 7.32 (s, 1H), 7.28 (s, 1H), 4.16 (d, *J* = 7.6 Hz, 2H), 2.88–2.81 (m, 4H), 2.79–2.69 (m, 4H), 2.44 (t, *J* = 6.9 Hz, 2H), 2.21–2.13 (m, 1H), 2.07 (s, 1H), 1.93–1.85 (m, 2H), 1.78–1.69 (m, 4H), 1.69–1.62 (m, 10H), 1.50–1.06 (m, 60H), 0.95–0.80 (m, 22H). **^{13}C NMR** (126 MHz, $CDCl_3$): δ_C = 142.8, 142.4, 142.3, 141.4, 133.1, 132.5, 132.3, 132.3, 123.3, 123.0, 122.9, 122.7, 122.6, 122.2, 122.0, 120.8, 120.7, 120.6, 119.8, 112.3, 106.8, 98.4, 95.7, 95.4, 94.0, 88.4, 88.4, 81.2, 65.9, 48.0, 37.9, 34.5, 34.4, 34.3, 34.3, 32.0, 31.9, 31.9, 31.9, 31.7, 31.0, 30.9, 30.8, 30.8, 30.1, 29.8, 29.6, 29.5, 29.5, 29.4, 29.4, 26.7, 26.6, 22.8, 22.8, 22.8, 22.8, 22.7, 21.5, 21.0, 18.4, 18.2, 14.3, 14.3, 14.2, 14.2, 11.9, 9.9. **MS** (MALDI-TOF) *m*/*z*: $[M+H]^+$ calcd for $C_{85}H_{123}N_2OSi$, 1216.94; found 1216.95. **Anal.** Calcd for $C_{85}H_{122}N_2OSi$: C, 83.96; H, 10.11; N, 2.30. Found: C, 83.70; H, 10.03; N, 2.43.

Homo Dimer 2-{ethynyl[2-(ethynyl)-7-[(4-ethynyl-2,5-dihexylphenyl)-2-methylbut-3-yn-2-ol]-9-(2-hexyldecyl)-carbazole]}-7-[(4-ethynyl-2,5-dihexylphenyl)-2-methylbut-3-yn-2-ol]-9-(2-hexyldecyl)-carbazole (4.11)

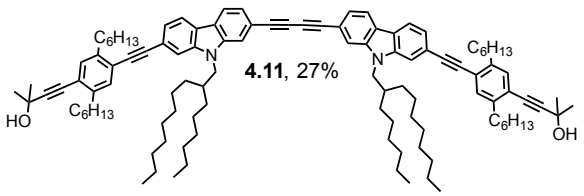

The diacetylene homocoupled product **4.11** was isolated by column chromatography from the reaction mixture from the above procedure as a yellow oil (39.4 mg, 27%). **^{1}H NMR** (400 MHz, $CDCl_3$): δ_H = 8.02 (dd, *J* = 8.1, 4.1 Hz, 3H), 7.74 (d, *J* = 16.0 Hz, 1H), 7.65–7.58 (m, 2H), 7.58 (d, *J* = 1.3 Hz, 1H), 7.53 (s, 1H), 7.46–7.35 (m, 6H), 7.28 (s, 1H), 7.08 (d, *J* = 15.9 Hz, 1H), 4.14 (d, *J* = 7.5 Hz, 4H), 2.83 (dd, *J* = 9.1, 6.5 Hz, 4H), 2.71 (dd, *J* = 9.1, 6.5 Hz, 4H), 2.20–2.10 (m, 2H), 2.07 (s, 2H), 1.78–1.56 (m, 20H), 1.50–1.15 (m, 72H), 0.95–0.78 (m, 24H). **^{13}C NMR** (101 MHz, $CDCl_3$): δ_C = 189.1, 143.5, 142.4, 142.3, 141.6, 141.1, 134.9, 132.5, 132.3, 130.6, 129.1, 128.5, 125.6, 123.7, 123.4, 123.1, 122.8, 122.5, 122.0, 121.2, 120.7, 120.6, 119.0, 113.5, 112.3, 98.4, 95.3, 88.6, 83.5, 81.2, 77.4, 74.2, 65.9, 48.1, 37.9, 34.3, 34.3, 32.0, 31.9, 31.7, 30.8, 30.8, 30.1, 29.8, 29.8, 29.6, 29.6, 29.4, 29.4, 26.6,

26.6, 22.8, 14.3, 14.3, 14.2. **MS** (MALDI-TOF) *m/z*: $[M–H]^-$ calcd for $C_{110}H_{148}N_2O_2$, 1529.16; found 1529.27.

2-Bromo-7-(ethynyl-H)-9-(2-hexyldecyl)-carbazole (4.12)

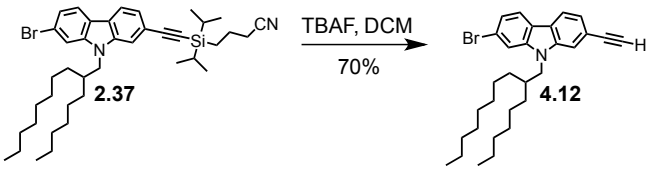

To a stirred solution of **2.37** (20 mg, 29.6 μmol) in DCM (1 mL) was added dropwise TBAF (1M in THF, 26 μL, 88.8 μmol) and the reaction monitored by TLC and after 10 min the crude reaction mixture was loaded onto a small column of SiO_2 (1:1 hexane:dcm) fractions evaporated to afford **4.12** as a yellow wax. (10.3 mg, 70%). $\mathbf{R_f}$ = 0.69 (SiO_2; hexane/DCM 1:1). **^{1}H NMR** (400 MHz, $CDCl_3$): δ_H = 7.93 (dd, *J* = 29.5, 8.1 Hz, 2H), 7.51 (s, 2H), 7.35 (dd, *J* = 13.7, 8.1 Hz, 2H), 4.08 (d, *J* = 7.5 Hz, 2H), 3.15 (s, 1H), 2.09 (s, 1H), 1.46–1.13 (m, 24H), 0.97–0.79 (m, 6H). **^{13}C NMR** (101 MHz, $CDCl_3$): δ_C = 123.5, 122.5, 121.8, 120.3, 119.3, 113.2, 112.4, 48.0, 37.8, 32.0, 31.9, 31.8, 30.0, 29.7, 29.6, 29.4, 26.6, 22.8, 22.8, 14.3, 14.2. **MS** (ESI, *m/z*): 492.4 $[M–H]^-$ 100%, requires 492.2. **MS** (MALDI-TOF) *m/z*: $[M+H]^+$ calcd for $C_{30}H_{40}BrN$, 495.23; found 495.17.

2-Bromo-7-[(4-ethynyl-2,5-dihexylphenyl)-2-methylbut-3-yn-2-ol]-9-(2-hexyldecyl)-carbazole (4.13)

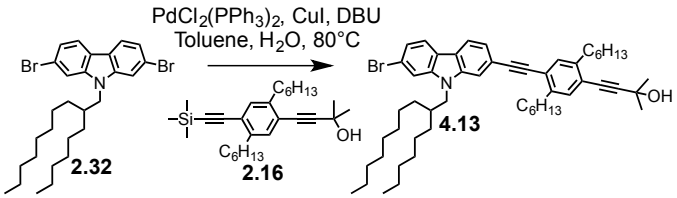

A solution of **2.16** (153 mg, 360 μmol) dissolved in toluene (5 mL) was transferred to a two neck flask. Then the catalytic system was added; $PdCl_2(PPh_3)_2$ (21.9 mg, 30.9 μmol), CuI (9.8 mg, 51.5 μmol) and then DBU (480 mg, 471 μL, 3.09 mmol) was added and dissolved in toluene (5 mL) with water (0.37 mL) was added. Finally the **2.32** (283 mg, 515 μmol) was added and the solution degassed by bubbling through with argon and the reaction mixture heated to 80°C overnight. When the reaction was deemed complete by TLC, Et_2O and H_2O were added. Brown sludge in the organic phase was washed 2M HCl (aq), H_2O, brine and dried over Na_2SO_4. The crude was passed through a column on SiO_2 (2:1 cyclohexane:DCM) fractions combined to afford **4.13** as a yellow oil (78 mg, 26%). **^{1}H NMR** (400 MHz,

$CDCl_3$): δ_H = 8.00 (d, *J* = 8.0 Hz, 1H), 7.91 (d, *J* = 8.3 Hz, 1H), 7.52 (s, 2H), 7.41–7.32 (m, 3H), 7.26 (d, *J* = 4.4 Hz, 1H), 4.11 (d, *J* = 7.1 Hz, 2H), 2.83 (t, *J* = 7.6 Hz, 2H), 2.71 (t, *J* = 7.7 Hz, 2H), 2.12 (s, 1H), 2.00 (s, 1H), 1.75–1.53 (m, 10H), 1.47–1.15 (m, 36H), 0.96–0.80 (m, 12H). **^{13}C NMR** (101 MHz, $CDCl_3$): δ_C = 142.5, 142.4, 142.3, 140.8, 132.5, 132.3, 123.1, 122.9, 122.5, 122.5, 122.0, 121.7, 121.6, 120.8, 120.3, 119.9, 112.4, 112.3, 98.4, 95.3, 88.3, 81.2, 65.9, 48.0, 37.8, 34.3, 34.3, 32.0, 31.9, 31.9, 31.9, 31.7, 30.8, 30.8, 30.1, 29.7, 29.6, 29.4, 29.4, 26.6, 26.6, 22.8, 22.8, 14.3, 14.3, 14.2, 14.2. **MS** (MALDI-TOF) *m*/*z*: $[M+H]^+$ calcd for $C_{53}H_{74}BrNO$, 819.50; found 819.83.

2,7-Dibromo-9-(12-bromododecyl)-carbazole (4.15)

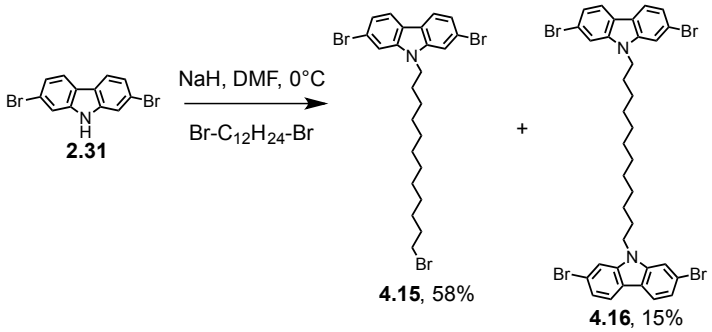

A two-neck 50mL round bottom flask with reflux condensor attached was charged with 2,7-dibromo-carbazole **2.31** (306 mg, 0.942 mmol) and dried in vaccuo for 30 min. Then dry DMF (5 mL) was added and the solution cooled with an ice bath. Then NaH (60% w/w dispersion in mineral oil, 57 mg, 1.41 mmol) was added and the solution stirred for 30 min. Then 1,12 dibromoalkane (1.545 g, 4.71 mmol) was added and the reaction stirred for 12 hr, two spots are observed by TLC. The mixture was quenched with water and extracted with DCM. The organic layer was washed with 2M HCl (aq), brine and dried over $MgSO_4$. The crude was passed through a column of SiO2 (5:1 cyclohexane:DCM) fractions combined and solvent removed to afford **4.15** as a low melting point white powder (313 mg, 58%). **^{1}H NMR** (400 MHz, $CDCl_3$): δ_H = 7.84 (d, *J* = 8.3 Hz, 2H), 7.50 (d, *J* = 1.6 Hz, 2H), 7.32 (dd, *J* = 8.3, 1.6 Hz, 2H), 4.13 (t, *J* = 7.3 Hz, 2H), 3.41 (t, *J* = 6.9 Hz, 2H), 1.91–1.74 (m, 4H), 1.47–1.19 (m, 16H). **^{13}C NMR** (101 MHz, $CDCl_3$): δ_C = 141.4, 122.6, 121.5, 121.3, 119.8, 112.0, 43.4, 34.2, 32.9, 29.6, 29.6, 29.5, 29.5, 29.4, 28.8, 28.3, 27.2. **MS** (EI +, 70 eV) *m*/*z* (%) = 571.0 (100%), 573.0 (98%) [M^+]. **MS** (MALDI-TOF) *m*/*z*: $[M+H]^+$ calcd for $C_{24}H_{30}Br_3N$, 572.0; found 572.01. **Anal.** Calcd for $C_{24}H_{30}Br_3N$: C, 50.38; H, 5.28; N, 2.45. Found: C, 50.41; H, 5.15; N, 2.50.

1,12-Bis(2,7-dibromo-9H-carbazol-9-yl)dodecane (4.16)

The disubstituted dodecal chain **4.16** was isolated by column chromatography from the reaction mixture from the procedure describe above as a white, poorly soluble solid (59 mg, 15%). **^{1}H NMR** (500 MHz, $CDCl_3$): δ_H = 7.88 (d, *J* = 8.3 Hz, 4H), 7.52 (d, *J* = 1.6 Hz, 4H), 7.33 (dd, *J* = 8.3, 1.7 Hz, 4H), 4.18 (t, *J* = 7.3 Hz, 4H), 3.40 (dt, *J* = 9.4, 6.9 Hz, 2H), 1.89–1.78 (m, 4H), 1.40–1.19 (m, 14H). **^{13}C NMR** (126 MHz, $CDCl_3$): δ_C = 141.5, 122.7, 121.6, 121.4, 119.8, 112.2, 43.5, 29.5, 29.5, 29.4, 28.9, 27.3. **MS** (MALDI-TOF) *m*/*z*: $[M–Br]^+$ calcd for $C_{36}H_{37}Br_3N_2$, 735.04; found 735.42. $[M–2Br]^+$ calcd for $C_{36}H_{37}Br_2N_2$, 658.14; found 658.52. $[M–3Br]^+$ calcd for $C_{36}H_{37}BrN_2$, 578.23; found 578.59.

2,7-Bis(4,4,5,5-tetramethyl-1,3,2-dioxaborolan-2-yl)-9-(12-bromododecyl)-carbazole (4.18)

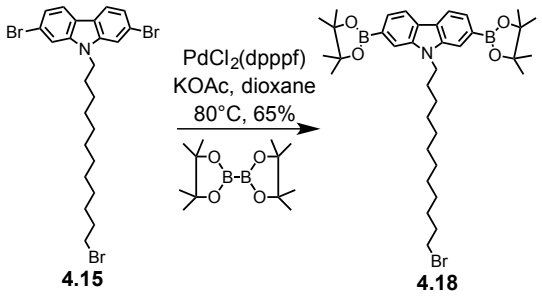

Adapting a literature procedure,[261] a 25 mL round bottom flask equipped with reflux condenser was charged with **4.15** (445 mg, 0.778 mmol), Bis(pinacolato)diboron (408 mg, 1.61 mmol) and KOAc (412 mg, 4.19 mmol) and dried under vacuum. then dry dioxane (8 mL) was added and the solution bubble purged with argon for 15 min. Then $PdCl_2$(dppf) (114 mg, 0.14 mmol) was added and the reaction stirred at 80°C overnight. The reaction was quenched with water, and extracted with DCM. The organic layer was washed with brine and dried over $MgSO_4$. The crude was passed through a column of SiO_2 (1:1 cyclohexane:DCM), fractions combined and solvent removed to afford **4.18** as a dark oil (337 mg, 65%). **^{1}H NMR** (500 MHz, $CDCl_3$): δ_H = 8.12 (dd, *J* = 7.8, 0.5 Hz, 2H), 7.88 (s, 2H), 7.68 (dd, *J* = 7.8, 0.7 Hz, 2H), 4.38 (t, *J* = 7.4 Hz, 2H), 3.39 (t, *J* = 6.9 Hz, 2H), 1.93–1.79 (m, 4H), 1.46–1.20 (m, 40H). **^{13}C NMR** (126 MHz, $CDCl_3$): δ_C = 140.5, 125.2, 125.0, 120.1, 115.4, 83.9, 43.0, 34.2, 33.0, 29.7, 29.6, 29.6, 29.5, 29.3, 28.9, 28.3, 27.3, 25.1. **MS** (EI +, 70 eV) *m*/*z* (%) = 665.3 (100%) $[M^+]$. **MS** (MALDI-TOF) *m*/*z*: $[M+H]^+$ calcd for $C_{36}H_{54}B_2BrNO_4$, 666.34; found 666.26. **Anal.** Calcd for $C_{36}H_{54}B_2BrNO_4$; C, 64.89; H, 8.17; N, 2.10. Found: C, 64.57; H, 7.95; N, 2.33.

12-(2,7-Diiodo-9H-carbazol-9-yl)dodecyl formate (4.21)

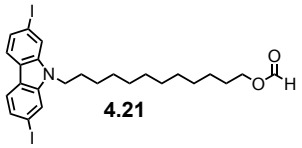

4.21

This compound was formed by decomposition. See Scheme 4.5 for details. **^{1}H NMR** (400 MHz, $CDCl_3$): δ_H = 8.05 (s, 1H), 7.75 (d, *J* = 8.2 Hz, 2H), 7.71 (d, *J* = 1.2 Hz, 2H), 7.50 (dd, *J* = 8.2, 1.4 Hz, 2H), 4.18 – 4.08 (m, 4H), 1.86 – 1.73 (m, 2H), 1.71 – 1.59 (m, 2H), 1.39 – 1.17 (m, 16H). **^{13}C NMR** (101 MHz, $CDCl_3$): δ_C = 161.3, 141.3, 128.3, 121.9, 118.1, 90.9, 64.3, 43.3, 29.6, 29.6, 29.6, 29.6, 29.4, 29.3, 28.9, 28.6, 27.2, 27.0, 25.9. **MS** (EI +, 70 eV) *m*/*z* (%) = 631.0 (100%) [M^+]. **MS** (MALDI-TOF) *m*/*z*: [M]$^+$ calcd for $C_{25}H_{31}I_2NO_2$, 631.04; found 630.17. **Anal.** Calcd for $C_{25}H_{31}I_2NO_2$: C, 47.56; H, 4.95; N, 2.22. Found: C, 47.14; H, 4.75; N, 2.08.

12-(2,7-Diiodo-9*H*-carbazol-9-yl)dodecan-1-ol (4.22)

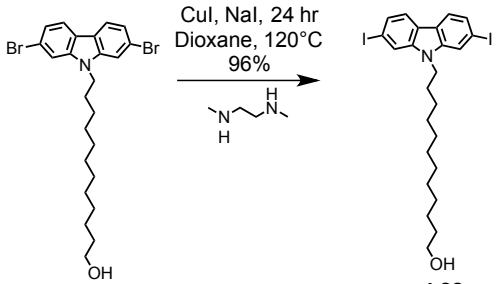

4.23 **4.22**

Adapting a literature procedure,[209] **4.23** (417 mg, 0.819 mmol) was placed in a 5 mL microwave vial that can be pressure sealed. Then CuI (15.5 mg, 0.082 mmol) and NaI (491 mg, 3.27 mmol) were added and the vial sealed and placed under vaccum for 30 min. Then dry Dioxane (1.5 mL) was added under N_2 followed by N,N'-dimethylethylendiamine (20.7 µL, 0.164 mmol) the vial sealed and heated to 120°C, left stirring for 24 hr. The resulting sludge was diluted with 30% Ammonia (aq) and water, extracted with DCM. The organic layer was washed with brine and dried over $MgSO_4$, solvent removed to afford **4.22** as a colourless oil (0.476 mg, 96%). **mp** 123.4–124.2 °C. **^{1}H NMR** (400 MHz, $CDCl_3$): δ_H = 7.77 (d, *J* = 8.2 Hz, 2H), 7.72 (d, *J* = 1.3 Hz, 2H), 7.52 (dd, *J* = 8.2, 1.4 Hz, 2H), 4.16 (t, *J* = 7.3 Hz, 2H), 3.64 (t, *J* = 6.6 Hz, 2H), 1.87–1.75 (m, 2H), 1.56 (dt, *J* = 13.9, 6.7 Hz, 2H), 1.43 (s, 1H), 1.39–1.22 (m, 16H). **^{13}C NMR** (101 MHz, $CDCl_3$): δ_C = 141.4, 128.3, 121.9, 121.9, 118.1, 90.9, 63.2, 43.4, 33.0, 29.7, 29.7, 29.7, 29.6, 29.5, 29.4, 28.9, 27.3, 25.9. **MS** (EI +, 70 eV) *m*/*z* (%) = [M^+] 603.0 (100%).

12-(2,7-Dibromo-9*H*-carbazol-9-yl)dodecan-1-ol (4.23)

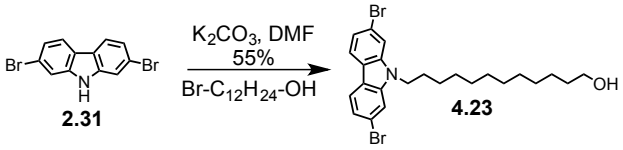

A round bottom flask cooled with ice was charged with **2.31** (1.00 g, 3.08 mmol), 12-Bromo-1-dodecanol (0.833 mg, 3.08 mmol) and K_2CO_3 (0.515 mg, 3.69 mmol) dissolved in DMF (20 mL). The reaction mixture was stirred for 12 hr at RT. Then water was added and the reaction mixture extracted with DCM. The organic layer was washed with 2M HCl (aq), brine and dried over $MgSO_4$. The crude was passed through a column of SiO_2 (DCM), fractions combined and solvent removed to afford **4.23** as a colourless oil (0.86 g, 55%). **^{1}H NMR** (400 MHz, $CDCl_3$): δ_H = 7.85 (dd, *J* = 8.3, 2.4 Hz, 2H), 7.51 (s, 2H), 7.32 (d, *J* = 8.3 Hz, 2H), 4.14 (t, *J* = 7.3 Hz, 2H), 3.63 (t, *J* = 6.6 Hz, 2H), 1.80 (q, *J* = 7.0 Hz, 2H), 1.56 (p, *J* = 6.7 Hz, 2H), 1.42 (s, 1H), 1.29 (d, *J* = 31.6 Hz, 16H). **^{13}C NMR** (101 MHz, $CDCl_3$): δ_C = 141.4, 122.6, 121.6, 121.3, 119.8, 112.1, 63.2, 43.4, 32.9, 29.7, 29.6, 29.6, 29.6, 29.5, 29.4, 28.9, 27.3, 25.8.

2-Iodo-7-[(4-ethynyl-2,5-dihexylphenyl)-2-methylbut-3-yn-2-ol]-9-(2-hexyldecyl)-carbazole (4.24)

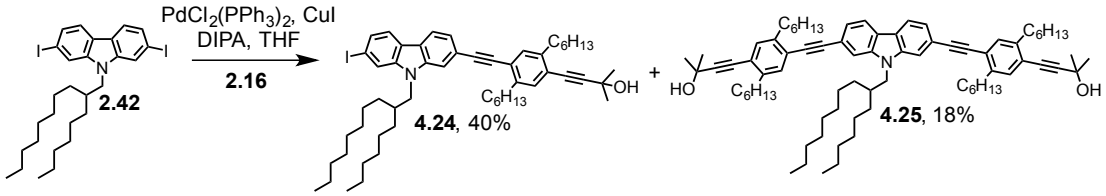

A round bottom flask was charged with **2.42** (579 mg, 0.90 mmol) dissolved in DIPA (7 mL) and THF (3 mL). Then the catalytic system of $PdCl_2(PPh_3)_2$ (31.9 mg, 45 μmol) and CuI (8.74 mg, 45 μmol) was added and the solution degassed with argon. Finally the acteylene **2.16** (317 mg, 0.9 mmol) dissolved in pre-degassed THF (20mL) was added slowly. After complete addition the reaction mixture was left stirring at RT overnight. When the reaction was deemed complete by TLC water was added and extracted with DCM. The organic fraction was washed with 2M HCl (aq), brine and dried over $MgSO_4$. The crude was passed through a column of SiO_2 (1:1 cyclohexane:DCM moving to DCM to remove the final spot), fractions combined and solvent evaporated to afford **4.25** as a yellow oil (314 mg, 40%). **^{1}H NMR** (400 MHz, $CDCl_3$): δ_H = 8.01 (d, *J* = 8.0 Hz, 1H), 7.80 (d, *J* = 8.2 Hz, 1H), 7.73 (d, *J* = 1.1 Hz, 1H), 7.52 (dd, *J* = 8.2, 1.3 Hz, 2H), 7.42–7.35 (m, 2H), 7.27 (s, 1H), 4.10 (d, *J* =

7.5 Hz, 2H), 2.91–2.78 (m, 2H), 2.77–2.67 (m, 2H), 2.12 (s, 1H), 1.65 (s, 10H), 1.40–1.15 (m, 36H), 0.87 (ddt, *J* = 10.4, 7.0, 5.1 Hz, 12H). **^{13}C NMR** (101 MHz, $CDCl_3$): δ_C = 142.7, 142.4, 142.3, 140.5, 132.5, 132.3, 128.2, 123.1, 123.1, 122.9, 122.5, 122.1, 122.0, 121.0, 120.4, 118.4, 112.3, 98.4, 95.3, 90.9, 88.4, 85.0, 65.9, 48.0, 37.8, 34.3, 34.3, 32.0, 31.9, 31.9, 31.9, 31.9, 31.7, 30.8, 30.8, 30.1, 29.8, 29.7, 29.4, 29.4, 27.1, 26.6, 26.6, 22.8, 22.8, 22.8, 14.3. **MS** (MALDI-TOF) *m*/*z*: $[M+H]^+$ calcd for $C_{53}H_{74}INO$, 868.48; found 868.58. $[M–I]^+$ calcd for $C_{53}H_{74}NO$, 742.58; found 742.75.

2-[4-Ethynyl-2,5-dihexylphenyl)-2-methylbut-3-yn-2-ol]-7-[(4-ethynyl-2,5-dihexylphenyl)-2-methylbut-3-yn-2-ol)]-9-(2-hexyldecyl)-carbazole (4.25)

The disubstituted dodecal chain **4.25** was isolated by column chromatography from the reaction mixture from the procedure describe above as a yellow oil (184 mg, 19%). **^{1}H NMR** (400 MHz, $CDCl_3$): δ_H = 8.04 (d, *J* = 8.1 Hz, 2H), 7.54 (s, 2H), 7.44 – 7.36 (m, 4H), 7.29 (s, 2H), 4.16 (d, *J* = 7.5 Hz, 2H), 2.90 – 2.80 (m, 4H), 2.80 – 2.67 (m, 4H), 2.17 (s, 1H), 2.09 (s, 2H), 1.77 – 1.70 (m, 4H), 1.66 (s, 16H), 1.49 – 1.15 (m, 48H), 0.98 – 0.77 (m, 18H). **^{13}C NMR** (101 MHz, $CDCl_3$): δ_C = 142.4, 142.3, 141.4, 132.5, 132.3, 123.0, 122.9, 122.7, 122.0, 120.8, 120.5, 112.3, 98.4, 95.4, 88.4, 81.3, 65.9, 48.0, 38.0, 34.4, 34.3, 32.0, 31.9, 31.9, 31.7, 30.8, 30.8, 30.1, 29.8, 29.6, 29.4, 29.4, 29.4, 26.7, 26.6, 22.8, 22.8, 22.8, 22.8, 14.3, 14.3, 14.2, 14.2. **MS** (MALDI-TOF) *m*/*z*: $[M]^+$ calcd for $C_{78}H_{109}NO_2$, 1091.85; found 1092.00.

4,4'-(buta-1,3-diyne-1,4-diylbis(2,5-dihexyl-4,1-phenylene))bis(2-methylbut-3-yn-2-ol) (4.14)

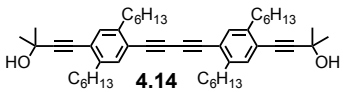

4.14

This compound was isolated from the above reaction conditions. **^{1}H NMR** (400 MHz, $CDCl_3$): δ_H = 7.32 (s, 2H), 7.23 (s, 2H), 2.76 – 2.70 (m, 4H), 2.70 – 2.64 (m, 4H), 2.01 (s, 2H), 1.67 – 1.57 (m, 20H), 1.34 (dt, *J* = 11.1, 6.6 Hz, 24H), 0.89 (q, *J* = 5.7 Hz, 12H). **^{13}C NMR** (101 MHz, $CDCl_3$): δ_C = 143.8, 142.4, 133.4, 132.5, 123.0, 121.3, 99.1, 81.6, 81.0, 78.2, 65.9, 34.2, 34.0, 31.9, 31.8, 31.6, 30.7, 30.6, 29.3, 29.2, 22.8, 22.7, 14.3, 14.2.

3,3'',5,5''-Tetramethoxy-1,1':4',1''-terphenyl (4.28)

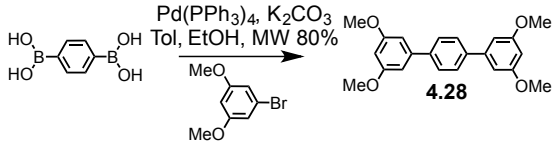

A microwave vial was charged with Benzene-1,4-diboronic acid (500 mg, 3.02 mmol), 1-Bromo-3,5-dimethoxybenzene (1.69 g, 7.54 mmol) and K_2CO_3 (1.685 g, 12.1 mmol) dissolved in toluene (15 mL) and EtOH (5 mL). This mixture was bubble purged with argon for 10 min and then $Pd(PPh_3)_4$ (176 mg, 151 umol) was added and the tube sealed. The reaction mixture was then subjected to microwave conditions (5 min pre-stirring, normal absorbance, 40 min at 110°C). After microwaving the reaction mixture was tested by TLC and deemed complete. The mixture was then poured onto a plug of celite in THF and the crude further purified by coloumn chromatography on SiO_2 (1:1 cyclohexane:DCM), fractions combined and solvent removed to affored **4.28** as a white powder (845 mg, 80%). **^{1}H NMR** (400 MHz, $CDCl_3$): δ_H = 7.64 (s, 4H), 6.77 (d, J = 2.3 Hz, 4H), 6.48 (t, J = 2.3 Hz, 2H), 3.86 (s, 12H). **^{13}C NMR** (101 MHz, $CDCl_3$): δ_C = 161.2, 143.1, 140.5, 127.6, 105.5, 99.5, 55.6. **MS** (EI +, 70 eV) *m*/*z* (%) = 350.2 (100) [M^+]. **MS** (MALDI-TOF) *m*/*z*: $[M]^+$ calcd for $C_{22}H_{22}O_4$, 350.15; found 350.12.

6-(4'-Bromo-[1,1'-biphenyl]-4-yl)hex-5-yn-1-ol (4.30)

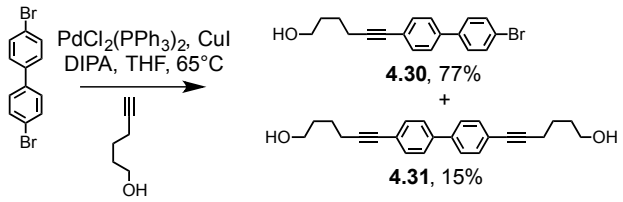

A 50 mL two neck flask was charged with 4,4'-Dibromobiphenyl (1.872 mg, 6.0 mmol), $PdCl_2(PPh_3)_2$ (42.5 mg, 0.06 mmol) and CuI (19 mg, 0.1 mmol) and dried under vacuum for 45 min. Then THF (10 mL) and DIPA (2 mL) were added and bubble purged with argon. Finally 5-hexyn-1-ol (196 mg, 2.0 mmol) was added dropwise. The reaction mixture was heated to 65°C for 16 hr. Then water was added and extracted with TBME. The organic layer was washed with 1M HCl (aq), brine and dried over $MgSO_4$. The crude was passed through a column of SiO_2 (1:1 Cyclohexane:EtOAc), fractions combined and solvent removed to afford **4.30** as a white solid (504 mg, 77%). **^{1}H NMR** (400 MHz, $CDCl_3$): δ_H = 7.58–7.52 (m, 2H), 7.47 (dd, J = 9.3, 1.3 Hz, 4H), 7.45–7.41 (m, 2H), 3.72 (t, J = 6.1 Hz, 2H), 2.48 (t, J = 6.7 Hz, 2H), 1.89–1.64 (m, 4H), 1.54 (s, 1H). **^{13}C NMR** (101 MHz, $CDCl_3$): δ_C = 139.5, 139.1, 132.2, 132.0, 128.6, 126.8, 123.4, 121.9, 91.1, 80.8, 62.6, 32.0, 25.1, 19.4. **MS** (EI +, 70 eV)

m/z (%) = 328.1 (100%), 330.1 (98%) [M^+]. **Anal.** Calcd for $C_{18}H_{17}BrO$: C, 65.67; H, 5.20. Found: C, 65.69; H, 5.44.

6-(4'-Bromo-[1,1'-biphenyl]-4-yl)hex-5-yn-1-ol (4.31)

Di-substituted biphenyl **4.31** was isolated by column chromotagraphy on SiO_2 from the reactions conditions (52 mg, 15%). **^{1}H NMR** (400 MHz, $CDCl_3$): δ_H = 7.53–7.48 (m, 4H), 7.47–7.42 (m, 4H), 3.72 (t, *J* = 6.1 Hz, 4H), 2.48 (t, *J* = 6.7 Hz, 4H), 1.83–1.65 (m, 8H), 1.41 (s, 2H). **^{13}C NMR** (101 MHz, $CDCl_3$): δ_C = 139.7, 132.1, 126.8, 123.2, 91.0, 80.9, 62.6, 32.1, 25.2, 19.4. **MS** (MALDI-TOF) *m/z*: $[M]^+$ calcd for $C_{24}H_{26}O_2$, 346.19; found 346.48.

4-Bromo-4'-(6-bromohex-1-yn-1-yl)-1,1'-biphenyl (4.32)

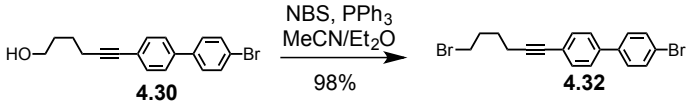

A 250 mL round bottom flask was charged with **4.30** (2.47 g, 7.5 mmol) and triphenylphosphine (3.94 g, 15 mmol) and the flask dried under vacuum. Then the compounds were dissolved in a 1:1 mixture of dry MeCN:Et_2O (30 mL:30 mL), cooled with an ice bath and then N-Bromosuccinimide (2.7 g, 15 mmol) was added portion-wise to the stirred reaction mixture under argon. After allowing to warm to RT over 6 hr the reaction mixture is passed through a celite plug and then a column of SiO_2 (1:1 cyclohexane:DCM), fractions combined and solvent removed to afford **4.32** as a white solid (2.88g, 98%). **^{1}H NMR** (400 MHz, $CDCl_3$): δ_H = 7.58–7.53 (m, 2H), 7.50–7.40 (m, 6H), 3.48 (t, *J* = 6.7 Hz, 2H), 2.48 (t, *J* = 6.9 Hz, 2H), 2.07 (dt, *J* = 14.5, 6.8 Hz, 2H), 1.78 (dt, *J* = 9.3, 7.0 Hz, 2H). **^{13}C NMR** (101 MHz, $CDCl_3$): δ_C = 139.5, 139.3, 132.2, 132.1, 128.7, 126.8, 123.3, 121.9, 90.4, 81.1, 33.4, 31.9, 27.3, 18.9. **MS** (EI +, 70 eV) *m/z* (%) = 392.0 (100) [M^+]. **Anal.** Calcd for $C_{18}H_{16}Br_2$: C, 55.13; H, 4.11. Found: C, 55.18; H, 4.01.

4-Bromo-4'-(6-bromohexyl)-1,1'-biphenyl (4.33)

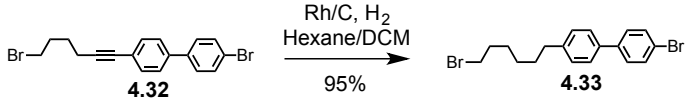

An autoclave vial was charged with temp3 (453 mg, 1.16 mmol) and Rhodium (5% activated carbon, 119 mg, 57.8 μmol) dissolved in a 1:1 mixture of hexane:DCM (5 mL:5 mL). The solution was degassed by bubble purging with argon and then placed in an autoclave, placed

under 10 Bar H_2 atmosphere and stirred for 16 hr. Then the crude was passed through a celite plug and then column of SiO_2 (4:1 cyclhexane:DCM), fractions combined and solvent removed to afford **4.33** as a white solid (0.434 g, 95%). **^{1}H NMR** (400 MHz, $CDCl_3$): δ_H = 7.57 – 7.51 (m, 2H), 7.49 – 7.41 (m, 4H), 7.24 (d, *J* = 7.5 Hz, 2H), 3.40 (t, *J* = 6.8 Hz, 2H), 2.70 – 2.59 (m, 2H), 1.93 – 1.79 (m, 2H), 1.66 (dt, *J* = 15.2, 7.6 Hz, 2H), 1.52 – 1.43 (m, 2H), 1.43 – 1.34 (m, 2H). **^{13}C NMR** (101 MHz, $CDCl_3$): δ_C = 142.3, 140.2, 137.5, 131.9, 129.1, 128.7, 126.9, 121.3, 35.6, 34.1, 32.8, 31.3, 28.5, 28.1. **MS** (EI +, 70 eV) *m*/*z* (%) = 396.0 (100), 394.1 (51), 398.1 (49) [M^+]. **Anal.** Calcd for $C_{18}H_{20}Br_2$: C, 54.57; H, 5.09. Found: C, 54.58; H, 5.19.

6-(4'-Iodo-[1,1'-biphenyl]-4-yl)hex-5-yn-1-ol (4.34)

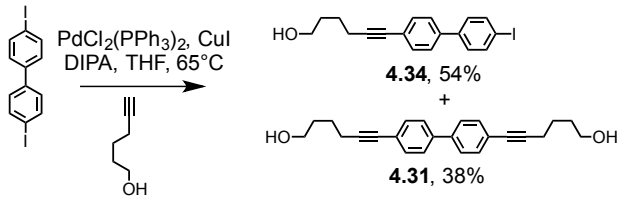

A 100 mL two neck flask was charged with 4,4'-Diiodobiphenyl (4.00 mg, 9.75 mmol), $PdCl_2(PPh_3)_2$ (137 mg, 195 µmol) and CuI (61.9 mg, 325 µmol) and dried under vacuum for 45 min. Then THF (30 mL), toluene to dissolve better (20 mL) and DIPA (7 mL) were added and bubble purged with argon. Finally 5-hexyn-1-ol (0.74 mL, 6.5 mmol) was added dropwise. The reaction mixture was heated to 65°C for 16 hr. Then water was added and extracted with TBME. The organic layer was washed with 1M HCl (aq), brine and dried over $MgSO_4$. The crude was passed through a column of SiO_2 (1:1 Cyclohexane:EtOAc), fractions combined and solvent removed to afford **4.34** as a white solid (1.32 mg, 54%). **^{1}H NMR** (400 MHz, $CDCl_3$): δ_H = 7.78 – 7.72 (m, 2H), 7.50 – 7.42 (m, 4H), 7.34 – 7.28 (m, 2H), 3.72 (t, *J* = 5.8 Hz, 2H), 2.48 (t, *J* = 6.7 Hz, 2H), 1.83 – 1.66 (m, 4H), 1.36 (s, 1H). **^{13}C NMR** (101 MHz, $CDCl_3$): δ_C = 140.1, 139.2, 138.0, 132.2, 128.9, 126.8, 123.5, 117.1, 93.4, 91.1, 80.8, 77.2, 62.6, 32.1, 25.2, 19.4. **MS** (EI +, 70 eV) *m*/*z* (%) = 376.0 (100) [M^+]. **Anal.** Calcd for $C_{18}H_{17}IO$: C, 57.46; H, 4.39. Found: C, 57.25; H, 4.39.

4-(6-Bromohex-1-yn-1-yl)-4'-iodo-1,1'-biphenyl (4.35)

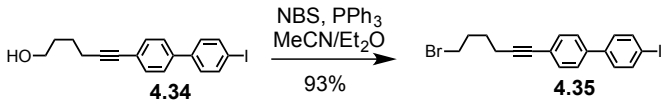

A 250 mL round bottom flask was charged with **4.34** (1.32 g, 3.52 mmol) and triphenylphosphine (1.27 g, 7.04 mmol) and the flask dried under vacuum. Then the compounds were dissolved in a 1:1 mixture of dry MeCN:Et_2O (20 mL:20 mL), cooled with an ice bath and then N-Bromosuccinimide (1.85 g, 7.04 mmol) was added portion-wise to the stirred reaction mixture under argon. After allowing to warm to RT over 6 hr the reaction mixture is passed through a celite plug and then a column of SiO_2 (1:1 cyclohexane:DCM), fractions combined and solvent removed to afford **4.35** as a white solid (1.44g, 93%). **^{1}H NMR** (400 MHz, $CDCl_3$): δ_H = 7.79 – 7.72 (m, 2H), 7.51 – 7.42 (m, 4H), 7.35 – 7.28 (m, 2H), 3.48 (t, *J* = 6.7 Hz, 2H), 2.49 (t, *J* = 6.9 Hz, 2H), 2.11 – 2.00 (m, 2H), 1.85 – 1.73 (m, 2H). **^{13}C NMR** (101 MHz, $CDCl_3$): δ_C = 140.1, 139.4, 138.1, 132.2, 128.9, 126.8, 123.4, 93.4, 90.5, 81.1, 33.4, 31.9, 27.3, 18.9. **Anal.** Calcd for $C_{18}H_{16}BrI$: C, 49.23; H, 3.67. Found: C, 49.20; H, 3.65.

Tetra-bromo Template (4.36)

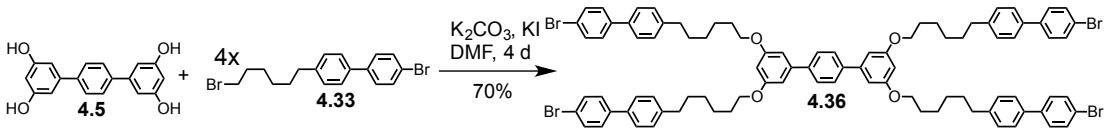

A 50 mL round bottom flask was charged with **4.5** (59 mg, 0.2 mmol), **4.33** (397 mg, 1 mmol), K_2CO_3 (140 mg, 1.0 mmol) and KI as a nucleophilic catalyst (67 mg, 0.401 mmol). These were dissolved in DMF (20 mL) and the reaction mixture stirred at 70°C for 4 d. The mixture was diluted with DCM and water. The organic phase was washed with 2M HCl (aq) and lots of water. Then the organic layer was passed through a plug of celite to obtain a clear yellow solution. The crude was adsorbed onto silica from DCM and passed through a column of SiO_2 (1:1 cyclohexane:DCM), fractions combined to afford **4.36** as a white solid (219 mg, 70%). **^{1}H NMR** (400 MHz, $CDCl_3$): δ_H = 7.61 (s, 4H), 7.55 – 7.50 (m, 8H), 7.48 – 7.40 (m, 16H), 7.23 (s, 4H), 6.75 (d, *J* = 2.2 Hz, 4H), 6.46 (t, *J* = 2.1 Hz, 2H), 4.00 (t, *J* = 6.4 Hz, 8H), 2.72 – 2.58 (m, 8H), 1.86 – 1.76 (m, 8H), 1.69 (dt, *J* = 15.2, 7.6 Hz, 8H), 1.58 – 1.48 (m, 8H), 1.43 (dt, *J* = 9.9, 6.4 Hz, 8H). **^{13}C NMR** (101 MHz, $CDCl_3$): δ_C = 160.7, 142.9, 142.5, 140.5, 140.2, 137.5, 131.9, 129.1, 128.7, 127.6, 126.9, 121.3, 106.0, 100.5, 68.2, 35.6, 31.5, 29.4, 29.1, 26.1. **Anal.** Calcd for $C_{90}H_{90}Br_4O_4$: C, 69.50; H, 5.83. Found: C, 69.51; H, 6.03.

Ethyl 4''-(6-bromohexyl)-[1,1':4',1''-terphenyl]-4-carboxylate (4.37)

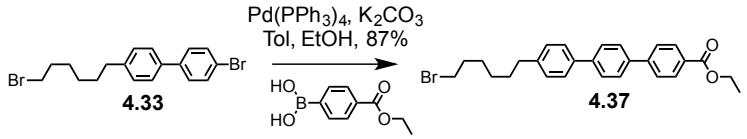

A microwave vial was charged with **4.33** (420 mg, 1.06 mmol), $Pd(PPh_3)_4$ (61.3 mg, 53 µmol), K_2CO_3 (296 mg, 2.12 mmol) and 4-Ethoxycarbonyl-phenyl-boronic acid (226 mg, 1.17 mmol) dissolved in a degassed mixture of toluene (10 mL) and EtOH (5 mL). The MW vial was sealed and irradiated in the MW (5 min pre-stirring, normal absorbance, 45 min at 120°C). Then the mixture was poured into water, and extracted with TBME. The organic layer was washed with 2M HCl (aq), brine and dried over $MgSO_4$. The crude was passed through a column of SiO_2 (1:1 cyclohexane:DCM), fractions combined and solvent removed to afford **4.37** as a white solid (428 mg, 87%). **^{1}H NMR** (400 MHz, $CDCl_3$): δ_H = 8.15–8.12 (m, 2H), 7.73–7.69 (m, 6H), 7.59–7.55 (m, 2H), 7.31–7.26 (m, 2H), 4.42 (q, *J* = 7.1 Hz, 2H), 3.42 (t, *J* = 6.8 Hz, 2H), 2.73–2.63 (m, 2H), 1.93–1.83 (m, 2H), 1.74–1.65 (m, 2H), 1.55–1.46 (m, 2H), 1.44–1.40 (m, 5H). **^{13}C NMR** (101 MHz, $CDCl_3$): δ_C = 166.7, 145.2, 142.2, 141.0, 138.7, 138.0, 130.2, 129.1, 127.7, 127.6, 127.1, 127.0, 61.1, 35.6, 34.1, 32.9, 31.4, 28.6, 28.2, 14.5. **MS** (EI +, 70 eV) *m*/*z* (%) = 466.1 (100), 464.1 (98) [M^+].

((4'-(6-Bromohex-1-yn-1-yl)-[1,1'-biphenyl]-4-yl)ethynyl)triisopropylsilane (4.38)

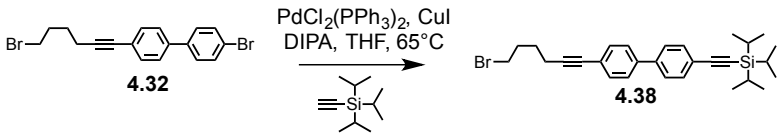

A two neck round bottom flask with reflux condenser attached was charged with **4.32** (724 mg, 1.85 mmol) dissolved in THF (100 mL) and DIPA (60 mL) and degassed by bubble purging with argon by for 15 min. Then CuI (17.6 mg, 92.5 µmol) and $PdCl_2(PPh_3)_2$ (131 mg, 0.185 mmol) were added. Finally TIPS-A (512 mL, 2.22 mmol) was added dropwise by syringe. The reaction mixture was heated to 60°C and left stirring for 16.5 hr. By TLC (1:1 cyclohexane:DCM) sm was still present, therefore a further 131 mg of $PdCl_2(PPh_3)_2$ and 0.5 mL of TIPS-A were added to the reacton mixture and stirred for a further 24 hr. After diluting with water and extraction with TBME, the organic layer was washed with 2M HCl (aq), brine and dried over $MgSO_4$. The crude was passed through a column of SiO_2 (4:1 cyclohexane:DCM), fractions combined and solvent removed to afford **4.38** as white solid (0.709 g, 78%). **^{1}H NMR** (400 MHz, $CDCl_3$): δ_H = 7.56–7.48 (m, 6H), 7.47–7.43 (m, 2H), 3.49 (t, *J* = 6.7 Hz, 2H), 2.49 (t, *J* = 6.9 Hz, 2H), 2.13–2.01 (m, 2H), 1.85–1.72 (m, 2H), 1.19–1.10 (m, 21H). **GC-MS** *m*/*z*; 17.20 min, 494 [$M]^+$.

Ethyl 4''-(6-bromohex-1-yn-1-yl)-[1,1':4',1''-terphenyl]-4-carboxylate (4.39)

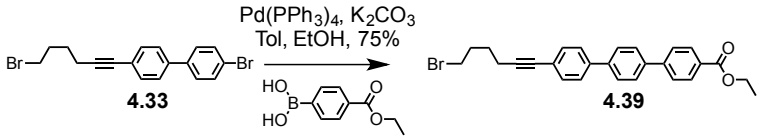

A microwave vial was charged with **4.32** (644 mg, 1.64 mmol), $Pd(PPh_3)_4$ (94.9 mg, 82.1 µmol), K_2CO_3 (460 mg, 3.28 mmol) and 4-Ethoxycarbonyl-phenyl-boronic acid (350 mg, 1.81 mmol) dissolved in a degassed mixture of toluene (10 mL) and EtOH (5 mL). The MW vial was sealed and irradiated in the MW (5 min pre-stirring, normal absorbance, 45 min at 120°C). Then the mixture was poured into water, and extracted with TBME. The organic layer was washed with 2M HCl (aq), brine and dried over $MgSO_4$. The crude was passed through a column of SiO_2 (1:1 cyclohexane:DCM), fractions combined and solvent removed to afford **4.39** as a white solid (459 mg, 75%). **^{1}H NMR** (500 MHz, $CDCl_3$): δ_H = 8.16 – 8.11 (m, 2H), 7.73 – 7.66 (m, 6H), 7.60 – 7.56 (m, 2H), 7.51 – 7.47 (m, 2H), 4.42 (q, *J* = 7.1 Hz, 2H), 3.50 (t, *J* = 6.7 Hz, 2H), 2.50 (t, *J* = 7.0 Hz, 2H), 2.13 – 2.02 (m, 2H), 1.85 – 1.75 (m, 2H), 1.43 (t, *J* = 7.2 Hz, 3H). **^{13}C NMR** (126 MHz, $CDCl_3$): δ_C = 166.6, 144.9, 140.2, 139.6, 139.2, 132.2, 130.2, 129.4, 127.8, 127.5, 126.9, 126.9, 123.1, 90.4, 81.2, 61.1, 33.4, 31.9, 27.2, 18.8, 14.5. **GC-MS** *m/z*; 17.45 min, 382 $[M\text{-}Br]^{\bullet+}$. **Anal.** Calcd for $C_{27}H_{25}BrO_2$: C, 70.29; H, 5.46. Found: C, 70.51; H, 5.19.

3,3'',5,5''-tetrakis((6-(4'-((triisopropylsilyl)ethynyl)-[1,1'-biphenyl]-4-yl)hex-5-yn-1-yl)oxy)-1,1':4',1''-terphenyl (4.41)

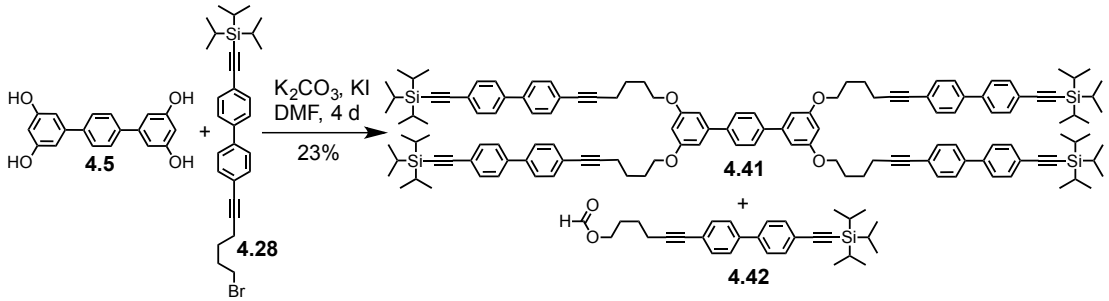

A 100 mL round bottom flask with reflux condenser was charged with **4.28** (693 mg, 1.4 mmol), K_2CO_3 (163 mg, 1.17 mmol), KI (78.4 mg, 0.468 mmol) and finally **4.5** (68.8 mg, 0.234 mmol) and dried under vacuum for 10 min. Then these solids were dissolved in dry, degassed DMF (20 mL) and the mixture heated to reflux under argon for 4 d accompanied by slow formation of a precipitate. Testing by TLC (8:6 cylohexane:DCM) shows the reaction was complete. The mixture was passed through a plug of celite in DCM, solvent removed to

give 1.11 g crude. This crude was adsorbed to silica by dissolving in with DCM/EtOAc and loaded onto a column of SiO_2. Fractions combined to afford **4.42** as a white solid and 0.322 g of the product. This was further purified by semi-prep GPC in $CHCl_3$, fractions combined and solvent removed to afford **4.41** as a yellow wax (0.104 g, 23%). **^{1}H NMR** (400 MHz, $CDCl_3$): δ_H = 7.62 (s, 4H), 7.55 – 7.46 (m, 24H), 7.46 – 7.41 (m, 8H), 6.77 (d, *J* = 2.1 Hz, 4H), 6.49 (t, *J* = 2.0 Hz, 2H), 4.08 (t, *J* = 6.2 Hz, 8H), 2.53 (t, *J* = 6.9 Hz, 8H), 2.05 – 1.93 (m, 8H), 1.84 (dd, *J* = 14.7, 7.1 Hz, 8H), 1.14 (s, 84H). **^{13}C NMR** (101 MHz, $CDCl_3$): δ_C = 160.7, 143.0, 140.5, 140.4, 139.6, 132.6, 132.2, 127.6, 126.9, 126.8, 123.4, 122.8, 107.0, 106.0, 100.5, 91.7, 90.9, 81.0, 67.7, 28.7, 25.5, 19.4, 18.8, 11.5.

2,7-Bis(ethynyl-TIPS)-9-(dodecan-1-ol)-carbazole (4.48)

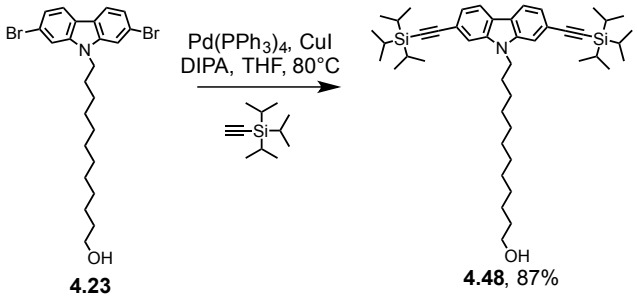

4.23 **4.48**, 87%

A 50 mL round bottom flask was charged with **4.23** (426 mg, 0.836 mmol) dissolved in THF (4 mL) and DIPA (4mL) and bubble purged with argon for 20min. Then CuI (8.0 mg, 42 µmol) and $Pd(PPh_3)_4$ (101 mg, 89 µmol) were added followed by TIPS-A (1.55 mL, 6.69 mmol) and the reaction stirred under argon at 80°C overnight. Water was added and extracted with TBME. The organic layer was washed with 2M HCl (aq), brine and dried over $MgSO_4$. The crude was passed through a column of SiO_2 (DCM), fractions combined and solvent removed to afford **4.48** as a yellow oil (517 mg, 87%). **^{1}H NMR** (400 MHz, $CDCl_3$): δ_H = 7.96 (d, *J* = 8.0 Hz, 2H), 7.49 (s, 2H), 7.35 (dd, *J* = 8.0, 1.1 Hz, 2H), 4.26 (t, *J* = 7.3 Hz, 2H), 3.63 (t, *J* = 6.7 Hz, 2H), 1.87 (p, *J* = 7.2 Hz, 4H), 1.56 (p, *J* = 6.6 Hz, 4H), 1.44–1.11 (m, 55H). **^{13}C NMR** (101 MHz, $CDCl_3$): δ_C = 140.7, 123.5, 122.7, 120.8, 120.4, 112.4, 108.6, 90.4, 63.2, 43.2, 33.0, 29.7, 29.7, 29.7, 29.6, 29.6, 29.5, 29.1, 27.3, 25.9, 18.9, 17.8, 11.6.

2-[4-(Ethynyl-2,5-dihexylphenyl)-2-ethynyl-H]-7-(4-{(2,5-dihexyl-4-((triisopropylsilyl)ethynyl)phenyl)ethynyl)}-9-(2-hexyldecyl)-carbazole (4.49)

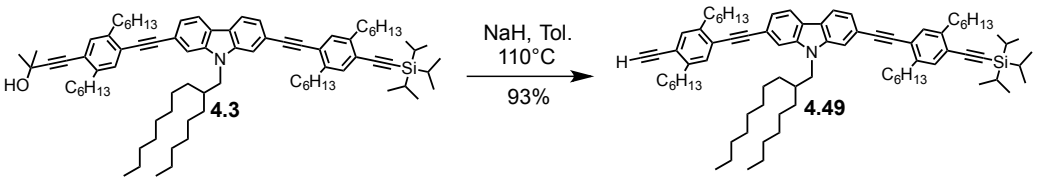

A round bottom flask was charged with **4.3** (383 mg, 322 µmol) dissolved in toluene (2 mL) and bubble purged with argon. Then NaH (dispersion of NaH 60% mineral oil, 25.7 mg, 643 µmol) and heated to 110°C for 1.5 hr until complete by TLC (DCM). Then the reaction mixture was passed through a plug of SiO_2 (DCM), collecting the main fraction to afford **4.49** as a yellow oil (340 mg, 93%). **^{1}H NMR** (400 MHz, $CDCl_3$): δ_H = 8.05 (d, J = 8.1 Hz, 2H), 7.55 (s, 2H), 7.45–7.38 (m, 4H), 7.35 (d, J = 10.1 Hz, 2H), 4.18 (d, J = 7.5 Hz, 2H), 3.32 (s, 1H), 2.91–2.82 (m, 4H), 2.79 (q, J = 7.2 Hz, 4H), 2.19 (s, 1H), 1.80–1.62 (m, 8H), 1.51–1.13 (m, 66H), 0.96–0.81 (m, 21H). **MS** (MALDI-TOF) m/z: $[M+H]^+$ calcd for $C_{81}H_{118}NSi$, 1132.90; found 1133.52.

7.4 Compounds from Chapter 5

1,3,5-Tris((4-(phenylethynyl)phenyl)ethynyl)benzene (5.1)

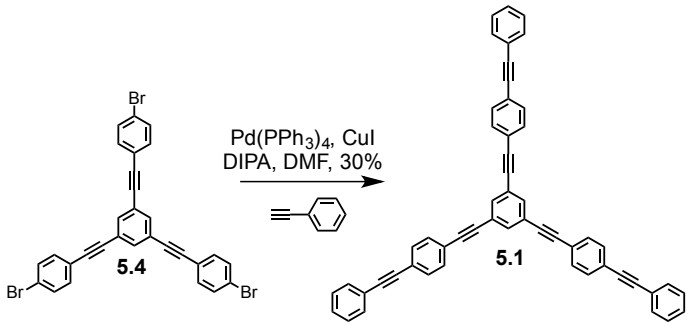

A two neck rb flask was charged with **5.4** (152 mg, 0.247 mmol) and CuI (2.35 mg, 12.4 µmol) and $Pd(PPh_3)_4$ (14.3 mg, 12.4 µmol) and dried under vacuum for 30 min. Then dry THF (10 mL) and DIPA (5 mL) were added and bubble purged with argon for 20 min. Finally Phenyl acetylene (109 µL) was added dropwise and the reaction mixture stirred under argon for 16 hr. After work-up and multiple columns, and a recrystalisation from DCM/Hexane the product **5.1** was isolated as a white solid. $\mathbf{R}_f$ = 0.23 (SiO_2; cyclohexane/DCM 4:1). **^{1}H NMR** (400 MHz, $CDCl_3$): δ_H = 7.67 (s, 3H), 7.53 (m, 18H), 7.36 (m, 9H). **^{13}C NMR** (101 MHz, $CDCl_3$): δ_C = 134.2, 131.7, 131.7, 131.6, 128.6, 128.4, 124.0, 123.6, 123.0, 122.6, 91.5, 90.4, 89.5, 89.0. **MS** (MALDI-TOF) m/z: $[M+H]^+$ calcd for $C_{54}H_{31}$, 679.23; found 679.31.

See also crystal structure data!

4-Iodo-1,1'-biphenyl (5.7)

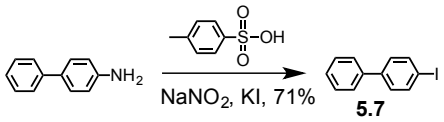

Following a literature procedure,[267] a round bottom flask was charged with 4-aminobiphenyl (508 mg, 3.00 mmol) and p-Toluenesulfonic acid monohydrate (1.71 g 9.01 mmol) dissolved in MeCN (12 mL). Then a solution of Sodium nitrite (414 mg, 6.00 mmol) and Potassium iodide (1.26 g, 7.51 mmol) dissolved in H2O (15 mL) was added dropwise. A further 12 mL of MeCN was added to aid stirring of the sludge that formed. After 6 hr the reaction was diluted with TBME and extracted. The organic layer was washed with brine and dried over $MgSO_4$ and the crude passed through a short column on SiO_2 (cyclohexane), fractions combined and solvent removed to afford **5.7** as a whte solid (594 mg, 71%). **^{1}H NMR** (500 MHz, $CDCl_3$): δ_H = 7.77 (dd, *J* = 8.6, 2.0 Hz, 2H), 7.58 – 7.53 (m, 2H), 7.48 – 7.41 (m, 2H), 7.38 (d, *J* = 7.2 Hz, 1H), 7.37 – 7.30 (m, 2H). **^{13}C NMR** (126 MHz, $CDCl_3$): δ_C = 140.9, 140.2, 138.0, 129.2, 129.0, 127.8, 127.0, 93.2. **MS** (EI +, 70 eV) *m/z* (%) = 280.0 (100) [M^+]. **Anal.** Calcd for $C_{12}H_9I$: C, 51.46; H, 3.24. Found: C, 51.60; H, 3.16.

1,3,5-Tris([1,1'-biphenyl]-4-ylethynyl)benzene (5.5)

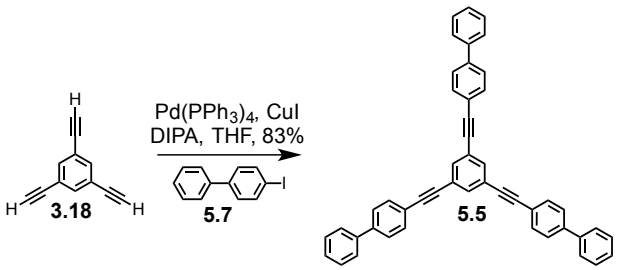

A round bottom flask was charged with **5.7** (463 mg, 1.65 mmol) and catalytic system of CuI (3.93 mg, 20.6 µmol) and $Pd(PPh_3)_4$ (47.7 mg, 42.3 µmol) dissolved in DIPA and THF. Finally **3.18** (62 mg, 413 µmol) dissolved in THF was added dropwsie and the reaction stirred overnight giving a yellow solution. Extraction with DCM, the organic layer washed with 2M HCl (aq), brine and dried over $MgSO_4$. After two sequential columns were made on SiO_2 (10:1 cyclohexane:DCM), fractions combined and solvent removed to afford **5.5** as a white crystalline solid (208 mg, 83%). **^{1}H NMR** (400 MHz, $CDCl_3$): δ_H = 7.69 (s, 3H), 7.64 – 7.59 (m, *J* = 5.7 Hz, 18H), 7.46 (t, *J* = 7.6 Hz, 6H), 7.37 (t, *J* = 7.4 Hz, 3H). **^{13}C NMR**

(126 MHz, $CDCl_3$): δ_C = 141.5, 140.4, 134.2, 132.3, 129.0, 127.9, 127.2, 127.2, 124.2, 121.8, 90.6, 88.7. **MS** (MALDI-TOF) *m/z*: $[M–H]^-$ calcd for $C_{48}H_{29}$, 605.23; found 605.00.
Also See the X-ray data!

1,3,5-Tris((4-((E)-styryl)phenyl)ethynyl)benzene (5.6)

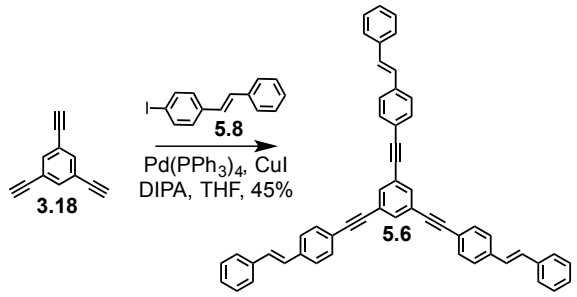

A 50 mL three neck round bottom flask was charged with (*E*)-1-iodo-4-styrylbenzene **5.8** (212 mg, 693 µmol), CuI (1.65 mg, 8.66 µmol) $Pd(PPh_3)_4$ (10.1 mg, 8.66 µmol) and **3.18** (26 mg, 173 µmol) dissolved in THF (10 mL) and DIPA (4.5 mL). The solution was bubble purged with argon for 20 min, and then stirred at RT overnight. Water was added and extracted with DCM. The organic phase was washed with H_2O, 2M HCl (aq), brine and dried over $MgSO_4$. The crude was passed through a column of SiO_2 (3:1 cyclohexane:DCM). The mixed fractions recovered were passed though a second column of SiO_2 (2:1 cyclohex:dcm), fractions combined and solvent removed to afford **5.6** as a white solid (58.1 mg, 49%). **^{1}H NMR** (500 MHz, $CDCl_3$): δ_H = 7.56 – 7.50 (m, 3H), 7.38 (t, *J* = 7.6 Hz, 1H), 7.29 (t, *J* = 7.3 Hz, 1H), 7.13 (q, *J* = 16.3 Hz, 1H). **^{13}C NMR** (126 MHz, $CDCl_3$): δ_C = 137.8, 137.2, 134.1, 132.2, 130.0, 128.9, 128.1, 128.0, 126.8, 126.6, 124.2, 121.9, 90.9, 88.9. **MS** (MALDI-TOF) *m/z*: $[M]^+$ calcd for $C_{54}H_{36}$, 684.28; found 684.52.

4',4'',4'''-(Benzene-1,3,5-triyltris(ethyne-2,1-diyl))tris(([1,1'-biphenyl]-3-ol)) (5.9)

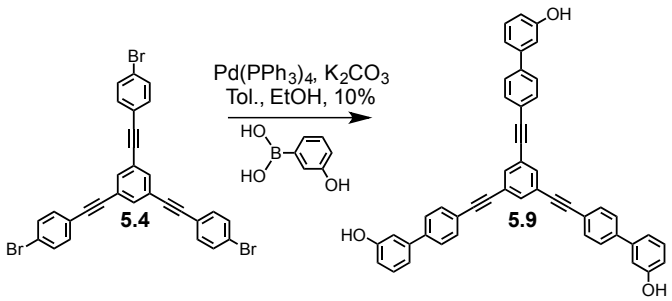

A microwave vial was charged with **5.4** (102 mg,166 µmol), $Pd(PPh_3)_4$ (9.58 mg, 8.29 µmol), K_2CO_3 (76.4 mg, 547 µmol) and 3-Hydroxyphenylboronic acid (91.5 mg, 663 µmol) dissolved in a degassed mixture of toluene (10 mL) and EtOH (5 mL). The MW vial was

sealed and irradiated in the MW (5 min pre-stirring, normal absorbance, 45 min at 120°C). Then the mixture was poured into water, and extracted with TBME. The organic layer was washed with 2M HCl (aq), brine and dried over $MgSO_4$. The crude was passed through a column of SiO_2 (1:1 cyclohexane:DCM), fractions combined and the crude passed through recycling GPC (loaded in CHCl3, cruse is not very soluble at all so only what was dissolved in 2 mL was purified) and solvent removed to afford **5.9** as a white solid (10.2 mg, 10%). **^{1}H NMR** (400 MHz, $CDCl_3$): δ_H = 7.64 (s, 3H), 7.61 (s, 12H), 7.25 (t, *J* = 7.9 Hz, 3H), 7.09 (d, *J* = 7.8 Hz, 3H), 7.06 (d, *J* = 1.8 Hz, 3H), 6.80 (dd, *J* = 8.1, 1.7 Hz, 3H). **^{13}C NMR** (101 MHz, $CDCl_3$): δ_C = 159.1, 142.9, 142.8, 134.8, 133.2, 131.0, 128.1, 125.7, 122.8, 119.2, 115.8, 114.7, 91.6, 89.1. **MS** (MALDI-TOF) *m*/*z*: $[M]^+$ calcd for $C_8H_{30}O_3$, 654.22; found 654.26.

See crystal structure data, under refinement!

4',4''',4''''''-(Benzene-1,3,5-triyltris(ethyne-2,1-diyl))tris(([1,1'-biphenyl]-3,5-diol)) (5.10)

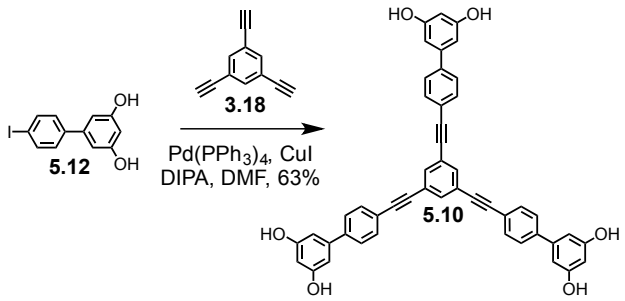

A 25 mL two neck flask with reflux condenser attached was charged with **5.12** (319 mg, 1.02 mmol) dissolved in DMF (2 mL) and DIPA (5 mL) and degassed by bubble purging with argon. Then $Pd(PPh_3)_4$ (22.3 mg, 19.3 µmol) amd CuI (18.4 mg, 96.6 µmol) were added. Finally the acetylene **3.18** (29 mg, 193 µmol) was added from a 5 mL solution of DMF, freshly degassed by bubble purge with argon. The reaction mixrure was gently heated to 45°C and left under argon overnight. The solvent was removed under reduced pressure and the crude loaded cirectly into a column of SiO_2 using EtOAC, ramping with some MeOH in the eluent. The collected crude was then passed through an RP column (C18, 40-60Å) in MeOH and the collected fraction passed through a third column SiO_2 (EtOAc), fractions combined and solvent removed to afford **5.10** as an offwhite solid (86.1 mg, 63%). **^{1}H NMR** (400 MHz, MeOD): δ_H = 7.64 (s, 3H), 7.59 (s, 12H), 6.58 (d, *J* = 2.2 Hz, 6H), 6.30 (t, *J* = 2.1 Hz, 3H). **^{13}C NMR** (101 MHz, MeOD): δ_C = 160.1, 143.5, 143.1, 134.8, 133.1, 128.0, 125.7, 122.8, 106.5, 103.1, 91.6. **MS** (ESI, *m*/*z*): 701.4 $[M–H]^-$ 100%, requires 701.2.

4'-Iodo-[1,1'-biphenyl]-3,5-diol (5.12)

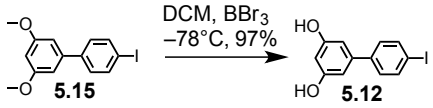

A 100 mL round bottom flask was charged with **5.15** (480 mg, 1.41 mmol) dissolved in in dry DCM (30 mL) under argon. The solution was cooled to –78°C and then BBr3 (1M solution in DCM, 10 mL, 10 mmol) was added by syringe dropwise. The reaction was left stirring to warm up overnight. The reaction was quenched by the slow addition of water, and extracted with DCM. The organic phase was washed and dried over $MgSO_4$. The crude was passed through a column of SiO_2 (1:1 cylclohexane:EtOAc), fractions combined and solvent removed to afford **5.12** as a colourless oil (427 mg, 97%). **NMR** (400 MHz, CD_3CN): δ_H = 7.79 – 7.71 (m, 2H), 7.38 – 7.29 (m, 2H), 7.04 (s, 2H), 6.56 (d, *J* = 2.2 Hz, 2H), 6.31 (t, *J* = 2.2 Hz, 1H). **^{13}C NMR** (101 MHz, CD_3CN): δ_C = 159.4, 143.0, 141.3, 138.7, 129.8, 106.5, 102.8, 93.5.**^{1}H NMR** (400 MHz, MeOD): δ_H = 7.74 – 7.68 (m, 2H), 7.33 – 7.27 (m, 2H), 6.52 (d, *J* = 2.2 Hz, 2H), 6.29 (t, *J* = 2.2 Hz, 1H). **^{13}C NMR** (101 MHz, MeOD): δ_C = 160.0, 143.3, 142.1, 138.8, 129.8, 106.3, 102.9, 93.4. **MS** (EI +, 70 eV) *m*/*z* (%) = 312.0 (100) [M^+]. **GC-MS** *m*/*z*; 12.91 min, 314 [M]$^{\bullet+}$ **Anal.** Calcd for $C_{12}H_9IO_2$: C, 46.18; H, 2.91. Found: C, 46.34; H, 3.06.

3,3-Diethyl-1-(4-iodophenyl)triaz-1-ene (5.13)

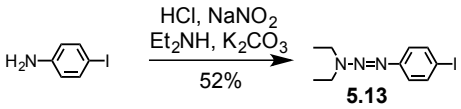

To a suspension of 4-Iodanilin (4.00 g, 18.3 mmol) in concentrated hydrochloride acid (35%, 26 mL) was added a solution of $NaNO_2$ (1.39 g 20.1 mmol) in water (6 mL) at 0°C. After stirring at 0°C for 30 min, the resulting mixture was added dropwise slowly at 0°C to a suspension of K_2CO_3 (20.4 g, 146 mmol), diethylamine (17 mL), and water (80 mL). The reaction mixture was then warmed to room temperature and stirred for 1 h. After extraction with ethyl acetate, the organic layer was evaporated, and the residue was passed through a coloum (1:1 cyclohexane/DCM), fractions combined and solvent removed to afford **5.13** as a red oil (2.92 g, 53%). **^{1}H NMR** (400 MHz, $CDCl_3$): δ_H = 7.64 – 7.59 (m, 2H), 7.19 – 7.13 (m, 2H), 3.75 (q, *J* = 7.2 Hz, 4H), 1.26 (t, *J* = 6.4 Hz, 6H). **^{13}C NMR** (101 MHz, $CDCl_3$): δ_C = 151.0, 137.8, 122.6, 89.1. **GC-MS** *m*/*z*; 304 [M+H]$^{\bullet+}$.

1-(3',5'-Dimethoxy-[1,1'-biphenyl]-4-yl)-3,3-diethyltriaz-1-ene (5.14)

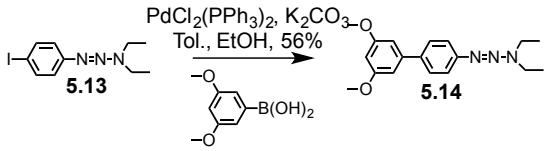

A microwave vial was charged with **5.13** (1.11 g, 3.68 mmol), $PdCl_2(PPh_3)_2$ (261 mg, 368 µmol), K_2CO_3 (1.54 g, 11.0 mmol) and 3,5-Dimethoxyphenylboronic acid (0.704 g, 3.68 mmol) dissolved in a degassed mixture of toluene (10 mL) and EtOH (5 mL). The MW vial was sealed and irradiated in the MW (5 min pre-stirring, normal absorbance, 45 min at 120°C). Then the mixture was poured into water, and extracted with TBME. The organic layer was washed with 2M HCl (aq), brine and dried over $MgSO_4$. The crude was passed through a column of SiO_2 (1:1 cyclohexane:DCM), fractions combined and solvent removed to afford **5.14** as a yellow oil (640 mg, 56%). **^{1}H NMR** (400 MHz, $CDCl_3$): δ_H = 7.55 (dd, *J* = 8.3, 2.0 Hz, 2H), 7.47 (dd, *J* = 8.4, 2.1 Hz, 2H), 6.75 (t, *J* = 2.4 Hz, 2H), 6.44 (d, *J* = 2.3 Hz, 1H), 3.86 – 3.84 (m, 6H), 3.78 (dt, *J* = 6.6, 5.8 Hz, 4H), 1.28 (t, *J* = 6.8 Hz, 6H). **^{13}C NMR** (101 MHz, $CDCl_3$): δ_C = 161.1, 151.0, 143.5, 137.8, 127.7, 120.8, 105.3, 99.1, 55.6.

4'-Iodo-3,5-dimethoxy-1,1'-biphenyl (5.15)

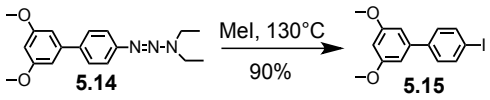

A 5 mL sealed tube was charged with **5.14** (388 mg, 1.24 mmol) using DCM to transfer this oil, the solvent was evaporated and then **5.14** was dissolved in MeI (3 mL) the tube sealed and heated to 130°C overnight. Then the MeI was distilled off inside a fume hood, and the crude left behind passed through a short column on SiO2, fractions evaporated to afford **5.15** as a dark oil (378 mg, 90%). **^{1}H NMR** (400 MHz, $CDCl_3$): δ_H = 7.74 (d, *J* = 8.2 Hz, 2H), 7.30 (d, *J* = 8.2 Hz, 2H), 6.67 (d, *J* = 2.1 Hz, 2H), 6.47 (t, *J* = 2.1 Hz, 1H), 3.83 (s, 6H). **^{13}C NMR** (101 MHz, $CDCl_3$): δ_C = 161.3, 142.4, 140.8, 137.9, 129.1, 105.4, 99.7, 93.4, 55.6.

((4'-Iodo-[1,1'-biphenyl]-3,5-diyl)bis(oxy))bis(triisopropylsilane) (5.16)

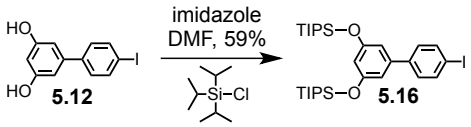

A 50 mL round bottom flask was charged with **5.12** (49.4 mg, 157 umol) and imidazol (64 mg, 94 µmol) and the flask dried under vacuum. Then dry DMF (2 mL) was added and still under argon Chlortriisopropylsilan (104 mL, 47 µmol) was added and the reaction stirred

at RT for 2 hr. The reaction was diluted with water and extracted with DCM, the organic phase was washed with water several times to remove traces of DMF, then brine and dried over $MgSO_4$. The crude was passed through a short column of SiO2 (4:1 cyclohexane:DCM), fractions combined and solvent removed to afford **5.16** as a colourless oil (58 mg, 59%). **^{1}H NMR** (400 MHz, $CDCl_3$): δ_H = 7.73 (d, J = 8.4 Hz, 2H), 7.26 (d, J = 8.4 Hz, 2H), 6.67 (d, J = 2.1 Hz, 2H), 6.43 (t, J = 2.1 Hz, 1H), 1.31 – 1.20 (m, 6H), 1.11 (d, J = 7.3 Hz, 36H). **^{13}C NMR** (101 MHz, $CDCl_3$): δ_C = 157.4, 141.8, 140.8, 137.9, 129.0, 111.9, 111.1, 93.1, 18.1, 12.8. **MS** (EI +, 70 eV) m/z (%) = 624.2 (100) [M^+]. **MS** (MALDI-TOF) m/z: $[M+H]^+$ calcd for $C_{30}H_{50}IO_2Si_2$, 625.23; found 625.67.

1,3,5-Tris((3',5'-bis((triisopropylsilyl)oxy)-[1,1'-biphenyl]-4-yl)ethynyl)benzene (5.17)

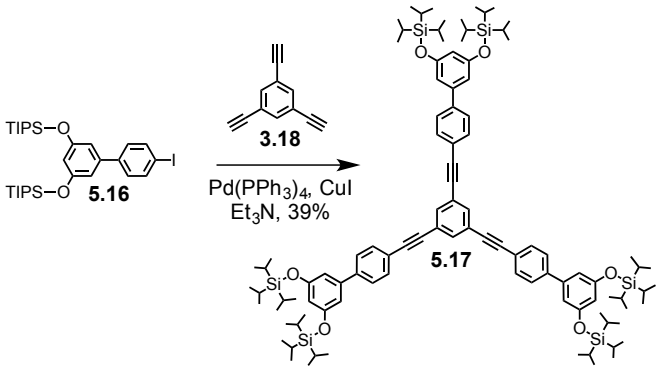

A 10 mL round bottom flask was charged with **5.16** (58.2 mg, 93.2 µmol), $Pd(PPh_3)_4$ (2.7 mg, 23.3 µmol) and CuI (0.22 mg, 11.7 µmol) and the flask placed under argon. The mixture was dissolved in degassed Et_3N (2 mL). Then **3.18** triethynylbenzene (3.5 mg, 23.3 µmol) was added dropwise from a solution of degassed Et_3N. The reaction was diluted with water and extracted with DCM. The organich phase was washed with 2M HCl (aq), brine and dried over $MgSO_4$. The crude was passed through a column of SiO_2. The collected product fraction was then loaded onto a prepretive TLC plate, SiO_2 (8:2 cyclohexane:DCM) and the product line scratched off, loaded onto to a frit and washed extensively with DCM to obtain **5.17** as a yellow oil (14.8 mg, 39%). **^{1}H NMR** (400 MHz, $CDCl_3$): δ_H = 7.70 (s, 3H), 7.59 (d, J = 8.3 Hz, 6H), 7.54 (d, J = 8.2 Hz, 6H), 6.74 (d, J = 2.1 Hz, 6H), 6.44 (t, J = 2.1 Hz, 3H), 1.27 (ddd, J = 13.6, 12.7, 7.3 Hz, 18H), 1.13 (d, J = 7.2 Hz, 108H). **^{13}C NMR** (101 MHz, $CDCl_3$): δ_C = 157.4, 142.1, 141.4, 134.2, 132.2, 127.1, 124.3, 121.9, 112.1, 111.2, 90.7, 88.6, 18.1, 12.9.

7.5 X-ray Crystal Structures

Carbazole crystal compound 2.22

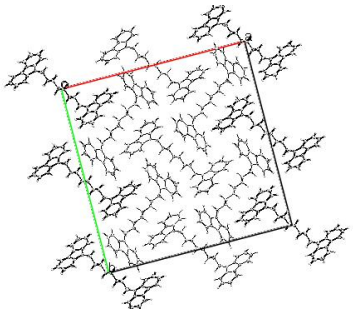

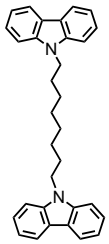

Crystal data for expt. eaton207

formula	$C_{32}H_{32}N_2$
formula weight	444.62
Z, calculated density	8, 1.224 Mg · m^{-3}
F(000)	1904
description and size of crystal	colourless plate, 0.030 · 0.190 · 0.220 mm^3
absorption coefficient	0.071 mm^{-1}
min/max transmission	1.00 / 1.00
temperature	123K
radiation(wavelength)	Mo K_α (λ = 0.71073 Å)
Crystal system, space group	tetragonal, I $4_1/a$
a	28.6475(10) Å
b	28.6475(10) Å
c	5.8815(3) Å
α	90°
β	90°
γ	90°
V	4826.8(3) $Å^3$
min/max Θ	1.422° / 32.694°
number of collected reflections	54013
number of independent refections	4417 (merging r = 0.054)
number of observed reflections	2887 (I>2.0σ(I))
number of refined parameters	154

r	0.0482
rW	0.0888
goodness of fit	1.0974

Phenyl acetylene star 5.1

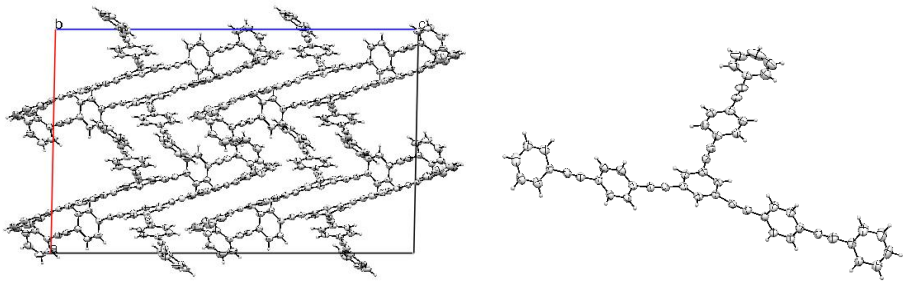

Crystal data obtained from expt. Eaton91

Formula	$C_{54}H_{30}$
formula weight	678.78
Z, calculated density	8, 1.204 Mg · m^{-3}
F(000)	2832
description and size of crystal	colourless plate, 0.02 · 0.21 · 0.34 mm^3
absorption coefficient	0.068 mm^{-1}
temperature	150(2)K
radiation(wavelength)	MoK_α (λ = 0.71073 Å)
Crystal system, space group	monoclinic, C2/c
a	20.361(4) Å
b	11.046(2) Å
c	33.312(7) Å
α	90.00°
β	91.19(3)°
γ	90.00°
V	7491(3) $Å^3$
min/max Θ	2.00° / 25.00°
number of collected reflections	16658
number of independent refections	6491 (merging r = 0.1863)
number of observed reflections	6491 (>2sigma(I))
number of refined parameters	487
r	0.1160

rW	0.2800
goodness of fit	1.067

Biphenyl star 5.5

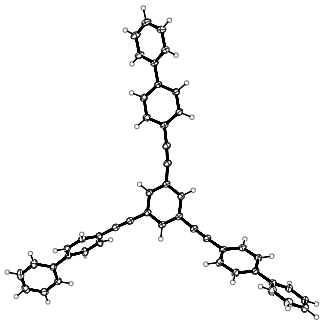

Crystal data for expt. eaton62	
formula	$C_{48}H_{30}$
formula weight	606.77
Z, calculated density	4, 1.207 Mg · m^{-3}
F(000)	1272
description and size of crystal	colourless block, 0.090 · 0.140 · 0.210 mm^3
absorption coefficient	0.068 mm^{-1}
min/max transmission	0.99 / 0.99
temperature	123K
radiation(wavelength)	Mo K_α (λ = 0.71073 Å)
Crystal system, space group	monoclinic, P 2_1/c
a	9.6393(13) Å
b	10.6477(14) Å
c	32.761(4) Å
α	90°
β	96.789(3)°
γ	90°
V	3338.9(8) $Å^3$
min/max Θ	2.012° / 32.629°
number of collected reflections	59189
number of independent refections	12147 (merging r = 0.045)
number of observed reflections	7487 (I>2.0σ(I))

number of refined parameters	433
r	0.0524
rW	0.0976
goodness of fit	1.1097

Tri-hydroxy star 5.9

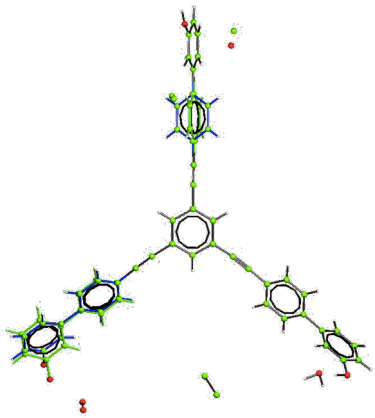

The star **5.9** was crystallised and a diffraction pattern was measured, however the packing is highly disordered, requiring intensive refinement to obtain an approximation to the unit cell. At this time we have confirmation of molecular identity, with two predominate sites of the biphenyl arms in the unit cell.

8 References:

[1] C. Toumey, *Nat. Nanotechnol.* **2009**, *4*, 783–784.
[2] G. Binnig, H. Rohrer, C. Gerber, E. Weibel, *Phys. Rev. Lett.* **1982**, *49*, 57–61.
[3] T. J. J. Müller, U. H. F. Bunz, Eds., *Functional Organic Materials – Syntheses, Strategies and Applications*, Wiley-VCH, Weinheim, **2007**.
[4] E. Negishi, L. Anastasia, *Chem. Rev.* **2003**, *103*, 1979–2018.
[5] X. F. Wu, P. Anbarasan, H. Neumann, M. Beller, *Angew. Chem. Int. Ed.* **2010**, *49*, 9047–9050.
[6] "The Nobel Prize in Chemistry 2010 - Scientific Background," can be found under http://nobelprize.org/nobel_prizes/chemistry/laureates/2010/sci.html, **2010**.
[7] F. Diederich, P. J. Stang, R. R. Tykwinski, Eds., *Acetylene Chemistry - Chemistry, Biology and Material Science*, Wiley-VCH, **2005**.
[8] K. Sonogashira, *J. Organomet. Chem.* **2002**, *653*, 46–49.
[9] R. R. Tykwinski, *Angew. Chem. Int. Ed.* **2003**, *42*, 1566–1568.
[10] K. Sonogashira, Y. Tohda, N. Hagihara, *Tetrahedron Lett.* **1975**, *16*, 4467–4470.
[11] N. Weibel, S. Grunder, M. Mayor, *Org. Biomol. Chem.* **2007**, *5*, 2343–2353.
[12] J. N. Wilson, U. H. F. Bunz, *J. Am. Chem. Soc.* **2005**, *127*, 4124–4125.
[13] M. Fischer, G. Lieser, A. Rapp, I. Schnell, W. Mamdouh, S. De Feyter, F. C. De Schryver, S. Höger, *J. Am. Chem. Soc.* **2004**, *126*, 214–222.
[14] K. C. Nicolaou, P. G. Bulger, D. Sarlah, *Angew. Chem. Int. Ed.* **2005**, *44*, 4442–4489.
[15] A. L. K. Shi Shun, E. T. Chernick, S. Eisler, R. R. Tykwinski, *J. Org. Chem.* **2003**, *68*, 1339–1347.
[16] M. Kivala, F. Diederich, *Pure Appl. Chem.* **2008**, *80*, 411–427.
[17] J. P. Hermes, F. Sander, P. Torsten, C. Cioffi, P. Ringler, T. Pfohl, M. Mayor, *Small* **2011**, *7*, 920–929.
[18] A. Schaate, M. Schulte, M. Wiebcke, A. Godt, P. Behrens, *Inorganica Chim. Acta* **2009**, *362*, 3600–3606.
[19] D. Evrard, F. Lambert, C. Policar, V. Balland, B. Limoges, *Chem. - Eur. J.* **2008**, *14*, 9286–9291.
[20] J. E. Reeve, H. A. Collins, K. D. Mey, M. M. Kohl, K. J. Thorley, O. Paulsen, K. Clays, H. L. Anderson, *J. Am. Chem. Soc.* **2009**, *131*, 2758–2759.
[21] N. Miyaura, A. Suzuki, *J. Chem. Soc. Chem. Commun.* **1979**, 866.
[22] D. Milstein, J. K. Stille, *J. Am. Chem. Soc.* **1978**, *100*, 3636–3638.
[23] S. Chopin, F. Chaignon, E. Blart, F. Odobel, *J. Mater. Chem.* **2007**, *17*, 4139.
[24] U. H. F. Bunz, *Macromol. Rapid Commun.* **2009**, *30*, 772–805.
[25] C. Wang, A. S. Batsanov, M. R. Bryce, *J. Org. Chem.* **2006**, *71*, 108–116.
[26] Y. Cakmak, E. U. Akkaya, *Org. Lett.* **2009**, *11*, 85–88.
[27] T. E. O. Screen, I. M. Blake, L. H. Rees, W. Clegg, S. J. Borwick, H. L. Anderson, *J. Chem. Soc. [Perkin 1]* **2002**, 320–329.
[28] M. B. Nielsen, F. Diederich, *Chem. Rec.* **2002**, *2*, 189–198.
[29] C. D. Simpson, J. D. Brand, A. J. Berresheim, L. Przybilla, H. J. Räder, K. Müllen, *Chem. - Eur. J.* **2002**, *8*, 1424–1429.
[30] J. S. Moore, *Accounts Chem. Res.* **1997**, *30*, 402–413.

[31] B. Schmaltz, A. Rouhanipour, H. J. Räder, W. Pisula, K. Müllen, *Angew. Chem. Int. Ed.* **2009**, *48*, 720–724.
[32] L. Shu, M. Mayor, *Chem. Commun.* **2006**, 4134–4136.
[33] L. Shu, M. Müri, R. Krupke, M. Mayor, *Org. Biomol. Chem.* **2009**, *7*, 1081–1092.
[34] Z. Wu, S. Lee, J. S. Moore, *J. Am. Chem. Soc.* **1992**, *114*, 8730–8732.
[35] T. C. Bedard, J. S. Moore, *J. Am. Chem. Soc.* **1995**, *117*, 10662–10671.
[36] N. Weibel, A. Mishchenko, T. Wandlowski, M. Neuburger, Y. Leroux, M. Mayor, *Eur. J. Org. Chem.* **2009**, 6140–6150.
[37] A. Błaszczyk, M. Chadim, C. von Hänisch, M. Mayor, *Eur. J. Org. Chem.* **2006**, 3809–3825.
[38] K. Sato, T. Yoshimura, M. Shindo, K. Shishido, *J. Org. Chem.* **2001**, *66*, 309–314.
[39] M. Kivala, C. Boudon, J.-P. Gisselbrecht, P. Seiler, M. Gross, F. Diederich, *Angew. Chem. Int. Ed.* **2007**, *46*, 6357–6360.
[40] H. C. Kolb, M. G. Finn, K. B. Sharpless, *Angew. Chem. Int. Ed.* **2001**, *40*, 2004–2021.
[41] P. Siemsen, R. C. Livingston, F. Diederich, *Angew. Chem. Int. Ed.* **2000**, *39*, 2632–2657.
[42] E. J. Corey, *Chem. Soc. Rev.* **1988**, *17*, 111.
[43] A. L. Kanibolotsky, I. F. Perepichka, P. J. Skabara, *Chem. Soc. Rev.* **2010**, *39*, 2695–2728.
[44] T. Narita, M. Takase, T. Nishinaga, M. Iyoda, K. Kamada, K. Ohta, *Chem. - Eur. J.* **2010**, *16*, 12108–12113.
[45] M. Mayor, J.-M. Lehn, *J. Am. Chem. Soc.* **1999**, *121*, 11231–11232.
[46] M. Mayor, C. Didschies, *Angew. Chem. Int. Ed.* **2003**, *42*, 3176–3179.
[47] B. M. Trost, M. T. Sorum, C. Chan, G. Rühter, *J. Am. Chem. Soc.* **1997**, *119*, 698–708.
[48] R. Chinchilla, C. Nájera, *Chem. Rev.* **2007**, *107*, 874–922.
[49] P. Fitton, M. P. Johnson, J. E. McKeon, *Chem. Commun.* **1968**, 6–7.
[50] P. Fitton, E. A. Rick, *J. Organomet. Chem.* **1971**, *28*, 287–291.
[51] C. Amatore, A. Jutand, *Accounts Chem. Res.* **2000**, *33*, 314–321.
[52] C. Amatore, S. Bensalem, S. Ghalem, A. Jutand, Y. Medjour, *Eur. J. Org. Chem.* **2004**, 366–371.
[53] C. Amatore, A. Jutand, *J. Organomet. Chem.* **1999**, *576*, 254–278.
[54] L. Xue, Z. Lin, *Chem. Soc. Rev.* **2010**, *39*, 1692.
[55] G. P. McGlacken, I. J. S. Fairlamb, *Eur. J. Org. Chem.* **2009**, 4011–4029.
[56] S. Wu, M. T. Gonzalez, R. Huber, S. Grunder, M. Mayor, C. Schönenberger, M. Calame, *Nat. Nanotechnol.* **2008**, *3*, 569–574.
[57] R. L. Carroll, C. B. Gorman, *Angew. Chem. Int. Ed.* **2002**, *41*, 4378–4400.
[58] V. P. W. Böhm, W. A. Herrmann, *Eur. J. Org. Chem.* **2000**, 3679–3681.
[59] A. C. Hillier, G. A. Grasa, M. S. Viciu, H. M. Lee, C. Yang, S. P. Nolan, *J. Organomet. Chem.* **2002**, *653*, 69–82.
[60] A. F. Littke, G. C. Fu, *Angew. Chem. Int. Ed.* **2002**, *41*, 4176–4211.
[61] C. Torborg, J. Huang, T. Schulz, B. Schäffner, A. Zapf, A. Spannenberg, A. Börner, M. Beller, *Chem. - Eur. J.* **2009**, *15*, 1329–1336.
[62] S. Cacchi, P. G. Ciattini, E. Morera, G. Ortar, *Tetrahedron Lett.* **1986**, *27*, 3931–3934.
[63] S. Darses, G. Michaud, J.-P. Genêt, *Eur. J. Org. Chem.* **1999**, 1875–1883.
[64] G. Fabrizi, A. Goggiamani, A. Sferrazza, S. Cacchi, *Angew. Chem. Int. Ed.* **2010**, 4067–4070.
[65] D. Sahoo, S. Thiele, M. Schulte, N. Ramezanian, A. Godt, *Beilstein J. Org. Chem.* **2010**, *6*, DOI 10.3762/bjoc.6.57.
[66] H. Kukula, S. Veit, A. Godt, *Eur. J. Org. Chem.* **1999**, 277–286.
[67] S. Höger, *Liebigs Ann.* **1997**, 273–277.

[68] S. Höger, A. D. Meckenstock, S. Müller, *Chem.- Eur. J.* **1998**, *4*, 2423–2434.
[69] F. M. Irvine, J. C. Smith, *J. Chem. Soc. Resumed* **1927**, 74.
[70] M. Schelhaas, H. Waldmann, *Angew. Chem. Int. Ed. Engl.* **1996**, *35*, 2056–2083.
[71] U. Ziener, A. Godt, *J. Org. Chem.* **1997**, *62*, 6137–6143.
[72] P. Wuts, T. Greene, *Greene's Protective Groups in Organic Synthesis*, Wiley-VCH, **2006**.
[73] T. Kamikawa, T. Hayashi, *J. Org. Chem.* **1998**, *63*, 8922–8925.
[74] T. Sandmeyer, *Berichte Dtsch. Chem. Ges.* **1884**, *17*, 1633–1635.
[75] J. Louie, J. F. Hartwig, *Tetrahedron Lett.* **1995**, *36*, 3609–3612.
[76] A. S. Guram, R. A. Rennels, S. L. Buchwald, *Angew. Chem. Int. Ed. Engl.* **1995**, *34*, 1348–1350.
[77] H. Ku, J. R. Barrio, *J. Org. Chem.* **1981**, *46*, 5239–5241.
[78] N. Satyamurthy, J. R. Barrio, *J. Org. Chem.* **1983**, *48*, 4394–4396.
[79] J. S. Moore, E. J. Weinstein, Z. Wu, *Tetrahedron Lett.* **1991**, *32*, 2465–2466.
[80] J. Zhang, J. S. Moore, Z. Xu, R. A. Aguirre, *J. Am. Chem. Soc.* **1992**, *114*, 2273–2274.
[81] E. J. Corey, P. L. Fuchs, *Tetrahedron Lett.* **1972**, *13*, 3769–3772.
[82] J. C. Gilbert, U. Weerasooriya, *J. Org. Chem.* **1979**, *44*, 4997–4998.
[83] E. Negishi, A. O. King, J. M. Tour, *Org. Synth.* **1986**, *64*, 44.
[84] L. R. Jones, J. S. Schumm, J. M. Tour, *J Org Chem* **1997**, *62*, 1388–1410.
[85] F. Thiemann, T. Piehler, D. Haase, W. Saak, A. Lützen, *Eur. J. Org. Chem.* **2005**, *2005*, 1991–2001.
[86] I. Wallmann, M. Schiek, R. Koch, A. Lützen, *Synthesis* **2008**, 2446–2450.
[87] S. Takahashi, Y. Kuroyama, K. Sonogashira, N. Hagihara, *Synthesis* **1980**, 627–630.
[88] R. Eastmond, D. R. M. Walton, *Tetrahedron* **1972**, *28*, 4591–4599.
[89] U. Halbes-Letinois, J.-M. Weibel, P. Pale, *Chem. Soc. Rev.* **2007**, *36*, 759–769.
[90] R. Severin, J. Reimer, S. Doye, *J. Org. Chem.* **2010**, *75*, 3518–3521.
[91] S. Höger, K. Bonrad, *J. Org. Chem.* **2000**, *65*, 2243–2245.
[92] W. E. Davidsohn, M. C. Henry, *Chem. Rev.* **1967**, *67*, 73–106.
[93] F. Diederich, Y. Rubin, O. L. Chapman, N. S. Goroff, *Helv. Chim. Acta* **1994**, *77*, 1441–1457.
[94] S. Höger, A.-D. Meckenstock, *Chem. - Eur. J.* **1999**, *5*, 1686–1691.
[95] S. Kim, B. Kim, J. In, *Synthesis* **2009**, *2009*, 1963–1968.
[96] G. Gaefke, S. Höger, *Synthesis* **2008**, *2008*, 2155–2157.
[97] A. Ernst, L. Gobbi, A. Vasella, *Tetrahedron Lett.* **1996**, *37*, 7959–7962.
[98] Y. Li, C. M. Santos, A. Kumar, M. Zhao, A. I. Lopez, G. Qin, A. M. McDermott, C. Cai, *Chem. - Eur. J.* **2011**, *17*, 2656–2665.
[99] C. Cai, A. Vasella, *Helv. Chim. Acta* **1995**, *78*, 732–757.
[100] N. A. Bumagin, A. B. Ponomaryov, I. P. Beletskaya, *Synthesis* **1984**, 728–729.
[101] S. J. Havens, P. M. Hergenrother, *J. Org. Chem.* **1985**, *50*, 1763–1765.
[102] M. J. Dabdoub, V. B. Dabdoub, E. J. Lenardão, *Tetrahedron Lett.* **2001**, *42*, 1807–1809.
[103] J. G. Rodríguez, J. Esquivias, A. Lafuente, C. Díaz, *J. Org. Chem.* **2003**, *68*, 8120–8128.
[104] O. H. Omar, F. Babudri, G. M. Farinola, F. Naso, A. Operamolla, *Eur. J. Org. Chem.* **2011**, 529–537.
[105] S. Goeb, R. Ziessel, *Org. Lett.* **2007**, *9*, 737–740.
[106] J. G. Rodríguez, J. L. Tejedor, T. La Parra, C. Díaz, *Tetrahedron* **2006**, *62*, 3355–3361.
[107] A. Khatyr, R. Ziessel, *J. Org. Chem.* **2000**, *65*, 3126–3134.
[108] R. Ziessel, S. Diring, P. Retailleau, *Dalton Trans.* **2006**, 3285–3290.

[109] J. Luo, Q. Yan, Y. Zhou, T. Li, N. Zhu, C. Bai, Y. Cao, J. Wang, J. Pei, D. Zhao, *Chem. Commun.* **2010**, *46*, 5725–5727.
[110] N. Zhu, W. Hu, S. Han, Q. Wang, D. Zhao, *Org. Lett.* **2008**, *10*, 4283–4286.
[111] M. M. Haley, M. L. Bell, J. J. English, C. A. Johnson, T. J. R. Weakley, *J. Am. Chem. Soc.* **1997**, *119*, 2956–2957.
[112] M. J. Mio, L. C. Kopel, J. B. Braun, T. L. Gadzikwa, K. L. Hull, R. G. Brisbois, C. J. Markworth, P. A. Grieco, *Org. Lett.* **2002**, *4*, 3199–3202.
[113] H.-F. Chow, C.-W. Wan, K.-H. Low, Yeung, *J. Org. Chem.* **2001**, *66*, 1910–1913.
[114] P. N. W. Baxter, *Chem. - Eur. J.* **2003**, *9*, 5011–5022.
[115] A. M. McDonagh, C. E. Powell, J. P. Morrall, M. P. Cifuentes, M. G. Humphrey, *Organometallics* **2003**, *22*, 1402–1413.
[116] Y. Zhao, Y. Shirai, A. D. Slepkov, L. Cheng, L. B. Alemany, T. Sasaki, F. A. Hegmann, J. M. Tour, *Chem. Eur. J.* **2005**, *11*, 3643–3658.
[117] Y. Shirai, Y. Zhao, L. Cheng, J. M. Tour, *Org. Lett.* **2004**, *6*, 2129–2132.
[118] K. C. Nicolaou, S. E. Webber, *J. Am. Chem. Soc.* **1984**, *106*, 5734–5736.
[119] B. Alberts, A. Johnson, J. Lewis, M. Raff, K. Roberts, P. Walter, *Molecular Biology of the Cell*, Garland Science, New York, **2002**.
[120] G. McDermott, S. M. Prince, A. A. Freer, A. M. Hawthornthwaite-Lawless, M. Z. Papiz, R. J. Cogdell, N. W. Isaacs, *Nature* **1995**, *374*, 517–521.
[121] A. Rodríguez-Moreno, M. M. Kohl, J. E. Reeve, T. R. Eaton, H. A. Collins, H. L. Anderson, O. Paulsen, *J. Neurosci.* **2011**, *31*, 8564 –8569.
[122] N. Crivillers, S. Osella, C. Van Dyck, G. M. Lazzerini, D. Cornil, A. Liscio, F. Di Stasio, S. Mian, O. Fenwick, F. Reinders, et al., *Adv. Mater.* **2013**, *25*, 432–436.
[123] S. Linden, C. Enkrich, M. Wegener, J. Zhou, T. Koschny, C. M. Soukoulis, *Science* **2004**, *306*, 1351–1353.
[124] B. R. Sveinbjörnsson, R. A. Weitekamp, G. M. Miyake, Y. Xia, H. A. Atwater, R. H. Grubbs, *Proc. Natl. Acad. Sci.* **2012**, *109*, 14332–14336.
[125] H. Liu, J. He, J. Tang, H. Liu, P. Pang, D. Cao, P. Krstic, S. Joseph, S. Lindsay, C. Nuckolls, *Science* **2010**, *327*, 64–67.
[126] E. Orentas, M. Lista, N.-T. Lin, N. Sakai, S. Matile, *Nat. Chem.* **2012**, *4*, 746–750.
[127] I. Sunagawa, Ed., *Morphology of Crystals: Part A: Fundamentals Part B: Fine Particles, Minerals and Snow Part C: The Geometry of Crystal Growth*, Springer, **2013**.
[128] K. G. Libbrecht, *J. Cryst. Growth* **2003**, *258*, 168–175.
[129] C. T. Calderone, D. H. Williams, *J. Am. Chem. Soc.* **2001**, *123*, 6262–6267.
[130] A. Ciesielski, C.-A. Palma, M. Bonini, P. Samorì, *Adv. Mater.* **2010**, *22*, 3506–3520.
[131] J. W. Steed, P. A. Gale, Eds., *Supramolecular Chemistry: From Molecules to Nanomaterials*, John Wiley And Sons, **2012**.
[132] D. M. P. Mingos, Ed., *Supramolecular Assembly via Hydrogen Bonds*, Springer, **2004**.
[133] P. Metrangolo, G. Resnati, *Chem. - Eur. J.* **2001**, *7*, 2511–2519.
[134] S. Furukawa, K. Tahara, F. C. De Schryver, M. Van der Auweraer, Y. Tobe, S. De Feyter, *Angew. Chem. Int. Ed.* **2007**, *46*, 2831–2834.
[135] N. Lin, A. Dmitriev, J. Weckesser, J. V. Barth, K. Kern, *Angew. Chem. Int. Ed.* **2002**, *41*, 4779–4783.
[136] C. A. Hunter, J. K. M. Sanders, *J. Am. Chem. Soc.* **1990**, *112*, 5525–5534.
[137] K. K. Baldridge, F. Cozzi, J. S. Siegel, *Angew. Chem. Int. Ed.* **2012**, *51*, 2903–2906.
[138] R. E. Dawson, A. Hennig, D. P. Weimann, D. Emery, V. Ravikumar, J. Montenegro, T. Takeuchi, S. Gabutti, M. Mayor, J. Mareda, et al., *Nat. Chem.* **2010**, *2*, 533–538.

[139] B. Lewandowski, G. D. Bo, J. W. Ward, M. Papmeyer, S. Kuschel, M. J. Aldegunde, P. M. E. Gramlich, D. Heckmann, S. M. Goldup, D. M. D'Souza, et al., *Science* **2013**, *339*, 189–193.
[140] F. B. L. Cougnon, J. K. M. Sanders, *Accounts Chem. Res.* **2012**, *45*, 2211–2221.
[141] T. Aida, E. W. Meijer, S. I. Stupp, *Science* **2012**, *335*, 813–817.
[142] J. Rotzler, S. Drayss, O. Hampe, D. Häussinger, M. Mayor, *Chem. – Eur. J.* **2013**, *19*, 2089–2101.
[143] J. Rotzler, M. Mayor, *Chem. Soc. Rev.* **2012**, *42*, 44–62.
[144] J. V. Barth, G. Costantini, K. Kern, *Nature* **2005**, *437*, 671–679.
[145] L. Gross, *Nat Chem* **2011**, *3*, 273–278.
[146] L. Bartels, *Nat. Chem.* **2010**, *2*, 87–95.
[147] S. Gabutti, M. Knutzen, M. Neuburger, G. Schull, R. Berndt, M. Mayor, *Chem. Commun.* **2008**, 2370–2372.
[148] W. Azzam, C. Fuxen, A. Birkner, H.-T. Rong, M. Buck, C. Wöll, *Langmuir* **2003**, *19*, 4958–4968.
[149] R. Madueno, M. T. Raisanen, C. Silien, M. Buck, *Nature* **2008**, *454*, 618–621.
[150] C. B. Aakeröy, N. R. Champness, C. Janiak, *CrystEngComm* **2010**, *12*, 22–43.
[151] J. A. A. W. Elemans, S. Lei, S. De Feyter, *Angew. Chem. Int. Ed.* **2009**, *48*, 7298–7332.
[152] A. G. Slater (née Phillips), P. H. Beton, N. R. Champness, *Chem. Sci.* **2011**, *2*, 1440–1448.
[153] S. Kitagawa, R. Kitaura, S. Noro, *Angew. Chem. Int. Ed.* **2004**, *43*, 2334–2375.
[154] L. Lafferentz, V. Eberhardt, C. Dri, C. Africh, G. Comelli, F. Esch, S. Hecht, L. Grill, *Nat. Chem.* **2012**, *4*, 215–220.
[155] J. Cai, P. Ruffieux, R. Jaafar, M. Bieri, T. Braun, S. Blankenburg, M. Muoth, A. P. Seitsonen, M. Saleh, X. Feng, et al., *Nature* **2010**, *466*, 470–473.
[156] R. Wehlauch, J. Hoecker, K. Gademann, *ChemPlusChem* **2012**, *77*, 1071–1074.
[157] Z. Mu, L. Shu, H. Fuchs, M. Mayor, L. Chi, *Langmuir* **2011**, *27*, 1359–1363.
[158] Z. Mu, L. Shu, H. Fuchs, M. Mayor, L. Chi, *J. Am. Chem. Soc.* **2008**, *130*, 10840–10841.
[159] C. Pérez León, C. Sürgers, M. Mayor, M. Marz, R. Hoffmann, H. v. Löhneysen, *J. Phys. Chem. C* **2009**, *113*, 14335–14340.
[160] N. Kepčija, Y.-Q. Zhang, M. Kleinschrodt, J. Björk, S. Klyatskaya, F. Klappenberger, M. Ruben, J. V. Barth, *J. Phys. Chem. C* **2013**, DOI 10.1021/jp310606r.
[161] L. Shu, Z. Mu, H. Fuchs, L. Chi, M. Mayor, *Chem. Commun.* **2006**, 1862–1863.
[162] N. M. Jenny, H. Wang, M. Neuburger, H. Fuchs, L. Chi, M. Mayor, *Eur. J. Org. Chem.* **2012**, *2012*, 2738–2747.
[163] T. Bauer, Z. Zheng, A. Renn, R. Enning, A. Stemmer, J. Sakamoto, A. D. Schlüter, *Angew. Chem. Int. Ed.* **2011**, *50*, 7879–7884.
[164] W. Xiao, D. Passerone, P. Ruffieux, K. Aït−Mansour, O. Gröning, E. Tosatti, J. S. Siegel, R. Fasel, *J. Am. Chem. Soc.* **2008**, *130*, 4767–4771.
[165] K. Tahara, H. Yamaga, E. Ghijsens, K. Inukai, J. Adisoejoso, M. O. Blunt, S. De Feyter, Y. Tobe, *Nat. Chem.* **2011**, *3*, 714–719.
[166] T. A. Jung, R. R. Schlittler, J. K. Gimzewski, *Nature* **1997**, *386*, 696–698.
[167] A. Schramm, C. Stroh, K. Dössel, M. Lukas, M. Fischer, F. Schramm, O. Fuhr, H. v. Löhneysen, M. Mayor, *Eur. J. Inorg. Chem.* **2013**, 70–79.
[168] J. K. Gimzewski, C. Joachim, R. R. Schlittler, V. Langlais, H. Tang, I. Johannsen, *Science* **1998**, *281*, 531–533.
[169] T. Kudernac, N. Ruangsupapichat, M. Parschau, B. Macia, N. Katsonis, S. R. Harutyunyan, K.-H. Ernst, B. L. Feringa, *Nature* **2011**, *479*, 208–211.

[170] G. Pawin, K. L. Wong, K.-Y. Kwon, L. Bartels, *Science* **2006**, *313*, 961–962.
[171] U. Schlickum, R. Decker, F. Klappenberger, G. Zoppellaro, S. Klyatskaya, M. Ruben, I. Silanes, A. Arnau, K. Kern, H. Brune, et al., *Nano Lett.* **2007**, *7*, 3813–3817.
[172] U. Schlickum, R. Decker, F. Klappenberger, G. Zoppellaro, S. Klyatskaya, W. Auwärter, S. Neppl, K. Kern, H. Brune, M. Ruben, et al., *J. Am. Chem. Soc.* **2008**, *130*, 11778–11782.
[173] D. Kühne, F. Klappenberger, R. Decker, U. Schlickum, H. Brune, S. Klyatskaya, M. Ruben, J. V. Barth, *J. Am. Chem. Soc.* **2009**, *131*, 3881–3883.
[174] D. Kühne, F. Klappenberger, W. Krenner, S. Klyatskaya, M. Ruben, J. V. Barth, *Proc. Natl. Acad. Sci.* **2010**, *107*, 21332–21336.
[175] J.-M. Lehn, *Chem. Soc. Rev.* **2007**, *36*, 151–160.
[176] J. A. Theobald, N. S. Oxtoby, M. A. Phillips, N. R. Champness, P. H. Beton, *Nature* **2003**, *424*, 1029–1031.
[177] Y. Yang, C. Wang, *Chem. Soc. Rev.* **2009**, *38*, 2576–2589.
[178] M. Grunze, *Nature* **2008**, *454*, 585–586.
[179] C. Silien, M. Buck, *J. Phys. Chem. C* **2008**, *112*, 3881–3890.
[180] D. Oyamatsu, H. Kanemoto, S. Kuwabata, H. Yoneyama, *J. Electroanal. Chem.* **2001**, *497*, 97–105.
[181] C. Silien, M. T. Räisänen, M. Buck, *Angew. Chem. Int. Ed.* **2009**, *48*, 3349–3352.
[182] C. Silien, M. T. Räisänen, M. Buck, *Small* **2010**, *6*, 391–394.
[183] A. G. Phillips, L. M. A. Perdigão, P. H. Beton, N. R. Champness, *Chem. Commun.* **2010**, *46*, 2775–2777.
[184] M. T. Räisänen, A. G. Slater (née Phillips), N. R. Champness, M. Buck, *Chem. Sci.* **2012**, *3*, 84–92.
[185] N. M. Jenny, M. Mayor, T. R. Eaton, *Eur. J. Org. Chem.* **2011**, *2011*, 4965–4983.
[186] G. Collin, H. Höke, J. Talbiersky, in *Ullmanns Encycl. Ind. Chem.*, Wiley-VCH Verlag GmbH & Co. KGaA, **2000**.
[187] N. J. Sax, *Dangerous Properties of Industrial Materials*, Van Nostrand Reinhold Comp., London, **1979**.
[188] J. V. Grazulevicius, P. Strohriegl, J. Pielichowski, K. Pielichowski, *Prog. Polym. Sci.* **2003**, *28*, 1297–1353.
[189] J. Li, A. C. Grimsdale, *Chem. Soc. Rev.* **2010**, *39*, 2399–2410.
[190] H. Jian, J. M. Tour, *J. Org. Chem.* **2003**, *68*, 5091–5103.
[191] F. Camerel, B. Donnio, R. Ziessel, *Soft Matter* **2011**, *7*, 412–428.
[192] Schaerlaekens M., Hendrickx E., Hameurlaine A., Dehaen W., Persoons A., *Chem. Phys.* **2002**, *277*, 43–52.
[193] J. Bouchard, M. Belletête, G. Durocher, M. Leclerc, *Macromolecules* **2003**, *36*, 4624–4630.
[194] S. Kato, S. Shimizu, H. Taguchi, A. Kobayashi, S. Tobita, Y. Nakamura, *J Org Chem* **2012**, 3222–3232.
[195] J.-F. Morin, M. Leclerc, *Macromolecules* **2002**, *35*, 8413–8417.
[196] P.-L. T. Boudreault, N. Blouin, M. Leclerc, in *Polyfluorenes* (Eds.: U. Scherf, D. Neher), Springer Berlin Heidelberg, Berlin, Heidelberg, **n.d.**, pp. 99–124.
[197] P. A. S. Smith, B. B. Brown, *J. Am. Chem. Soc.* **1951**, *73*, 2438–2441.
[198] J.-F. Morin, M. Leclerc, *Macromolecules* **2001**, *34*, 4680–4682.
[199] X. Pan, S. Liu, H. S. O. Chan, S.-C. Ng, *Macromolecules* **2005**, *38*, 7629–7635.
[200] F. Dierschke, A. C. Grimsdale, K. Müllen, *Synthesis* **2003**, 2470–2472.
[201] A. W. Freeman, M. Urvoy, M. E. Criswell, *J. Org. Chem.* **2005**, *70*, 5014–5019.
[202] D. Patrick, D. Boykin, W. Wilson, F. Tanious, J. Spychala, B. Bender, J. Hall, C. Dykstra, K. Ohemeng, R. Tidwell, *Eur. J. Med. Chem.* **1997**, *32*, 781–793.

[203] S.-H. Jung, W. Pisula, A. Rouhanipour, H. J. Räder, J. Jacob, K. Müllen, *Angew. Chem. Int. Ed.* **2006**, *45*, 4685–4690.
[204] M. Kastler, W. Pisula, D. Wasserfallen, T. Pakula, K. Mullen, *J. Am. Chem. Soc.* **2005**, *127*, 4286–4296.
[205] A. Lerchner, E. M. Carreira, *J. Am. Chem. Soc.* **2002**, *124*, 14826–14827.
[206] T. Kamikawa, T. Hayashi, *J. Org. Chem.* **1998**, *63*, 8922–8925.
[207] S. W. Thomas, T. M. Swager, *Macromolecules* **2005**, *38*, 2716–2721.
[208] E. L. Dane, S. B. King, T. M. Swager, *J Am Chem Soc* **2010**, *132*, 7758–7768.
[209] A. Klapars, S. L. Buchwald, *J. Am. Chem. Soc.* **2002**, *124*, 14844–14845.
[210] D. S. Surry, S. L. Buchwald, *Chem Sci* **2010**, *1*, 13–31.
[211] N. Berton, F. Lemasson, J. Tittmann, N. Stürzl, F. Hennrich, M. M. Kappes, M. Mayor, *Chem. Mater.* **2011**, *23*, 2237–2249.
[212] F. Lemasson, J. Tittmann, F. Hennrich, N. Stürzl, S. Malik, M. M. Kappes, M. Mayor, *Chem. Commun.* **2011**, 7428–7430.
[213] F. A. Lemasson, T. Strunk, P. Gerstel, F. Hennrich, S. Lebedkin, C. Barner-Kowollik, W. Wenzel, M. M. Kappes, M. Mayor, *J. Am. Chem. Soc.* **2011**, *133*, 652–655.
[214] F. Lemasson, N. Berton, J. Tittmann, F. Hennrich, M. M. Kappes, M. Mayor, *Macromolecules* **2012**, *45*, 713–722.
[215] P. Gerstel, S. Klumpp, F. Hennrich, O. Altintas, T. R. Eaton, M. Mayor, C. Barner-Kowollik, M. M. Kappes, *Polym. Chem.* **2012**, *3*, 1966.
[216] H. Kukula, S. Veit, A. Godt, *Eur. J. Org. Chem.* **1999**, *1999*, 277–286.
[217] M. Rehahn, A.-D. Schlüter, W. J. Feast, *Synthesis* **1988**, *1988*, 386–388.
[218] S. Höger, K. Bonrad, *J. Org. Chem.* **2000**, *65*, 2243–2245.
[219] R. L. Carroll, C. B. Gorman, *Angew. Chem. Int. Ed.* **2002**, *41*, 4378–4400.
[220] A. Aviram, M. A. Ratner, *Chem. Phys. Lett.* **1974**, *29*, 277–283.
[221] N. J. Tao, *Nat. Nano.* **2006**, *1*, 173–181.
[222] I. Díez-Pérez, J. Hihath, Y. Lee, L. Yu, L. Adamska, M. A. Kozhushner, I. I. Oleynik, N. Tao, *Nat Chem* **2009**, *1*, 635–641.
[223] S. Grunder, R. Huber, S. Wu, C. Schönenberger, M. Calame, M. Mayor, *Eur. J. Org. Chem.* **2010**, *2010*, 833–845.
[224] V. B. Engelkes, J. M. Beebe, C. D. Frisbie, *J Am Chem Soc* **2011**, *126*, 14287–14296.
[225] A. Salomon, D. Cahen, S. Lindsay, J. Tomfohr, V. B. Engelkes, C. D. Frisbie, *Adv. Mater.* **2003**, *15*, 1881–1890.
[226] I. Diez-Perez, J. Hihath, T. Hines, Z.-S. Wang, G. Zhou, K. Mullen, N. Tao, *Nat Nano* **2011**, 226–231.
[227] D. Vonlanthen, J. Rotzler, M. Neuburger, M. Mayor, *Eur. J. Org. Chem.* **2010**, *2010*, 120–133.
[228] D. Vonlanthen, A. Mishchenko, M. Elbing, M. Neuburger, T. Wandlowski, M. Mayor, *Angew. Chem. Int. Ed.* **2009**, *48*, 8886–8890.
[229] W. Lai, Y. Xing, Z. Ma, *J. Phys. Condens. Matter* **2013**, *25*, 205304.
[230] Y. Wada, *Pure Appl. Chem.* **1999**, *71*, 2055–2066.
[231] L. A. Bumm, J. J. Arnold, M. T. Cygan, T. D. Dunbar, T. P. Burgin, L. Jones, D. L. Allara, J. M. Tour, P. S. Weiss, *Science* **1996**, *271*, 1705–1707.
[232] E. Lörtscher, C. J. Cho, M. Mayor, M. Tschudy, C. Rettner, H. Riel, *ChemPhysChem* **2011**, *12*, 1677–1682.
[233] A. K. Flatt, S. M. Dirk, J. C. Henderson, D. E. Shen, J. Su, M. A. Reed, J. M. Tour, *Tetrahedron* **2003**, *59*, 8555–8570.
[234] H. Valkenier, E. H. Huisman, P. A. van Hal, D. M. de Leeuw, R. C. Chiechi, J. C. Hummelen, *J. Am. Chem. Soc.* **2011**, *133*, 4930–4939.

[235] M. A. Mangold, M. Calame, M. Mayor, A. W. Holleitner, *J. Am. Chem. Soc.* **2011**, *133*, 12185–91.
[236] U. Ziener, A. Godt, *J. Org. Chem.* **1997**, *62*, 6137–6143.
[237] J. C. Cuevas, E. Scheer, *Molecular Electronics: An Introduction to Theory and Experiment (Nanotechnology and Nanoscience)*, World Scientific Publishing Company, **2010**.
[238] S. M. Luber, M. Bichler, G. Abstreiter, M. Tornow, *Nanotechnology* **2011**, *22*, 065301.
[239] S. Strobel, S. Harrer, G. P. Blanco, G. Scarpa, G. Abstreiter, P. Lugli, M. Tornow, *Small* **2009**, *5*, 579–582.
[240] F. Sander, T. Peterle, N. Ballav, F. von Wrochem, M. Zharnikov, M. Mayor, *J. Phys. Chem. C* **2010**, *114*, 4118–4125.
[241] T. Peterle, P. Ringler, M. Mayor, *Adv. Funct. Mater.* **2009**, *19*, 3497–3506.
[242] T. Peterle, A. Leifert, J. Timper, A. Sologubenko, U. Simon, M. Mayor, *Chem. Commun.* **2008**, 3438–3440.
[243] E. O. Stejskal, J. E. Tanner, *J. Chem. Phys.* **1965**, *42*, 288–292.
[244] A. Macchioni, G. Ciancaleoni, C. Zuccaccia, D. Zuccaccia, *Chem. Soc. Rev.* **2008**, *37*, 479–489.
[245] M. Mayor, C. Didschies, *Angew. Chem. Int. Ed.* **2003**, *42*, 3176–3179.
[246] J. K. Sprafke, D. V. Kondratuk, M. Wykes, A. L. Thompson, M. Hoffmann, R. Drevinskas, W.-H. Chen, C. K. Yong, J. Kärnbratt, J. E. Bullock, et al., *J. Am. Chem. Soc.* **2011**, *133*, 17262–17273.
[247] V. G. Veselago, *Sov. Phys. Uspekhi* **1968**, *10*, 509–514.
[248] J. B. Pendry, A. J. Holden, D. J. Robbins, W. J. Stewart, *Microw. Theory Tech. Ieee Trans.* **1999**, *47*, 2075–2084.
[249] R. A. Shelby, D. R. Smith, S. Schultz, *Science* **2001**, *292*, 77–79.
[250] S. Linden, C. Enkrich, M. Wegener, J. Zhou, T. Koschny, C. M. Soukoulis, *Science* **2004**, *306*, 1351–1353.
[251] J. M. Keller, K. S. Schanze, *Organometallics* **2009**, *28*, 4210–4216.
[252] S. Höger, *J. Polym. Sci. Part Polym. Chem.* **1999**, *37*, 2685–2698.
[253] S.-H. Jung, W. Pisula, A. Rouhanipour, H. J. Räder, J. Jacob, K. Müllen, *Angew. Chem. Int. Ed.* **2006**, *45*, 4685–4690.
[254] S. C. Simon, B. Schmaltz, A. Rouhanipour, H. J. Räder, K. Müllen, *Adv. Mater.* **2009**, *21*, 83–85.
[255] B. Schmaltz, A. Rouhanipour, H. J. Räder, W. Pisula, K. Müllen, *Angew. Chem. Int. Ed.* **2009**, *48*, 720–724.
[256] S. Hoger, A.-D. Meckenstock, H. Pellen, *J. Org. Chem.* **1997**, *62*, 4556–4557.
[257] M. F. Jacobsen, C. S. Andersen, M. M. Knudsen, K. V. Gothelf, *Org. Lett.* **2007**, *9*, 2851–2854.
[258] H. Kukula, S. Veit, A. Godt, *Eur. J. Org. Chem.* **1999**, *1999*, 277–286.
[259] M. Rehahn, A.-D. Schlüter, W. J. Feast, *Synthesis* **1988**, *1988*, 386–388.
[260] G. Battagliarin, C. Li, V. Enkelmann, K. Müllen, *Org. Lett.* **2011**, *13*, 3012–3015.
[261] G. W. Kabalka, M. R. Akula, J. Zhang, *Nucl. Med. Biol.* **2002**, *29*, 841–843.
[262] M. Roberti, D. Pizzirani, M. Recanatini, D. Simoni, S. Grimaudo, Di Cristina, V. Abbadessa, N. Gebbia, M. Tolomeo, *J. Med. Chem.* **2006**, *49*, 3012–3018.
[263] C. Oger, L. Balas, T. Durand, J.-M. Galano, *Chem. Rev.* **2013**, *113*, 1313–1350.
[264] M. Hoffmann, C. J. Wilson, B. Odell, H. L. Anderson, *Angew. Chem. Int. Ed.* **2007**, *46*, 3122–3125.
[265] F. Würthner, F. Schlosser, J. Sung, P. Kim, D. Kim, *Chem. Sci.* **2012**, 2778–2785.
[266] T. R. Eaton, D. M. Torres, M. Buck, M. Mayor, *CHIMIA* **2013**, *67*, 222–226.

[267] E. Krasnokutskaya, N. Semenischeva, V. Filimonov, P. Knochel, *Synthesis* **2007**, *2007*, 81–84.
[268] M. C. O'Sullivan, J. K. Sprafke, D. V. Kondratuk, C. Rinfray, T. D. W. Claridge, A. Saywell, M. O. Blunt, J. N. O'Shea, P. H. Beton, M. Malfois, et al., *Nature* **2011**, *469*, 72–75.
[269] G. Gaefke, S. Höger, *Synthesis* **2008**, *2008*, 2155–2157.
[270] C. Maeda, T. Yoneda, N. Aratani, M.-C. Yoon, J. M. Lim, D. Kim, N. Yoshioka, A. Osuka, *Angew. Chem. Int. Ed.* **2011**, *50*, 5691–5694.
[271] O. Mongin, C. Papamicaël, N. Hoyler, A. Gossauer, *J. Org. Chem.* **1998**, *63*, 5568–5580.